Modelling and Design Methodology for Fully-Active Fixtures

Thomas Nikolaou Papastathis
MEng, Mechanical and Aeronautics Engineering

Thesis submitted to The University of Nottingham

for the degree of Doctor of Philosophy

December 2010

Abstract

Fixtures are devices designed to repeatedly and accurately locate the processed workpiece in a desired position and orientation, and securely hold it in the location throughout the manufacturing process. Fixtures are also charged with the task of supporting the workpiece to minimise deflection under the loads arising from the manufacturing process. As a result, fixtures have a large impact on the outcome of a manufacturing process, especially when the workpiece presents low rigidity. Traditionally, in manufacturing environments, where thin-walled components are produced, the utilised fixtures are dedicated solutions, designed for a specific workpiece geometry. However, in the recent decades, when the manufacturing philosophy has shifted towards mass customisation, there is a constant technological pull towards manufacturing equipment that exhibits high production rates and increased flexibility/reconfigurability, without any compromise in the quality of the end result. Therefore, fixtures have been the focal point of a plethora of research work, targeting mainly towards either more reconfigurable, or more intelligent/adaptive solutions. However, there have been no attempts so far to merge these two concepts to generate a new fixturing approach. Such an approach, referred to in this work as fully-active fixrturing, would have the added ability to reposition its elements and adapt the forces it exerts on-line, maximising the local support to the workpiece, and thus reducing vibration amplitude and elastic deformation. This results in a tighter adherence to the nominal dimensions of the machined profile and an improved surface-finish quality.

This research work sets out to study the impact of such fixturing solutions, through developing suitable models which reflect the fixture-workpiece system behaviour, and a design methodology that can support and plan the operation of fully-active fixtures. The developed model is based on a finite elements representation of the workpiece, capturing the dynamic response of a thin-walled workpiece that is being subjected to distributed moving

harmonic loads. At the same time, the workpiece is in contact with an active element that operates in closed-loop control. An electromechanical actuator is charged with the role of the active elements, and it is modelled via first-principle based equations. Two control strategies are examined experimentally to identify the best performing approach. The direct force/torque control strategy with a Proportional-Integral action compensator is found to lead to a system that responds faster. This control architecture is included in the model of the active elements of the fixture. The behaviour of the contact between the fixture and the workpiece is approximated via a combination of a spring and a damper. The overall model is assembled using the impedance coupling technique and has been verified by comparing its response with the time-domain response of an experimental set-up.

The developed model serves as the backbone of the fully-active fixture design methodology. The latter is capable of establishing important fixturing parameters, such as the pattern of motion of the movable fixture element, the points on the surface of the workpiece that formulate the motion path of the fixture element, the time instant at which the element needs to change position, and the clamping forces the fixture needs to apply and maintain. The methodology is applied on a thin plate test case. Such a plate has been also used in a series of machining experiments, for which the fixturing parameters used are those that resulted from the test case. A very good quantitative agreement between both experiments and theory was observed, revealing the capabilities of the methodology itself and of the fully-active fixturing approach in general.

Και πολλὰ μὲλλει να μὰθεις,

αν το Ασὴμαντο εμβαθὺνεις.

Το Ἀξιον Εστὶ, Οδυσσὲας Ελὺτης, 1911-1996

You'll come to learn a great deal

if you study the Insignificant in depth.

The Axion Esti - It is Worthy, Odysseas Elytis, 1911-1996

Acknowledgements

Through these lines I would like to thank all those people that contributed to this research work, either directly or indirectly. First of all, I would like to express my deepest gratitude to my supervisors Prof. Svetan Ratchev and Dr. Atanas Popov for their inspiring and invaluable guidance throughout my work. Their input has been determinant for the successful completion of this study.

I am also truly thankful towards Dr. Kevin Hin Leong Phuah for helping me in my initial steps in the field of fixturing with his knowledge and experience.

Furthermore, I would like to thank all my colleagues and friends at the Precision Manufacturing Centre. A special mention needs to be made of my esteemed colleague Marco Ryll and my treasured friend Otto Jan Bakker, for sharing with me this research quest in the field of fixturing, and for making my involvement in the AFFIX project such a pleasure. I would also like to express my gratitude towards everyone in C32 and A37 for making my time in Nottingham one that I will never forget. Also, I would like to acknowledge Ruth Strickland, Rachel Watson, and Rachel Brereton for their everyday support.

Many thanks go to the technicians Colin Astill, Mark Strickland, Paul Wentworth, Dave Smith, Mark Dane, and Tom Buss for their valuable help and advice on the experimental work of this study.

Finally, I would like to thank from the depths of my heart my father Nicholas, my mother Georgia, and my sister Vicky for their unbound love and continuous support in everything I do.

Contents

Abstract **i**

Acknowledgements **iv**

List of Figures **ix**

List of Tables **xvii**

List of Symbols **xxi**

List of Abbreviations **xxix**

1 Introduction **1**

1.1 Background and Motivation 1

1.2 Research Objectives 5

1.3 Thesis Outline 6

2 Literature Review **9**

2.1 Introduction 9

2.2 The Basics of Fixturing 10

2.3 Fixturing Concepts 12

2.3.1 Dedicated Fixtures 12

2.3.2 Modular Fixtures 13

2.3.3 Phase-Change Fixtures 14

2.3.4 Conformable Fixtures 16

2.3.5 Sensor-Integrated Fixtures 17

2.3.6 Numerically-Controlled Fixtures 18

2.3.7 Active/Adaptive Fixtures 20

2.3.8 Pallet Fixtures . . . 22
2.4 Fixture-Workpiece Dynamics . . . 23
2.4.1 Friction and its Effect on the Workpiece-Fixture System Dynamics . 23
2.4.2 Modelling of Fixture and Workpiece Considering their Dynamic Interaction . . . 24
2.4.3 Fixture Design Methods Accounting for System Dynamics . . . 29
2.5 Control Strategies for Active Fixtures . . . 30
2.6 Modelling of the Full Dynamic Nature of Machining Loads . . . 31
2.7 Summary of Key Findings and Identification of Knowledge Gaps . . . 33

3 Research Methodology 36
3.1 Introduction . . . 36
3.2 Research Objectives, Assumptions and Limitations . . . 38
3.2.1 Research Objectives . . . 38
3.2.2 Assumptions and Limitations . . . 42
3.3 Validation Procedures . . . 47
3.3.1 Analytical Validation Procedures . . . 47
3.3.2 Experimental Validation Procedures . . . 48
3.3.3 Fully-Active Fixture Concept . . . 49
3.3.4 Fully-Active Fixture Prototype . . . 55
3.4 Conclusions . . . 59

4 A Comprehensive Model for Fixture-Workpiece Systems 61
4.1 Introduction . . . 61
4.2 Finite Elements Model of a Workpiece . . . 62
4.2.1 Natural Frequency Prediction Accuracy . . . 63
4.2.2 Elastic Deformation of a Plate under a Moving Load . . . 69
4.3 Model of the Active Fixturing Elements . . . 78
4.3.1 Modelling of the Actuating Unit . . . 82
4.3.2 Modelling the Actuator Controller . . . 84
4.4 Model Formulation in a Matrix Form . . . 85
4.4.1 Expressing the Workpiece Model in Matlab . . . 86
4.5 Coupling of Actuator and Workpiece Models . . . 89

4.6 Experimental Validation 95
4.7 Conclusions 99

5 Control Strategies for Active Fixture Elements 101

5.1 Introduction 101
5.2 Overall System Control Architecture 102
5.3 Control Algorithms 103
5.3.1 Position Control Related Tasks 104
5.3.2 Force Control Related Tasks 104
5.3.3 Selection of Suitable Force/Torque Control Strategy 110
5.4 Modelling the Closed-Loop Operation of the Clamps 116
5.4.1 Modelling the Motion Controller 118
5.4.2 Modelling the Charge Amplifier 119
5.4.3 Generating the Full System Model 121
5.5 Tuning the Controller of the Modelled System 123
5.5.1 Ultimate Sensitivity Ziegler-Nichols Design Method 124
5.5.2 Manual Tuning 125
5.5.3 Discussion on the Tuning Results for the Modelled System 125
5.6 Validation of the Fixture-Workpiece System Model 131
5.7 Conclusions 134

6 Fully-Active Fixture Design Methodology 137

6.1 Introduction 137
6.2 Fixture Design Methodology 139
6.2.1 Discretisation of the Structure 140
6.2.2 Formulation of Problem in Matlab 147
6.2.3 Optimisation Process 152
6.3 Beam Workpiece Test Case 169
6.4 Conclusions 177

7 Verification of the Fixture Design Methodology 179

7.1 Introduction 179
7.2 The Thin Plate Test Case 180

7.2.1 Phase 1: Discretisation of the Structure . . . 181
7.2.2 Phase 2: Formulation of the Problem in Matlab . . . 184
7.2.3 Phase 3: Optimisation Process. . . . 187
7.3 Experimental Set-Up . . . 198
7.3.1 Fixture Hardware . . . 198
7.3.2 Controlling Hardware . . . 201
7.3.3 Workpiece . . . 203
7.3.4 Workpiece Baseplate . . . 206
7.4 Experimental Procedure . . . 208
7.5 Results . . . 213
7.5.1 Passive and Static Clamp at P1 (X,Y)=(75,25) . . . 213
7.5.2 Passive and Static Clamp at P2 (X,Y)=(75,10) . . . 214
7.5.3 Passive and Moving Clamp - Continuous Motion . . . 217
7.5.4 Active and Static Clamp at P2 (X,Y)=(75,10) . . . 218
7.5.5 Active and Moving Clamp - Continuous Motion . . . 221
7.6 Discussion . . . 223
7.7 Conclusions . . . 227

8 Conclusions and Future Work 230
8.1 Contributions . . . 230
8.1.1 Literature Survey . . . 231
8.1.2 Identification of Research Objectives, Assumptions and Limitations 232
8.1.3 Fulfilment of the Research Objectives . . . 233
8.1.4 Validation of the Developed Model and Methodology . . . 237
8.2 Future Work . . . 238

Bibliography 239

A Validation of FEA and Analytical Workpiece Models 254
A.1 Validation of Natural Frequencies Obtained from the Literature . . . 254
A.2 Validation of Analytical Model of SFSF Plate Subjected to Moving Load . 255
A.2.1 Static Deflection of Beam Versus Deflection of Beam Under Slowly Moving Load . . . 257

A.2.2 Deflection of Beam Under Moving Load Versus Literature Results . 258

B Detailed Natural Frequency Prediction Results 261

C Detailed Elastic Deformation Prediction Results for Plate 266

C.1 Elastic Deformation of a SFSF Plate Calculated Using S4 Finite Elements . 267

C.2 Elastic Deformation of a SFSF Plate Calculated Using S3 Finite Elements . 270

List of Figures

2.1 Schematic of a modular fixture designed for to improve fixturing performance for thin-walled flexible objects [119]. 14
2.2 (a) The principle of Reference Free Part Encapsulation [76]. (b) The principle of phase-change base plate fixturing [10] 16
2.3 Two NC fixturing concept utilising the (a) double revolver and (b) translational movement principles [138] 19
2.4 The adaptive fixture presented by Nee *et al.* (a) Picture of the developed fixture [98] (b) Schematic of the DC motor-based active clamp and its components [97]. 21

3.1 (a) Normal and tangential forces experienced by a workpiece undergoing a grinding operation. (b) Power spectrum density of normal forces [27] 39
3.2 CAD representation of the proposed fully-active fixture concept. 50
3.3 A detailed view of the transport component and its various components. (a) The transport component along with the runner-base and the transport component base. (b) A closer detail highlighting the runners, the ball-screw nut, and the linear-guides base. 51
3.4 Placement of the actuators relative to motion direction of the runners on the linear guides. The local Cartesian axes for the transport component are highlighted. 54
3.5 The hardware instantiation of the fully-active fixture prototype. (a) A general view of the overall system. (b) A more detailed view showing the two transport components and the passive locating elements that comprise the fixture. 56

3.6 The control architecture of the fully-active fixture that is used during experimental validation procedures. 58

4.1 (a) Boundary conditions applied to a plate represented by a 3D extruded solid body. (b) Boundary conditions applied to a plate represented by a 2D planar solid body. 66

4.2 Representation of a moving load $P(t)$ and the resulting nodal loads [142]. . 71

4.3 Moving concentrated load $P(t) = 150\,(1 + \cos\omega t)$ with $\omega = 10$ Hz and its Resulting Nodal Forces on the two Nodes of the Second Element (S4). . . 72

4.4 Moving distributed harmonic load of magnitude $P = 12$ N/mm traversing a SFSF plate. 78

4.5 Schematic of an active clamping fixture element and its necessary components. 81

4.6 Block diagram of the actuator and its peripherals in open-loop operation. . 81

4.7 Mechanical model of the actuator in contact with a simplified workpiece through springs and dampers. 83

4.8 Electrical model of the actuator motor [50]. 83

4.9 Electrical diagram of RC-filter circuit. 85

4.10 Experimental set-up for the verification of the open-loop active clamp-plate coupled model. 96

4.11 Simulated and experimental response of the active clamp-plate system to a (a) step input of 1 V and a (b) sinusoidal input of 0.5 V amplitude, 0.5 V offset and 1 Hz excitation frequency. 98

5.1 Block diagram of the position control closed-loop system. Digital to Analogue conversion is signified as DAC, and the linear gain in the voltage to current transformation is signified as G_{ac}. 104

5.2 Block diagram of the cascaded force/torque control architecture. Based on information obtained from [83]. 105

5.3 Schematic representation of the active clamp system operating under the cascaded force/position control scheme [98]. 106

5.4 Response of a DC motor-based active clamping system to 10 N step inputs [83]. 107

5.5 Response of a DC motor active clamping system to a ramp input [98]. . . 107
5.6 Block diagram of the direct force/torque control architecture. 109
5.7 Transient response of a PMAC actuator-based active clamp with direct force control, in contact with a 150 × 50 × 3 mm 7075-T6 aluminium plate, to a 600 count (73.26 N) step input. 112
5.8 Transient response of a PMAC actuator-based active clamp with direct force control, in contact with a 150 × 50 × 3 mm 7075-T6 aluminium plate, to a train of ascending and descending 600 count (73.26 N) steps. 113
5.9 Step response and Bode diagram of the force sensor amplifier with the low-pass filter turned on ($F_c = 10000$ Hz). 121
5.10 Simplified block diagram of the fixture-workpiece system. $C(s)$ is the resultant transfer function of the PID controller and the DAC, $\mathbf{D}(s)$ is the transfer function of the coupled actuator-workpiece system, and $H_{fb}(s)$ is the resultant transfer function of the amplifier and the ADC. 122
5.11 Response of the fixture-workpiece system with different controller parameters, to a 600 count force command input. From top: Actuator force output, angular velocity of the actuator motor axis, angular position of actuator motor axis, displacement of the midpoint (connecting point) of plate. . . . 126
5.12 Frequency response of the force output of fixture-workpiece system with different controller parameters, to a force command input. (a) Response magnitude and phase in the 1 to 10^6 rad/s range, (b) A more detailed view of the response magnitude and phase in the 1 to 1000 rad/s range. 127
5.13 Step responses of the experimental and the modelled system, with various controller designs. 132

6.1 Schematic representation of the 1st phase of the Fixture Planning Methodology. Rhomboids signify user inputs, whilst rectangles signify processes. 141
6.2 Schematic representation of the 2nd phase of the fully-active fixture design methodology. Rhomboids signify user inputs, rectangles signify processes and double rectangles refer to the predefined processes of phase 1 and phase 3. 148

6.3 Schematic representation of the 3rd phase of the Fixture Planning Methodology. 153

6.4 Illustrative representation of a five-sided-box-shaped workpiece held by a 3-2-1 fixture with point contacts. The machined area in each case is designated as light grey. The working area of each fixture is designated as dark grey. Locators are marked as L and clamps as C. (a) Optimisation process to be applied on clamp C2. (b) Optimisation process to be applied on clamp C1. 156

6.5 Schematic representation of the overall fully-active fixture planning methodology. 170

6.6 Beam workpiece FEA model. Numbering of the nodes was automatically generated by the FEA software. 171

6.7 Concentrated constant moving load and the reactions it induces to the nodes of the beam workpiece. 173

6.8 Dynamic response of the midpoint of the beam to a moving constant and concentrated load of 100 N magnitude. Left: Steady-state response. Right: Full dynamic response. 174

6.9 Displacement of the workpiece at the point of the cutting tool, when the fixture element is positioned at (a) nodes 3 and 4 and (b) nodes 4 and 5. . . 176

6.10 Resultant force at the fixturing element during the manufacturing process. The figure reflects all positions that the fixel occupies during the discretely-moving-fixel strategy. 177

7.1 Schematic representation of the geometric model of thin-plate workpiece. The spring and damper, shown in the side and top views, represent a passive fixture element. The position of the passive element constitutes the initial solution for the optimisation step of the fixture design methodology, applied on the thin-plate test case (Section 7.2.3). Key points on the surface of the plate are highlighted. All coordinates are expressed in millimetres. 182

7.2 Transverse elastic deformation of the workpiece, as the cutting tool traverses the plate, as predicted by the fixture-workpiece model. A single clamping element positioned at P1 (Figure 7.1) is used. The applied clamping force is 20 N 189

7.3 Transverse elastic deformation of the workpiece, as the cutting tool traverses the plate, after the optimisation phase of the design methodology has been applied. A single clamping element is positioned at point P2, as shown in Figure 7.1. 190

7.4 Elastic deformation of the point of contact between locator and workpiece (P2), as the load traverses the plate. (a) Full time history and (b) a closer look at $t = 0 \div 0.1$ s, where the resultant force is closer to violating the minimum force criterion. 191

7.5 Transverse elastic deformation of the workpiece, as the cutting tool traverses the plate, after the optimisation phase of the design methodology has been applied. The clamping element moves, in discrete steps, from point P3 to point P6, as presented in Figure 7.1. 193

7.6 Comparison of the elastic deformation of the thin-plate workpiece at $Y =$ 25 mm, for different positions of the fixture element. (a) The cases where the fixture element is at P3 and at P4. (b) The cases where the fixture element is at P4 and at P2. (c) The cases where the fixture element is at P2 and at P5. (d) The cases where the fixture element is at P5 and at P6. These graphs are used for determining the time instants, when the fixture element needs to change positions, during the discrete-moving-fixel case. 194

7.7 The resultant force on the fixture element at two positions during the discrete-moving-fixture-element case. (a) Resultant force on the fixel while it is positioned at P3. (b) Resultant force on the fixel while it is positioned at P4. 195

7.8 Transverse elastic deformation of the thin-plate workpiece, at various points on its surface, with $Y = 0$, $Y = 10$, and $Y = 25$, as the cutting tool traverses the plate, after the optimisation phase of the design methodology has been applied. The clamping element moves continuously, following exactly the movement, of the tool. 196

7.9 The resultant force on the fixture element as it traverses the plate, continuously following the motion of the tool. 197

7.10 Picture of the fully-active fixture used for the experimental verification of the design methodology. The fixture comprises a single clamping element that can operate in both passive and active modes. The position of the element on the linear guides is controlled by the LGME actuator. 198

7.11 The two active element tips used for the fully active fixture. (a) A normal point-contact fixture tip that is used when the active elements maintain their position or change it in a discrete fashion. (b) A rolling point-contact tip enabling constant movement of the active elements with the need to disengage the workpiece surface. 200

7.12 Schematic representation of the control architecture of the fully-active fixture used during the experiments. 203

7.13 Drawing of the rectangular thin-plate workpiece. All dimensions are in mm. The thickness of the plate is $h = 3.17$ mm. The shaded areas with four through-holes designate the parts of the workpiece that are used for clamping. 203

7.14 The frequency response plot of the aluminium 6068 test workpiece. (a) Response magnitude in dB. (b) Response phase in degrees. 206

7.15 The workpiece baseplate with the thin-plate workpiece. Some of the most important features are highlighted in this photograph. 207

7.16 The frequency response of the workpiece baseplate. (a) Response of the baseplate when excited at the turret with the accelerometer. (b) Response of the baseplate when excited at the turret without the accelerometer. . . . 209

7.17 A view of the experimental set-up and equipment. The controlling hardware arrangement is shown positioned next to the machine tool. 210

7.18 The fully-active fixture with one transport component and one active clamp, positioned on the bed of the Hurco VM1 machining centre. 210

7.19 A typical surface profile of the aluminium 7075-T6 thin-plate workpieces. Obtained at $Y = 5$ mm and from $X = 35$ mm to $X = 115$ mm on the surface of a thin-plate workpiece that is to be machined. 213

7.20 Surface measurement results for the fixturing scenario, where a passive clamp ($F_c = 20$ N) is constantly positioned at P1 with coordinates $(X, Y) = (75, 25)$, as shown in Figure 7.1. 215

7.21 Three-dimensional representation of the measured surface profile of a thin-walled workpiece machined under the fixturing scenario where a passive clamp ($F_c = 20$) N is positioned at P1 with coordinates $(X, Y) = (75, 25)$. . 215

7.22 Surface measurement results for the fixturing scenario, where a passive clamp ($F_c = 20$ N) is constantly positioned at P2 with coordinates $(X, Y) = (75, 10)$. This is the point that was indicated after the application of the methodology on the thin-plate test case, and when a static fixture layout was assumed. 216

7.23 Three-dimensional representation of the measured surface profile of a thin-plate workpiece machined under the fixturing scenario, where the passive clamp ($F_c = 20$) N is positioned at P2 $(X, Y) = (75, 10)$. 216

7.24 Surface measurement results for the fixturing scenario, where a passive clamp ($F_c = 20$ N) is moving along the surface of the plate in a discrete manner occupying five points, as shown in Table 7.8. 218

7.25 Three-dimensional representation of the measured surface profile of a thin-plate workpiece machined under the fixturing scenario, where the passive clamp ($F_c = 20$) N moves in a discrete manner, occupying the five points that were suggested by the fully-active fixture design methodology (see Table 7.8). 218

7.26 Surface measurement results for the fixturing scenario, where a passive clamp ($F_c = 20$ N) is moving along with the cutting tool. The path of the fixture element is a straight line with Y-coordinate $Y = 10$ mm. 219

7.27 Three dimensional representation of the measured surface profile of a thin-plate workpiece machined under the fixturing scenario, where the passive clamp ($F_c = 20$) N is continuously moving, following the motion of tool. . . 219

7.28 Surface measurement results for the fixturing scenario, where an active clamp ($F_c = 20$ N) is constantly positioned at P2 with coordinates $(X, Y) = (75, 10)$. 220

7.29 Three-dimensional representation of the measured surface profile of a thin-plate workpiece machined under the fixturing scenario, where an active clamp ($F_c = 20$) N is positioned at P2 $(X, Y) = (75, 10)$. 220

7.30 Surface measurement results for the fixturing scenario, where an active clamp ($F_c = 20$ N) is moving along with the cutting tool. The path of the fixture element is a straight line with coordinate $Y = 10$ mm. 221

7.31 Three-dimensional representation of the measured surface profile of a thin-plate workpiece machined under the fixturing scenario, where an active clamp ($F_c = 20$) N is continuously moving, following the motion of tool. . . 222

A.1 Graphical Representation of a simply supported beam subjected to a static load. 258

A.2 Response of the midpoint of a simple supported beam excited by a moving constant load, under different speed cases (a) as calculated using Equations (A.7) and (A.9) and (b) as presented in [52]. In this figure α designates ratio of load speed to critical speed, β refers to damping, $T = ct/l$ is the time period necessary for the load to travel one full length of the beam. . . 259

List of Tables

2.1 Characteristics of fixtures compared to other work-holding devices. Based on [96]. 11

3.1 Physical properties of the selected plate workpiece. 44

4.1 Natural frequencies of an aluminium SFSF plate with $\phi = 1/3$ [57]. Values shown in Hertz (Hz). 65

4.2 Comparison of results from the investigated element types against the set performance indicators. SFSF Case. 67

4.3 Natural frequencies of a thin plate with SFSF boundary conditions as predicted using S3 finite elements. 68

4.4 Comparison of results from the investigated element types against selected performance indicators. CFCF case. 69

4.5 Comparison of transverse displacement of a SFSF plate excited by a distributed load of 12 N/mm applied from $x = 0$ to $x = 25$ mm. The load traverses the length of the plate at 33 mm/sec. Results from Kirchhoff plate theory are denoted as PT and from FEA as S4 or S3, depending on the elements used. Displacement values measured at $t = 1.515$ s, i.e. when the moving load is at $x = 50$ mm. The % differences calculated via Equation (4.3). Coordinate values are in mm and displacement values are in μm. 79

4.6 Statistical comparison of results from transverse elastic deformation of a SFSF plate. 79

4.9 Definition of input variables, state variables and output variable 94

4.10 Numerical values of the variables of active clamp-plate model. 97

5.1 Comparison of the response characteristics of the system using the control strategy proposed by Mannan and Sollie [83] and the control strategy proposed by thus study. 113
5.3 Controller parameter settings according to the Ziegler-Nichols ultimate sensitivity method, based on data from [50]. 124
5.4 Controller parameters after applying the Ziegler-Nichols ultimate sensitivity method. 124
5.5 Comparison between the time-response characteristics of the comprehensive fixture-workpiece system model under different controller parameters, and the manually tuned PI controller of the experimental fixture-workpiece system. 128
5.6 Comparison of the time response performance between the experimental and the modelled system. 133
5.7 Comparison of the time response performance between the experimentally-deployed PI and the theoretical Ziegler-Nichols-tuned PID controllers. . . . 134

6.1 Maximum transverse displacement of planar beam workpiece under various static fixture scenarios. 174
6.2 Comparison of static and fully-active fixturing strategies. 177

7.1 Mechanical properties of aluminium 7075-T6. 182
7.2 Summary of maximum elastic deformation reduction, as the direct result of the application of the fully-active fixture design methodology on a thin-plate workpiece test case. A passive fixture element is assumed. 197
7.3 The first five natural frequencies of the thin-plate aluminium 6068 workpiece extracted using different methods. Experimental and FE-based results are compared. 205
7.4 The first three natural frequencies of the thin-plate aluminium 7075-T6 workpiece extracted using FE-based calculations and experimental modal analysis. 206
7.5 Cutting process parameters. 209
7.6 The parameters of the fixturing scenarios used during the experiments. . . 211

7.7 Detailed results from the surface characteristics analysis. Bold letters and numbers indicate measurement results that were obtained from machined plates, the profile of which is also presented graphically. 214
7.8 Cutting process parameters. 217
7.9 Statistical comparison of surface measurement results. Results shown are in comparison to the static, passive clamp at P2 fixturing strategy (Eq. (7.6)). 223
7.10 Statistical comparison of surface measurement results. Results shown are in comparison to the passive and continuously moving clamp strategy (Eq. (7.7)). Positive values indicate a reduction, whilst negative values indicate an increase, compared to the passive continuously-moving clamp strategy. 223
7.11 Statistical comparison of experimental results and the percentile reduction in the maximum elastic deformation of the plate, as predicted by the fully-active fixture design methodology, when applied on the thin-plate test case. Results shown are in comparison to the fixturing strategy where a static and passive clamp is positioned at point P2 $(X, Y) = (75, 10)$ of the plate. . . . 227

A.1 Comparison between natural frequencies of the aluminum plate with $\phi = 1/3$ calculated using beam theory and Kirchhoff plate theory [57]. Values in Hz. 255
A.3 Comparison of transverse deflection between a simply supported beam and a simply supported plate (values from $y = 25$ mm) under a 300 N moving load ($c = 33$ mm/s). All displacement values in μm. 260
A.4 Comparison of transverse deflection of a simply supported beam under a 300 N static load, applied at different positions along the span of a beam and the same beam under a slow moving 300 N load ($c = 0.1$ mm/s). All displacement values in μm. 260

B.1 Natural frequencies of a thin plate with SFSF boundary conditions as predicted using (a) S4 finite elements (341 nodes) and (b) S4R finite elements (341 nodes). Values in Hz. 261
B.2 Natural frequencies of a thin plate with SFSF boundary conditions as predicted using (a) S8R finite elements (981 nodes) and (b) S3 finite elements (341 nodes). Values in Hz. 262

B.3 Natural frequencies of a thin plate with SFSF boundary conditions as predicted using (a) STRI65 finite elements (7701 Nodes) and (b) C3D8 finite elements (7904 Nodes). Values in Hz. 262

B.4 Natural frequencies of a thin plate with SFSF boundary conditions as predicted using (a) C3D8R finite elements (7904 Nodes) and (b) C3D20 finite elements (4947 Nodes). Values in Hz. 263

B.5 Natural frequencies of a thin plate with SFSF boundary conditions as predicted using (a) C3D20R finite elements (4947 Nodes) and (b) C3D15 finite elements (6812 Nodes). Values in Hz. 263

B.6 Natural frequencies of a thin plate with SFSF boundary conditions as predicted using (a) SC8R finite elements (1500 Nodes) and (b) SC6R finite elements (1504 Nodes). Values in Hz. 264

B.7 Natural frequencies of a thin plate with CFCF boundary conditions as predicted using (a) S4 finite elements (341 Nodes) and (b) S3 finite elements (341 Nodes). Values in Hz. 264

B.8 Natural frequencies of a thin plate with CFCF boundary conditions as predicted using (a) SC8R finite elements (1500 Nodes) and (b) C3D20 finite elements (4947 Nodes). Values in Hz. 265

C.1 Elastic deformation of a SFSF plate at time $t = 0.1515$ s - S4 Elements. . . 267

C.2 Elastic deformation of a SFSF plate at time $t = 0.7575$ s - S4 Elements. . . 268

C.3 Elastic deformation of a SFSF plate at time $t = 1.515$ s - S4 Elements. . . . 268

C.4 Elastic deformation of a SFSF plate at time $t = 2.272$ s - S4 Elements. . . . 269

C.5 Elastic deformation of a SFSF plate at time $t = 0.1515$ s - S3 Elements. . . 270

C.6 Elastic deformation of a SFSF plate at time $t = 0.7575$ s - S3 Elements. . . 271

C.7 Elastic deformation of a SFSF plate at time $t = 1.515$ s - S3 Elements. . . . 271

C.8 Elastic deformation of a SFSF plate at time $t = 2.272$ s - S3 Elements. . . . 272

List of Symbols

Latin Symbols

$[0]$	zero matrix	[-]
A	generic numerical constant	[-]
$[C]$, $[C_w]$	damping matrix of the workpiece	[-]
$[C_C]$	damping matrix of coupled system	[-]
C	capacitance of an RC low-pass filter	[F]
$C\,(s)$	combined transfer function of PID controller and DAC	[V/counts]
$C_{PID}\,(s)$	transfer function of a PID controller	[-]
C_f	capacitance of the low-pass filter of the force-sensor amplifier	[F]
C_g	capacitance of a range capacitor	[F]
D	bending stiffness (flexural rigidity) of a plate	[Nm]
$\mathbf{D}\,(s)$	transfer function of the MIMO open-loop actuator-workpiece model	[-]
E	Young's modulus of elasticity	[Pa]
$[F]$	state-space model system matrix	[-]
F_A	actuator force	[N]
F_c	cut-off frequency of low-pass filter	[Hz]
F_e	reaction force from spring and damper element	[N]
$F_k(t)$	resultant force in the direction of fixture element k at time t	[N]
F_{max}	maximum required actuator force	[N]

F_{sl}	user defined force safety limit	[N]
F_r	force reference value	[N]
$[G]$	state-space model input matrix	[-]
G_{ac}	gain of transconductance amplifier	[A/V]
G_{mc}	gain of the motion controller	[V/counts]
G_{rr}	gearing ratio	[-]
$[H]$	state-space model output matrix	[-]
$H_{ADC}(s)$	transfer function of the analogue-to-digital converter	[counts/V]
$H_{DAC}(s)$	transfer function of the digital-to-analogue converter	[V/counts]
$H_{af}(s)$	transfer function of the low-pass filter in the force-sensor amplifier	[-]
$H_{amp}(s)$	transfer function force-sensor amplifier	[V/N]
$H_{(i,j)}(s)$	transfer function of input i to output j of the forward path of the closed-loop fixture-workpiece model	[-]
$\mathbf{H}_{sys}(s)$	transfer function of the closed-loop fixture-workpiece system model	[-]
$H_{sys_{(i,j)}}(s)$	transfer function of input i to output j of the closed-loop fixture-workpiece system model	[-]
$[I]$	unit matrix	[-]
I_{in}	input current to a low-pass filter	[A]
I_m	motor input current	[A]
I_{out}	current output from the low-pass filter	[A]
$[J]$	state-space model direct transmission term matrix	[-]
J_{tot}	total moment of inertia of rotating components of the actuator	[kgm^2]
$[K]$, $[K_w]$	stiffness matrix of the workpiece	[-]
$[K_C]$	stiffness matrix of coupled system	[-]

K_D	derivative gain of a PID controller	[-]
K_I	integrative gain of a PI or PID controller	[-]
K_T	motor torque constant	[Nm/A]
K_{emf}	electromotive force coefficient	[Vs/rad]
K_p	proportional gain of a P, PI, or PID controller	[-]
L_m	motor armature inductance	[H]
$[M]$, $[M_w]$	mass matrix of the workpiece	[-]
$[M_C]$	mass matrix of coupled system	[-]
M	concentrated mass	[kg]
N_i	Shape function of a finite element, $i = 1 \ldots 4$	[-]
P	constant load amplitude	[N]
$P(t)$	load amplitude at time t	[N]
Q	charge produced by a PZT force sensor	[C]
Q_s	charge sensitivity	[C/N]
R	resistance of an RC low-pass filter	[Ω]
R_a	average surface roughness	[μm]
R_f	resistance of the low-pass filter of the force-sensor amplifier	[Ω]
R_m	motor armature resistance	Ω
R_z	maximum surface profile height	[μm]
$R_{z\mathrm{JIS}}$	Japanese industrial standard ten point average surface roughness	[μm]
$[S_C]$	coupled actuator-workpiece model - system of equations in matrix form	[-]
$[S_{ac}]$	actuator - system of equations in matrix form	[-]
$[S_w]$	workpiece - system of equations in matrix form	[-]
T_e	external torque	[Nm]
V_{cc}	control voltage applied to the actuator controller	[V]

V_{in}	input voltage to a low-pass filter	[A]
V_m	motor input voltage	[V]
V_{out}	voltage output from the low-pass filter	[V]
$W(i,j,t)$	two-dimensional Fourier finite sine transformation of $w(x,y,t)$	[-]
X	X-axis or coordinate	[m]
Y	Y-axis or coordinate	[m]
Z	Z-axis or coordinate	[m]
c	traversing velocity of a moving load	[m/s]
c_c	contact damping coefficient	[Ns/m]
c_{cr}	critical damping	[Ns/m]
c_i	damping coefficients of damping element i	[Ns/m]
c_s	damping coefficient of a single-degree-of-freedom system	[Ns/m]
d	number of degrees of freedom per node	[-]
dt	time increment	[s]
e	Euler's number	[-]
$\{f_C\}$	force vector of coupled system	[-]
$\{f_w\}$	force vector of discretised model	[-]
f_i	nodal force along the i^{th} degree of freedom	[N]
$f_i^{(s)}(t)$	for $i = 1, 3$: shear nodal force on a node of element s, at time t	[N]
	for $i = 2, 4$: nodal moment on a node of a element s, at time t	[Nm]
f_r	viscous damping coefficient of motor	[Nm s/rad]
h	plate (workpiece) thickness	[m]
k_c	contact stiffness coefficient	[N/m]
k_i	stiffness coefficient of spring element i	[N/m]

k_{ij}	stiffness matrix element (i^{th} row, j^{th} column)	[N/m]
k_s	stiffness coefficient of a single-degree-of-freedom system	[N/m]
l	length of a finite element	[m]
l_x	length of a plate	[m]
l_y	width of a plate	[m]
m_s	mass of a single-degree-of-freedom system	[kg]
n	number of nodes	[-]
p	actuator ball-screw pitch	[m/rev]
$p(x, y, t)$	external load applied at point (x, y) at time t	[N]
q	modal coordinates	[-]
s	Laplace variable	[-]
t	time	[s]
$\{u_C\}$	vector of degrees of freedom of the coupled system	[-]
$\{\mathrm{u}_i\}$	vector of state-space model inputs	[-]
$\{u_w\}$	vector of degrees of freedom of discretised model	[-]
u	distance of the load from the node through which a load enters a finite element	[m]
u_{in}	command input to the closed-loop system	[counts]
$w_{(j)}(y)$	function that satisfies the boundary conditions	[-]
$w(x, y, t)$	transverse displacement of plate at point (x, y) at time t	[m]
$\{\mathrm{x}_i\}$	vector of state variables	[-]
x	displacement along the x-axis	[mm]
x_A	displacement of the actuator tip	[m]
x_M	displacement of mass M	[m]
$\{\mathrm{y}_i\}$	vector of state-space model outputs	[-]
y	displacement along the y-axis	[mm]
z	displacement along the z-axis	[mm]

Greek Symbols

$[\Delta C]$	added subsystem damping matrix	[Ns/m]
$[\Delta K]$	added subsystem stiffness matrix	[N/m]
$[\Delta M]$	added subsystem mass matrix	[kg]
$[\Psi]$	unscaled mode-shape matrix	[-]
$[\Phi]$	mass-normalised mode-shape matrix	[-]
Δx, Δy, Δz	elastic deformation in the three Cartesian coordinates	[m]
α	constant of the mass matrix contribution in the proportional damping formula	[s^{-1}]
α_{jk}	individual frequency response function (FRF) interrelating the response of degree of freedom j to an input at degree of freedom k	[-]
β	constant of the stiffness matrix contribution in the proportional damping formula	[s]
β_ν	damping coefficient of PMAC controller	[-]
δ	Dirac function	[-]
ζ_r	damping ratio of mode shape r	[-]
η	a line parallel to the x-axis	[-]
η_2	reverse efficiency coefficient of ball-screw	[-]
η_r	structural damping loss factor for mode r	[-]
θ	angular displacement of motor	[rad]
λ, ω_r^2	eigenvalue	[-]
μ	mass per unit area	[kg/m^2]
ν	Poisson's ratio	[-]
π	mathematical constant pi	[-]
ρ	density	[kg/m^3]

τ	time instant within the time t	[s]
ϕ	width-to-length ratio	[-]
$\{\phi_r\}$	mass-normalised eigenvector corresponding to eigenvalue r	[-]
$\{\psi_r\}$	unscaled eigenvector corresponding to eigenvalue r	[-]
ω	excitation frequency	[rad/s]
$\omega_{(i,j)}$	natural frequency of plate with a mode shape that exhibits i half-sine waves along the x-direction and j half-sine waves along the y-direction of a plate	[rad/s]
ω_r	r^{th} natural frequency	[rad/s]
ω_ν	bandwidth of the controller	[Hz]

List of Abbreviations

2D:	Two-Dimensional
3D:	Three-Dimensional
AC:	Alternating Current
ADC:	Analogue-to-Digital Converter
AFD:	Automated Fixture Design
ARMA:	Autoregressive-Moving Average model
CAD:	Computer-Aided Design
CAFD:	Computer-Aided Fixture Design
CFCF:	Clamped-Free-Clamped-Free boundary conditions
CMM:	Coordinate Measurement Machine
CNC:	Computer Numerically-Controlled
DAC:	Digital-to-Analogue Converter
DADS:	Dynamic Analysis and Design System
DC:	Direct Current
DOF:	Degrees-of-Freedom
FE:	Finite Element
FEA:	Finite Element Analysis
FEM:	Finite Element Method

FFFF:	Free-Free-Free-Free boundary conditions
FMS:	Flexible Manufacturing System
FNS:	Fixel Nodes Set
FRF:	Frequency Response Function
FXLMS:	Filtered Input Least-Mean Squares
GMV:	Generalised Minimum Variance
HMI:	Human-Machine Interface
HP:	High Pressure rotor
LGME:	Linear-Guide-Motion-Enabling actuators
LS:	Least Squares
MFS:	Modular Fixturing System
MIMO:	Multi-Input-Multi-Output
NC:	Numerically-Controlled
NGV:	Nozzle Guide Vain
ODE:	Ordinary Differential Equation
OEM:	Original Equipment Manufacturer
P:	Proportional controller
PCI:	Peripheral Component Interconnect bus
PI:	Proportional, Integrative controller
PID:	Proportional, Integrative, Derivative controller
PMAC:	Permanent Magnet Alternating Current motor
PMSM:	Permanent Magnet Synchronous Motor
PZT:	Piezoelectric Transducer

RFPE: Reference Free Part Encapsulation

SDA: Translational Spring Damper Actuator element

SFSF: Simply Supported-Free-Simply Supported-Free boundary conditions

SISO: Single-Input-Single-Output model

SNS: Solution Nodes Set

TSDA: Translational Spring-Damper-Actuator elements

ZN: Ziegler-Nichols tuning method

Chapter 1

Introduction

1.1 Background and Motivation

The advent of computer numerically-controlled (CNC) machine tools and machining centres, in combination with the infiltration of information technologies and the advance of computer science in manufacturing environments, have triggered a paradigm shift from mass manufacturing to mass customisation. Modern manufacturing systems are called to produce large numbers of small-sized batches of different products, or different product variants, in a cost efficient manner. At the same time, the quality of the product must be maintained high in order to remain competitive. The automotive manufacturing sector is perhaps the most prominent example of this trend, with some manufacturers offering such customisation abilities that each model can have more than 1000 different variants.

In order for contemporary manufacturing industries to be able to competitively output their final products and maintain a prominent position in the global market, they need to invest in flexibility and product quality. Flexibility is a measure of how responsive to changes a production environments really is. A series of flexibility characteristics, as described by [26], outline the behaviour that manufacturing environments need to display:

- Machine flexibility, the ease of making changes required to produce a given set of part types.
- Process flexibility, the ability to produce a given set of part types, possibly using different materials, in different ways.
- Product flexibility, the ability to change over to produce new (set of) products very

economically and quickly.

- Routing flexibility, the ability to handle breakdowns and to continue producing a given set of part types.
- Volume flexibility, the ability to operate profitably at different production volumes.
- Expansion flexibility, the ability to expand the system easily and in a modular fashion.
- Operation flexibility, the ability to interchange the ordering of several operations for each part type.
- Production flexibility, the universe of part types that the manufacturing system can produce.

On the other hand, increasing the quality of the made products requires the use of specialised equipment that ensures minimal deviation from the designed attributes. As a result of the above, research and development activities in the manufacturing sector have focused on investigating and developing technologies and equipment that constantly push the boundaries of flexibility and cycle times, whilst minimising production costs without the loss of quality of the end result. Fixtures are an integral part of manufacturing systems and, as such, they have received considerable research attention.

Fixtures are devices that are designed to repeatedly and accurately locate the processed workpiece in a desired position and orientation, and securely hold it in that location throughout the manufacturing process. These work-holding devices are composed of three main elements:

Locators: These are critical elements with no actuation ability, used to locate the workpiece in a desired position and orientation.

Clamps: These are critical elements with actuation ability, used to apply the forces that securely hold (clamp) the workpiece in its position.

Supports: These are optional elements with no actuation ability, used to improve the performance of the fixture by reducing the elastic deformations experienced by the workpiece during the manufacturing process and improve the stability of the fixture-workpiece system.

Traditionally, passive and purely mechanical devices, fixtures are regarded as one of the most important aspects in the manufacturing chain that greatly affect the production cycle times and the quality of the final product. Furthermore, the capital investment for fixtures could constitute a large part of the overall cost of the production process. Indicatively, Bi and Zhang [17] state that fixtures might occupy up to $10 \div 20\%$ of the total cost of a Flexible Manufacturing System (FMS). However, the adoption of appropriate fixturing technologies, for example modular fixturing systems (MFS) over dedicated fixtures, could reduce fixture manufacturing time by 90%, lead time by 85%, and fixture manufacturing costs by 80% [144].

As fixtures are in immediate contact with the workpiece, they affect the result of the manufacturing process in two ways. First of all, incorrect workpiece localisation due to positional and dimensional deviations of the locating elements, and/or deformation due to over-clamping and slippage during clamping, could lead to significant deviations from the nominal dimensions and the form of the workpiece. Additionally, the dynamic nature of loads, like machining forces, set the workpiece in vibration, which, if not treated properly, could lead to increased surface roughness and loss of contact between the fixture and the part. The results of such phenomena are reduced product quality, catastrophic damage to the workpiece or the machine tool, and even serious injury to the operator.

The effects of fixtures on the end result of a manufacturing process are more prominent in the case of thin-walled low-rigidity components. Such components can be found in virtually any industrial sector, and especially in the aerospace or automotive. Their importance is evermore increasing, as reduction in the weight of the final product translates into increased performance and reduced fuel consumption. Such factors play a pivotal role in the success of a product. Moreover, the maximum gains in terms of weight reduction with limited sacrifice in structural rigidity can be achieved trough monolithic parts, i.e. parts stemming from a single block of raw material that do not need assembly to obtain their final design. To manufacture such parts, material removal processes are often preferred, especially when these parts are made of metallic materials.

The above discussion, however, reveals a fundamental issue. In traditional cutting processes, like milling, and when rigid workpieces are machined, the fundamental natural frequency of the workpiece and the excitation frequency from the process lie far apart. This means that the vibration experienced by the workpiece during machining is not significant.

As the weight of the workpieces is reduced, their fundamental natural frequencies are pushed down. On the other hand, as machining times need to be reduced, usually by increasing the tool feed rates and the spindle speed, the workpiece is inevitably excited at higher frequencies. This results in more intense vibration of the workpiece, ultimately leading to the negative effects discussed earlier. Fixtures could play an important role in eliminating these effects.

Many researchers have focused attention in this issue and have attempted to develop models, tools and methodologies that reflect the effect of the fixture on the workpiece response. However, in most cases the fixture-workpiece system is treated as static or pseudo-static. In other cases the workpiece is considered rigid and only the time-varying amplitude of the machining forces is captured. However, as tool traverses the workpiece, machining forces change the areas at which they are applied. This affects the dynamics of the system. Reflecting this, along with the full dynamic response of the fixture-workpiece system is important in order to improve the outcome of manufacturing processes and design better and more efficient fixturing solutions.

Another approach towards improving the dynamic response of fixture-workpiece systems is that of active/adaptive fixtures. This fixturing solution constitutes a para- digm shift and does not approach fixtures as purely mechanical and passive equipment. Active fixtures are work-holding systems with sensor-integrated locators and supports, and clamps that adapt the forces they apply based on the reactions recorded by the sensors. This mechatronic approach on fixturing eliminates the need to design the fixture parameters on a worst-case-scenario basis and leads to the concept of optimal clamping at any given instant. Active fixtures have also been developed to suppress the vibrations experienced by the workpiece during machining. These usually take the form of an active pallet or base-plate, on which passive fixture elements are assembled. Active fixture solutions aim at eliminating the drawbacks of traditional fixturing solutions that could negatively affect the quality of the produced part. Indicatively, active fixturing systems could improve the surface finish by reducing the average surface roughness R_a by up to 41.29% [110] and improve the surface profile of the machined workpiece, as well as enhance fixturing stability [97].

Despite the apparent benefits of active fixtures, their adaptive capabilities have so far only been studied in isolation from the dynamic response of the workpiece. However, the response of the active elements to external stimuli does affect the dynamic response of the

fixture-workpiece system. Therefore, it is important to reflect this interaction in the models, tools and methodologies that are being developed and that target a better understanding and improvements in fixturing solutions.

Moreover, so far, the proposed active fixtures lack the ability to reconfigure. Active fixtures are designed for a single product or, at best, for a small-sized product family. Just as in traditional solutions, the changeover from one fixture or fixture set-up to another, in order to accommodate for a new product, can be a labour- and time-intensive process. This could drastically lengthen the production cycle time and prevent the manufacturing plant from utilising the flexibility of modern CNC machine tools and assembly lines. From a manufacturing perspective, it becomes apparent that the combination of the active fixture and reconfigurable fixture paradigms could greatly benefit industry. Such fixtures, namely ones that can automatically reposition their fixturing elements before and during the manufacturing process, and/or actively adapt the clamping forces they apply on the workpiece, are called fully-active fixtures. The potential positive impact of such fixtures lies beyond the fact that flexibility and adaptivity appear simultaneously in one solution. Fully-active fixtures could lead to new fixturing strategies, where not only the clamping forces are adapted to be optimal at any given instant, but so does the layout of the entire fixture too.

This brief analysis clearly highlights the importance of fixtures on the process outcome and the performance of a production system, especially in the case of thin-walled workpieces. It also underlines the positive impact of active fixtures and the potential of fully-active fixtures. An investigation in the field constitutes the overarching objective of the research work that is described throughout this thesis.

1.2 Research Objectives

This work primarily targets the improvement of the quality of manufactured parts by implementing more efficient and better performing fixturing solutions. The improvement of the dynamic response of the workpiece is treated as the key to improving the quality of the end result. This improvement is sought through the capabilities of fully-active fixtures. In order to support this, it is necessary to develop models and methods that capture and reflect the effects of fully-active fixtures and the manufacturing process on the workpieces,

and especially for thin-walled components. Therefore, the main objectives of this work can be summarised as follows:

- To investigate the performance of new fixturing strategies that stem from the capabilities of fully-active fixtures.
- To develop suitable models that reflect the dynamic response of the fixture-workpiece system under such fixturing strategies.
- To capture within the proposed models the effects of the constantly changing point of application of the dynamic machining forces on the dynamic response of a thin-walled workpiece.
- To identify suitable control algorithms for fully-active fixtures in order to enhance their performance.
- To integrate the adaptive nature of fully-active fixtures in the developed models.
- To establish methods and methodologies that facilitate the design and parameter selection of the fixturing process through fully-active fixtures.
- To develop a prototype fully-active fixture that can be used as the basis of a feasibility study and the validation of the developed models.

The adoption of fully-active fixturing strategies is envisaged to increase the quality and form accuracy of produced parts and to shorten production times through a fixturing approach that is more flexible and more cost-efficient when compared to contemporary fixturing solutions. Furthermore, by integrating the adaptive side of the fixturing elements, the moving and time-varying machining loads and the dynamic response of thin-walled workpieces into a comprehensive model, it is expected to augment the accuracy of the model, rendering it a powerful tool for planning and designing fully-active fixturing solutions. This shall help accelerate the development process and reduce associated costs.

1.3 Thesis Outline

The thesis is split into 8 chapters, including this one. A brief description of the content of each chapter is presented bellow:

Chapter 1 - Introduction. The motivation behind this research work is revealed. Key research objectives and a thesis outline are also presented.

Chapter 2 - Literature Survey. A comprehensive survey of the open literature on the background of the relevant for this work research fields of fixturing. The available results are presented. The knowledge gaps that need to be filled in order to achieve the objectives of this work are discussed.

Chapter 3 - Research Methodology. In this chapter the research objectives are revisited and defined in more detail. The methodology that is followed in order to achieve the set objectives is described, along with the assumptions and limitations that govern the work.

Chapter 4 - Fixture-Workpiece Model. A finite element-based (FE-based) structural dynamics modelling approach of a thin-walled workpiece is introduced. Appropriate finite elements are selected. A method to include the moving nature of machining loads is presented and proven analytically. Finally, the modelling method for the active fixture elements is presented. This chapter focuses only on the uncontrolled or open-loop response of the active elements. Finally, the coupling of the various sub-models, i.e. workpiece and fixture elements, is described.

Chapter 5 - Active-Clamp Control Strategy. Various closed-loop control architectures to control the forces applied from the active elements of active and fully-active fixtures are introduced, explained and evaluated. The best performing architecture is modelled and introduced into the fixture-workpiece model, producing its final and comprehensive version.

Chapter 6 - Fully-Active Fixture Design Methodology. A design methodology that is primarily based on the developments of Chapters 4 and 5 is proposed and explained in detail. The methodology is applied on a simplified test case, involving a thin beam workpiece and a fully-active fixture with passive elements.

Chapter 7 - Verification of the Fully-Active Fixture Design Methodology. A prototype fully-active fixture system that is used as the backbone of the experimental process is presented. The research methodology presented in Chapter 6 is applied on a

thin-walled plate workpiece. A series of experiments is conducted to allow comparisons between simulated and experimental results. The key findings from these experiments and the verification of the developed design methodology are described.

Chapter 8 - Conclusions and Future Work. The main findings from the analysis and experiments, and the key contributions of this research work are summarised. Open issues are discussed and future work to tackle these is proposed.

Chapter 2

Literature Review

2.1 Introduction

Work-holding devices and systems, such as fixtures, are of paramount importance within a manufacturing environment. They exist in virtually any manufacturing environment, instantiated in geometries and layouts that span from a simple vice to a complicated robotic cell. Fixtures possess a prominent position within the work-holding systems family and are mostly used when precise an repeatable localisation of the processed workpiece is required.

As observed in the previous chapter, fixtures can affect the performance of a manufacturing line in two ways. On one hand, the flexibility of the line is largely dictated by the selected fixturing solution. A fixturing system that demands significant effort to be adjusted to accept a new product geometry, could negate the benefits of modern numerically-controlled (NC) machine-tools and automated manufacturing cells.

On the other hand, fixtures, due to their immediate contact with the workpiece largely determine the outcome of the manufacturing process. Geometrical variations in the features of the fixture reduce the localisation accuracy of the workpiece relative to the global coordinate frame of the manufacturing process. This could result in the production of out of tolerance parts. Furthermore, fixtures affect the static and dynamic rigidity of the workpiece. A poorly designed fixture may result in over-clamping and excess vibration. These, in turn, lead to dimensional inaccuracies, reduced surface quality and even separation between the fixture and the workpiece, causing the part to be released, damaging the processing station, halting the production and injuring personnel.

The previous clearly highlight the importance of fixtures. This is why intensive research

efforts have been dedicated to the field of fixtures, especially over the last few decades. This chapter intends to provide a comprehensive review of the these efforts and identify relevant knowledge gaps. Attention is mainly placed on available fixturing solutions and their effects on the dynamic response of thin-walled low-rigidity workpieces, as these are the subjects around which this work revolves.

The chapter commences by giving a brief overview of the basic theory behind fixtures and fixturing practices in Section 2.2. Then, in Section 2.3, various fixture concepts are reviewed. In Section 2.4, modelling methods, which have been applied to capture the dynamics behind the fixture-workpiece systems, and have been implemented to facilitate and augment the fixture-design process, are reviewed. Section 2.5 looks into the strategies that have been proposed for fixtures with adaptive characteristics, often referred to as active fixtures, whilst Section 2.6 deals with the methods that have been proposed to capture the dynamic and moving nature of machining loads. Finally, the knowledge gaps which this literature survey reveals, and which are addressed in this thesis, are outlined and explained in Section 2.7.

2.2 The Basics of Fixturing

A fixture is a device designed to repeatedly and accurately locate a workpiece in a position and orientation, relative to another workpiece or the reference frame of a machine tool or measurement machine. This process is often referred to as localisation. Moreover, fixtures must be able to securely hold the workpiece in the desired location throughout the duration of a manufacturing process. Fixtures can be used in assembly, machining or measurement operations. They belong to the greater family of work-holding devices. They can be identified and differentiated from other work-holding family members through their comprising elements and their functionalities. Some of the most prominent work-holding technologies and their characteristics are presented in Table 2.1. More detailed information can be found in [62, 96]. In general, a fixture comprises three fundamental elements:

Locators: Statically positioned elements with no actuation ability, used to locate the workpiece in a desired position and orientation. A typical fixture has at least 6 locators.

Clamps: Statically positioned elements with actuation ability, used to exert the forces that

securely hold the workpiece in its position. A typical fixture has at least 2 clamps.

Supports: Statically positioned elements with no actuation ability, used to locally reduce the elastic deformations experienced by the workpiece due to the loads applied by the manufacturing process. They can also improve the stability of the fixture-workpiece system. There is no limitation to the number of supporting elements used in fixtures. Contrary to clamps and locators, the existence of supports is not compulsory.

Table 2.1: Characteristics of fixtures compared to other work-holding devices. Based on [96].

	Elements			Functionality	
	Locators	Clamps	Supports	Workpiece Localisation	Tool Localisation
Fixtures	✓	✓	✓	✓	×
Jigs	✓	✓	✓	✓	✓
Vices	✓(1)	✓(1)	×	×	×
Chucks	×	✓(≥ 3)	×	×	×
Grippers	×	✓	×	×	×

Although simple in concept and role, the design of a fixture requires extensive experience and expertise but also imagination and intuition. For this reason, some might state that the design of a fixture is a combination of engineering science and art. Nevertheless, there are some generic guidelines and principles [96] that the designer can use as the springboard for their work. One very important aspect during the design of a fixturing system is the type of contact between the fixture and the workpiece. This is determined by the geometrical characteristics of the tips of the fixturing elements. Point contact exists when the fixture elements present a spherical formation at their tips. Surface contact is possible when the ends of the fixture elements are flat surfaces or when they mimic directly the local geometry of the workpiece. Finally, line contact is feasible when the tip of fixture elements takes the form of a (half-)cylinder.

Perhaps the most commonly used principle in fixturing is the 3-2-1. According to this principle, the designer must identify three major datums on the workpiece, namely the primary, the secondary and the tertiary. The first one is usually the largest flat surface or three points that are as far apart as possible. The normal vector to these points must be the same or very similar. The secondary datum is defined by a flat surface that is perpendicular to the primary datum, or a set of two points with normal vectors perpendicular to the

normal vector of the primary datum. Finally, the tertiary datum is a surface (usually the smallest of all datum surfaces), or a single point, with normal vector perpendicular to both the primary and the secondary datums. Three point contact locators or a surface locator, are used on the primary datum. Two point contact locators or a line contact is used on the secondary datum. Finally, a single point contact is used on the tertiary datum. Once the locating datums are defined, the clamping strategy needs to be determined. A minimum of two clamps are necessary to fully remove any degrees of freedom from the system. Three clamps, one opposite each of the locating datums, are the most common and secure clamping strategy. Careful analysis and experimentation determines the coordinates of the contact points (locators and clamps) or the size of the contact surfaces and lines. Through this analysis, the necessity of supporting elements is also identified.

The previous constitute a brief introduction in the basis of fixturing. Of course, each workpiece, each manufacturing process and each manufacturing environment have their own unique fixturing requirements. This explains the immense research and development efforts that have gone into developing new fixturing concepts and technologies. The most prominent ones are presented briefly through the next paragraph.

2.3 Fixturing Concepts

2.3.1 Dedicated Fixtures

This form of fixturing is perhaps the oldest fixturing solution. They are called dedicated because they are designed for fixturing one specific workpiece and, sometimes, one workpiece for only one stage of the manufacturing process. This lack of flexibility is the main disadvantage of dedicated fixtures. This, in conjunction with their increased cost, renders dedicated fixtures economical only in mass production schemes. When multiple fixtures are used, the inevitable change-over from one fixture to the next during the manufacturing cycle introduces an extra bottleneck and increases the production down-time. Despite these drawbacks, dedicated fixtures are still used in large- and small-batch production sites, where increased accuracy is the prerequisite for the final result.

Research activities concentrate on overcoming the problems and disadvantages of dedicated fixtures. Efforts are therefore focused on developing alternative fixturing concepts or tools that assist the fixture designer and accelerate the design process. Various Computer-

Aided Fixture Design (CAFD) tools [19, 25, 106, 118] and methods [121, 137, 143] for rapid concept generation and verification have been proposed.

2.3.2 Modular Fixtures

Modular fixtures are perhaps the first solution against the drawbacks of dedicated fixtures and maybe the most industrially applicable and flexible fixturing solution available. The concept of modular fixtures dates back to the Second World War and was proposed by John Warton [96]. Modular fixturing systems are fixtures that consist of a number of standard elements, called modules, that can be used in various combinations to create fixture assemblies that can accommodate different workpieces. The modules include various forms of clamps, locators, supports, base plates and connections. An extensive review on modular fixtures can be found in [63, 96].

The main advantage of modular fixtures is that standard elements can be re-used to build a large variety of different set-ups. This renders modular fixtures most appropriate for highly-flexible manufacturing environments, like workshop facilities. Bi and Zhang [17] identify the main shortcoming of fixtures. These are:

- Large original capital investment.
- Large amount of knowledge and time needed for fixture planning. This problem is magnified as the workpiece geometry and the process complexity increases.
- Decreased accuracy stemming from the stacking up of the tolerances of the various elements forming the fixture.
- Reduced capacity for bearing large clamping loads.
- Disability to hold parts with very complicated geometry. The more complicated the geometry the larger the inventory of modules needs to be.
- Efficient scheduling of the utilisation of fixture modules is extremely complicated.

Research activities have concentrated on improving the performance of modular fixtures. In more detail, Automated Fixture Design (AFD) tools and methodologies [54, 58, 64, 120, 129] have been proposed in order to speed up the planning phase and increase the efficiency of fixture module utilisation. Modular fixture assembly through external machinery [74,

100, 122, 123] has also received significant attention. The goal of such work is to consolidate the knowledge and expertise of operators in a computer environment, which can then be utilised by a robotic assembly station to complete the assmby of the fixture. The desired result is the speeding-up of the assembly process, which in turn positively affects the change-over time and down-time within a manufacturing system. Finally, new modular fixturing kits have been proposed [58, 119, 122, 123]. These intend to facilitate automated assembly or improve the performance of the modular fixture. An example of such a modular fixture is presented in Figure 2.1. This fixture consists of modules that are assembled on a base-plate that bears unidirectional T-slots. The modules are formed by vertically oriented rods mounted on cross-block with engraved dimensional scales. Both the locators and the clamps possess tiltable heads, however clamps are equipped with an additional clamping mechanism. The position of the modules and their height can be manually adjusted. This fixture is targeted towards thin-walled sheet-like workpieces.

The previously mentioned research fields fall outside the scope of this work and, therefore, will not be discussed further.

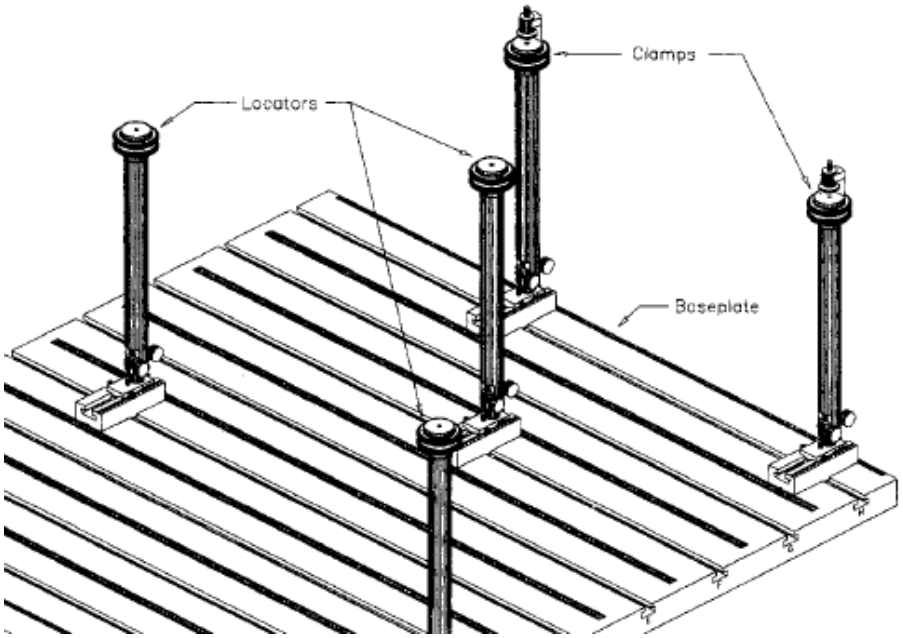

Figure 2.1: Schematic of a modular fixture designed for to improve fixturing performance for thin-walled flexible objects [119].

2.3.3 Phase-Change Fixtures

Another concept of reconfigurable fixtures that has received considerable research attention is based on phase-change materials. The term "phase-change" implies the utilisation of the

transition from one material state to another, usually from liquid to solid. In detail, these fixtures deploy a bed filled with a material, which constitutes the fixturing medium. When the medium is in liquid, or pseudo-liquid state, the workpiece can be inserted and localised. Clamping takes place through solidification of the medium.

The family of phase-change fixtures can be separated into two major groups [55], namely the pseudo-phase-change and the authentic phase-change fixtures. The first group takes advantage of the ability to manipulate the density of sand-like materials in powder or particle form, by introducing a stream of a gas medium through the material bed. When the gas flow is on, the density of the fixturing medium is reduced, creating a pseudo-liquid state. The workpiece can then be easily introduced into the fixture. When the gas flow ceases,the fixturing medium is returned to its original, solid state, firmly holding the part. These fixtures are known as Fluidized Bed fixtures [56, 96, 134] or Particulate Bed fixtures [2–6]. In this type of fixtures the workpiece is partially immersed in the medium.

Authentic phase-change fixtures utilise the thermally-induced change of state of low melting point materials, known as fusible or eutectic materials. Thermally induced phase-change is used in the principles of Reference Free Part Encapsulation (RFPE) [7, 75, 76, 117] and Phase-Change Baseplate Fixturing [10]. In RFPE the workpiece is fully immersed in a eutectic material in liquid state. The material is then solidified creating a solid block, which can be localised and machined. During the latter, both the solidified fixturing medium and the workpiece experience material removal. If a set-up change is necessary to machine additional features on the workpiece, the removed fixturing medium is first restored, recreating the original encapsulating block, and then the entire block is repositioned according to the process needs. The new features can then be machined.

The phase-change baseplate fixturing principle is based on a chamber containing a low-melting tempretature alloy, and bearing locating pins. The champer is used to contain the fixturing medium and has features that allow the change of the position of the fixturing pins. When the fixturing medium is in liquid state, the fixture pins can be repositioned to match the geometry of the workpiece, The low-melting temperature alloy is then solidified, securing the pins in place. The workpiece can then be loaded and clamped. The principles behind RFPE and the phase-change baseplate fixturing are shown in Figure 2.2.

Other types of authentic phase-change fixtures are based on electrically-induced phase change. Examples of such fixtures using magnetorheological and electrorheological fluids

as fixturing media are presented in [114] and [68] respectively.

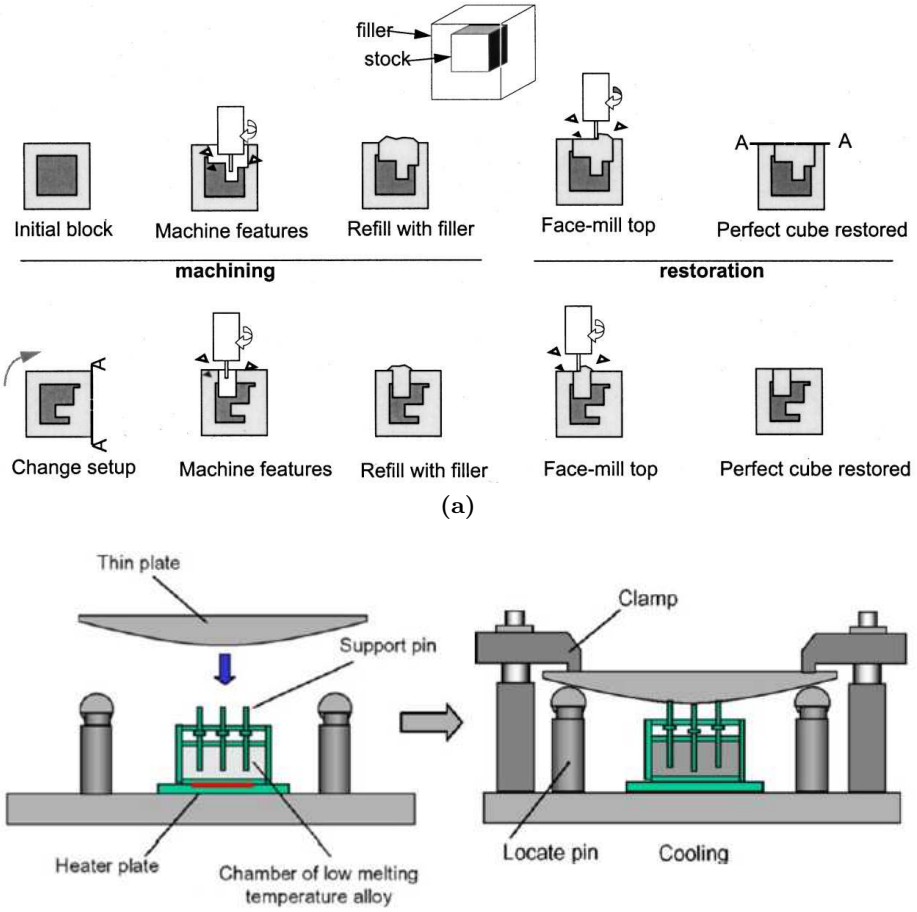

Figure 2.2: (a) The principle of Reference Free Part Encapsulation [76]. (b) The principle of phase-change base plate fixturing [10]

The main advantage of phase-change fixtures is the ability to grasp even the most complex workpieces using simple fixturing devices. Additionally, the RFPE method can produce extremely thin-walled structures with complicated geometries, as the fixture provides maximum support. The need for specialized fixtures for each different process set-up is eliminated. Amongst the disadvantages are the large set-up changeover times and the contamination of the workpiece from the fixturing medium. Finally, the solidification of the fixturing medium can induce displacement of the workpiece from its desired position, leading to uncertainty in the localisation process [9, 10, 117].

2.3.4 Conformable Fixtures

Conformable fixtures is another flexible fixturing solution often met in the literature. They are commonly referred to as pin-array fixtures or pin-type fixtures. In principle, they

comprise a bed of independently adjustable pins that either manually or automatically [66] conform to the surface of the workpiece, providing support and localization to the workpiece. The part is then clamped from the opposing side. The clamping mechanism can vary from a simple structure [124] to another pin-array formation that is pneumatically or hydraulically actuated [8].

Youcef-Toumi and Buitrago [146] have combined the principles of conformable fixtures with that of modular fixtures in an attempt to create an innovative hybrid fixturing solution.

Conformable fixtures have the advantage of evenly distributing the clamping and reaction forces exerted on the workpiece during the manufacturing process. As a result, part deformation is reduced. Additionally, they are able to hold a large group of different and very complicated part geometries. However, the part localization accuracy could be largely inferior compared to other fixturing solutions. Moreover, reconfiguration times can be comparably large in the case of passive pin-array fixturing. This drawback can be partially alleviated by introducing automated actuation of the pins (active pin-array fixtures) [139]. Nevertheless, the need for a separate actuator for each pin significantly increases the necessary capital investment.

A detailed review on conformable fixtures can be found in [90].

2.3.5 Sensor-Integrated Fixtures

These fixturing systems constitute the first step towards adaptive fixtures. They do not strictly constitute a separate category of fixture concepts as they take the form of any of the previously mentioned fixtures. The difference is that they bear sensing elements integrated into their structure. In the vast majority of cases, these elements are used to record clamping, reaction and external forces. However, position sensors have also been used to record workpiece displacement from its desired location.

The first attempt to integrate sensing capabilities into a work-holding device was made by Gupta *et al.* [60]. This work describes the fabrication of a simple vice comprising two V-blocks, one fixed and one movable. A piezoelectric dynamometer was placed on the fixed V-block to measure clamping forces. Another dynamometer, measuring thrust forces and torque from the drilling tool, was placed below the base of the two V-blocks. The recorded data was used to identify the safe and unsafe clamping force regions relatively to spindle speed and feed rate.

Hameed *et al.* [61] investigated the performance of a fixture with uniaxial-force-sensor-integrated elements for accurate monitoring of the cutting forces from milling operations. The goal was to alleviate the need for a multi-axis dynamometers.

De Meter and Hockenberger [38] instrumented a fixture with eddy current displacement sensors to record workpiece displacement from its desired position due to the clamping process. This information was used to compensate the tool path of a milling cutter.

Sensor-integrated fixtures intend to allow the on-line monitoring of key variables, which may affect workpiece and the outcome of the fixturing and/or the manufacturing processes. Such fixtures help in augmenting the operator's understanding of the performance of the fixtures. Recorded information can also be used to adjust the fixturing or processing parameters either on- or off-line. Sensor-integrated fixtures are the basis of numerically-controlled fixtures (see Section 2.3.6) and adaptive fixtures (see Section 2.3.7).

2.3.6 Numerically-Controlled Fixtures

Numerically-controlled (NC) fixtures belong to a category of fixturing concepts that drifts away from the traditional static solutions and moves towards the notion of a gripper. These fixtures are perhaps the first step towards more intelligent solutions. The flexibility here lies within the ability to automatically adjust the layout of the fixture, in order to grasp parts with different geometrical features. Numerically-controlled fixtures are identified by their ability to automatically reposition their locating, clamping or supporting elements.

To the best of the author's knowledge, the first NC fixtures were conceptualised and presented by Tuffentsammer [138]. In this work two NC fixturing principles were presented: the double revolver and the translational movement. The first one can achieve differentiation in fixture element position by using independently actuated revolvers, called the primary and the secondary. The primary revolvers take the form of disks, on which a variable number of secondary revolvers is assembled. Each revolver is able to rotate independently. Secondary revolvers, bear cylindrical-pin formations, which are positioned eccentrically to the revolvers axis of rotation and are able to extend and retract. By combining the movement of the primary and the secondary revolvers, different fixture set-ups are achieved for a variety of processes. Hydraulic linear actuators, which are positioned above the workpiece, are used to apply the required clamping forces.

The translational-movement-based system uses linear motion to achieve the necessary

readjustment of the position of the elements. Just as in the double-revolver concept, this fixture deploys cylindrical-pin formation that can extend and retract to conform to the workpiece geometry. Contrary to the previous concept, however, the clamping elements of this NC fixture are situated at the side of the workpiece and are positioned on slides with vertical orientation.

The two previously mentioned principles are presented schematically in Figure 2.3. These principles have also been used by Lin and Du [44, 79] in their proposals of NC fixturing concepts.

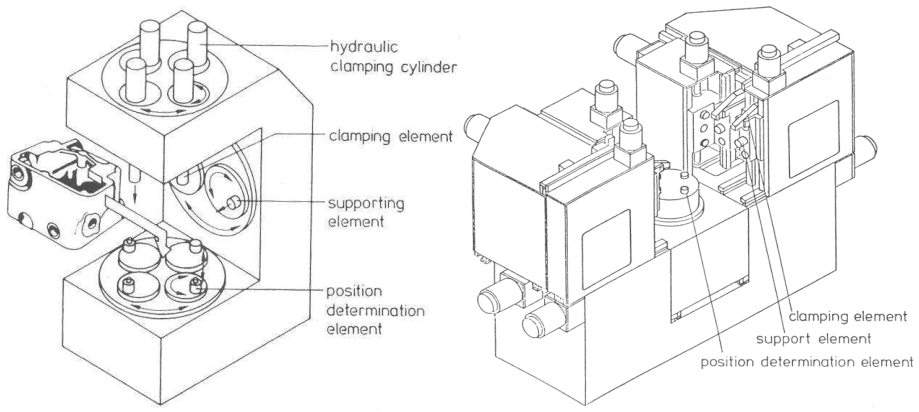

Figure 2.3: Two NC fixturing concept utilising the (a) double revolver and (b) translational movement principles [138]

Chan and Lin [24] proposed an NC fixture with modular structure. Each module is a standalone multi-finger electric-motor-based system. This concept combines the flexibility of modular fixtures with the added ability of automatic (re)configuration.

Kurz *et al.* [72, 73] described an NC fixture for welding processes. This mechanism is based on two hydraulic actuators that are mounted on a stable base via revolute joints. The actuators' piston ends are also joined together via a revolute joint. This layout allows for accurate plane-positioning of the overall mechanism tip. Sensors and microcomputers are responsible for controlling the position of the cylinders.

Lu *et al.* [81] introduced an electric-motor-based, quick action flexible fixture for clamping prismatic parts. The fixturing system is similar to a vice, but each jaw of the vice contains two half-cylinder formations (four in total). Chan *et al.* [23] introduced a modular numerically-controlled fixture consisting of a hole-type baseplate and a series of specially designed modules. These have integrated sensing and communication capabilities. The fixture, designed for assembly processes, has the ability to verify its proper connection with

other modules and the baseplate, sense the presence of a workpiece, extend or contract the camping and locating elements and adapt the clamping forces it applies. Pneumatic and hydraulic actuation is used. The entire fixture is put together by an external robotic manipulator, and is targeted towards assembly operations.

The most recent development on NC fixtures negotiates a concept called Swarm Fixtures. According to Molfino *et al.* [88] such fixtures implement a modular structure. Each module takes the form of a tripod mechanism with a support head that adapts to the local geometry of the workpiece. The base of these modules is moveable. These modules are called 'support agents'. The latter are assembled on a base plate that is designed to allow for the bases of the support agents to move without the need for human intervention. This reconfigurable swarm concept has been primarily developed for thin-walled sheet-like structures.

Numerically-controlled fixtures have the potential to reduce configuration times in reconfigurable fixturing solutions. On the other hand, such fixtures can be bulky, reducing accessibility to the workpiece, and the associated costs can be high.

2.3.7 Active/Adaptive Fixtures

Adaptive fixtures, also referred to as active fixtures, are perhaps the most recent development in fixturing technology. The family of adaptive fixtures includes fixturing systems with elements that can apply variable clamping forces, responding to external stimuli. These fixtures usually deploy clamping elements that incorporate actuation and sensing capabilities, rendering them able to operate in a closed-loop manner. Contrary to NC fixtures, adaptive fixtures are most often not reconfigurable.

The most comprehensive approach to adaptive fixtures thus far originates from a group of researchers at the National University of Singapore. In detail, Nee *et al.* [97, 98] introduced a fixturing system (Figure 2.4) that can adapt the applied clamping force online and they used this to investigate the advantages of the approach. The prototype fixture includes active clamping elements and passive locating elements with integrated force sensors. Each clamping element consists mainly of a direct current (DC) servomotor-based linear actuator, a piezoelectric load washer, and a rotary encoder. This formation allows for maintaining the position of and the forces applied from the clamps. The position and speed of the dynamic clamp are controlled by means of a digital controller, which feeds

back information on the rotational position and speed of the servomotors shaft through the rotary encoder. A schematic of the dynamic clamp is shown in Figure 2.4 (b). Mannan and Sollie [83] presented in detail the control strategy that is used to operate the clamps. Wang *et al.* [140] presented a version of the aforementioned adaptive fixture with hydraulic actuators instead of electromechanical, along with a methodology to calculate off-line the optimal clamping forces that the fixture should apply.

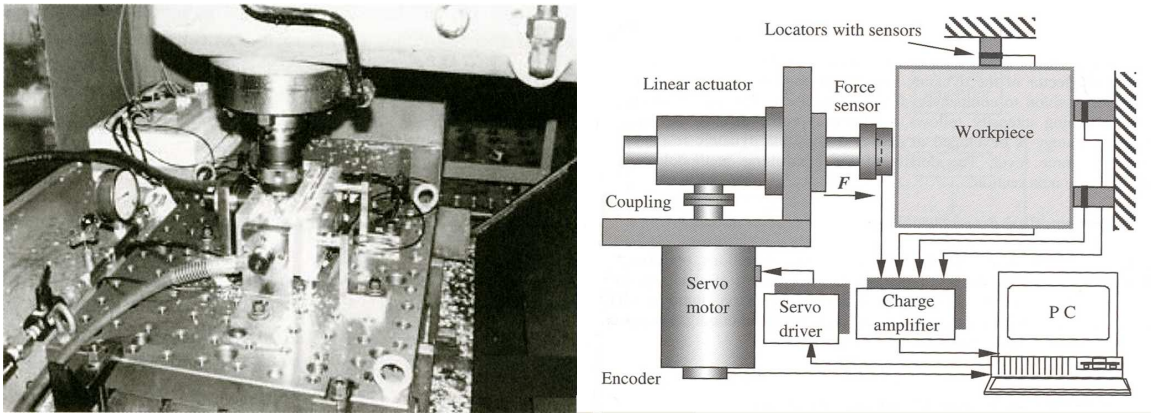

(a) **(b)**

Figure 2.4: The adaptive fixture presented by Nee *et al.* (a) Picture of the developed fixture [98] (b) Schematic of the DC motor-based active clamp and its components [97].

Another example of adaptive fixturing was developed by Chakraborty *et al.* [21, 22]. This fixture uses a Coordinate Measurement Machine (CMM) to probe important features on automotive engine blocks. This information is employed to identify the exact position and orientation of the surfaces to be machined. A micro-positioning base is adopted to reposition the workpiece to its ideal location.

Du *et al.* [45] used a combination of their three-fingered programmable fixture [44] and adaptive control strategies to augment the intelligence of the fixture and grant it adaptive capabilities. The result was a fixture for thin-walled ring-shaped workpieces that can identify the variations in the stiffness of the workpiece and adjust the clamping forces accordingly to reduce deformation. This is the first example where a reconfigurable fixture is granted adaptive capabilities.

Bukowski *et al.* described their take on an active fixturing system in [20]. Their concept utilises stepper motor actuators playing the role of the active fixture clamps. Laser and inductive sensors are used to detect large and small workpiece displacements respectively. Furthermore, the proposed active fixture bears force sensors to monitor the applied clamping forces and vision sensors that allow for establishing the position of the workpiece

relative to the reference frame of the fixture.

Papastathis *et al.* [103] describe the concept of an intelligent fixturing system that incorporates active fixture elements and possesses the additional ability automatically reconfigure. The fixture utilises position and force feedback sources to actively adapt the clamping forces it applies and autonomously change its set-up according the geometry of the workpiece. This approach provides the added capability to change the position of the fixturing elements throughout the manufacturing process. This strategy leads to increased local stiffness of the workpiece around the area where the machining process takes place. A prototype of such a fixturing system has been developed as part of this research work and will be described in more detail in Chapter 3 of this thesis.

Finally, Papastathis *et al.* developed an active fixture for the assembly of the high pressure (HP) rotor of the Trent family of Rolls-Royce aero-engines [102]. The fixture deploys a series of DC-motor and stepper motor-based linear and rotary actuators in a cylindrical formation. The developed fixture uses quadratic encoders as position feedback sources and strain gauges to monitor and control the clamping forces applied by the fixture. Apart from applying varying clamping forces and controlling them to reject external disturbances, the fixture has the ability to autonomously reconfigure. As a result, the same fixture can be used for the assembly of the HP rotor of five different aero-engine types.

Adaptive fixtures present numerous advantages. They offer a better understanding of the effect that fixtures have on the manufacturing process outcome and the possibility to adapt the fixture parameters to optimise the results. In essence, adaptive fixtures aim at eliminating the errors caused by the fixturing process and affect the quality of the end-result. In some cases, reconfigurability has been combined with adaptiveness to produce a flexible and highly-performing solution. The drawback of adaptive fixtures is the increased cost associated with the sensory and actuation equipment necessary.

2.3.8 Pallet Fixtures

Although, strictly speaking, pallet fixtures are not a distinct fixturing solution, a lot of interesting work has been carried out in this field. Therefore, they deserve a special mention. The term pallet fixture can be used for any of the previously mentioned fixturing technologies, so long as the fixture lies on a base-plate that is not permanently mounted on a surface. On the contrary, the fixture base-plate can be moved from one processing station

to another. Such base-plates, referred to as pallets, bear special locating formations that allow them to be mounted on the bed of a processing station without the need of referencing the fixture to the reference frame of the station. Fixtures can be assembled off-line and introduced with ease in the manufacturing line. Also, the change-over from one fixturing set-up to another is similarly straightforward. The concept of palletised fixtures is very old and has been widely adopted by industry.

In the last decade, pallet fixtures with adaptive capabilities have been presented. Rashid and Nicolescu [110] presented a pallet fixture system with active vibration control capabilities. It embodies piezoelectric actuators and force sensors used to sense and respond to machining forces from milling operations. Similar systems are now commercially available [130].

The presented pallet fixture systems target the dampening of vibrations induced from the time-varying machining forces. They can reduce the roughness of the machined surfaces and decrease the required processing times. Higher cost is the disadvantage of this fixturing technology.

The previous paragraphs summarised in brief the most prominent fixturing technologies that have been presented thus far. The field of fixturing has received considerable amount of research attention. Covering all fixturing-related work would exceed the scope of this thesis and would be impractical. Therefore, the focus is hereafter placed on the research areas that are of direct relationship with this study.

2.4 Fixture-Workpiece Dynamics

Fixturing devices are in direct contact with the processed workpiece, greatly affecting its dynamic response. Designing better performing and more efficient fixturing systems requires an in depth understanding of the effects they have on the workpiece behaviour and, therefore, the process outcome. As a result, the interaction between fixture and workpiece has received significant attention.

2.4.1 Friction and its Effect on the Workpiece-Fixture System Dynamics

One of the aspects of fixturing that has received considerable research attention is the friction at the contact points between the fixture and the workpiece. Friction affects the

dynamic behaviour of the system and is dynamically affected by the response of the fixture-workpiece system to external dynamic loads. The presence of friction increases the stability of the system and also helps dampen the vibrations experienced by the fixture and the workpiece during dynamic loading conditions. Hurtado and Melkote [67] aimed at experimentally establishing the coefficient of static friction between a cast aluminium workpiece and oxide-coated steel fixture elements, when excited by dynamic loading. A series of factors and their effects were investigated. These included the normal pre-load forces (clamping forces), the frequency of excitation in both the normal and tangential directions, and the vibration amplitude in the normal and tangential directions.

Fang *et al.* [49] examined the damping effect of friction on the stability of the fixture-workpiece system under machining conditions. More specifically, they formulated a model that included the vibration of the workpiece and the fixturing elements, which was solved using the finite elements method (FEM). It was observed that at specific levels of clamping forces, a "locking" effect is starting to emerge, significantly reducing the relative motion between the workpiece surface and the fixturing element. It should be noted that, in the case of multiple contact interfaces, this locking effect does not emerge simultaneously on all contacting points, but it appears sequentially.

Motlagh *et al.* [89] utilised the Armstrong non-linear friction model to improve the model developed by Fang *et al.* [49]. The addition of the Armstrong friction model renders the overall model able to converge to a solution even for high clamping forces. This is not possible with the model in [49]. The proposed approach enables the study of pre-sliding and micro-sliding at the fixture-workpiece contact points.

2.4.2 Modelling of Fixture and Workpiece Considering their Dynamic Interaction

Another area that has significantly attracted the attention of the research community is that of the modelling of fixture-workpiece systems and their dynamic behaviour. Models for both passive and active fixture systems have been presented.

2.4.2.1 Passive Fixture Systems

Mittal *et al.* [87] created a model for the dynamic analysis of the fixture-workpiece system. Their approach is based on the finite element method (FEM) and the Dynamic Analysis

and Design System (DADS) computer code. In this approach the workpiece is treated as rigid. The machining forces and torques are treated as having constant or linearly-varying magnitude. The fixturing elements are simulated as lumped, translational spring-damper-actuator (TSDA) elements. In this way, the local flexibility at the contact points between the fixture and the workpiece is captured. The stiffness in the TSDA elements is treated as linear and the actuator part of the TSDA element is approached as a constant clamping force. This model allows for the separation between workpiece and fixture. The model was used to evaluate stability of the system and the effects of clamping sequence and locator arrangement on the accuracy of the workpiece. It was shown that the relative placement of locators and clamps has a greater impact that the absolute placement of the locators alone. The sequence of application of the clamps was also observed to have a significant impact on the end result. The authors of this work also pointed out the utility of obtaining the vibration characteristics of the system, as this could help to design a fixture that can reduce surface finish variations.

Yeh and Liou [145] treated the fixture-workpiece system solely through the stiffness at the contact points. For this they proposed the use of virtual springs to simulate the interaction between the workpiece and the fixture. The mass of the virtual springs and the damping are considered negligible. A modified version of the Hertz contact theory was used to establish the stiffness of the virtual springs. Spring constants that stemmed from the above two models are incorporated in a FE model, which is used to calculate the natural frequencies and the frequency response of the simulated system. Experimental modal analysis results were used to prove the validity of the proposed modelling approach.

Behzadi and Arezoo [16] followed a similar approach to model the dynamic behaviour of a fixture-workpiece system. The workpiece is considered perfectly rigid and the rigidity of the fixturing elements is represented through spring-damper elements. The entire system is regarded to be linear. The developed model was implemented to investigate the effect of support elements to the flatness and roughness of a machine surface.

Deiab and Elbestawi [40] proposed a more comprehensive model of the fixture and workpiece system. This model treats both the workpiece and the fixture elements as flexible. Their interaction at the contact points is modelled through spring elements enhanced with a modified version of Coulomb's law of friction. This aims at reflecting the effects of friction. The model also integrates a three-dimensional (3D) model of the workpiece, the geometry

of the cutting edge of the tool, and modal characteristics of the machine tool. In this way, the dynamics induced by the cutting forces can be accounted for in the model, allowing for a more accurate calculation of the workpiece and the fixture dynamic deformations. The model was used to evaluate the effects of friction, location of fixture element and contact stiffness on the machining process outcome.

Liao and Hu [78] developed a Finite Element Analysis-based (FEA-based) model of the fixture-workpiece system, which treats the workpiece, the fixture elements and the fixture base as flexible. The dynamic compliance of the workpiece and the contact stiffness characteristics are also reflected in the model. The model can take into account the deflection experienced by the fixture and the workpiece due to the static clamping loads, instantaneous machining forces and the forced vibrations caused by the dynamically changing amplitude of the machining forces. The model is used to predict the surface flatness of fixtured parts under dynamic machining conditions.

Phuah [107] and Ratchev *et al.* [111, 112] also used the finite element (FE) approach to describe the dynamic behaviour of fixture-workpiece systems undergoing a grinding process. In this work the workpiece is a treated as a deformable solid and simulated in commercial FE software. The fixturing elements are introduced into the model as spring and damper elements. The stiffness profile of these elements was determined experimentally. The changing point of application of the dynamic machining loads is captured in the work, however, this is achieved in a pseudo-static manner.

Deng [41] worked on incorporating the effects of material removal due to a machining process on the dynamic behaviour of a workpiece. As in some of the previously described cases, this work treats the fixturing elements and the workpiece as deformable solids. The fixture base, however, is considered to be rigid. The mass removal effects were incorporated by considering both the mass characteristics of the workpiece and the rate of change of its inertia. The former was obtained through the geometric model of the workpiece in various phases of the machining process using the 3D ACIS modeller. The mass reduction rate was calculated through the forward finite differences method. The stiffness characteristics of the workpiece are obtained using the FEA commercial software ANSYS. The damping characteristics of the workpiece and fixture elements are not taken into account. Finally, the fixture-workpiece interaction is represented through a set of spring constants acting in all three translational Cartesian directions. This representation accounts for the stiffness

of the fixture elements and the stiffness of the contact. The model was used to investigate the dynamic stability of the system through the manufacturing process. It was also used to optimise the design of the fixturing process, and more specifically the applied clamping loads.

A simplified model of the above, one that treats the workpiece and the fixturing elements as rigid, was also established by Deng and Melkote [42]. This model includes the materilal removal effects and accounts for the dynamic nature of the machining loads. The model was developed using analytical expressions and was used to investigate the dynamic stability of the system and the effects of clamping forces.

2.4.2.2 Active Fixture Systems

In all the above cases, fixturing elements are treated as passive components. Locating elements are at best regarded as deformable bodies that present a reaction force when external loads are applied on the workpiece. Clamping elements present the same behaviour, but they are also granted the ability to apply constant forces on the workpiece. However, with the advent of active fixtures this approach is no longer adequate. The fixture elements can actively react to external forces, automatically adapting their position, reaction and clamping forces. The dynamic response of the fixturing elements of active fixtures should therefore be taken into consideration when modelling such fixturing systems. Bakker *et al.* [13] were perhaps the first to integrate the dynamic behaviour of active fixture elements to the model of a fixture-workpiece. In this work the active fixture elements take the form of hydraulic actuators, whose response is reflected by a first-principle-based analytic model. The workpiece is approached as a concentrated mass object. The compliance of the fixturing element and the workpiece are modelled as spring and damper pairs. The forces that are exerted on the system present time-varying amplitude. The developed model was used to theoretically investigate the performance of position-feedback and force-feedback control strategies, with various controller designs. Bakker *et al.* used the same modelling approach to investigate the performance of control strategies and controller designs for a fixture-workpiece system with piezoelectric actuators [12]. The workpiece is again treated as a concentrated mass-spring-damper system, connected to the active fixturing element through a lever mechanism.

Expanding the previous models, Bakker *et al.* [14] proposed a methodology through

which the dynamic behaviour of an active fixture-workpiece system can be extracted. The active fixture elements in this work are based on hydraulic actuation with closed-loop operation. The workpiece is described through a reduced finite elements model. The behaviour of the modelled system under various control strategies was investigated. The above methodology was also applied to establish the fixture-workpiece system of a thin-walled, box-shaped workpiece fixated by an active fixture with electromechanical actuators as clamps. Permanent magnet synchronous motor (PMSM) actuators were assumed. These were modelled using the first principle equations that apply for DC motors. Step forces were used as the source of excitation of the system. Different control strategies were investigated for their performance in minimising the workpiece displacement.

Moreover, in [11], Bakker implemented the aforementioned methodology to simulate the behaviour of a Nozzle Guide Vain (NGV) workpiece being processed by grinding. A reduced model of the workpiece was coupled with an analytical model of piezoelectric active clamps, operating in closed loop. The dynamic amplitude and moving nature of the forces exerted on the workpiece by the grinding process were also included.

Nee *et al.* presented another approach to modelling the active fixture-workpiece system [98]. This approach is based on system identification principles and the establishment of a parametric Autoregressive-Moving Average (ARMA) model. The least squares (LS) technique was proposed as the means of calculating the unknown parameters of the ARMA model. As this model is extracted from experimental data, it reflects all the parameters that contribute to the response of the system.

Finally, a special mention should be given to the following research activities, despite the fact that both treat the fixture workpiece system as quasi-static. Grochowski *et al.* [59] use commercial FEA software to model the workpiece. The active elements of the fixture, which are composed of stepper motor actuators, are modelled using first principles. Their closed-loop operation, controlled by a PID regulator, is reflected in the developed model. The latter is introduced to the FEA model of the workpiece through subroutines implemented in the Fortran77 programming language. The model was used to evaluate the performance of such a system in controlling the position of a point on a beam workpiece that experiences deflection due to externally applied forces. The point whose position is controlled does not coincide with the contact point between the fixture and the workpiece.

Nee *et al.* [98] do not reflect the dynamic behaviour of the active elements of their

system in their FE model of the workpiece. The fixture elements are represented as spring elements. For every time step for which the FE model is solved, the clamps can apply forces with different amplitude and different point of application. This way, the model reflects the ability of the fixture to dynamically adjust the position of the clamps and the clamping forces it exerts. This is the first and only instance where the effects of clamps that constantly change their positions during the manufacturing process are mentioned.

2.4.3 Fixture Design Methods Accounting for System Dynamics

In many cases, dynamic models of the fixture-workpiece systems have been used to assist the design of the fixture. Daimon *et al.* [30] formulated a fixture design method, based on the dynamic behaviour of a fixated workpiece. They used finite element simulation or experimental modal analysis data to evaluate the dynamic compliance of the workpiece under a certain fixture layout. The proposed method can be used to evaluate the positions where additional supports would reduce the dynamic compliance of the workpiece to acceptable levels. Similarly to the work by Mittal *et al.* [87], in this approach the fixture elements were simulated as sets of springs and dampers. The latter were treated as having constant stiffness and damping coefficient, respectively. The method was trialled on thin-walled cast iron and steel box-like workpieces.

Padmanaban and Prabhaharan [101] proposed another design method, also based on the dynamic behaviour of a fixture-workpiece. It uses Ant Colony and Genetic Algorithms to minimise the dynamic elastic deformations experienced by a workpiece, excited by harmonic forces. In this work the workpiece is treated as deformable, but the fixture itself is rigid. The objective function of the problem, generated by formulating the problem through finite element principles, is solved using the modal superposition method. The workpieces for which the method was tested are two-dimensional and are excited by purely harmonic forces acting in the plane of the workpiece.

Deiab [39] used the finite element analysis to investigate the effect that the position of supporting elements has on the dynamic response of a workpiece undergoing an end-milling operation. This model includes factors like cutting edge geometry, process parameters, fixture layout and others. Both the workpiece and the fixture elements are considered flexible. The model was used to identify the fixture layout that increases the stability of the system and reduces the maximum vibration amplitude experienced by the workpiece

under dynamic excitation. This study concentrates only on the positioning of passive support elements.

Li and Melkote [77] used a lumped mass and stiffness model to describe the dynamic response of the fixture-workpiece system. The fixturing elements are represented as a set of springs, two in the tangential and one in the normal direction of the surface of the workpiece at the point of contact. Damping and slippage at the contact points were not taken into account. The same holds true for the moving nature of the point of application of machining forces. An iterative algorithm was used to establish the fixture layout and clamping forces that resulted in the lowest positional/location error of workpiece.

Deng and Melkote [41, 43] implemented the model that was presented in Section 2.4.2.1 to optimise the clamping forces that are applied by the fixture per tool pass during the machining process. As already mentioned the model behind this fixture design method considers the dynamic response of the fixture-workpiece system, whilst also incorporating the effects of the material removal to the dynamic response of the system. The optimisation problem is solved using the Particle Swarm Optimisation technique.

2.5 Control Strategies for Active Fixtures

Another research area that is of great interest for this thesis is that of the control strategies that have been proposed for the regulation of the operation of active fixtures. Mannan and Sollie [83] proposed the cascaded position/force control algorithm for the operation of active clamping elements. This method utilises two feedback sources, namely a force sensor and a position sensor. The control loop implements two controllers; one implemented by means of a motion control card and the other implemented by means of software. The former is a PID controller and the latter is a simple P controller. The controlled variable in this work was the force applied by the clamping elements of a prototype active fixture.

Nee *et al.* [98] used the same approach with a slight variation in its application. In detail, the proportional controller in the force-feedback loop (external loop) that was utilised by Mannan and Sollie was replaced by a simplified version of the Generalised Minimum Variance (GMV) self-tuning controller.

Du *et al.* [45] described the utilisation of two separate control strategies to regulate the positioning and force application tasks of a prototype three-fingered intelligent fixture.

The direct position-feedback was used to control the positioning actions of the fixture. The feedback source for this loop was an optical encoder mounted on the axis of a DC motor. The direct force-feedback approach was used to control the forces exerted by the fixture on a thin-walled cylindrical workpiece. Strain gauges were utilised as the feedback source for this loop. A digital controller was in charge of regulating the response of the fixture. No further detail were given on the characteristics of this controller.

Bakker *et al.* [12–15] examined the effect of different control schemes on the response of the fixture-workpiece systemt. In detail, both force- and position-feedback with various controller designs were examined. The goal was to investigate which of the above schemes leads to a system that reacts to external loads in such a way that the workpiece displacement is minimised. The direct force-feedback and direct position-feedback algorithms were used. This work showed that position-feedback leads to a system that minimises the unwanted behaviour of the workpiece.

Grochowski *et al.* [59] applied a simple position-feedback loop architecture to control the displacement of a cantilever beam workpiece by using stepper motors as active fixture elements. A PID regulator was used to control the response of the system.

Most of the previously described approaches have the objective to minimize workpiece displacement and deformation under clamping either by controlling the applied clamping forces or by controlling the position of the tip of the active clamping elements. Looking into a possible capability of active fixturing systems, Rashid and Nicolescu [110] investigated the ability to actively control the vibration experienced by a workpiece undergoing end-milling processing. To achieve this, their palletised active fixture deploys three-component force sensors and piezoelectric actuators housed in the base-plate of the palletised fixture. The authors of this worked implemented the filtered input least-mean squares (FXLMS) algorithm to control the output of the actuators.

2.6 Modelling of the Full Dynamic Nature of Machining Loads

The simulation of moving loads to analyse the dynamic response of structures is definitely not a new subject. The effect of moving loads has been studied both analytically [52, 86] and through finite element analysis [37, 141, 142]. However, the constantly changing point

of application of the machining forces is an aspect that is very often disregarded during the analysis and design of fixtures for machining operations. In the majority of cases, the methods that have been proposed thus far treat machining loads solely through their changing amplitude.

Few are the cases where the moving nature of machining forces has been included in a fixture-workpiece model. However, the vast majority of these models treats the problem as static or pseudo-static. Such models are often based on FEA, e.g. [107]. Such modelling approaches fall outside the scope of this study and, therefore, will not be further analysed here. The following paragraphs focus on models and methods which capture the moving point of application of machining forces and the dynamic response of fixture-workpiece systems.

Liao and Hu [78] proposed a method for simulating the effect of moving loads to the dynamic response of a fixture-workpiece system. Finite element analysis was used as the basis of the proposed fixture-workpiece system. The FEA model was used to calculate the Frequency Response Function (FRF) of all nodal points. The dynamic response of the fixture-workpiece system was then calculated based on the nodes on which the machining forces where applied.

Behzadi and Arezoo [16] captured both the dynamic amplitude and point of application of the machining forces by introducing both a force amplitude and a moments vector in their analytical model. This method has been used for pseudo-static solution approaches [98], however, in this work the problem is treated as a dynamic one. The applied forces are considered purely harmonic and the workpiece is considered to be rigid. The same approach is used by Deng [41].

The aforementioned cases are tailored for passive fixtures. Bakker [11] is the only researcher thus far to have captured the moving nature of machining forces in a model focusing on active fixtures. The simulation method proposed by Bakker utilises the approach described in [142]. According to this, all the nodes of the FEA model of the workpiece, which are scanned by the cutting tool as it passes over the machined surface, are assigned a load. This load has a time-varying amplitude. When the tool lies over a node or between two nodes, then the amplitude of the loads that have been applied to these nodes are non-zero. All other loads are given a zero amplitude. The value of the non-zero-amplitude loads is function of the cutting force amplitude and its distance from the neighbouring elements.

The previously described method was used to simulate point moving loads from a grinding operation. Constant and time-varying cutting forces were considered.

2.7 Summary of Key Findings and Identification of Knowledge Gaps

From the conducted survey of the open literature it is possible to extract a series of noteworthy conclusions. To begin with, the field of fixturing is one of great interest for the research community. This stems from the fact that fixtures can greatly affect the outcome of a manufacturing process.

Fixtures can be used in almost any manufacturing operation, including assembly, machining, measurement and inspection. As a result, the fixturing technologies that have been proposed over the decades are numerous. In all cases, however, there are two key characteristics that a fixturing solution needs to possess; flexibility and performance.

Flexibility is a term that characterises the ability of a fixture to hold workpieces of different geometry. As a rule of thumb, the greater the number of different workpieces for a fixture, and the more the geometrical differences between workpieces, the more flexible a fixturing technology is considered.

Performance is a term used to describe how positive an effect does the fixture have on the outcome of the manufacturing process. Fixtures are in direct contact with the processed workpiece and, therefore, impact the behaviour of the workpieces. The performance of a fixture is measured through a series of key indicators. These include the stability, the localisation accuracy, the static deformation, the dynamic deformation, and the accessibility of the workpiece.

A review of the developed fixturing technologies, as presented in the first part of this chapter, reveals that these two characteristics are the driver behind the different fixturing concepts that have been proposed. Flexibility is the point of focus in many cases. Conformable fixtures, modular fixtures and phase-change fixtures are examples of highly flexible fixturing solutions. In most recent years, however, fixturing concepts have been developed with performance in mind. This is reflected from the increased attention that active fixtures have received during the past fifteen years. Fixture concepts behind which the combination of increased performance and flexibility is the driver have yet to be proposed.

Furthermore, the thus far active fixture solutions concentrate on the application of dynamically-adjusted clamping forces. Fully-active fixtures, which can vary the amplitude and point of application of clamping forces throughout the manufacturing process have only been suggested and discussed on a hypothetical basis. A hardware implementation of the concept of fully-active fixtures has not been encountered. This fixturing technology not only promises enhanced performance, but could also combine it with high levels of flexibility.

Apart from fixture concepts, another subject within the field of fixturing that has received considerable amount of attention is the investigation and modelling of the effects of fixtures on the behaviour of the workpiece. This of course directly relates to increased performance of fixturing solutions. Understanding how the fixture affects the outcome of the process is key in order to design better performing fixtures. Friction and the contact stiffness at the fixture and workpiece interface points, and how these affect the response of the workpiece to external stimuli, have been the focal point for many researchers. A series of modelling approaches, each with its own assumptions, simplifications and limitations, has attempted to enhance understanding of the fixture-workpiece system. The accurate simulation of the static and dynamic response of the fixture and workpiece system to the clamping forces and the externally applied forces has been the main goal of the proposed models. These models can be used for verifying the performance of a fixture in terms of its stability and the workpiece deformations, bypassing the need for building cost intensive prototypes.

Additionally, the developed models have been used as means of designing better performing fixtures. The careful placement of locating, supporting and clamping elements around the workpiece could amplify stability and reduce deformations and vibrations, experienced by the workpiece. Also, a fixture that performs as intended, with the minimum number of fixturing elements around the workpiece, helps improve accessibility.

However, the literature survey presented in this chapter also reveals a series of gaps within the knowledge which has been generated from the reviewed work. These can be summarised in the subsequent list.

1. The majority of the models that intend to predict the dynamic deformation experienced by the workpiece, treat the problem as static or pseudo-static. This approach is valid when the frequency of the dynamic loads that excite the workpiece is far away

from the natural frequencies of the fixture-workpiece system. However, the transient dynamic response of the system cannot be ignored when the excitation frequency is comparable to the natural frequencies of the fixture-workpiece system.

2. The results reported in a large percentile of the open literature are based on workpieces that present high levels of rigidity. Low-rigidity, thin-walled workpieces present unique fixturing demands and challenges that differ and should be carefully studied.

3. The moving point of application of external loads, such as machining forces, is often ignored even in research activities that deal with the dynamic response of fixture-workpiece systems.

4. In active fixtures the response of the active elements is regulated through feedback control. This, in turn, affects the dynamic response of the workpiece. This behaviour is not reflected by the vast majority of fixture-workpiece models that have been proposed so far.

5. Fixture-workpiece models that reflect the dynamic response of the workpiece, the dynamic response of active fixturing elements and the full dynamic nature of machining forces are almost non-existent.

6. The performance and capabilities of fully-active fixtures have not been examined in detail. Such fixtures have only been proposed in theory.

7. The effects of fully-active fixture on the workpiece dynamic response have barely been investigated.

8. Fixture design methodologies that can support fully-active fixturing systems have never been proposed.

The intention and goal of the research work that is reported through the pages of this thesis is to address these knowledge gaps. The proposed models and methodologies to achieve this goal are described in the next chapters.

Chapter 3

Research Methodology

3.1 Introduction

The literature review presented in Chapter 2 predominantly revealed that the field of active fixtures has only recently started to receive the attention needed to understand the full abilities of such advanced fixturing solutions. This thesis is targeted towards the investigation of the potential benefits of fully-active fixtures, also referred to as fully-adaptive fixtures. These cannot apply variable clamping loads over the duration of the manufacturing process, but also allow for variable positioning of fixturing elements. Therefore, such fixtures combine load compensation with manual and automated reconfigurability. The former attribute ensures the application of optimal fixturing process parameters at any given moment. The latter contributes towards achieving a high-performing flexible fixturing solution. This study shall concentrate on the adaptive side of fully-active fixtures, with the ultimate aim being the investigation of how such fixtures can be applied to improve the end result of the manufacturing process and/or to decrease the process's cycle time and cost. In order to achieve the desired results, a structured research methodology was followed for the completion of the thesis. This methodology will be analysed in the next paragraphs.

The research methodology followed comprises four core steps. At first, a detailed literature survey was completed, which helped to identify the current state of the art in fixturing technology and research trends in the field. Most importantly, this survey highlighted knowledge gaps which should be addressed in order to propel fixturing technology. The results of this first step have been presented in Chapter 2 of this thesis.

The second step of the methodology involves the translation of the identified knowledge gaps into clearly defined research objectives. Three are the main research objectives identified, namely:

1. The generation of a model that adequately describes the active fixture-workpiece system's response to external moving and oscillating loads.

2. The definition of appropriate control algorithms and strategies for the seamless operation of a fully-active fixture.

3. The composition of a fixture design methodology, which accounts for the capabilities of fully-active fixtures, and assists in drastically improving the results of a machining process in terms of surface quality and form accuracy.

At this step the assumptions and limitations that govern the developments of this study are clearly defined. Also, it was decided to focus the research efforts on fixtures used during conventional machining processes of thin-walled structures. Material-removal machining processes, like milling [128], affect the workpiece-fixture system due to the fluctuating amplitude of machining forces in combination with their constantly changing point of application. Thin-walled low-rigidity structures are most susceptible to deformation due to clamping and the dynamic effects induced by machining operations [98]. As a result, the developments described in this thesis are expected to be more beneficial to such structures. The core research objectives of this work, along with the assumptions and limitations that govern them, are presented in more detail in Section 3.2 of this chapter.

The third step of the research methodology involves the execution of the necessary activities towards achieving the core research objectives identified in the previous step. These activities and the theoretical developments that lead to the achievement of the research objectives, are described in depth through Chapters 4, 5 and 6 of the thesis.

The fourth and final step of the methodology involves the validation of the models and methods developed. To achieve this a combination of analytical and experimental approaches will be utilised. As part of this step of the methodology a fully-active fixture concept is proposed. Furthermore, a prototype, which is based on this concept, is developed, serving as the platform for all experimental validation processes. A brief summary of the activities within this step is presented in Section 3.3.

The first three steps of the methodology occur sequentially. However, the third and the fourth step of the research methodology were executed concurrently as one affects the other. Presenting the particulars of the fourth step before the developments within the third step, shall facilitate and enhance the reader's understanding of fully-active fixtures and the tools and methods proposed through in study. For this reason, the concept of a fully-active fixture, designed for the needs of this work, is presented in Section 3.3.3.

3.2 Research Objectives, Assumptions and Limitations

3.2.1 Research Objectives

As presented briefly in Section 3.1, three are the core research objectives of this PhD thesis. These are presented below.

3.2.1.1 Modelling of Active Clamping Elements and the Workpiece

Building a comprehensive model of the fixture-workpiece system constitutes the first objective of this work. This model should capture the dynamic response of the processed workpiece to the dynamic, moving loads of a machining process. Moreover, the active clamping elements and their reaction to external stimuli is a critical step towards the investigation and optimisation of the performance of fully-active fixturing systems. Successful models of both the workpiece and the fixturing elements could help predict the fixture-workpiece systems' behaviour. Therefore such models can assist in optimising the fixturing process and, subsequently, the outcome of the machining process.

Structural model of a workpiece. The dynamic response of a structure becomes increasingly important as the frequency of the external excitation (machining forces) is close or equal to a natural frequency of the excited structure [78]. Solid and very rigid structures usually have natural frequencies well above the excitation frequencies met in conventional machining operations like end-milling. Furthermore, solid structures suffer less deflection compared to thin-walled structures when statically loaded with the same clamping force. As presented in [83], thin-walled low-rigidity structures could benefit more from a carefully planned and adaptive fixturing process, one that can decrease the static deformation from the clamping forces and reduce the vibration experienced during the machining operation.

In order to reduce static deformation and vibration amplitude of low-rigidity workpieces, it is essential to establish a model of the workpieces behaviour under external excitation.

The excitation experienced by structures when undergoing machining operations is inherently dynamic. The machining forces are not constant, but instead their amplitude fluctuates over time. This amplitude fluctuation is the resultant of mainly the tool rotational speed, tool geometry, and variable depth of cut, as the tool teeth constantly engage and disengage the workpiece. Ideally, these sources of fluctuation are purely harmonic in nature. However, deviations from the ideal condition, such as the existence of tool eccentricity, non-ideal workpiece geometry, regenerative vibrations (chatter) and vibrations passed onto the machine tool from other operating equipment get superimposed as additional harmonic forces or noise on the cutting force amplitudes, resulting in a force profile that is almost random with a certain level of periodicity. Yet, the cutting force amplitude can be well approximated by a weighted sum of harmonic amplitudes as shown in Figure 3.1. Therefore the workpiece model should be able to accurately capture the behaviour of the workpiece under periodic excitation. Furthermore, machining forces are never applied statically at the same point on the workpiece. On the contrary, the point of application of machining loads changes constantly over the duration of a tool pass. This movement causes dynamic excitation of the workpiece [52] and needs to be reflected in the workpiece model.

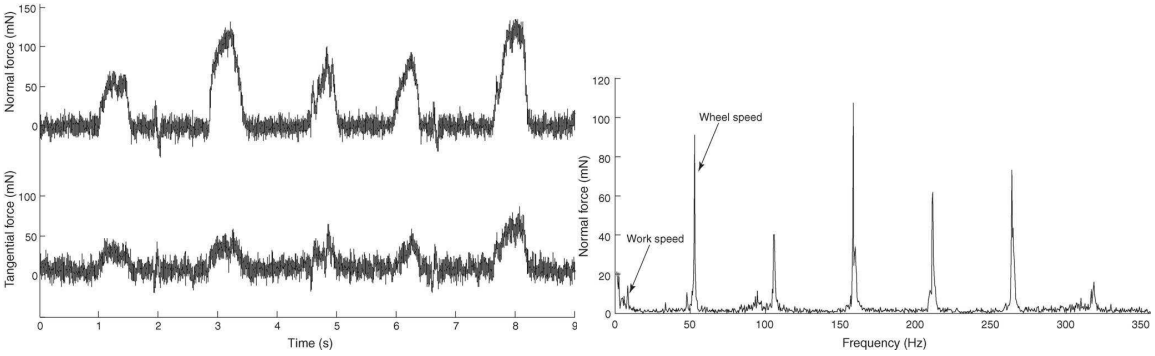

Figure 3.1: (a) Normal and tangential forces experienced by a workpiece undergoing a grinding operation. (b) Power spectrum density of normal forces [27]

For the simulation of the workpiece under the previously described loading conditions Finite Element Analysis (FEA) will be deployed. FEA is a powerful tool with which complicated continuous structures can be discretised into a number of small sections called finite elements [53]. The required behaviour of the structure under excitation, thermal, structural or other, can be calculated through calculating the behaviour of each individ-

ual element. In this way, the developed model of the workpiece should be irrelevant to its geometry, granting increased generality to the model. For example, the commercially available software Abaqus [127] can be used for the finite element analysis.

Active fixturing elements model. Apart from the workpiece, it is equally essential to grasp the behaviour of the active elements of the fixture. Traditional fixturing elements could be treated as simple spring-damper systems [87] which could apply a predefined amount of force onto the workpiece. However, active clamps of adaptive fixturing systems are dynamic systems themselves. Their response to input signals for a change in clamping force or clamp position can introduce dynamic phenomena into the workpiece-fixture system. These phenomena need to be sufficiently captured. Perhaps the most convenient way to model the active clamping elements' behaviour is by using a first-principle-based model. There are many different actuation technologies available. Pneumatic, hydraulic, electromechanical and piezoelectric are the most commonly used ones. Each of these actuation methods is based on different principles and therefore it would be impossible to develop a single model for every single actuator. For this reason, in this work a model for Permanent Magnet Alternating Current (PMAC) motor electromechanical actuators will be developed, as this is the actuation technology implemented on the experimental test-bed that is designed and built for the experimental validation of the developments and analyses in the thesis.

The model of the active clamp elements will be deployed in Matlab [84], a numerical computing environment and programming language. Matlab can create transfer functions and state-space models that can be integrated into closed-loop feedback system models in a straightforward manner. This allows for direct use of the developed model in the investigation of appropriate control algorithms and strategies. This constitutes the next main research objective of this work, which is described in the following paragraph.

The models of the PMAC actuator and the FEA model of the workpiece, will be coupled together to form one full fixture-workpiece model that can be used for theoretical prediction of the system's behaviour under external machining loads. The integration of these two models into a combined fixture-worpiece system model will also be executed in Matlab.

3.2.1.2 Formulation of Force Control Algorithm

A critical part of the performance of active fixtures is the control algorithms used to control the application of actively applied clamping forces. As there has been little attention to the investigation of appropriate closed-loop control strategies for active clamps in the fixturing domain, this will be another research objective of this work. A well-controlled clamp can significantly improve the outcome of the fixturing and manufacturing process. The response of the active element to command inputs needs to be fast, to reduce transient effects that could endanger the fixture-workpiece system to become unstable or deteriorate the quality of the produced surface. Also, as machining forces can have amplitudes that vary significantly in value, the active fixture elements need to be able to accommodate for the large fluctuations in the loads they are called to apply, in a fast and reliable manner. In general, a poorly performing control algorithm could result in inferior geometrical accuracy and surface quality of the end result, and even unstable work-holding.

The force that an active fixturing element applies can be controlled in two ways. One involves the control of the position of the tip of the element. The other involves the direct control of the force. Electromechanical actuating units, such as the PMAC-based actuators referred to previously, have the advantage that they easily and cost-effectively incorporate position- and force-feedback. For this reason, potential control algorithms that utilise these two feedback sources need to be evaluated in order to identify the appropriate approach for achieving the best results.

3.2.1.3 Fully-Active Fixture Design Methodology

Adaptive fixtures have received attention mainly in the last ten years. The vast majority of the research effort has been targeted towards the investigation of the effect of active clamps, which are able to adaptively apply forces, on the workpiece and the manufacturing process outcome. However, a fixture that automatically changes layout during the processing phase, could significantly reduce workpiece deformation and vibration during machining. The quality of the end product can hence be drastically improved. Therefore, the final objective of this thesis is to investigate the benefits of such a fixturing method and develop a methodology to assist in formulating the optimal fixturing strategy when deploying a fully-active fixture. The methodology will be based on the models described

previously and shall serve as a tool to define the optimal fixturing parameters. These include: the fixturing strategy, the number of fixture element-workpiece contact points, the coordinates of contact points, and the clamping force intensity. The identification of these optimal parameters can be achieved using available optimisation tools. The methodology will be deployed in Matlab, which offers many optimisation options, from simple logical loops to advanced optimisation algorithms, genetic algorithms, etc. The results obtained by implementing the developed methodology will then be validated experimentally, through measuring and comparing the form accuracy and surface finish of workpieces machined whilst fixed according to the off-line results of the methodology.

The aforementioned research objectives constitute the main driving force behind this research work. The field of fully-active fixtures is a completely new one. Nee *et al.* in [98] stated: 'In the ideal vision, a fully-automated numerically-controlled (NC) fixture would apply just enough sustainable locking forces to the workpiece in a self-adaptive manner. Such a visionary system would also adapt the clamping positions as fixed layout of clamping points may not be able to support the workpiece from the point of view of workpiece deflection'. Such a novel system pose a series of questions that demand scientific explanation. However, it is virtually impossible to answer all of them within the time span of a PhD. Therefore, and in order to achieve the formerly described research objectives, it is important to acknowledge that a number of assumptions need to be made and that the research work is governed by specific limitations. These are described in the following paragraphs.

3.2.2 Assumptions and Limitations

3.2.2.1 Workpiece Geometry and Rigidity

As mentioned earlier, thin-walled structures shall be the focus of this work as these structures can potentially benefit greatly from advanced fixturing solutions. Increased clamping loads lead to static deformations and excess vibrations, which can defer the dimensional and form accuracy as well as the surface finish of the final product. Fixtures can be carefully designed and implemented to partially, or even fully, resolve these issues.

Thin-walled low-rigidity structures are common in a number of industrial sectors, especially aerospace and automotive. In many cases these structures are machined from a

block of raw material, avoiding joining operations that produce increased weight and lower stiffness end results. The cost of production of these parts is however comparatively larger than that of their assembled counterparts and quite often the machining of these structures is never straightforward. In order for a structure to be classified as thin-walled it must exhibit a wall thickness of at least one order of magnitude smaller than its length and width. In other words the thickness to length or to width ratio must be smaller than 1/10. A good example of such a structure is a workpiece that resembles a lidless box. Each of the sides of such a workpiece in turn resembles a thin plate. In engineering, thin plates are defined as flat structures for which the width to length ratio is bigger than 1/10 whilst the thickness to width ratio is less than 1/10. Plate structures can be well described using classical plate theory, also known as Kirchhoff Plate Theory [52, 57]. Therefore, a direct comparison of FEA and analytic results can be achieved, indicating whether the FEA results hold true or not, without having to conduct time- and resource-consuming experiments. It has to be noted that Kirchhoff plate theory is based on the following assumptions [136]:

- The deformations arising in the body of the plate are small compared to its thickness.
- The relationship between the components of stress and the components of strain is linear (Hooke's Law) [135].
- There is no deformation in the middle plane of the plate. This plane remains neutral during bending.
- Points of the plate lying initially on a normal-to-the-middle plane of the plate remain on the normal-to-the-middle surface of the plate after bending.
- The normal stresses in the direction transverse to the plate can be disregarded.

For the reasons explained before, a simple thin-plate workpiece has been chosen to serve as a test case throughout this work in order to prove the developed concepts. The geometrical simplicity and mathematical description of the behaviour of such a workpiece can greatly facilitate the experimental verification of the developed models and concepts. It helps to minimize the uncontrolled parameters that could potentially affect experimental results and lead to erroneous conclusions. The selected workpiece will be made of 7075-T6 aluminium, a material commonly used in aerospace, and has the characteristics presented in Table 3.1. The plate will be fully constrained on its two opposing small sides (50 mm).

This type of boundary conditions fairly resemble the ones present when a plate-like elements constitute one or more sides of a generic workpiece. Also, such boundary conditions can be applied easily both in practice and in FEA procedures. Furthermore, these boundary conditions guarantee a firm hold of the workpiece during experimentation, thus reducing the possibility of damage to any of the experimental equipment in case of failure.

Table 3.1: Physical properties of the selected plate workpiece.

Plate Characteristics	
Material	Aluminum 7075-T6
Density	2810 kg/m^3
Young's Modulus	71.7 GPa
Poisson's Ratio	0.33
Length	150 mm
Width	50 mm
Thickness	3 mm

3.2.2.2 Fixturing Strategy

As discussed in the literature review presented in Chapter 2, there are many different fixturing strategies available. The most commonly used one is the 3-2-1 fixturing principle [96]. According to this principle, three locating elements are used on the largest planar surface or orthogonal datum surface of a workpiece (primary surface), two locating elements are used on a surface perpendicular to the plane of the primary surface (secondary surface), and one locating element in the mutually orthogonal surface (tertiary surface). In this way, the movement of the workpiece along one direction of each of the six spatial degrees of freedom is constrained. By adding clamps, usually one opposite the primary surface and one opposite the secondary or the tertiary surface, all movement is successfully constrained. The fixturing elements can allow for either surface contact with the workpiece, or point contact. In most cases point contact provides adequate stability and improved accessibility compared to surface contacts. In practice, however, when processing thin-walled parts, the preferred option is to use surface contacts, due to the increased rigidity they offer to the system. Achieving the same or even better results by using point contact fixtures is therefore an additional challenge, which, if fulfilled, should grant further generality and credibility to the outcomes of this work. Therefore, and for all the reasons mentioned previously, the fixturing principle that will be the basis of this thesis is the 3-2-1 with point

contact fixturing elements.

3.2.2.3 Manufacturing Process

Milling is a manufacturing process found in virtually any manufacturing environment where material removal processing capabilities are present. During a milling process, material is removed by a rotating cutter [128]. The position of the cutter usually remains stationary whilst the workpiece is being moved relative to the tool thus achieving the desired material removal operation. Milling is a very flexible process. It is predominantly used in a wide range of operations spanning from simple slotting to mould manufacturing. There are many different milling method variations, but mainly two categories can be identified: Peripheral (or Plain) Milling and Face (or End) Milling. The former generates surfaces parallel to the axis of rotation of the tool. The latter generates surfaces normal to the axis of rotation of the tool. For creating thin-walled box shaped workpieces, the most common milling process used is peripheral milling. For this reason, the developments of this work will seek experimental validation using peripheral milling operations. However, this does not reduce the generality of the results, as the tools used and the developed concepts do not depend on the process itself.

3.2.2.4 Cutting Tool

For this work, the flexibility of the processing tool will not be taken into consideration. In reality, the cutting tool in conventional machining processes, like milling, is not rigid, but presents a certain degree of flexibility. This flexibility, along with other aspects such as geometrical inaccuracy, eccentricity and processing parameters (feed rate, depth of cut, etc.) does affect the end result of a machining process. However, thin-walled workpieces like the ones used in this study are considerably more flexible than the cutting tools, rendering the tool itself comparatively rigid. Furthermore, factors like geometrical inaccuracy and eccentricity can be minimised by carefully selecting and mounting the tool to the machine tool spindle. Therefore, for the purpose of this work, the effects that these parameters have on the fixture-workpiece system are not taken into account.

Additionally, the axis of rotation of the tool during a machining process, such as peripheral milling, is vertical. Therefore, the weight and the mass of the tool can be neglected. So according to these assumptions the tool will be treated only through the forces it applies

during the machining process.

3.2.2.5 External/Machining Forces

External forces experienced by a workpiece undergoing a material removal process are the primary source of excitation of the workpiece-fixture system. Machining forces have components in all three Cartesian coordinates. Nevertheless, the thin plates and in general thin-walled parts present the highest deflections and vibration amplitudes in the transverse direction, i.e. the direction normal to the plate's largest surface. For this reason, fixturing elements are applied in such a way as to oppose these forces. Since this is the component of machining forces that is primarily important, and because this research work does not intend to concentrate on the external stimuli, machining forces shall be approximated by means of their transverse component only. Moreover, the boundary conditions applied on the thin-plate workpiece used for experimental validation help eliminate the displacement of the part in the other two directions.

Another assumption made regarding the external forces experienced by the workpiece-fixture system, is that these forces are periodic and purely harmonic with a single excitation frequency. As explained before machining forces, provided they present periodicity (Figure 3.1), can be decomposed into a weighted sum of simple harmonic components, also known as a Fourier series [47]. The approach used in this thesis focuses on simple harmonic forces. The workpiece-fixture system is treated as a linear system, hence the developed methods and methodologies can be expanded to multi-harmonic forces by simply calculating the effect of each force component separately and then superimposing the results.

Finally, another assumption made regarding the applied external forces is that the direction of these forces does not change as the workpiece deforms. The deformations experienced by the part are small enough to allow this assumption without significantly affecting the validity of the results.

3.2.2.6 Fully-Active Fixture Design Methodology Limitations

As the fully-active fixture design methodology is based on the models described in Sections 3.2.1.1 and 3.2.1.2, it is also affected by the limitations behind these models.

Therefore, it should by highlighted that the purpose behind the third research objective is not to use the proposed methodology in order to accurately predict the displacements

that the fixtured workpiece experiences during machining. Also, it is not intended to be used as a means of predicting the actual characteristics of the surface that is produced by the machining process. The tools used in this work have been proven for their ability to achieve the above in many occasions. This research work sets out to develop a methodology to a level, where it can be used as a design guideline, which can assists in selecting the better performing fixturing solution. This is deemed sufficient in order to explore the capabilities of both the methodology and fully-active fixtures, which is the overarching objective of this study. Further development of the methodology to a level, where it can be used to predict the behaviour of the workpiece to the extend mentioned at the beginning of this paragraph, falls outside the scope of this research work.

3.3 Validation Procedures

The developments of this work will be validated using analytical or experimental methods. These are described below.

3.3.1 Analytical Validation Procedures

One of the reasons behind the selection of a simple-geometry thin-plate workpiece was to facilitate validation. Plates are structures which are met in a wide range of engineering sectors, especially mechanical, aerospace and civil engineering. As such, they have been the focal point of a body of research work, both theoretical and experimental. A large number of proven analytical models of thin plates, under various loading and boundary conditions, exist. These will be employed to validate the FEA models, which in turn will be used to theoretically validate the results of the developed models and methodology. In detail, the following theoretical validation procedures are performed within this study:

- Comparison of FEA-extracted natural frequencies of the plate workpiece with exact solutions from literature. This is used to select suitable finite elements that accurately predict the modal characteristics of the plate. This procedure is summarised in Chapter 4 and presented in more detail in Appendix A.

- Comparison of the FEA-extracted natural frequencies of the plate workpiece with analytically calculated natural frequencies of a beam with dimensions similar to those

of the plate. This is to further fortify the justification behind the selection of finite elements. Results of this comparison are presented in Appendix B.

- Validation of the moving load modelling approach, which is used in the fully-active fixture design methodology (Chapter 6). This is achieved by comparing an FEA-based model to which the load modelling approach is implemented with an analytical model of a thin plate subjected to moving loads. Results of this procedure are presented in Chapter 4 (Section 4.2.2.2) and Appendix C.

- Validation of the analytical model of a plate subjected to moving load via comparison of elastic deformation results with this from an analytical model of a beam subjected to moving loads. This is presented in Appendix A.2.

- Validation of the developed fully-active fixture design methodology using a test case of a beam subjected to a moving load. This is achieved by comparing the elastic deformation results from the design methodology to those obtained by an FEA model. This model is validated as discussed in the previous bullet-point.

The above validation procedures are intended to establish confidence in the developed tools, models and methodologies, eliminating the need for time-consuming and increased-cost experiments. In some cases, for example the measurement of the elastic deformation of plate subjected to moving loads, is significantly complex to be performed experimentally. Therefore, theoretical validation is almost the only available option.

3.3.2 Experimental Validation Procedures

When possible, and in order to investigate the developed models and methodologies in a real-life manufacturing environment, experimental validation procedures were applied. The following experiments are conducted within the content of this work:

- Validation of the coupled electromechanical actuator and plate workpiece model. This is achieved by comparing the open-loop response of the experimental set-up to that of the model.

- Validation of the comprehensive fixture-workpiece model. This includes the previously-mentioned model and the response models of the controlling hardware, with the entire system operating in a closed loop.

- Verification of certain design features of the experimental set-up for machining experiments. For this, experimental modal analysis is used, in order to ensure that the correct boundary conditions are applied on the workpiece and that the mechanism for applying these boundary conditions does not affect the dynamics of the workpiece.

In order to be able to conduct these experiments, appropriate experimental set-up has to be commissioned. For this, the following fully-active fixturing system concept was developed.

3.3.3 Fully-Active Fixture Concept

As discussed in Section 3.2.1.3, a fixture is defined as fully-active fixture when it present the abilities to adaptively adjust the clamping forces it applies on the workpiece, and to automatically reposition the fixturing elements relative to the workpiece before and during the manufacturing process. Therefore, the concept and prototype of such a fixture should possess these capabilities.

With this in mind, and as part of the experimental validation requirements behind this research work, the fixture shown in Figure 3.2 was conceptualised. This figure shows a Computer-Aided Design (CAD) software drawing of a fixture, which is designed for holding simple prismatic workpieces. There are two main reasons behind this. To begin with, feedback from Original Equipment Manufacturers (OEM's) from the aerospace, automotive and white-goods industry [46] revealed that many of the workpieces that are manufactured by them:

- Have simple prismatic geometry.
- Have features with prismatic geometry.
- Have each of the datum-point sets positioned in such a way, that the datum surfaces (primary, secondary and tertiary) are flat and perpendicular to each other. This means that the datum surfaces create a virtual box around the workpiece. This statement applies in the case where the 3-2-1 fixturing is utilised.

The second reason behind the proposed design, stems from the fact that the hardware implementation of this concept, is intended to be used primarily for experimental validation purposes. With this in mind, a simple design can assist in isolating the investigated

experimental variables from unwanted influences, and facilitates experimental procedures by reducing set-up time, minimising costs, and reducing the risk of equipment failure.

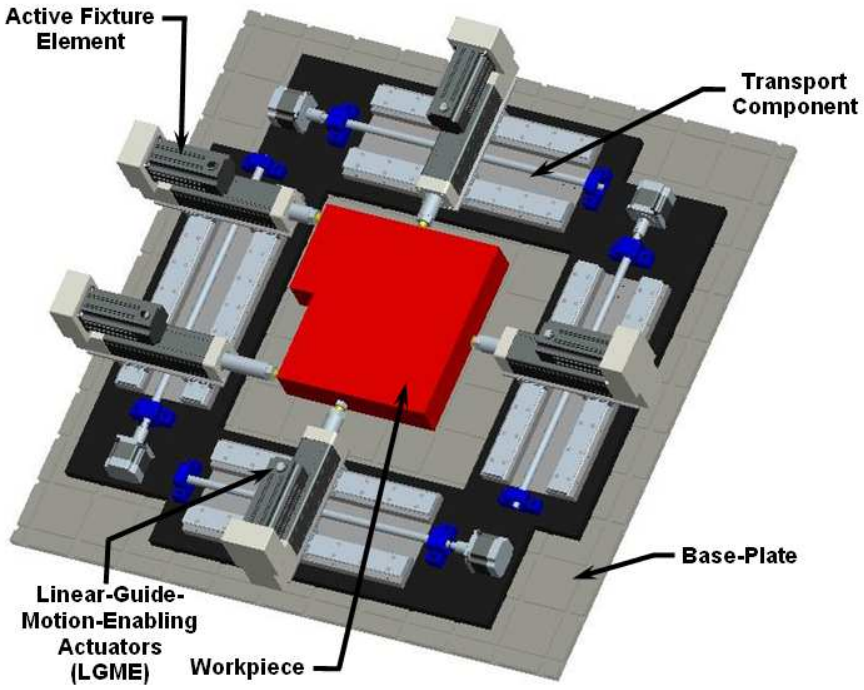

Figure 3.2: CAD representation of the proposed fully-active fixture concept.

The conceptual fully-active fixture employs a modular structure, granting it increased flexibility and manual or automatic reconfigurability. These attributes render the hardware implementation of the concept capable of being used for the needs of other research activities [115].

There are two specific characteristics that should be highlighted here. First of all, the fixturing strategy that is utilised by the fixture concept is the 3-2-1, with the baseplate playing the role of the primary locating arrangement of the fixture. It is reminded here that a surface equates to 3 locating points. Depending on the features of the baseplate, point-contact locating elements could also be used. Moreover, the fixture is capable of side-clamping only. No top-clamps where incorporated in the concept, as side-clamping is more than adequate for the experimental purposes for which the rig was built.

The fully-active fixture concept consists of a series of modules and sub-modules. These are described below:

Transport components. Transport components (Figure 3.3) are structures that serve as guideways for the active fixture elements to move. Each transport component constitutes a fixture module, which comprises three sub-modules:

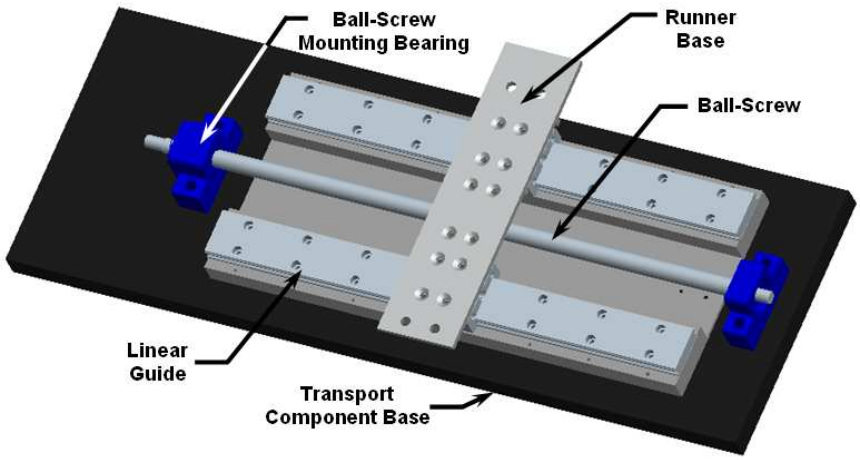

(a)

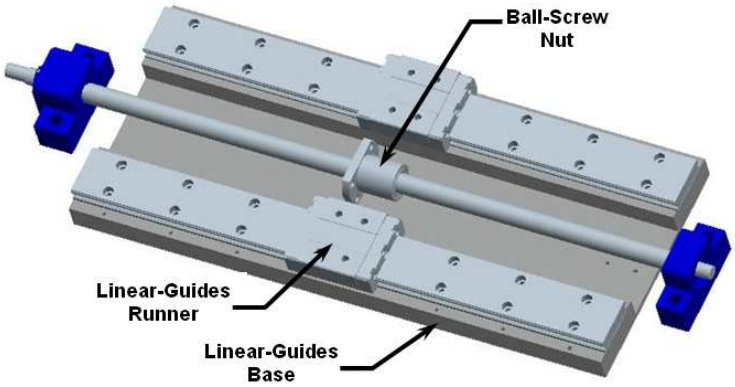

(b)

Figure 3.3: A detailed view of the transport component and its various components. (a) The transport component along with the runner-base and the transport component base. (b) A closer detail highlighting the runners, the ball-screw nut, and the linear-guides base.

Linear guides and runners. The linear guides are a set of straight metal beams, along which a variable number of runners is free to move. Two linear guides (pair) are used per transport component. These are machined together to ensure increased precision. Therefore, a pair of linear guides with their runners are regarded as one sub-module. The number of runners on each guide of each transport component must be the same.

The runners incorporate circulating ball formations, or other bearing technologies, to allow for virtually friction-free operation. Moreover, they are able to withstand loads in the radial, reverse radial and lateral directions. Finally, each runner incorporates end seals, side seals, inner seals and metal scrapers. This protects the circulating balls from contaminants like swarf and allows for trouble-free operation even when cutting fluids are used during the manufactur-

ing process.

Each pair of linear guides with their runners are permanently mounted on the Linear-Guides Base. This in turn is mounted on the Transport Component Base, as shown in Figure 3.3 (a). These are simple mechanical parts, machined out of high grade steel for increased rigidity. The linear-guides base is not only used as mounting means for the linear guides but also as a means to accurately locate them relative to each other. The required level of surface flatness and parallelism that the mounting surfaces for the guides require is thus easier to achieve.

The transport component base bears a series of features that allow for the mounting of other parts of the fully-active fixture. These will be described in more detail in the following paragraphs.

Ball-screw. The ball-screw is an assembly of a threaded shaft and nut, that transforms rotational motion to linear and vice-versa. The ball-screw nut is mounted in such a way that it cannot rotate freely. In this way, the rotational motion of the shaft can be translated into linear motion of the nut. Inside the nut, there is a circuit of circulating balls, in order to reduce friction during operation, and significantly increase performance and reduce heat generation. The ball-screw nut also incorporates a wiper-ring and sealing to prevent contaminants from entering the circulating balls.

The ball-screw shaft is mounted to the transport component base by means of two ball bearings, one on either side of the shaft, as shown in Figure 3.3. On one side the bearing and the mechanism that secures the shaft to it provide a fixed support. On that side, the shaft is threaded and bears a formation to accept a securing clip-ring. These features allow for the bearing to be sandwiched between a lock-nut that goes on the threaded part of the shaft an the clip-ring. As a result, all translational degrees-of-freedom (DOF) are removed from the shaft, which is only capable of rotating around its main axis. On the other side the shaft is secured on the bearing only on one side, by means of a securing clip-ring. This formation renders the ball-screw shaft simply supported. These bearings are directly bolted on the transport component base.

The ball-screw shaft is positioned between and parallel to the two linear guides, i.e. the main symmetry axis of the ball-screw is equidistant from the main

axes of the two guides. The ball-screw with its nut and the mounting bearings constitute the ball-screw sub-module.

Runner base. The runner base is another simple mechanical component. High grade steel is used for its manufacture. The runner base connects two runners - one from each linear guide of the pair - together. The nut of the ball-screw is also mounted on the runner base. This layout allows for the rotational motion of the ball-screw to be transformed into linear motion of the runners. Furthermore, the runner base is equipped with through holes that serve as mounting points of the actuators of the active fixture elements.

Actuation modules. Actuation modules are used to supply the necessary motion to the fully-active fixture and exert forces on the workpiece. There are two actuation module types used in the prototype fixture.

Active fixture elements. Off-the-shelf precision linear electromechanical actuators are used as active fixture elements. These have the ability to act as clamps or locators. Each actuator comprises a Permanent Magnet Alternating Current (PMAC) servomotor, a gearbox, a ball-screw and an extension shaft. The servomotor is positioned in parallel to the ball-screw and shaft axis, and it is used to drive the gearbox, which in turn drives the ball-screw axis. The nut of the ball-screw transforms the rotational motion into linear motion of the extension shaft. At the free end of the extension shaft the fixturing tips, i.e. the parts of the fixture that are in direct contact with the surfaces of the workpiece, are mounted.

Each actuator is placed in such a way that its axis of motion is perpendicular to the axis of motion of the linear guides, as shown in Figure 3.4. This formation creates modules with two degrees of freedom, a radial one, which always points towards the workpiece (Y-direction), and a lateral one (Z-direction), which translates into movement parallel to the locating and clamping surfaces on the workpiece. By extending or retracting the shaft of the actuator, the latter is capable of changing the radial position of the fixturing tips.

The motor of the linear actuator integrates a rotary encoder. This allows for the radial position of the extension shaft to be monitored. It is also used in the

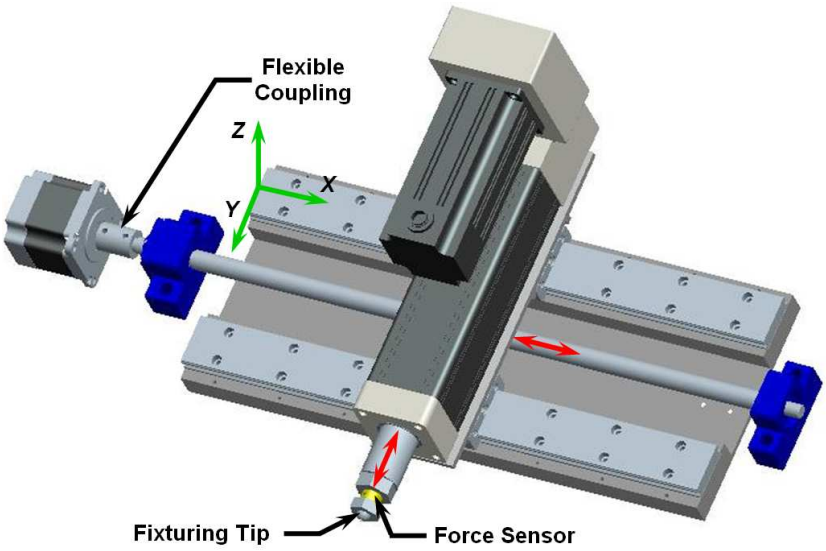

Figure 3.4: Placement of the actuators relative to motion direction of the runners on the linear guides. The local Cartesian axes for the transport component are highlighted.

direct position control strategy or the cascaded force/position control strategy (Section 5.3.2.1) as the means of feedback that closes the position control loop.

Linear-Guide-Motion-Enabling (LGME) actuators. These actuators, as their name reveals, are responsible for driving the runners on the linear guides, thus achieving the lateral movement of the fixturing elements. The LGME actuators are, in essence, simple PMAC servomotors. The same motor type, as that of the active fixture elements, is used for simplicity. These motors integrate rotary encoders at one end of their shaft. This possesses the role of a position feedback source. It is used to monitor the position of the set of runners that is driven by the motor. It is also the feedback source for the direct position control scheme (Section 5.3.1), with which the accurate and fast positioning of the modules on the linear guides is ensured.

The LGME actuator is positioned in line with the ball-screw shaft, as shown in Figure 3.4. It is connected directly to this shaft, by means of a flexible coupling, shown in the same figure. The latter caters for any minor misalignment there might be between the motor axis and the ball-screw axis. Finally, the LGME actuator is mounted on the linear guide base through a steel mounting plate.

Baseplate. The baseplate, shown in Figure 3.2, is a large metallic surface on which the entire fixture is assembled. This baseplate bears T-slot formations that allow for accurate positioning and secure holding of the fixture modules against the forces applied

from the fixture itself or the manufacturing process. The baseplate is considered as a separate module.

Sensing modules. The sensing modules play the role of feedback sources, or home and limit marks for the fully-active fixture. Three types of sensing modules are used.

Force sensor. Force sensors are positioned on all active elements that act as clamps and, conditionally, on active elements that act as locators. The force sensors on the clamps act as the feedback source for force control operations, or as clamping force monitoring sources when the clamps operate in position control mode. The force sensors on the locators are used solely for force monitoring tasks. Force sensor modules are sandwiched between the fixture tip and the free end of the extension shaft of a linear actuator, as shown in Figure 3.4.

Inductive switch. Inductive switches are used on the active fixture elements and provide reference marks, also referred to as home-position marks. They are used to identify the zero point of the motion of axis of the actuators in an accurate, automatic and repeatable way.

Mechanical switch. Mechanical switches are a cheap yet reliable alternative to the inductive switches, when mechanical activation is possible. In the proposed fixture concept, mechanical switches are used for two different operations. The first one deals with the marking of the home position of the axis of motion, which is controlled by the LGME actuators. The second one involves the utilisation of the switches as motion limits, which, when activated, inhibit the motion of the LGME actuators. Up to three mechanical switches per pair of linear guides can be used; one serving as a home switch and two serving as limit switches.

3.3.4 Fully-Active Fixture Prototype

The hardware implementation of the fully-active fixture concept was decided to be a simplified version of the design that was presented through Figure 3.2. This decision was made with cost-minimisation in mind, as a fixture with four transport components was not deemed necessary in order to satisfy the experimental validation requirements of this work. For this reason, only two sets of transport components were used in the actual prototype, positioned normal to each other, as shown in Figure 3.5. One of the transport components

bears two pairs of runners, whilst the other one only one pair. The rest of the fixture elements were replaced by passive metallic structures. It is considered that the baseplate grants the three locating points for the primary locating surface of the workpiece, according to the 3-2-1 principle [96].

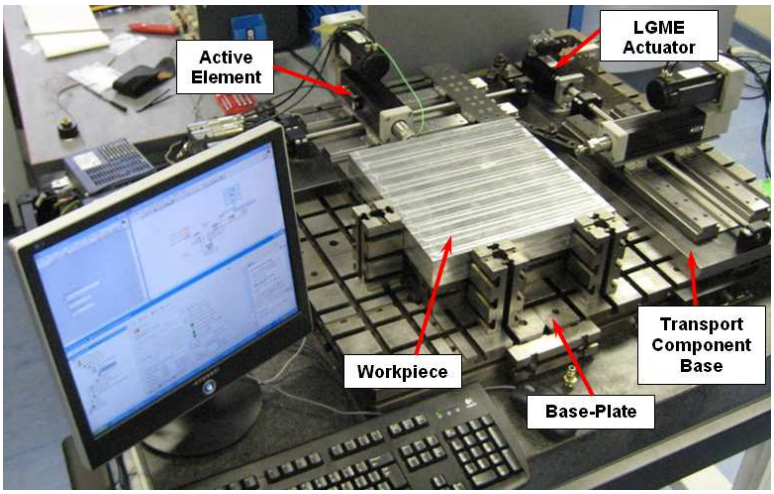

(a)

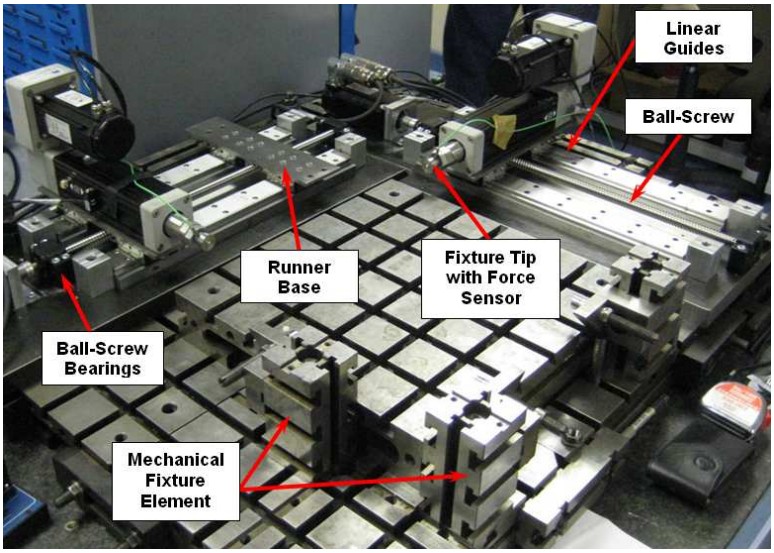

(b)

Figure 3.5: The hardware instantiation of the fully-active fixture prototype. (a) A general view of the overall system. (b) A more detailed view showing the two transport components and the passive locating elements that comprise the fixture.

In order to build the prototype the following off-the-shelf components were selected. The SHW-21CR1-ZZ-C1+400LP model, supplied by THK [133], was selected for the linear guides and runners. This model has a small profile, which helps reduce the torque that is applied on the parts of the transport component, this reducing deflection of the fixture structure. The ball-screw is a BNT1404-3.6-WW-G0+530LC-J1K, also from THK. The aforementioned runners and the ball-screw nut incorporate features that seal them from

contaminants that are expected during the machining experiments, namely cutting fluids and swarf. The ball-screw is secured in place by a BK10 bearing on one side, and a BF10 bearing on the other side, both sourced by THK [133].

For the role of the active fixture elements, the Kollmorgen EC2-BK23S-100-16B electromechanical actuator [32] was selected. This actuator is based on a Permanent Magnet Alternating Current (PMAC) motor and a gear-and-ball-screw mechanism, which transforms the rotary motion of the motor into linear. It has the ability to apply up to 2500 N of force and has a travel range of 60 mm. The Kollmorgen AKM23C [31] PMAC motor was selected as the linear-guides-motion-enabling actuators of the prototype fixture. These two actuation modules bear integrated rotary incremental encoders, which are used for position feedback and position monitoring activities.

Finally, a Kistler Type 9101A [70] piezoelectric transducer (PZT), also referred to as load washer, was charged with the force sensing tasks of the fixture.

Apart from the previously described modules, a series of controlling hardware is also necessary in order for the prototype to function. These are summarised hereafter:

Actuator controller. Also known as drive units, the controllers of the actuator are necessary for the actuators to work. They regulate and provide the power to the motor of the actuator, condition the voltage and current signals that control the speed and torque (force) of the actuator, supply the position feedback from the rotary encoders to other controlling hardware and stop the operation of the actuator in case a safety issue occurs. The selected model for the fully-active-fixture prototype is the Kollmorgen S200-VTS drive unit [35]. This is used for controlling both the motors of the active fixture elements and of the LGME actuators. One drive unit per actuation module is used.

Motion control card. This is a peripheral component interconnect (PCI) local-bus card that is mounted inside the personal computer that acts as the main control unit of the fixture and the human-machine interface (HMI) point. It incorporates a trajectory generator and a digital controller per motion axis, i.e. per actuation module. The selected card was the National Instrument PCI-7344 motion control card [92]. This can control all four actuation modules of the prototype fixture independently or simultaneously.

Controlling hardware interface. As the various controlling hardware was supplied from different manufacturers, an important issue is the integration of all the equipment into one fully-functional system. For this, the UMI-7774 board [94] from National Instruments was selected. This external board serves as a junction-point for any signal that goes to and from the motion control card.

Data acquisition card. As described earlier, fixture elements are equipped with force sensor. When the sensors are not used in the force-control closed loop operation, and if the signals from the sensors need to be monitored and/or recorded, then a data acquisition is necessary. A National Instruments PCI-6031E data acquisition card [91] was selected.

The above components are connected together to form the control system behind the fully-active fixture prototype. The control architecture of the prototype is shown in Figure 3.6.

The previously-mentioned prototype served as the platform for the experimental validation needs of this study and the work by Ryll [115]. Experimental modal tests, were conducted using the set-up, which is described in detail in Chapter 7, Section 7.3.3. For the sake of brevity, the description of this set-up is not reiterated here.

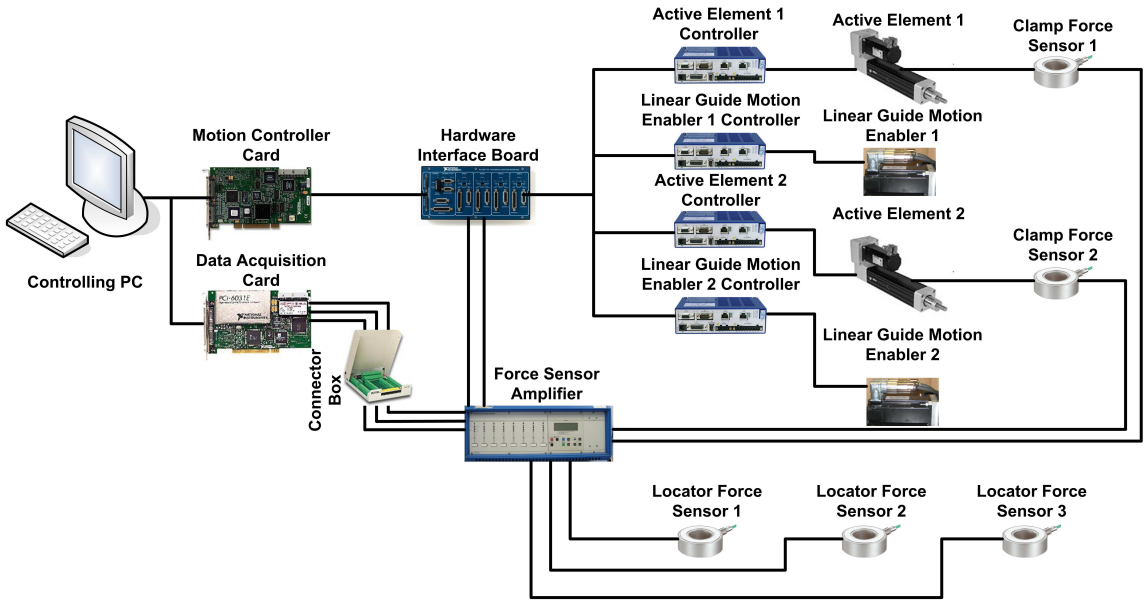

Figure 3.6: The control architecture of the fully-active fixture that is used during experimental validation procedures.

3.4 Conclusions

In this chapter, a detailed overview of the research methodology with which this work was approached, was presented. The key conclusions from the chapter are summarised below:

- A research methodology comprising four steps is used as the foundation of this research study. The four steps are:
  1. Conducting a literature survey on the relevant research field.
  2. Defining the research objectives, assumptions and limitations.
  3. Developing the tools, models and methodologies to achieve the set research objectives.
  4. Verifying the developed tools, models and methodologies via theoretical and experimental means.
- There are three core research objectives that this research work sets out to achieve:
  1. The generation of a model that adequately describes the active fixture-workpiece system's response to external moving and oscillating loads.
  2. The definition of appropriate control algorithms and strategies for the seamless operation of a fully-active fixture.
  3. The composition of a fixture design methodology, which accounts for the capabilities of fully-active fixtures, and assists in drastically improving the results of a machining process in terms of surface quality and form accuracy.
- This study shall concentrate on thin-walled low-rigidity workpieces. Theoretical validations and test cases shall revolve around a thin-plate workpiece, which abides to Kirchhoff plate theory and its assumptions.
- The proposed models, concepts and methodologies are based on point-contact fixturing and the 3-2-1 fixturing paradigm.
- External loads are assumed to comprise a single component applied in the transverse direction of the plate. Also, they are simple harmonic in nature.
- Peripheral milling is assumed to be the source of external excitation throughout this thesis. The rigidity and mass of the cutting tool are not taken into consideration.

- Due to the above limitations in the developed models, it is not expected to achieve an absolute agreement between the results from the design methodology and the results from experiments. A qualitative agreement between the two sets of results is sought within this study.

- Parts of the developments of this work shall be validated theoretically, based on analytical and FEA-based tools and methods.

- A fully-active fixture concept is proposed. Its various hardware instantiations will be used as the platform on which the experimental validation procedures shall be conducted.

Chapter 4

A Comprehensive Model for Fixture-Workpiece Systems

4.1 Introduction

In Chapter 3 the three key research objectives of this work, along with a comprehensive methodology towards achieving them, were presented. The first of these objectives, namely the generation of a suitable model to predict the response of the fixture-workpiece system under external excitation, will be analysed in this chapter.

Modelling of fixturing systems is a research field that has received considerable attention. Fixture and workpiece models can assist in understanding the behaviour of a system under various excitations. This is the basis of improving and optimising the design and operation of fixtures, which is the overall goal of this research work. The literature review presented in Chapter 2 revealed the plethora of research work devoted to modelling of fixturing systems. It also highlighted that this work can be mainly categorised as follows:

- Modelling of the fixture and fixturing elements. In such work, it is often the case that the workpieces is treated as being rigid.
- Modelling the contact stiffness between fixture and workpiece.
- Modelling the friction between fixturing elements and workpiece.
- Modelling the dynamic response of the fixtured workpiece.
- Modelling of the dynamic characteristics of active clamping element of fixtures.

These models constitute either the basis of design and optimisation methods and methodologies, or serve as the means towards better understanding and predicting the behaviour of fixture-workpiece systems. Nevertheless, all of the reported work so far fails to capture in a comprehensive manner the moving dynamic loads of machining operations, the dynamics of low rigidity workpieces, and the effects that active fixtures have on such workpieces. Industrial sectors, like the aerospace and high-performance automotive, often deal with thin-walled monolithic workpieces that need to be machined in order to obtain their final form. Such workpieces tend to deflect and vibrate, rendering the design of a suitable fixturing solution a complicated procedure. Advanced fixturing systems promise to significantly facilitate fixturing operations, by integrating adaptive and responsive characteristics. These eliminate the concept of 'worst-case-based' fixturing approach, where the fixture layout and clamping intensity are designed to perform at the worst anticipated conditions. This can lead to over-clamping or complex fixtures. Over-clamping reduces form accuracy, whilst the adoption of complex fixturing solutions increases associated costs and diminishes accessibility. On the contrary, active fixtures are able to apply varying clamping loads in order to adequately compensate for the effects of external time-varying loads. Fully-active fixtures possess the added capability of repositioning their elements in order to achieve the optimal fixture layout for any given time instant and for various part geometries.

A model that successfully reflects the effects of moving machining forces and fully-active fixtures to the dynamic response of thin-walled structures shall be presented in this chapter. The chapter will be thematically split into three distinct parts. The first one deals with the model of thin-walled structures under moving dynamic loads. The second one concerns the modelling of active fixturing elements. In the final part, these two models are coupled together to form a model of the fixture-workpiece system. In this chapter, the fixture-workpiece model will reflect the open-loop operation of the system only. The closed-loop controlled operation of the model shall be discussed in the following chapter.

4.2 Finite Elements Model of a Workpiece

Thin-walled structures present challenging difficulties during machining. High elastic deformation and large vibration amplitudes characterise their behaviour during manufacturing

processes, e.g. peripheral milling. At the same time, such structures are widely met in aerospace, automotive and other industries, where low-weight, high-performance parts are of paramount importance. Therefore, and as thin-walled parts benefit more from advanced fixturing solutions [83], this research work targets such structures.

The modelling approach that will be described in this chapter, and which is based on Finite Element Analysis (FEA) [148], needs to be presented and proven through an example. Thin-walled structures often bear features with long flat surfaces, resembling thin plates and slender beams [86]. These features can be described using analytical expressions. As a result, a direct comparison FEA and analytical results is possible, allowing for theoretical validation of the developed models. Additionally, plate workpieces can easily be produced in bulk from sheet raw material, thus facilitating experimental work. For these reasons, a thin plate is defined as the primary workpiece within this thesis. This does not reduce the generality of the developed model. FEA is perhaps the most versatile method of modelling structural behaviour of parts, regardless of their geometry. As such, the same modelling approach developed here can be implemented on various different parts.

The plate workpiece, which is used as an example in this study, is made of aerospace grade aluminium alloy 7075-T6 and has a size of $150 \times 50 \times 3$ mm (length×width×thickness). The alloy presents a Young's modulus of elasticity of $E = 71.9$ GPa, Poisson's ratio $\nu = 0.33$ and a density of $\rho = 2800$ kg/m^3. These characteristics are summarised in Table 3.1.

One of the first steps when establishing an FEA-based model is the selection of appropriate finite elements. This selection shall be based on two aspects, namely the ability to predict the natural frequencies and the elastic deflection of a workpiece subjected to dynamic moving loads.

4.2.1 Natural Frequency Prediction Accuracy

The accuracy of the candidate elements in predicting the natural frequencies and the corresponding mode shapes of the system is of paramount importance. The reason behind this criterion is that the method that will be used to obtain the response of the plate workpiece to external dynamic loads, is based on modal parameters, such as its natural frequencies and mode shapes [47]. To identify the elements that best predict these characteristics, an exhaustive study was carried out. Two boundary condition cases were investigated. The

first involves a plate that is simply supported on its two opposite shorter sides (50 mm) and is free at the other two, and the second is a plate that has its two opposite shorter sides fully-constrained and the other two free. The former, referred to as Simply Supported-Free-Simply Supported-Free (SFSF) case was selected as it is the most commonly studied support case in the open literature. This facilitates validation of FEA results by means of established literature results. The latter, referred to as Clamped-Free-Clamped-Free (CFCF) case, was selected as it represents more closely the actual set-up that will be used during experimental work.

4.2.1.1 The Simply Supported-Free-Simply Supported-Free (SFSF) Case

The free vibration of the SFSF thin plate is perhaps the most commonly studied thin-plate scenario in literature. As a result, it is possible to find the natural frequencies and mode shapes of such plates readily available [18, 57]. Therefore, the need for experimental modal analysis to validate FEA results is drastically reduced. In this work, the eigenvalues from [57], calculated through Kirchhoff Plate Theory, are used. The natural frequencies can be evaluated from these eigenvalues using Equation (4.1).

$$\lambda_{(i,j)}^2 = \omega_{(i,j)} l_y^2 \sqrt{\frac{\rho}{D}} \tag{4.1}$$

where

$$D = \frac{Eh^3}{12(1-\nu^2)} \tag{4.2}$$

In the above equations D is the bending stiffness of the plate, h is the thickness of the plate, l_y is the width of the plate, λ is the eigenvalue and $\omega_{(i,j)}$ is the natural frequency in radians per second, with a corresponding mode shape that presents i half-sine waves along the X-direction, and j half-sine waves along the Y-direction of the plate. The first 64 natural frequencies of a SFSF aluminium plate with a width-to-length ratio of $\phi = 1/3$, are summarised in Table 4.1.

Abaqus [127], the FEA software used in this work, allows for 3 ways in which the thin plate can be approached [126]:

- A three-dimensional (3D) Deformable Planar Solid, using Structural Shell Square or Triangular elements, linear or quadratic, namely S4, S4R, S8R, S3 and STRI65

- A 3D Deformable Extruded Solid, using 3D stress, General Purpose Continuum Hexahedron, Tetrahedron or Wedge elements, linear or quadratic, namely C3D8, C3D8R, C3D20, C3D20R and C3D15.
- A 3D Deformable Extruded Solid, using 3D Continuum Shell Hexahedron or Wedge linear elements, namely SC8R and SC6R

Table 4.1: Natural frequencies of an aluminium SFSF plate with $\phi = 1/3$ [57]. Values shown in Hertz (Hz).

		j							
		1	2	3	4	5	6	7	8
i	1	307.12	1276.3	7124.8	18654	36081	59358	88477	123410
	2	1242.9	2780.3	8573.3	19994	37350	60568	89628	124530
	3	2822.8	4684.9	10745	22133	39385	62515	91545	126390
	4	5050.8	7101.2	13509	24982	42188	65259	94200	129010
	5	7924.3	10084	16828	28473	45669	68681	97593	132350
	6	11444	13668	20699	32570	49829	72841	101660	136390
	7	15613	17872	25142	37232	54609	77650	106470	141140
	8	20424	22702	30151	42483	60007	83108	111900	146570

A thin plate with the dimensions and properties shown in Table 3.1 was input in Abaqus and appropriate boundary conditions were imposed. When the plate is simulated as a 3D deformable planar solid, simply supported boundary conditions are set at the two shorter edges of the plate. Note that in this case the plate appears as a two-dimensional (2D) object in the user interface environment Abaqus/CAE. Simply supported boundary conditions are simulated by disallowing movement along the X-, Y- and Z-axis at one of the small edges (50 mm), and Y- and Z-axis at the other. All other points on the plate are free to move along all available degrees of freedom (DOF). When the plate is simulated as a 3D extruded solid, it appears as a three-dimensional object in the user interface. In this case, the same combination of axis movement constraints are applied at the lower small edges of the 3D object. This is schematically depicted in Figure 4.1.

The plate was then discretised using the previously mentioned element types and natural frequencies and mode shapes of the solid body were calculated. The first twenty frequencies and their corresponding mode shapes were requested as an output. The resulting natural frequencies obtained were sorted according to the standing half-sine waves in their mode shapes. They were then compared to the natural frequencies from literature (4.1). To facilitate the selection of the most appropriate type of finite elements, the performance

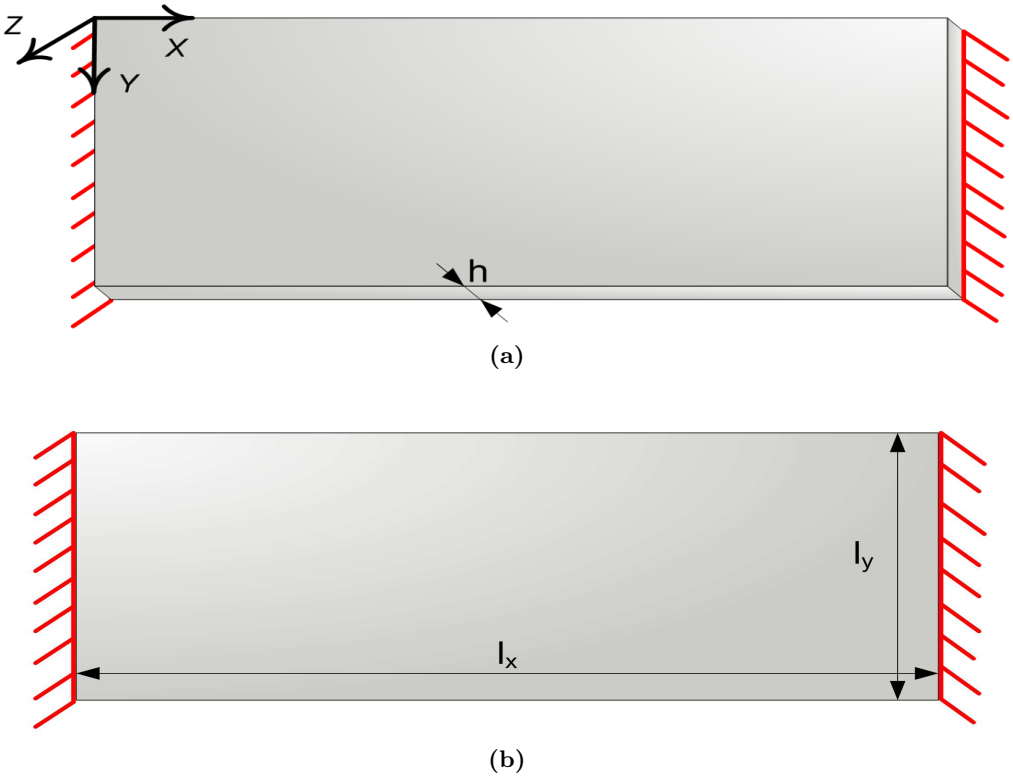

Figure 4.1: (a) Boundary conditions applied to a plate represented by a 3D extruded solid body. (b) Boundary conditions applied to a plate represented by a 2D planar solid body.

of each finite element type against four performance indicators is investigated. The first indicator is the prediction accuracy of the 1st natural frequency. In conventional milling operations, the spindle rotates at speeds from around 300 to 5000 rpm. Therefore the plate is excited at a frequency of 20 to 333 Hz, when a four-flute cutting tool is used. This, and since the fundamental natural frequency of the SFSF supported plate is above or very close to the previously-mentioned value, means that the frequency that will affect the behaviour of the system mostly is the fundamental frequency.

The second performance indicator is the maximum natural frequency prediction error. This constitutes a "worst-case-scenario" for every element.

The third performance indicator is the mean prediction error, which is calculated by averaging the prediction errors for the first twelve frequencies. These are the natural frequencies with mode shapes that exhibit no more that four standing half-sine waves along the X-direction, and no more that three standing half-sine waves along the Y-direction. This indicator assists in understanding how each element performs on average. In combination with the fundamental frequency error (smallest error) and the maximum error, one can understand how consistent the finite element is throughout the checked frequencies.

The final performance indicator is the number of nodes used to predict the natural frequencies. This number is critical as the more nodes needed, the bigger the system matrices become. As presented later within this chapter, large sized system matrices could lead to computational problems. Therefore, the FEA model was solved for natural frequencies and was checked for convergence. It is assumed that convergence is achieved when the resulting frequency values from two consecutive calculations, with different element grid densities, differ by no more than 3%. The lowest density is accepted as the final solution. The number of nodes reported in Table 4.2 was obtained after convergence was achieved, without violating the previously mentioned requirement.

The results from the above analysis are presented in Table 4.2. By denoting the FEA-derived results as FEA and the plate theory derived results as PT, all values in this table are percentages and were calculated according to:

$$\epsilon = \frac{FEA - PT}{FEA} \times 100\% \tag{4.3}$$

Table 4.2: Comparison of results from the investigated element types against the set performance indicators. SFSF Case.

Element Type	1st Frequency % Error	Max. % Error	Mean % Error	Nodes
S4	**0.10**	**-2.40**	**-0.74**	**341**
S4R	-0.03	4.00	-1.77	341
S8R	-0.05	-4.23	-1.94	981
S3	**0.09**	**-2.52**	**-0.13**	**341**
STRI65	-0.03	-3.60	-1.59	7701
C3D8	6.58	6.58	1.32	7904
C3D8R	-5.78	-9.93	-7.65	7904
C3D20	-0.15	4.82	-1.84	4947
C3D20R	-0.15	4.96	-1.91	4947
C3D15	-0.15	4.92	-1.89	6812
SC8R	-0.05	4.39	0.41	1500
SC6R	-0.07	5.28	1.62	1504

On these grounds, there are two elements that seem to be the ideal candidate for the FEA tasks of this research work. These are the S3 and the S4 elements. These elements not only predict accurately the natural frequencies of the workpiece, but also have the advantage of fast convergence and low computational power requirements. A detailed comparison between FEA results using all the previously mentioned finite elements and plate-theory-based data from Gorman [57] are given in Appendix B. As an example, obtained results by

using S3 elements are presented in Table 4.3.

Before a selection between the S3 and the S4 elements can be made, the CFCF case and elastic deformation prediction need to be considered.

Table 4.3: Natural frequencies of a thin plate with SFSF boundary conditions as predicted using S3 finite elements.

			j		
			1	2	3
i	1	PT	307.12	1276.3	7124.8
		FEA	307.40	1244.9	7081.0
		% Diff.	**0.09**	**-2.52**	**-0.62**
	2	PT	1242.9	2780.3	8573.3
		FEA	1265.0	2763.7	8533.1
		% Diff.	**1.75**	**-0.60**	**-0.47**
	3	PT	2822.8	4684.9	10745
		FEA	2834.8	4679.3	10732
		% Diff.	**0.42**	**-0.12**	**-0.12**
	4	PT	5050.8	7101.2	13509
		FEA	5087.8	7126.4	13575
		% Diff.	**0.73**	**0.35**	**-0.49**

4.2.1.2 The Clamped-Free-Clamped-Free (CFCF) Case

The above procedure was repeated for the Clamped-Free-Clamped-Free (CFCF) plate case. The plate used in this case is the same as the one in the SFSF case. The only aspect that changes is the boundary conditions. In the case where the plate is simulated as a planar solid, the boundary conditions are applied on the same edges as in the SFSF case. In the case where the plate is simulated as a three-dimensional solid, the boundary conditions are applied on the surfaces normal to the X- and Y-axes of the plate, as depicted in Figure 4.1. In both cases all six DOFs were constrained. Again, for comparison with FEA results, the natural frequencies of this system were calculated through the eigenvalues presented by [57] and by using Equation (4.1).

The same finite element types as in the SFSF case were examined for the CFCF case. The revealed pattern is similar to that of the simply supported boundary conditions. For this reason, only information about the best performing elements (SFSF case) from each of the three workpiece modelling approaches are documented in this section. These are the S4, S3, C3D20 and SC8R.

Just like in the SFSF case, for CFCF boundary conditions the 2D elements S4 and S3 present the best behaviour. S3 elements are only marginally more accurate compared to the S4 ones. Also, S4 elements under-predict the 1st natural frequency. On the contrary, S3 elements tend to over-predict it. Furthermore, these elements also present the most consistent prediction and the smallest maximum error. Comparison results between the best performing finite elements are summarised in Table 4.4.

Detailed results for each of the elements mentioned in Table 4.4 can be found in Appendix B. The previous analysis clearly pinpoints that either of the S4 or S3 finite elements is ideal for the FEA-based models of the thin-plate workpiece in this work. It should be noted that for workpieces with different geometrical features, other than plates, different elements are likely to present the best behaviour. It is therefore important that this analysis is repeated for different workpieces. When the geometrical features of the workpiece allow it, FEA results could be compared to theoretical ones. However, as the geometry of the workpiece becomes more complex, experimental modal analysis would be the preferred means of validation.

Table 4.4: Comparison of results from the investigated element types against selected performance indicators. CFCF case.

Element Type	1st Frequency % Error	Max. % Error	Mean % Error	Nodes
S4	**-0.02**	**-2.87**	**-0.74**	**341**
S3	**0.02**	**-0.73**	**-0.13**	**341**
C3D20	-1.33	-4.58	-2.58	4947
SC8R	-0.06	-7.32	-2.60	1500

4.2.2 Elastic Deformation of a Plate under a Moving Load

The analysis described in the previous paragraphs revealed that finite elements S3 and S4 can accurately predict the natural frequencies of the selected plate workpiece. Before a final decision between these two elements can be made, it is necessary to investigate their performance in predicting the elastic deformation of the workpiece due to time-varying moving external loads. A method to simulate these loads needs to be established first.

4.2.2.1 Simulation of Dynamic Moving Loads

In order to obtain a solution on the deformation of the workpiece, the forces applied on the structure need to be defined. In the following analysis it will be assumed that the load

moves in a straight line marked by a series of nodes, along one of the Cartesian axis, with a constant speed. Furthermore, it is assumed that the grid of nodes can be defined in a structured way, i.e. each node is separated by its neighbouring nodes by a fixed distance. As the load moves along one Cartesian axis and it passes through a series of equidistant nodes, it can be concluded that the load always travels on one of the edges of an element. For instance, if a square finite element with four nodes is used for the analysis (S4 element), then the load must always travel along one of the edges of the element and between the two nodes that define that edge. Finally, the subsequent analysis is focused on a concentrated moving load. However, the approach can be applied with no adaptation to the case of moving distributed loads. This is because in FEA, distributed loads can be simulated as a series of concentrated loads. Therefore, the same analysis applies to each one of these concentrated loads.

Abaqus offers two ways to solve a problem. One is through Abaqus/Standard and the other through Abaqus/Explicit [127]. In both solvers, there is not a straightforward way for dynamic moving loads to be simulated. Additionally, Abaqus/Explicit, although tailored for dynamic problems, is computationally extremely expensive and even simple problems could require hours of processing time to reach a solution. Therefore, an indirect method of simulating the moving nature of machining loads needs to be established. A number of researchers have dealt with the approximation of moving loads applied to discretised structures, e.g. [37, 113, 142]. A similar approach to the one presented in [142] for beams is used in this work. In FEA software like Abaqus, loads can only be defined on nodes. As a load moves from one node to another, it is possible to approximate the load by a set of forces and moments applied on the two neighbouring nodes, between which the load moves (Figure 4.2).

In Figure 4.2 the number of the element within which the load moves is denoted by s, u is the distance of the load from the node through which the load entered the element, l is the length of the element, $f_1^{(s)}(t)$, $f_3^{(s)}(t)$ are the resulting nodal shear forces of the two nodes, and $f_2^{(s)}(t)$, $f_4^{(s)}(t)$ are the nodal moments, respectively. These quantities can be calculated through:

$$f_1^{(s)}(t) = N_1 P(t) \tag{4.4}$$

$$f_2^{(s)}(t) = N_2 P(t) \tag{4.5}$$

$$f_3^{(s)}(t) = N_3 P(t) \tag{4.6}$$

$$f_4^{(s)}(t) = N_4 P(t) \tag{4.7}$$

with N_1, N_2, N_3, and N_4 being the shape functions of the elements. They depend on the type of the element used. As shown in [142], moments can be ignored without significant loss of accuracy in predicted displacements. Also, as the load moves between two nodes, and for small elements, the problem can be further simplified by ignoring the shape functions and assuming that the loads at the nodes can be simply calculated through linear interpolation. The relationship between the moving load and the nodal forces can then be calculated by implementing Newton's First Law. If c is the velocity with which the load traverses the structure, t it time and $s = 1, 2, \ldots, n$ is the sequential number of each element that the load passes over, then the nodal loads for every element are given by:

$$f_1^{(s)}(t) = P(t)\left(1 - \frac{ct - sl}{l}\right) \tag{4.8}$$

$$f_3^{(s)}(t) = P(t)\left(\frac{ct - sl}{l}\right) \tag{4.9}$$

The values of the nodal forces need to be defined in a discrete fashion. To do this, time t is defined as $t = m\Delta t$, with m signifying the number of time steps. For a simple harmonic concentrated load $P(t) = 150(1 + \cos \omega t)$, with $\omega = 198$ Hz and $c = 0.033$ m/s, moving on the centreline parallel to the X-axis of the plate workpiece, the nodal forces on the second element and the overall moving load are presented in Figure 4.3.

The calculated force amplitudes need to be incorporated in Abaqus and the model is

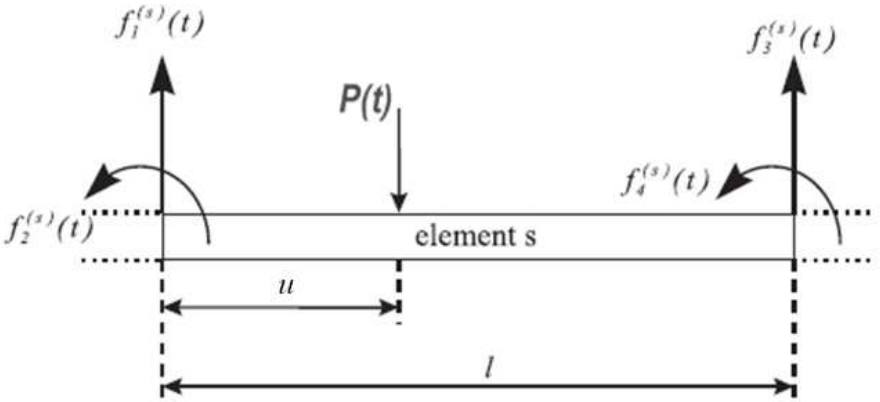

Figure 4.2: Representation of a moving load $P(t)$ and the resulting nodal loads [142].

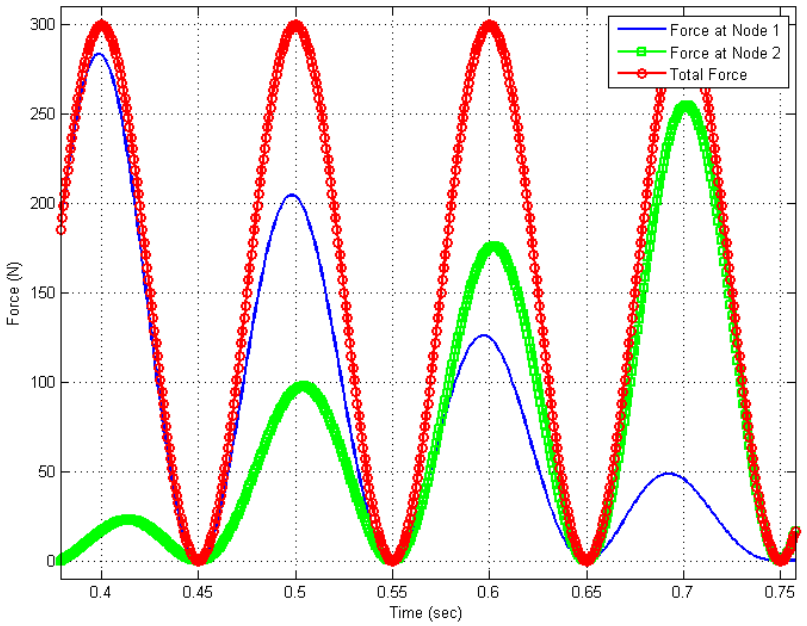

Figure 4.3: Moving concentrated load $P(t) = 150\,(1 + \cos\omega t)$ with $\omega = 10$ Hz and its Resulting Nodal Forces on the two Nodes of the Second Element (S4).

then solved for elastic deformation. The first aspect than needs to be defined in Abaqus before the nodal forces can be defined, is an analysis step. In Abaqus/Standard dynamic problems can be solved using one of the available Linear Perturbation steps. However, only one step produces the general solution (transient and steady-state), whilst allowing for the definition of loads in the time domain. This step is the Modal Dynamics step [125]. This step requires as a minimum input the time duration for which Abaqus should produce a solution and the size of each time step. Then, Abaqus will produce a solution for every time point.

The nodal forces caused by the moving load and their amplitudes, calculated earlier, can now be introduced in the FEA software. Abaqus offers the possibility to enter the force amplitudes in the form of a matrix. This is the most convenient way to introduce the nodal forces. In the first column of this matrix, time is defined. Each row represents the amplitude of the load at a time instant. In the second column the amplitude of the force applied to a node can be defined. Each of these amplitudes remains constant between two consecutive time instants. The force at each node has a zero amplitude until the moving load reaches the element, to which the node belongs to. From that time instant, until the instant where the moving load leaves the element, the force obtains non-zero values according to the amplitude values per instant calculated earlier. From the time instant that the load leaves the element until the end of the simulation time, the nodal force is

again set at a zero-amplitude value. With all nodal forces and their amplitudes defined, the problem can then be solved.

4.2.2.2 Elastic Deformation of a Workpiece

In order to select the most appropriate element type, it is necessary to calculate the displacement experienced by the workpiece as the load traverses it. In Abaqus, and after having established an element type, a loading case and an analysis step, solving the problem is straightforward. Nevertheless, it is of paramount importance to establish a method through which the obtained FEA results can be validated. This will also assist in proving the correctness of the method for simulating moving loads and supply a measure, against which the displacement prediction performance of the different types of elements can be compared. Validation of results can be achieved either by experimental or analytical means. The former poses numerous difficulties. Assuming a thin-walled and plate-like workpiece, fixtured by a fully-active fixture, then both of the main surfaces of the workpiece are in contact with moving elements. On one side, the cutting tool traverses the workpiece while removing material, and on the other side the element of the fixture changes position. As a result, the placement of contact-based sensors is almost entirely prohibited. Non-contact sensing methods are also particularly hard to implement, as the sensing elements could be obstructed from the fixture, or the machine tool. On top of that, the cost, time and effort required for such experiments are large. So, unless there is no other appropriate way of validation, experiments could be successfully substituted by theoretical means, especially when initial validation is the goal. When using simplified geometry workpieces, one can deploy analytical models to describe the response of such structures, hence reducing the need for experimental validation, at least at the initial stages of development. This was also one of the primary reasons for selecting a thin plate as the test workpiece for this research work.

Analytical model of SFSF plate excited by a moving distributed harmonic load. There has been a lot of interest from the research community for plate structures and consequently analytical models are available and could be used for validation of the FEA models developed within the context of this work. The analytical model that will be used throughout this thesis is the one described by Frýba [52]. The model concerns a thin-plate

that is simply supported on two opposite sides with no constraints on the other two sides. The equation that describes the motion of a plate under a time varying moving load is given by:

$$D\left[\frac{\partial^4 w\left(x,y,t\right)}{\partial x^4}+2\frac{\partial^4 w\left(x,y,t\right)}{\partial x^2\partial y^2}+\frac{\partial^4 w\left(x,y,t\right)}{\partial y^4}\right]+\mu\frac{\partial^2 w\left(x,y,t\right)}{\partial t^2}=p\left(x,y,t\right) \tag{4.10}$$

In the above equation:

$w(x,y,t)$: Transverse displacement of plate at point (x,y) at time t

D: Bending rigidity of plate

E: Young's Modulus

h: Plate Thickness

ν: Poisson's Ratio

μ: Mass per unit area

$p(x,y,t)$: External load applied at point (x,y) at time t

In the case of an evenly distributed moving line load, moving at constant speed along the X-axis of the plate, as the ones experienced by a workpiece undergoing a milling operation, the load can be expressed by:

$$p\left(x,y,t\right)=\delta\left(x-ct\right)\int_{\eta_1}^{\eta_2}P(t)\delta\left(y-\eta\right)dy \tag{4.11}$$

In Equation (4.11), c is the constant speed with which the load moves along the X-axis, t designates time, η designates the line parallel to the X-axis, along which the force moves, and $P(t)$ is the load magnitude at time instant t. Furthermore, δ signifies the Dirac function. For the SFSF case the boundary conditions are expressed mathematically as:

For $y=0$ mm and $y=l_y$:

$$w=0,\quad \frac{\partial^2 w}{\partial x^2}+\nu\frac{\partial^2 w}{\partial y^2}=0 \tag{4.12}$$

For $x=0$ mm and $x=l_x$:

$$\frac{\partial^2 w}{\partial x^2}+\nu\frac{\partial^2 w}{\partial y^2}=0,\quad \frac{\partial^3 w}{\partial x^3}+\left(2-\nu\right)\frac{\partial^3 w}{\partial x\partial y^2}=0 \tag{4.13}$$

Zero initial conditions are assumed, i.e. the system is initially at rest, which can be

expressed as:

$$w(x,y,0)=0, \quad \frac{\partial w(x,y,0)}{\partial t}=0 \tag{4.14}$$

Multiplying Equation (4.10) with $\sin({}^{i\pi x}/_{l_x})w_{(j)}(y)$, integrating both sides twice, along both the X- and Y-axis and using the two-dimensional Fourier finite sine-integral transformation, and by using the substitution:

$$W(i,j,t)=\int_0^{l_x}\int_0^{l_y} w(x,y,t)\sin\frac{i\pi x}{l_x}w_{(j)}(y)dydx \tag{4.15}$$

Equation (4.10), transforms into:

$$\ddot{W}(i,j,t)+\omega_{(i,j)}^2 W(i,j,t)=\frac{1}{\mu}\sin\omega_x t\int_{\eta_1}^{\eta_2} P(t)w_{(j)}(k)dy \tag{4.16}$$

The Laplace-Carson transformation is deployed to solve this equation [52]. After finding the solution and applying the inverse transformation, the general expression for the transverse displacement of an SFSF plate subjected to a time-varying load moving parallel to the x-axis at constant speed is:

$$\begin{aligned} w(x,y,t) \;=\; & \sum_{i=1}^{\infty}\sum_{j=1}^{\infty}\frac{2\mu}{l_x W_j}\sin\left(\frac{i\pi x}{l_x}\right)w_j(y)\frac{1}{\mu\omega_{(i,j)}}\times \\ & \int_0^t P(\tau)\sin(\omega_x\tau)\,w_{(j)}(\eta)\sin\left[\omega_{i,j}(t-\tau)\right]d\tau \end{aligned} \tag{4.17}$$

where:

$$W_j=\int_0^{l_y}\mu w_{(j)}^2(y)dy \tag{4.18}$$

Here, $w_{(j)}(y)$ is a function that satisfies the boundary conditions on the edges $y=0$ and $y=l_y$, as well as the equation of the free vibration of the plate. For a detailed expression of $w_{(j)}(y)$ please refer to [52] pp. 257-259. Also, $w_{(j)}(\eta)$ is the same expression for $y=\eta$. Circular natural frequencies of the plate are designated by $\omega_{(i,j)}$. Additionally,

$$\omega_x=\frac{i\pi c}{l_x} \tag{4.19}$$

is the excitation frequency due to the movement of the external load. Equation (4.17) is valid for $0\le t\le l_x/c$. As mentioned in Section 3.2.2 of Chapter 3, the external forces

from the machining process could be simplified to harmonic loads. In the case of milling operations, the force magnitude fluctuates between zero value (no tool teeth engaged) to full value (maximum depth of cut). Therefore, these loads can be expressed in the form $P(t) = \int_{\eta_1}^{\eta_2} P(\eta)(1 + \cos\omega_f t)d\eta$. If this form is substituted into Equation (4.17) and for a constant amplitude concentrated moving load $P(t) = P$ [52]:

$$\begin{aligned} w(x,y,t) &= \sum_{i=1}^{\infty}\sum_{j=1}^{\infty} \frac{2P}{l_x W_j} \frac{1}{\omega_{(i,j)}^2 - \omega_x^2} \sin\left(\frac{i\pi x}{l_x}\right) w_{(j)}(\eta) w_{(j)}(y) \times \\ &\quad \left[\sin(\omega_x t) - \frac{\omega_x}{\omega_{(i,j)}} \sin\left(\omega_{(i,j)} t\right)\right] \end{aligned} \tag{4.20}$$

the transverse displacement of the thin-plate can be expressed as:

$$\begin{aligned} w(x,y,t) &= \sum_{i=1}^{\infty}\sum_{j=1}^{\infty} \frac{2}{l_x W_j} \frac{1}{\omega_{(i,j)}^2 - \omega_x^2} \sin\left(\frac{i\pi x}{l_x}\right) w_{(j)}(y) \times \\ &\quad \int_{\eta_1}^{\eta_2} P w_{(j)}(\eta) d\eta \left[\sin(\omega_x t) - \frac{\omega_x}{\omega_{(i,j)}} \sin\left(\omega_{(i,j)} t\right)\right] + \\ &\quad \sum_{i=1}^{\infty}\sum_{j=1}^{\infty} \frac{2P}{l_x W_j} \sin\left(\frac{i\pi x}{l_x}\right) \int_{\eta_1}^{\eta_2} P w_{(j)}(\eta) d\eta w_{(j)}(y) \times \\ &\quad \frac{1}{\omega_{(i,j)}} \int_0^t \cos(\omega_f \tau) \sin(\omega_x \tau) \sin\left[\omega_{(i,j)}(t-\tau)\right] d\tau \end{aligned} \tag{4.21}$$

where τ expresses a time instant within the time span $0 \leq t \leq l_x/c$. The above formula calculates the steady-state transverse displacement of a homogeneous thin plate, excited by a harmonic distributed moving load applied normal to the plate. This is schematically depicted in Figure 4.4. The plate is only supported at its edges that are parallel to the Y-axis. The load is distributed along a line parallel to the Y-axis. The load is distributed between $y = \eta_1$ and $y = \eta_2$. It moves at a constant speed along the X-axis. The traverse displacement can be conveniently calculated through Equation (4.21) using software like Matlab, and then it can be compared to FEA results. Before this model can be confidently applied for validation purposes, it would be wise to ensure that it is correct. The validation of this model is presented in Appendix A.2.

Selection of finite elements based on elastic deformation prediction and validation of the FEA model. In order to reach a final decision on which of the S4 and S3 elements are better suited for the structural workpiece model, the previously established

FEA problem was solved using both elements. The results of these were then compared to results obtained by solving the analytical expression for the displacement of a SFSF plate under a distributed moving harmonic load (Equation (4.21)). The elastic deformations at various points on the plate, when the tool is at $x = 50$ mm ($t = 1.515$ s), are summarised in Table 4.5. For results from other time instants within the duration of the machining load movement, please refer to Appendix C. As stated before, the moving load is a distributed one, applied in the upper half of the plate ($y = 0$ to $y = 25$ mm), as shown in Figure 4.4. Table 4.6 presents a comparison between the two element types of interest against three performance indicators. These are the minimum, the maximum and the mean percentage error. The first one represents the best agreement between FEA and analytic results, whilst the second one reflects the worst. The mean percentage error, calculated by used the data from all the tables presented in Appendix C, gives a good indication of how consistently does a finite element predict the elastic deformation of the workpiece correctly.

From these two tables it can be concluded that the best performing finite element is the S4 element, even though only marginally. In more detail, the utilisation of S4 elements leads to a smaller minimum percentage error and a marginally better (by 0.01%) mean percentage error. This means that, on average, the S4 element produce elastic deformation results that are closer to the ones produced by the analytic model. A closer look in Table 4.5 further underlines this claim. In this table, the S4 elements predicts the elastic deformation of the workpiece better at 17 out of the 20 points presented. On the other hand, S3 elements lead to a smaller maximum percentage error. This is the only performance indicator for which the S3 elements outperform the S4 ones. Based on the above, and since the developed model has the overall scope of predicting workpiece displacement as accurately as possible, the S4 elements are considered as the better option and shall, therefore, be used in the finite element (FE) models throughout this study.

The results in Tables 4.5 and 4.6 also prove the validity of the developed FEA-based plate workpiece model. At this stage, a suitable model of the thin plate workpiece excited by moving harmonic distributed loads has been successfully established. This includes the identification of appropriate finite elements, method of simulation of moving loads in FEA, and the analysis step. Although the previous results correspond to SFSF conditions, the developed model is still valid for other types of boundary conditions. This is justified through the results on the natural frequency prediction, which were presented in

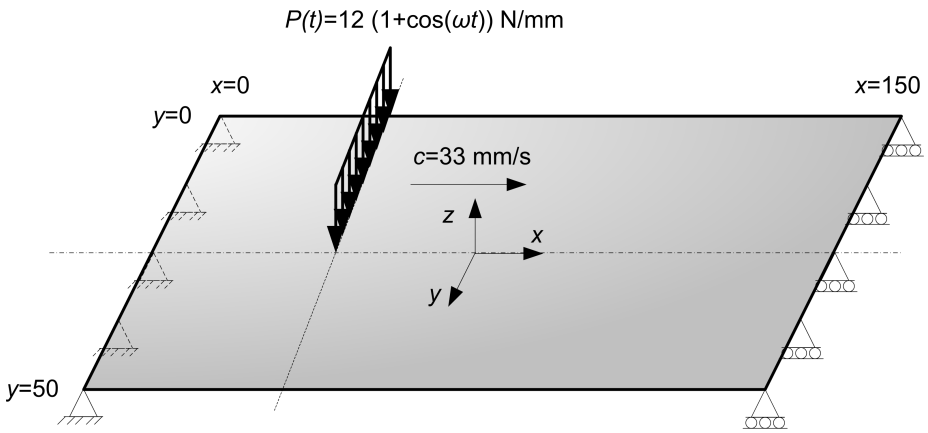

Figure 4.4: Moving distributed harmonic load of magnitude $P = 12$ N/mm traversing a SFSF plate.

Section 4.2.1, and through which it was shown that the FE model can accurately predict the modal characteristics of the workpiece for the two cases of boundary conditions that were investigated.

4.3 Model of the Active Fixturing Elements

With the structural dynamic model of the workpiece established, the attention can now be focused on the active fixturing elements. Due to the complexity and diversity in localisation and fixating needs of the different workpieces, many work-holding concepts have been presented over the history of manufacturing. These include vices, chucks, jigs and fixtures. The latter, and especially its 3-2-1 principle-based variation [96] has been widely used for its accuracy and robustness. Nevertheless, 3-2-1 fixtures could greatly benefit from introducing adaptive and intelligent capabilities into them. Fixtures have three types of fixturing elements, namely clamps, locators and supports. Locators are used to position and orientate the workpiece. Traditionally, they are considered passive. However, in fully-active fixtures, like the ones studied throughout this research work, it is necessary for these elements to be active and able to change their position and orientation in space. The same applies to clamps. In traditional fixtures, clamps are static elements with the ability to apply a fixed force. This force is used to push the workpiece against the locators and hence hold it in place. In an active fixturing solution, clamps have the added capability of applying time-varying forces, adapting to external force stimuli. In fully-active fixturing systems, clamps not only modify the force they apply, but they can also reposition during

Table 4.5: Comparison of transverse displacement of a SFSF plate excited by a distributed load of 12 N/mm applied from $x = 0$ to $x = 25$ mm. The load traverses the length of the plate at 33 mm/sec. Results from Kirchhoff plate theory are denoted as PT and from FEA as S4 or S3, depending on the elements used. Displacement values measured at $t = 1.515$ s, i.e. when the moving load is at $x = 50$ mm. The % differences calculated via Equation (4.3). Coordinate values are in mm and displacement values are in μm.

Time=1.515 sec, Load @ x=50 mm					
		x=5	x=25	x=50	x=75
y=0	PT	-372.20	-1773.59	-3007.21	-3252.20
	S4	-386.18	-1855.59	-3118.95	-1412.23
	% Diff.	3.62	4.42	3.58	3.53
	S3	-388.02	-1853.63	-3137.98	-3391.43
	% Diff.	4.08	4.32	4.17	4.11
y=10	PT	-352.61	-1679.40	-2848.59	-3101.91
	S4	-363.98	-1752.23	-2946.26	-3208.40
	% Diff.	3.12	4.16	3.32	3.32
	S3	-366.53	-1751.10	-2965.87	-3229.88
	% Diff.	3.80	4.09	3.95	3.96
y=25	PT	-332.04	-1280.53	-2680.39	-2947.11
	S4	-341.63	-1643.19	-2764.17	-3038.88
	% Diff.	3.12	3.81	3.03	3.02
	S3	-344.63	-1643.01	-2785.32	-3062.42
	% Diff.	3.65	3.80	3.77	3.76
y=40	PT	-321.65	-1530.14	-2592.24	-2873.81
	S4	-330.46	-1586.00	-2666.51	-2954.35
	% Diff.	2.67	3.52	2.79	2.73
	S3	-333.68	-1586.49	-2689.33	-2980.50
	% Diff.	3.60	3.55	3.63	3.58
y=50	PT	-320.88	-1525.90	-2584.98	-2873.18
	S4	-329.21	-1578.56	-2652.90	-2947.85
	% Diff.	2.53	3.34	2.56	2.53
	S3	-332.69	-1579.41	-2678.09	-2975.93
	% Diff.	3.55	3.39	3.48	3.45

Table 4.6: Statistical comparison of results from transverse elastic deformation of a SFSF plate.

Element Type	Min. % Error	Max. % Error	Mean % Error
S4	1.83	6.15	3.78
S3	2.76	5.54	3.79

the manufacturing process. Therefore, they are similar in operation to locating elements, with the added ability to exert forces on the workpiece. It is then obvious that locators are a sub-category of active clamping elements of a fully-active fixture. Therefore, the focus of the following analysis shall be placed on clamping elements, but it applies in full to locating elements too. Supports are extra elements used to increase the local stiffness of the fixture-workpiece system. Such elements are not strictly necessary in fully-active fixturing systems and will not be covered by this work.

Active clamping elements constitute a key component of advanced fixturing solutions. They are the source of the actively-changing forces applied from the fixture. Many actuation technologies have been proposed as the basis of the active clamping elements, such as hydraulic [13, 14], electromechanical [15, 98] and piezoelectric [12, 110]. The technology used to achieve the necessary force adaptation depends heavily on the desired results. Active vibration compensation through the fixture can only be realised using an actuation technology with the ability to react fast to system changes, since vibration is characterised by high acceleration. Piezoelectric actuators constitute an example of an actuation technology with such abilities. However, piezoelectric actuators present significantly limited travel ranges. For this reason they are often used as part of a hybrid actuation solution [80, 99]. When adaptation of the clamping forces is only necessary at a lower frequency, then electromechanical actuation solutions are more than adequate. Electromechanical actuators have the added benefit of large travel ranges and integrated position and (in some cases) force-sensing ability. Also, they are more compact, they respond faster, and are easier to control compared to hydraulic solutions. For these reasons, this work shall focus on electromechanical clamps. The actuators used will be Permanent Magnet Alternating Current (PMAC) motor-based ones. These actuators can deliver larger forces from small-sized motors compared to Direct Current (DC) motor electromechanical units [83, 98]. Furthermore, PMAC actuators respond faster to inputs.

A typical active clamping element operating in a closed-loop fashion is presented in Figure 4.5. In brief, the closed-loop system comprises a computer with a motion controller, an interface board (connector box), the controller of the actuator, and the actuator itself. The position-feedback loop is closed by using a built-in incremental quadrature encoder and the actuator controller. The force-feedback loop requires a force sensor to feed the force signals back to the motion controller. The force sensor signal needs first to be condi-

tioned through an appropriate amplifier, and then fed to the motion controller through the connector box. Please note that this configuration is not the only possible one. Depending on the supplier of the necessary equipment, different set-ups could be deployed. However, the principle and the core components remain the same.

In this chapter the focus will be placed upon the open-loop operation of the actuator. The closed-loop will be covered in the following chapter. The open-loop configuration, comprising the actuator and its controller, can be represented through the block diagram shown in Figure 4.6. According to this figure, the system accepts a voltage V_{cc} as the command input, which is referred to as control voltage. This is applied on the actuator controller, which comprises two parts, namely a transconductance amplifier and a low-pass filter. The first is charged with the task of transforming the applied voltage into current (I_{in}). The latter is conditioned by the low-pass filter, producing the current I_m, which is applied to the motor winding (armature) of the actuator. With electric current applied on the armature of the motor, a voltage V_m is also generated. The rotor of the motor is then forced to turn, causing the displacement of the tip of the actuator. Provided that the actuator is in contact with an object, the actuator generates a force F_A on the object.

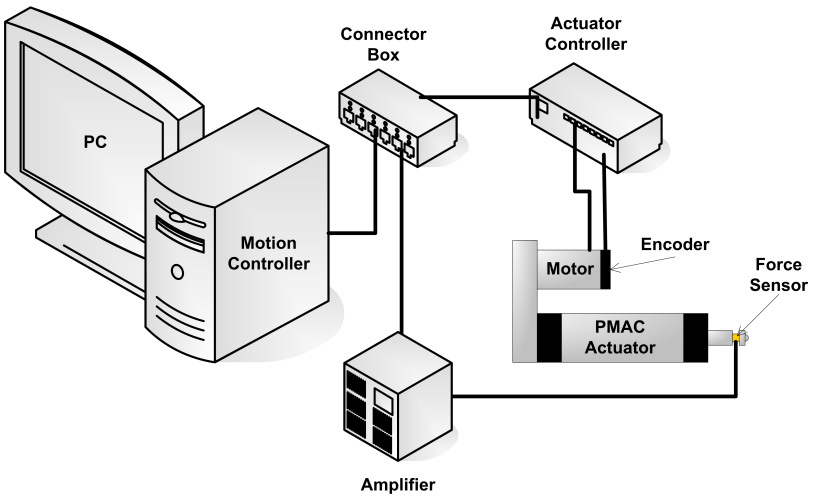

Figure 4.5: Schematic of an active clamping fixture element and its necessary components.

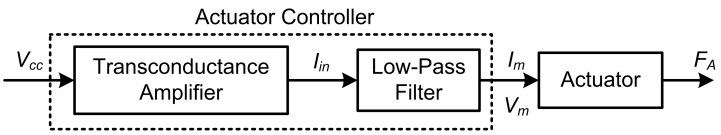

Figure 4.6: Block diagram of the actuator and its peripherals in open-loop operation.

4.3.1 Modelling of the Actuating Unit

In order to capture the dynamic response of an actuating systems, such as the one presented in Figures 4.5 and 4.6, the preferred method is by using analytical expressions. In this way the response of the actuator due to both its mechanical and electrical components can be captured. Modelling and analysis of AC motors are more complicated and cumbersome than that of DC motors. However, according to Franklin *et al.* [50], when dealing with a high-resistance AC motor, then the system can be approximated as a DC motor.

Electromechanical actuators are usually composed of two distinct parts. The electrical motor and the gears and ball-screw mechanism. The former supplies the movement to the actuating unit in form of rotation. The gears and ball-screw mechanism transforms the rotary motion into linear motion. When the actuator is in contact with a simple system, like e.g. a mass-spring-damper one, the mechanical parts of the actuator can be schematically represented as shown in Figure 4.7. In this figure x_A, k_i and c_i are the displacement of the actuator tip, stiffness coefficients and damping coefficients respectively. Using the notation:

- J_{tot}: Moment of inertia of rotating components within the actuator in kg m^2
- θ: Angular displacement of motor in rad
- K_T: Motor torque constant in Nm/A
- f_r: Viscous damping coefficient of motor in Nm/rpm
- T_e: Externally applied torque in Nm
- I_m: Motor input current in A
- V_m: Motor input voltage in V
- L_m: Motor armature inductance in H
- R_m: Motor armature resistance in Ω
- K_{emf}: Electromotive force coefficient in V/rpm

the mechanical side of the actuator can then be mathematically described as:

$$J_{tot}\ddot{\theta} + f_r\dot{\theta} = K_T I_m - T_e \tag{4.22}$$

The electrical circuit of the motor can be simplified to the one shown in Figure 4.8 and

is mathematically described by:

$$L_m \dot{I}_m + R_m I_m = V_m - K_{emf} \dot{\theta} \tag{4.23}$$

The external torque can be calculated as:

$$T_e = \frac{p \eta_2 F_e}{2\pi G_{rr}} \tag{4.24}$$

with:

p: Actuator ball screw pitch in mm/rev

η_2: Reverse efficiency coefficient of ball-screw

F_e: Reaction force from spring and damper in N

G_{rr}: Gear ratio

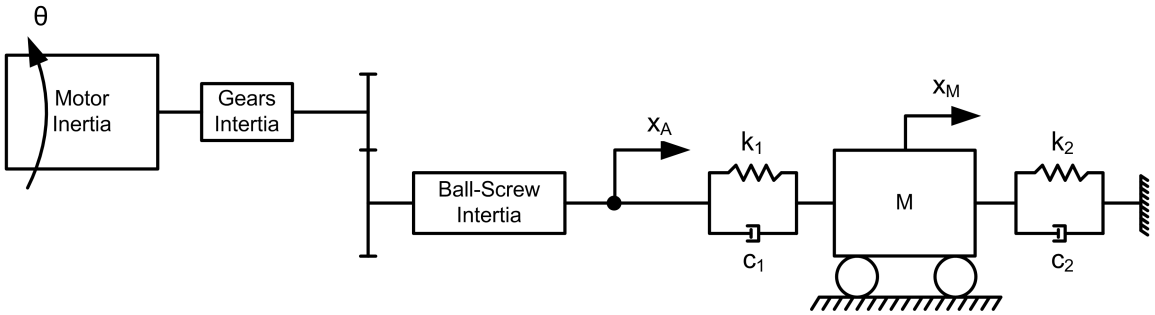

Figure 4.7: Mechanical model of the actuator in contact with a simplified workpiece through springs and dampers.

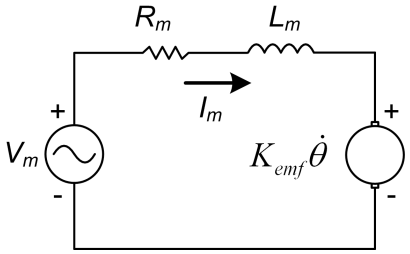

Figure 4.8: Electrical model of the actuator motor [50].

Furthermore, from the free body diagram of mass M, the following equation is derived:

$$M\ddot{x}_M = k_1 (x_A - x_M) + c_1 (\dot{x}_A - \dot{x}_M) - k_2 x_M - c_2 \dot{x}_M \tag{4.25}$$

where:

k_1: Actuator tip-mass connecting spring stiffness in N/m

k_2: Earth-mass connecting spring stiffness in N/m

c_1: Actuator tip-mass connecting damper coefficient in Ns/m

c_2: Earth-mass connecting damper coefficient in Ns/m

x_A: Actuator tip displacement in m

x_M: Actuator tip displacement in m

The reaction force F_e induced on the actuator by the spring-damper system between actuator tip and mass can be calculated as:

$$F_e = k_1 (x_A - x_M) + c_1 (\dot{x}_A - \dot{x}_M) \tag{4.26}$$

Finally, the actuator tip displacement and the angular displacement of the motor can be related through:

$$x_A = \frac{p\theta}{2\pi G_{rr}} \tag{4.27}$$

4.3.2 Modelling the Actuator Controller

The actuator controller affects the response of the actuator and should therefore be included in the system model too. In general, the actuator controller can be approached as a black box, where the control voltage applied to it and the voltage outputted by the controller to the actuator can be related through [15]:

$$\frac{V_m}{V_{cc}} = \frac{1}{\frac{1}{\omega_\nu^2} s^2 + \frac{2\beta_\nu}{\omega_\nu} s + 1} \tag{4.28}$$

where:

V_{cc}: Control voltage applied to the controller in V

s: Laplace variable

ω_ν: The bandwidth of the controller in Hz

β_ν: Damping coefficient

However, if the controller's block diagram is known, then a more precise model can be formulated. In the experimental device used in this work (Sections 3.3.4 and 7.3), the selected actuator controller [35], when in torque/current mode, operates in a simple manner. Its sole role is to condition the input voltage signal by transforming it into current

and passing it through a low-pass filter.

The transformation of input voltage takes place through a transconductance amplifier. The operation of the amplifier, based on the notation used in Figure 4.6, can be described by:

$$G_{ac} = \frac{I_{in}}{V_{cc}} \tag{4.29}$$

with I_{in} being the current from the amplifier, measured in Ampères (A), and G_{ac} being the gain of the amplifier. The low-pass filter can be approached as a simple Resistor-Capacitor Circuit (RC) as the one shown in Figure 4.9. The differential equation describing the

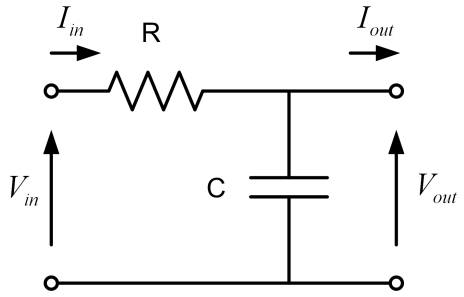

Figure 4.9: Electrical diagram of RC-filter circuit.

relationship of input and output voltage is:

$$V_{out} + RC\dot{V}_{out} = V_{in} \tag{4.30}$$

C is the capacitor constant (capacitance) of the filter, measured in Farad (F), R is the resistance value of the filter, in Ohm (Ω), and V_{in} and V_{out} are the input and output voltage, respectively, in Volts (V). However, based on Ohm's law $V_{in} = RI_{in}$ and as $V_{out} = V_m$, Equation (4.30) can be rewritten as:

$$V_{out} + RC\dot{V}_{out} = RI_{in} \tag{4.31}$$

4.4 Model Formulation in a Matrix Form

Before the actuator model and the workpiece model can be coupled, it is first necessary to express the system in a matrix form. At this stage, only Equations (4.22) and (4.24)-(4.27), are formulated into a system of equations taking a matrix form. This is due to the fact that Equation (4.23), contrary to the previously-mentioned equations, is a first order ordinary differential equation (ODE). If all equations are expressed in a matrix form at the same

time, then one of the system matrices will contain rows and columns with zero elements. This will lead to numerical issues when attempting to transfer the system into state-space.

Equations (4.22), (4.24), (4.26), and (4.27) can be combined into the following equation:

$$J_{tot}\ddot{x}_A + f_r\dot{x}_A = \left(\frac{p}{2\pi G_{rr}}\right)^2 K_T I_m - \left(\frac{p}{2\pi G_{rr}}\right)^2 \eta_2 \left[k_1 \left(x_A - x_M\right) + c_1 \left(\dot{x}_A - \dot{x}_M\right)\right] \quad (4.32)$$

The above equation, along with Equation (4.25) can be expressed as follows:

$$[M_{ac}] \begin{Bmatrix} \ddot{x}_M \\ \ddot{x}_A \end{Bmatrix} + [C_{ac}] \begin{Bmatrix} \dot{x}_M \\ \dot{x_A} \end{Bmatrix} + [K_{ac}] \begin{Bmatrix} x_M \\ x_A \end{Bmatrix} = \begin{Bmatrix} 0 \\ \left(\frac{p}{2\pi G_{rr}}\right)^2 K_T I_m \end{Bmatrix} \quad (4.33)$$

with:

$$[M_{ac}] = \begin{bmatrix} M & 0 \\ 0 & J_{tot} \end{bmatrix} \quad (4.34)$$

$$[C_{ac}] = \begin{bmatrix} c_1 + c_2 & -c1 \\ -c_1 \left(\frac{p}{2\pi G_{rr}}\right)^2 \eta_2 & f_r + c_1 \left(\frac{p}{2\pi G_{rr}}\right)^2 \eta_2 \end{bmatrix} \quad (4.35)$$

$$[K_{ac}] = \begin{bmatrix} k_1 + k_2 & -k1 \\ -k_1 \left(\frac{p}{2\pi G_{rr}}\right)^2 \eta_2 & k_1 \left(\frac{p}{2\pi G_{rr}}\right)^2 \eta_2 \end{bmatrix} \quad (4.36)$$

In order to apply the previous process on the workpiece model and the active element model, the workpiece model needs to be expressed in a matrix form too. This is achieved through discretising the model of the workpiece in FEA software like Abaqus. However, and as most commercially available FE software do not offer the capability of model coupling, the latter will need to take place in an alternative environment. The alternative is to use software with extensive matrix handling and computational capabilities. Matlab [84] is therefore an ideal option. As a result, the workpiece model apart from being discretised in Abaqus, it also needs to be transferred into Matlab.

4.4.1 Expressing the Workpiece Model in Matlab

There are two aspects in this operation. The first one includes the establishment of the system matrices and the second the representation of the moving loads.

4.4.1.1 Introduction of System Matrices

There are three matrices that need to be outputted. These are the mass $[M]$, stiffness $[K]$ and damping $[C]$ matrices. In order to export the latter matrix, the damping present in the system must have first been defined in the FEA environment. Extraction of the system matrices takes place through a linear perturbation analysis step [127]. Natural Frequency extraction is such a step. It is easy to implement, as it requires limited computational resources, and it has already be used during the selection process of finite elements. It should be pointed out that the global matrix extraction process should only be performed on the free workpiece, i.e. with no boundary conditions imposed. If this rule is violated, the generated matrices could contain erroneous information that lead to false results and numerical problems. To force the program to output the requested matrices, the following code needs to be integrated to the input file of the FEA problem, right after the code that controls the Natural Frequency extraction step.

```
*STEP, NAME=(User Defined Name)
*MATRIX GENERATE, STIFFNESS, MASS, STRUCTURAL DAMPING
*END STEP
```

The input file is the file containing the pseudo-code that Abaqus accepts as the problem definition. It is usually generated automatically according to the user selections through the user-interface environment Abaqus/CAE. However, in the current version of Abaqus (v6.9) the generation of global system matrices is not supported through the user interface and needs to be introduced manually in the input file, as described previously. By integrating the above pseudo-code in the input file, Abaqus outputs three separate ASCII format files with .mtx extension, one for each of the system matrices. These files can be imported into Matlab. The information in these files can then be re-formulated in Matlab matrix variables.

As soon as the system matrices have been formulated as Matlab variables, boundary conditions can be integrated. To do this, it is necessary to know which nodes correspond to the points on the workpiece, where boundary condition are applied physically. In simple structures this task is straightforward. However, as the complexity of the workpiece increases, the need for a more structured way to deal with boundary nodes is necessary. In such cases, boundary nodes are identified by applying the required boundary conditions

in the FEA software and requesting the output of the input file. The boundary nodes are included in this file as a set of nodes. The numbers of the nodes can be transferred into Matlab and a vector variable containing them in increasing order can be created.

Each node contributes to a specific set of elements in the global system matrices. In essence each node presents their own mass, stiffness and damping matrix entries [48, 148]. The size of the matrix depends on the degrees of freedom (DOF) of a node. If the node has k degrees of freedom, then the local matrix has a size of $k \times k$. The global matrices are then assembled by combining all the local matrices together. Each local matrix takes its position within the global matrix depending on the number of each node. If, for example, a node is assigned number b ($b = 1, 2, \ldots,$ Max Node) then its local matrix will occupy elements $[b \times k - (k-1)] \times [b \times k - (k-1)]$ to $(b \times k) \times (b \times k)$ within the global matrix.

Moreover, when applying zero displacement boundary conditions, which is the case with most commonly used typical boundary conditions, then the following takes place. In essence, the contribution of the degree of freedom, along which zero displacement/rotation is imposed, is completely suppressed. In the case of a discrete system with no damping, its equation of motion can be expressed as:

$$\begin{bmatrix} m_{11} & m_{12} & \cdots & m_{1n} \\ m_{21} & m_{22} & \cdots & m_{2n} \\ \vdots & \vdots & \ddots & \vdots \\ m_{n1} & m_{n2} & \cdots & m_{nn} \end{bmatrix} \begin{Bmatrix} \ddot{x}_1 \\ \ddot{x}_2 \\ \vdots \\ \ddot{x}_n \end{Bmatrix} + \begin{bmatrix} k_{11} & k_{12} & \cdots & k_{1n} \\ k_{21} & k_{22} & \cdots & k_{2n} \\ \vdots & \vdots & \ddots & \vdots \\ k_{n1} & k_{n2} & \cdots & k_{nn} \end{bmatrix} \begin{Bmatrix} x_1 \\ x_2 \\ \vdots \\ x_n \end{Bmatrix} = \begin{Bmatrix} f_1 \\ f_2 \\ \vdots \\ f_m \end{Bmatrix} \tag{4.37}$$

Assuming that a zero displacement boundary condition needs to be imposed on the second degree of freedom of the six DOF Node 1, i.e. $x_2 = 0$, then the entire 2^{nd} row and column of the mass and stiffness matrices do not contribute to the solution of the problem. As a result they are completely removed from the system matrices. Following this method, zero displacement boundary conditions can be implemented. Non-zero displacement conditions can be applied as described in [48] and also in Section 6.2.2 of the thesis. Therefore, the subject will not be further analysed at this stage.

4.4.1.2 Introduction of Moving Loads in Matlab

After formulating the system matrices in Matlab, and including boundary conditions, the next step is to define the external loads. For this, the same approach as the one for the

FEA workpiece model will be followed here. In FEA, the moving load was represented by the force it induces at the nodes as it moves along the workpiece. The amplitudes of these nodal forces were defined as matrices. Each of these matrices had two columns, the first one representing time and the second one representing amplitude at the corresponding time instant. The direction of the forces was defined separately by defining the DOF of the node, along which each nodal force is applied. The above information can lead to the generation of local force matrices, from which the global ones can be assembled.

Each local force matrix has a number of rows equal to the degrees of freedom of the node. The number of columns equals the number of time instants, for which a solution is required. The sum of these time instants equals to the entire time for which a solution is required and not only the time for which the nodal force is active. The magnitude of the load per time instant is placed along the row that corresponds to the DOF along which the load is applied. For example, for nodes with 6 DOFs, and a load applied in the Z-direction of the workpiece, namely the 3^{rd} DOF of the node, and for time $t = [0, 1]$ defined through 101 time instants, the local force matrix will have dimensions 6×101. The 3^{rd} row will contain the amplitude of the load per time instant. All other elements in the matrix will have zero values.

With all local force matrices defined, the global force matrix can then be established. This is achieved following the same procedure as the one used for the assembly of the global system matrices. In detail, in the previous example, if the mentioned node was node number 23, then its local matrix will occupy the elements of rows $23 \times 6 - (6 - 1)$ to 23×6 of the global force matrix.

Equation (4.37) reveals that forces need to be defined in a vector format. The moving nature of the load is the reason behind the formulation of a matrix instead of a vector. In order to obtain the solution of the problem over time, the system of equations shown in Equation (4.37) is solved for every time instant separately. Each time, a column of the global force matrix can be used as the excitation force vector.

4.5 Coupling of Actuator and Workpiece Models

With all elements of the workpiece and the actuator models defined, the coupling of the models can commence. In order to couple the models of the workpiece and the actuator,

the system must be brought to the form of Equation (4.33). To do that, the impedance coupling technique in spatial coordinates will be used [82]. This method works as follows. The workpiece model is defined as a second order ordinary differential equation:

$$[M_w]\{\ddot{u}_w\} + [C_w]\{\dot{u}_w\} + [K_w]\{u_w\} = \{f_w\} \tag{4.38}$$

According to Maia *et al.* [82] Equation (4.38) can be expanded as:

$$\begin{aligned} &\begin{bmatrix} [{}_wM_{ii}] & [{}_wM_{ic}] \\ [{}_wM_{ci}] & [{}_wM_{cc}] \end{bmatrix} \begin{Bmatrix} \{{}_w\ddot{u}_i\} \\ \{{}_w\ddot{u}_c\} \end{Bmatrix} + \begin{bmatrix} [{}_wC_{ii}] & [{}_wC_{ic}] \\ [{}_wC_{ci}] & [{}_wC_{cc}] \end{bmatrix} \begin{Bmatrix} \{{}_w\dot{u}_i\} \\ \{{}_w\dot{u}_c\} \end{Bmatrix} \\ &\qquad + \begin{bmatrix} [{}_wK_{ii}] & [{}_wK_{ic}] \\ [{}_wK_{ci}] & [{}_wK_{cc}] \end{bmatrix} \begin{Bmatrix} \{{}_wu_i\} \\ \{{}_wu_c\} \end{Bmatrix} = \begin{Bmatrix} \{{}_w0_i\} \\ \{{}_wf_c\} \end{Bmatrix} \end{aligned} \tag{4.39}$$

with c denoting the degrees of freedom that are involved in the physical connection, and i denoting the remaining degrees of freedom of the discretised workpiece model. Similarly, Equation (4.32) can be re-written as:

$$\begin{aligned} &\begin{bmatrix} [{}_{ac}M_{ii}] & [{}_{ac}M_{ic}] \\ [{}_{ac}M_{ci}] & [{}_{ac}M_{cc}] \end{bmatrix} \begin{Bmatrix} \{{}_{ac}\ddot{u}_i\} \\ \{{}_{ac}\ddot{u}_c\} \end{Bmatrix} + \begin{bmatrix} [{}_{ac}C_{ii}] & [{}_{ac}C_{ic}] \\ [{}_{ac}C_{ci}] & [{}_{ac}C_{cc}] \end{bmatrix} \begin{Bmatrix} \{{}_{ac}\dot{u}_i\} \\ \{{}_{ac}\dot{u}_c\} \end{Bmatrix} \\ &\qquad + \begin{bmatrix} [{}_{ac}K_{ii}] & [{}_{ac}K_{ic}] \\ [{}_{ac}K_{ci}] & [{}_{ac}K_{cc}] \end{bmatrix} \begin{Bmatrix} \{{}_{ac}u_i\} \\ \{{}_{ac}u_c\} \end{Bmatrix} = \begin{Bmatrix} \{{}_{ac}0_i\} \\ \{{}_{ac}f_c\} \end{Bmatrix} \end{aligned} \tag{4.40}$$

The coupling of the above systems, namely $[S_w]$ and $[S_{ac}]$, is symbolised as:

$$[S_C] = [S_w] \oplus [S_{ac}] \tag{4.41}$$

and results in the following:

$$[M_C] = \begin{bmatrix} [{}_wM_{ii}] & [{}_wM_{ic}] & [0] \\ [{}_wM_{ci}] & [{}_{ac}M_{cc}] + [{}_wM_{cc}] & [{}_{ac}M_{ci}] \\ [0] & [{}_{ac}M_{ic}] & [{}_{ac}M_{ii}] \end{bmatrix} \tag{4.42}$$

$$[C_C] = \begin{bmatrix} [{}_wC_{ii}] & [{}_wC_{ic}] & [0] \\ [{}_wC_{ci}] & [{}_{ac}C_{cc}] + [{}_wC_{cc}] & [{}_{ac}C_{ci}] \\ [0] & [{}_{ac}C_{ic}] & [{}_{ac}C_{ii}] \end{bmatrix} \tag{4.43}$$

$$[K_C] = \begin{bmatrix} [{}_wK_{ii}] & [{}_wK_{ic}] & [0] \\ [{}_wK_{ci}] & [{}_{ac}K_{cc}] + [{}_wK_{cc}] & [{}_{ac}K_{ci}] \\ [0] & [{}_{ac}K_{ic}] & [{}_{ac}K_{ii}] \end{bmatrix} \tag{4.44}$$

For the plate workpiece, discretised through a set of 300 S4 finite elements and 341 six-degree-of-freedom nodes, the system matrices have dimensions 2046×2046. Assuming the actuator needs to be placed in the middle of the plate, i.e. at point $(x, y) = (75, 25)$ mm, the coupling node is Node 171, as revealed by the input file. The direction of the actuator is parallel to the Z-axis of the system, hence along the 3^{rd} DOF of the node. The physical coupling takes place, therefore, at the 1023^{rd} degree-of-freedom of the discretised workpiece model, and the coupling procedure results in the following matrices:

$$[M_C] = \begin{bmatrix} m_{1,1} & 0 & \cdots & 0 & 0 \\ 0 & m_{2,2} & \cdots & 0 & 0 \\ \vdots & \vdots & & \vdots & \vdots \\ 0 & 0 & \cdots & m_{2046,2046} & 0 \\ 0 & 0 & \cdots & 0 & J_{tot} \end{bmatrix} \tag{4.45}$$

$$[C_C] = \begin{bmatrix} c_{1,1} & c_{1,2} & & \cdots & & c_{1,2046} & 0 \\ \vdots & \vdots & & \vdots & & \vdots & 0 \\ c_{1023,1} & c_{1023,2} & \cdots & c_{1023,1023} + c_1 & \cdots & c_{2046,2046} & -c1 \\ \vdots & \vdots & & \vdots & & \vdots & 0 \\ c_{2046,1} & c_{2046,2} & & \cdots & & c_{2046,2046} & 0 \\ 0 & 0 & \cdots & -c_1 \left(\frac{p}{2\pi G_{rr}}\right)^2 \eta_2 & \cdots & 0 & f_r + c_1 \left(\frac{p}{2\pi G_{rr}}\right)^2 \eta_2 \end{bmatrix} \tag{4.46}$$

$$[K_C] = \begin{bmatrix} k_{1,1} & k_{1,2} & & \cdots & & k_{1,2046} & 0 \\ \vdots & \vdots & & \vdots & & \vdots & 0 \\ k_{1023,1} & k_{1023,2} & \cdots & k_{1023,1023} + k_1 & \cdots & k_{2046,2046} & -k1 \\ \vdots & \vdots & & \vdots & & \vdots & 0 \\ k_{2046,1} & k_{2046,2} & & \cdots & & k_{2046,2046} & 0 \\ 0 & 0 & \cdots & -k_1 \left(\frac{p}{2\pi G_{rr}}\right)^2 \eta_2 & \cdots & 0 & k_1 \left(\frac{p}{2\pi G_{rr}}\right)^2 \eta_2 \end{bmatrix} \tag{4.47}$$

The degrees-of-freedom vector becomes:

$$\{u_C\} = \begin{bmatrix} x_1 & x_2 & \cdots & x_{2046} & x_A \end{bmatrix}^T \tag{4.48}$$

and the force vector becomes:

$$\{f_C\} = \begin{bmatrix} f_1 & f_2 & \cdots & f_{2046} & \left(\frac{p}{2\pi G_{rr}}\right)^2 K_T I_m \end{bmatrix}^T \tag{4.49}$$

Boundary conditions need to be applied to the previous model before a solution can be reached. If both small edges of the plate are assumed to be fully constrained, according to paragraph 4.4.1.1, the rows and columns of the matrices and vectors in Equations (4.45)-(4.49), corresponding to the degrees of freedom of the nodes that lie on the constrained edges of the plate, need to be removed. In this case, there are 22 boundary nodes. Therefore, the $22 \times 6 = 132$ rows and 132 columns that correspond to the boundary nodes are removed from the system matrices. Furthermore, the same 132 rows are removed from the displacement and force vectors. The system matrices are reduced to a size of 1915×1915 for the mass, stiffness, and damping matrices, and 1915×1 for the force and the degrees-of-freedom vectors. Also, the degree-of-freedom where the physical connection of the workpiece and the actuator model are coupled, corresponds to element $(957, 957)$ within the system matrices and element $(957, 1)$ within the system vectors. The model can now be solved for either forces or displacements of the actuator and the workpiece.

Please note, that even after the incorporation of boundary conditions, the matrices of the system, even for such a small number of finite elements, is significantly large. With increasing FEA model complexity, the computational power requirements to provide a so-

lution rapidly increase. When the system matrices become so large that cannot be handled efficiently, model condensation techniques can be applied to reduce the computational effort [11, 28, 108]. This subject falls out of the scope of this work and will not be analysed further here.

The next step towards completing the model coupling process is to introduce the equation that described the response of the electric circuit of the actuator, i.e. Equation (4.23). For this, Equations (4.29) and (4.31) are combined into the following:

$$V_m + RC\dot{V}_m = RG_{ac}V_{cc} \tag{4.50}$$

The system equations need to be transferred in state-space format:

$$\{\dot{\mathrm{x}}_i\} = [F]\{\mathrm{x}_i\} + [G]\{\mathrm{u}_i\} \tag{4.51}$$

$$\{\mathrm{y}_i\} = [H]\{\mathrm{x}_i\} + [J]\{\mathrm{u}_i\} \tag{4.52}$$

where $\{\mathrm{x}_i\}$ are the state variables, $\{\mathrm{u}_i\}$ are the inputs of the model, $\{\mathrm{y}_i\}$ are the outputs of the model, $[F]$ is the system matrix, $[G]$ is the input matrix, $[H]$ is the output matrix, and $[J]$ is the direct transmission term matrix [50]. To achieve this, the variables shown in Table 4.9 are defined.

The coupled system of equations can be re-written:

$$[M_C]\begin{Bmatrix}\{\dot{\mathrm{x}}_{(1,i)}\}\\ \dot{\mathrm{x}}_{1915}\end{Bmatrix} + [C_C]\begin{Bmatrix}\{\mathrm{x}_{(1,i)}\}\\ \mathrm{x}_{1915}\end{Bmatrix} + [K_C]\begin{Bmatrix}\{\mathrm{x}_{(2,i)}\}\\ \mathrm{x}_{3830}\end{Bmatrix} =$$

$$= \begin{bmatrix} 1 & 0 & \cdots & 0 & 0 \\ 0 & 1 & \cdots & 0 & 0 \\ \vdots & \vdots & & \vdots & \vdots \\ 0 & 0 & \cdots & 1 & 0 \\ 0 & 0 & \cdots & 0 & \left(\frac{p}{2\pi G_{rr}}\right)^2 K_T G_{ac} \end{bmatrix} \begin{Bmatrix}\{\mathrm{u}_{1,i}\}\\ \mathrm{u}_{1915}\end{Bmatrix} \tag{4.53}$$

Similarly, Equation (4.23) can be written as:

$$L_m\dot{\mathrm{x}}_{3831} + R_m\mathrm{x}_{3831} = \mathrm{x}_{3832} - K_{emf}\frac{2\pi G_{rr}}{p}\mathrm{x}_{3830} \tag{4.54}$$

and Equation (4.50) as:

$$\mathrm{x}_{3832} + RC\dot{\mathrm{x}}_{3832} = RG_{ac}\mathrm{u}_{1915} \tag{4.55}$$

Also, the force which the actuator applies on the workpiece, along the 957^{th} degree of freedom, is derived from Equation (4.26) and it is given by:

$$\mathrm{y}_2 = k_c\left(\mathrm{x}_{3830} - \mathrm{x}_{2872}\right) + c_x\left(\mathrm{x}_{1915} - \mathrm{x}_{957}\right) \tag{4.56}$$

where k_c and c_c are the stiffness and damping constant coefficients, respectively, describing the behaviour of the contact between the fixture and the workpiece. Equations (4.50), (4.53), and (4.55) are solved for the first order derivatives. These, along with Equation (4.56) and the exit variables from Table 4.9, are finally merged into a system of equations, which represents the state-space model of the system, thus completing the model coupling task. The coupled model is presented below:

Table 4.9: Definition of input variables, state variables and output variable

Input	State Variables	Output
$f_i = \mathrm{u}_{(1,i)}$, $i = 1, \ldots, 1914$	$\dot{x}_i = \mathrm{x}_{(1,i)}$, $i = 1, \ldots, 1914$	$x_i = \mathrm{y}_{(1,i)}$, $i = 1, \ldots, 1914$
$V_{cc} = \mathrm{u}_{1915}$	$\dot{x}_A = \mathrm{x}_{1915}$	$F_A = \mathrm{y}_{1915}$
	$x_i = \mathrm{x}_{(2,i)}$, $i = 1, \ldots, 1914$	
	$x_A = \mathrm{x}_{3830}$	
	$I_m = \mathrm{x}_{3831}$	
	$V_m = \mathrm{x}_{3832}$	

$$\begin{Bmatrix} \{\dot{\mathrm{x}}_{(1,i)}\} \\ \dot{\mathrm{x}}_{1915} \\ \{\dot{\mathrm{x}}_{(2,i)}\} \\ \dot{\mathrm{x}}_{3830} \\ \dot{\mathrm{x}}_{3831} \\ \dot{\mathrm{x}}_{3832} \end{Bmatrix} = [F] \begin{Bmatrix} \{\mathrm{x}_{(1,i)}\} \\ \mathrm{x}_{1915} \\ \{\mathrm{x}_{(2,i)}\} \\ \mathrm{x}_{3830} \\ \mathrm{x}_{3831} \\ \mathrm{x}_{3832} \end{Bmatrix} + [G] \begin{Bmatrix} \{\mathrm{u}_{(1,i)}\} \\ \mathrm{u}_{1915} \end{Bmatrix} \tag{4.57}$$

$$\begin{Bmatrix} \{y_{(1,i)}\} \\ y_{1915} \end{Bmatrix} = [H] \begin{Bmatrix} \{x_{(1,i)}\} \\ x_{1915} \\ \{x_{(2,i)}\} \\ x_{3830} \\ x_{3831} \\ x_{3832} \end{Bmatrix} + [J] \tag{4.58}$$

with:

$$[F] = \begin{bmatrix} -[M_C]^{-1}[C_C] & -[M_C]^{-1}[K_C] & \{0\}_{1914} & \{0\}_{1914} \\ & & \left(\frac{p}{2\pi G_{rr}}\right)^2 K_T G_{ac} & 0 \\ [I]_{1915} & [0]_{1915} & \{0\}_{1915} & \{0\}_{1915} \\ 0 \quad \cdots & -\frac{K_{emf}}{L_m}\frac{2\pi G_{rr}}{p} & -\frac{R_m}{L_m} & \frac{1}{L_m} \\ 0 \quad \cdots & 0 & 0 & -\frac{1}{RC} \end{bmatrix} \tag{4.59}$$

$$[G] = \begin{bmatrix} [M_C]^{-1}[I]_{1914} & \{0\}_{1914} \\ [0]_{1,1195} & \\ [0]_{1196,1195} & \\ [0]_{1,1194} & \frac{G_{ac}}{C} \end{bmatrix} \tag{4.60}$$

$$[H] = \begin{bmatrix} [0]_{1914,1915} & [I]_{1194,1914} & [0]_{3,1914} \\ [0]_{1,956} \quad -c_c \quad [0]_{1,957} & c_c \quad [0]_{1,956} & -k_c \quad [0]_{1,957} \quad k_c \quad 0 \quad 0 \end{bmatrix} \tag{4.61}$$

$$[J] = [0]_{1915} \tag{4.62}$$

In the above equations $[I]$ is the unit matrix, $[0]$ is a matrix with zero elements, and 0 is a vector with zero elements. The indicators next to the matrices and vectors designate their size. When a single indicator is shown then the matrix is square.

4.6 Experimental Validation

A simple experimental set-up was devised to examine the validity of the developed fixture-workpiece model. This is based on the fixture prototype that was described in detail in

Section 3.3.4. The experimental set-up, shown in Figure 4.10, comprises a single transport component with an active clamp. The latter is a Kollmorgen EC2-BK23S-100-16B electromechanical actuator [32]. This actuator has a pitch of $p = 16$ mm/rev. The gearing ratio of the actuator is $G_{rr} = 10/1$. The motor of the actuator is a Kollmorgen AKM23D PMAC motor [31]. The controller of the actuator is a Kollmorgen S200 drive unit [35].

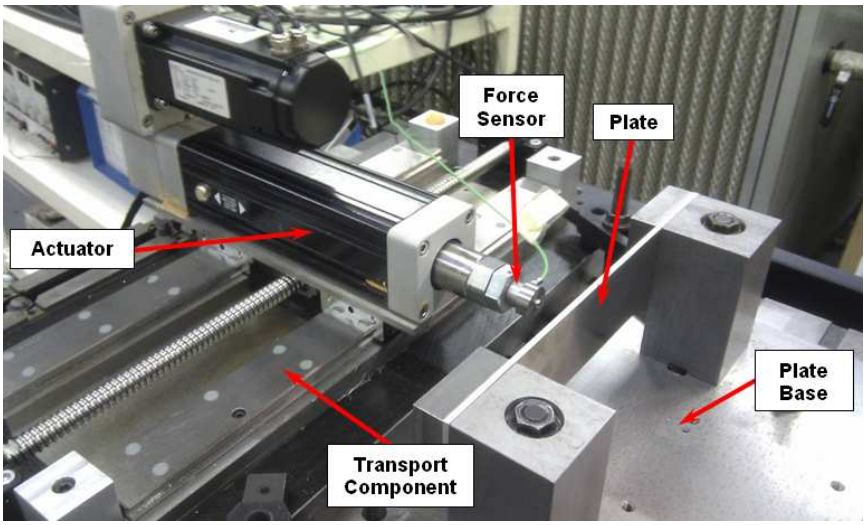

Figure 4.10: Experimental set-up for the verification of the open-loop active clamp-plate coupled model.

A Kistler Type 9101A PZT [70] single force component load washer (force sensor) was used to measure the forces applied by the actuator. The sensor's signal was conditioned and amplified by a Kistler Type 5017A charge amplifier [69].

An aluminium plate with the characteristics presented in Table 3.1 was securely clamped at both its small edges. This was achieved by a custom steel base, designed to be significantly more rigid than the plate. The base was also designed to provide a free span of 150 mm, whilst clamping an area of 50×50 mm^2 at the edges of the plate. The contact point between plate and actuator is the midpoint of the free plate span, i.e. point $(x, y) = (75, 25)$ mm.

A National Instruments PCI-6031E data acquisition card [91] was used to monitor and record the force applied by the actuator. The same card was also used to generate voltage profiles that were passed as command signals to the actuator controller. The controller and the card were connected through a National Instrument SCB-100 connector box [93].

Two types of input signals were used to evaluate the validity of the developed model. A step voltage signal with 1 V amplitude was first fed to the actuator controller. The second input signal was a harmonic sinusoidal force with 0.5 V amplitude, 0.5 V offset and 1 Hz

excitation frequency. In both cases the resulting actuating forces were recorded through the load washers mounted at the tip of the active clamp. The model of Equations (4.45)-(4.49) was solved for the same input signal. To solve this model, the values presented in Table 4.10 were assigned to the system variables. The resistance and capacitance values for the RC-filter (low-pass filter), were selected randomly, so that the steady-state value of the response of the filter is 1 V for a 1 V input, and so that the cut-off frequency of the filter is $F_c = 1457.28$ Hz ($F_c = 1/(2\pi RC)$), which is the only value that could be adjusted in the settings of the controller. A comparison between theoretical and experimental responses of the system are shown in Figure 4.11.

Table 4.10: Numerical values of the variables of active clamp-plate model.

Active Clamp Variables [1, 33, 34]		
J_{tot}	=	$1.86295e^{-5}$ kg m^2
K_T	=	0.52 Nm/A
f_r	=	$6.5e^{-6}$ Nms/rad
L_m	=	0.0173 H
R_m	=	8.77 Ω
K_{emf}	=	0.0338 Vs/rad
G_{rr}	=	10
p	=	0.016 m/rev
η_2	=	62%
Actuator Controller Variables [35]		
F_c	=	1457.28 Hz
C	=	$100e^{-9}$ F
G_{ac}	=	0.217 A/V
Other Model Variables		
k_c	=	100 MN/m
c_c	=	0 Ns/m

The diagrams show a fair agreement between experimental and simulated responses. A 2 ms output delay was introduced in the active clamp model to reflect more accurately the actual system. For the step response, it is noticed that the simulated response approaches well the experimentally obtained response. However, the experimental system appears to respond faster to the step input.

The rise time of the experimental system is approximately 90 ms, in comparison to the 142.9 ms rise time of the simulated system. Similar comments can be made on the settling times of the two systems, with the experimental system reaching the steady-state value after 100 ms, and the simulated system after 150 ms.

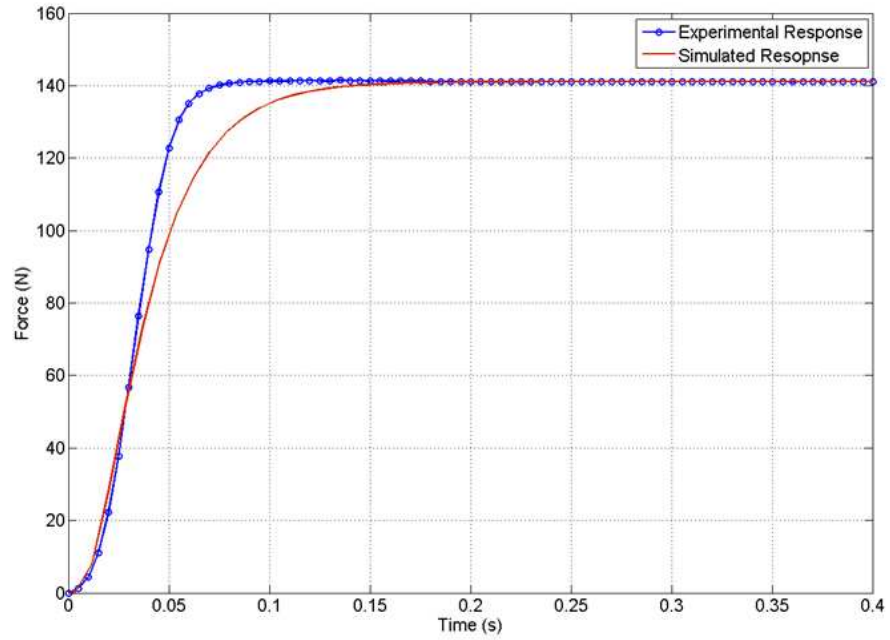

(a)

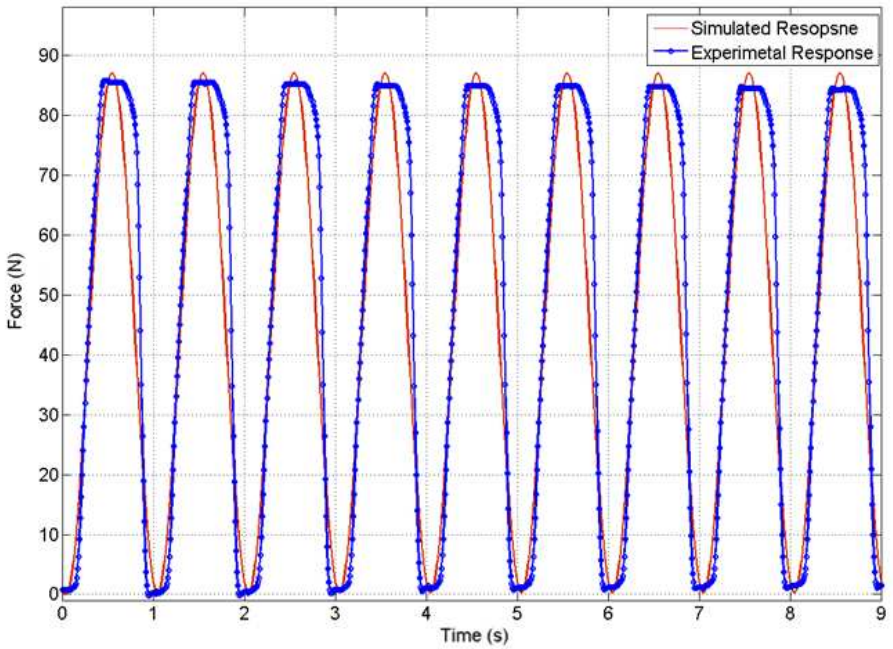

(b)

Figure 4.11: Simulated and experimental response of the active clamp-plate system to a (a) step input of 1 V and a (b) sinusoidal input of 0.5 V amplitude, 0.5 V offset and 1 Hz excitation frequency.

For the harmonic response, it is noted that the recorded forces present flat peaks and valleys. This is attributed to the backlash in mechanism of the actuator, gears and balls-screw. As the motor changes direction, there is a phase were the motor turns without turning the gears or the ball-screw. Therefore, although the motor responds to the input

signals, during that phase, the mechanical components do not move. Therefore, the tip of the active clamp remains at the same position, and, hence, the applied force does not change. Backlash is an inherent drawback of electromechanical actuators and is the result of manufacturing tolerances. It should also be noted, that the response amplitude for the two inputs is not the same. In a purely linear system, the response amplitude should remain the same for the same input amplitude (1 V). Non-linearities in the system lead to deviations from the previously mentioned statement. These non-linearities are captured by adapting the reverse efficiency coefficient η_2, within the active clamp-plate coupled model. For the harmonic input, the efficiency factor was set to $\eta_2 = 37.5\%$.

The above results highlight the validity of the developed open-loop model. The closed-loop model, which is based on the fixture-workpiece model that was presented through this chapter, can now be developed in confidence.

4.7 Conclusions

This chapter dealt with the modelling of the open-loop response of a fixture-workpiece system. A thin plate was used as the simulated workpiece, while a PMAC motor-base electromechanical actuator played the role of the active fixture element. The key conclusions from this chapter are presented hereafter:

- A method to formulate a model that reflects the dynamic open-loop response of an active fixture-workpiece system was presented.
- Four-node tetrahedron shell S4 elements were chosen for the discretisation of the workpiece structure in finite elements.
- The S4 elements outperformed all other investigated elements in the prediction of the natural frequencies and the elastic deformation of the plate workpiece. The S4 elements underestimate the natural frequencies of a thin plate by 0.47% on average, and overestimate the elastic deformation of the plate by 3.78% on average. These percentages stem from the comparison of FEA results to results from Kirchhoff plate-theory and the analytical model of a thin plate subjected to moving loads, respectively.
- A method to simulate in FEA and Matlab the elastic deformation of a workpiece under moving distributed loads was proposed and validated.

- A first-principle based model for the Permanent Magnet Alternating Current (PMAC) electromechanical actuator, that constitutes the active element of a fully-active fixture, was developed. It was assumed that the PMAC motor of the actuator could be approached as a Direct Current (DC) motor.

- The workpiece model and the actuator/actuator-controller models were coupled using the impedance coupling technique in spatial coordinates. The process was executed in Matlab.

- The developed fixture-workpiece open-loop model was validated experimentally. The response of the model and the experimental device, to step and harmonic input signals.

- The experimental and modelled responses agree quite well. The experimental system responds faster than the modelled system. From the obtained results, the open-loop models is considered validated and the assumption that the actuator motor can be approached as a DC motor verified.

- The backlash that is present in the mechanical components of the actuator affects the response of the system to the sinusoidal signal input.

- The experimental system responds with different force amplitudes for the two signals that where tested. This non-linearity can be accounted for by calibrating the reverse efficiency factor in the coupled workpiece-fixture model. For the step response the efficiency factor was set to $\eta_2 = 65\%$, while for the sinusoidal response it was set to $\eta_2 = 37.5\%$.

Chapter 5

Control Strategies for Active Fixture Elements

5.1 Introduction

The previous chapter dealt with the structural dynamics model of thin-walled workpieces and the dynamic response model of active fixture elements. The latter focused on electromechanically actuated elements and their open-loop behaviour. However, the operation of these active elements in a closed-loop condition is critical to the overall performance of active fixtures and needs to be studied in detail.

In general, a fully-active fixturing system is required to perform the following operations:

- Positioning and orientating of fixturing elements relative to the fixturing system's reference frame.
- Positioning of the locating elements' tips to accurately locate the workpiece.
- Positioning of clamping elements tips to a stand-by position.
- Apply desirable clamping force profiles over time.

The first three operations are closely linked to the automatic configuration and reconfiguration of a fully-active fixture. The fourth operation concerns the adaptive clamping force capabilities of the fixture. In both cases, the performance of the fixturing system needs to be as high as possible. This translates to fast response to input signals and accurate results

in terms of the desirable output, namely position or force. The control architecture and algorithm play a vital role in the performance of fully-active fixturing systems.

This chapter is, therefore, dedicated to the investigation of the performance of different control algorithms and the modelling of the full workpiece-fixturing system. At first, the overall system architecture is presented. The control algorithms behind position and force control tasks are discussed afterwards. The main focus is placed on force-control tasks. Finally, a model of the complete fixture-workpiece system, with active fixture elements operating in a closed-loop manner, is presented and analysed.

5.2 Overall System Control Architecture

As mentioned earlier, fully-active fixtures need to perform a series of operations that demand precise positioning and application of force. These control requirements of fixturing systems can span from very simple to highly complicated. Depending on the requirements of each application, different control architectures may be implemented. Additionally, possible control strategies and algorithms are largely dictated by the controlling hardware and its capabilities. Hence, it is important to analyse the control architecture and hardware before discussing possible control algorithms. In this work, and as it has been presented in Section 3.3.4 (see Figure 4.5), the architecture described below has been selected for each active fixture element.

A simple Windows XP-based computer is used as the overarching controller. It also plays the role of the point of interface between the user interface and the controlling and fixturing hardware. The command signal from the computer is translated into a command voltage from the motion controller. This is a peripheral component interconnect (PCI) local-bus card with an integrated digital Proportional-Integral-Derivative (PID) controller and a trajectory generator. The command voltage passes through a connector box (or board), which is used as the wiring interface point for the various equipment. The connector box does not alter or condition the signals in any way, i.e. it is a pass-through device.

The command signal, after passing through the connector box is fed to the controller of the actuator, also referred to as drive unit. The drive unit, in this work, is in charge of supplying the motor of the actuator with the correct electrical current and voltage. The voltage signal from the motion controller is applied to the transconductance amplifier

within the drive unit, and it is transformed into current. The gain of the transconductance amplifier is adjustable. The current is the passed through a low-pass filter, which conditions the signal, blocking any abrupt and large changes in the current amplitude. Then, the current is applied on the winding of the motor of the actuator.

An electromechanical Permanent Magnet Alternating Current (PMAC) motor-based linear actuator plays the role of the active fixture element. A gear-and-ball-screw mechanism is responsible for transforming the rotary motion of the motor into linear motion of the actuator's tip.

The actuator assembly includes a rotary quadratic incremental encoder on the axis of the motor. The signals from the encoder are fed back to the actuator controller. The latter transform these into a signal that can be read from the motion controller, through the connector board. This loop is used for position-control tasks.

At the tip of the actuator, there is mounted a piezoelectric transducer (PZT) that takes the form of a load washer. As the sensor compresses, due to the forces that are applied on the tip of the active fixture element, a change in its charge occurs. The signal from this sensor is fed to a charge amplifier, which transforms it into voltage, which in turn is amplified to take a value between 0 and 10 V. This voltage value is applied to the motion controller, through the connector box. This loop is used for force-control tasks.

This architecture, along with the selected hardware, have certain advantages. It can be used for both simple and complicated positioning and force control operations, whilst maintaining associated costs to a minimum. It can cater for either accurate and repeatable positioning of components to a predefined location, or maintaining constant velocity throughout an operation cycle, or applying a predefined force profile. Given these constraints, and the operations that a fully-active fixturing system should be able to complete successfully, two control algorithms can be identified. These are described in detail in the following paragraphs.

5.3 Control Algorithms

The previously described system is used for both position- and force-related control tasks. The control algorithms behind each of these tasks are being discussed below.

5.3.1 Position Control Related Tasks

Although the control of position related tasks of fully-active fixtures fall outside the scope of this work, a brief discussion shall be presented for the sake of facilitating understanding of the overall control requirements.

As mentioned earlier, fully-active fixtures need to perform a series of operations that demand precise positioning. The operations are closely linked to the automatic configuration and reconfiguration of a fully-active fixture, as well as the active change of fixture element positions during the process. The control algorithm behind these tasks is reflected through the block diagram presented in Figure 5.1.

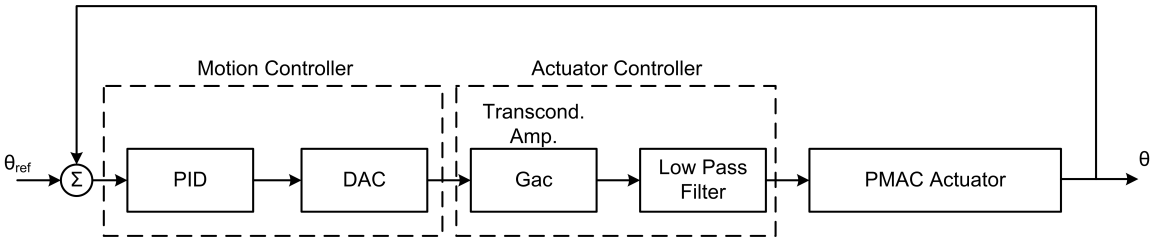

Figure 5.1: Block diagram of the position control closed-loop system. Digital to Analogue conversion is signified as DAC, and the linear gain in the voltage to current transformation is signified as G_{ac}.

The variable that is controlled according to the block diagram of Figure 5.1 is the angular position of the axis of the motors. A linear relationship between linear displacement and angular displacement is therefore assumed. For backlash-free systems or when backlash is small enough to produce acceptable positioning accuracy, this is an adequate approximation. In such cases, encoders mounted on the motor axes can be used as position-feedback devices. This is certainly the case in this work.

Position-controlled operations of fully-active fixturing systems and their control will not be discussed further in this thesis as they fall outside the scope of this work.

5.3.2 Force Control Related Tasks

The only force-controlled operation of a fully-active fixture is the application of clamping forces. These secure the workpiece in its desired position and orientation throughout the duration of the manufacturing process. There are two ways through which the applied forces can be controlled. Either directly using force feedback or indirectly by controlling the position of tip of the clamping element. These methods are discussed in detail in the following paragraphs.

5.3.2.1 Cascaded Position/Force-Feedback Control Algorithm

When the actuating elements is in contact with the workpiece, then a displacement of the tip of the actuator results in a change of the magnitude of the applied force. With this in mind, the clamping force can be actively controlled by controlling the displacement of the actuator.

Cascaded force control, also referred to as hybrid position/force-control algorithm, was first introduced by [109] for robotic manipulators. It has been the main control strategy in active fixturing systems that are based on electromechanical actuation technology [83, 98]. According to this strategy, the control architecture comprises two loops, namely an inner loop that controls the absolute position of an active fixture element, and an outer loops that controls the force applied by the element. The force loop also acts as a relative position correction. In detail, the operator assigns both a force and an absolute position reference. Assuming a linear relationship between force and displacement, through a contact stiffness coefficient k_c, the force reference is compared to the force applied by the active element, which can be read via a force sensor. The comparison result is transformed into a relative position error. This is then compared to the absolute position reference and the current position of the active element's tip, read by the encoder, which is integrated in the motor of the element. This causes the element to extend or contract until both the position and the force references have been satisfied. The block diagram of the cascaded force control algorithm is presented in Figure 5.2, whilst a schematic representation of an active fixture element operating under this algorithm is shown in Figure 5.3.

To the best of the author's knowledge, off-the-shelf motion controllers, which are nec-

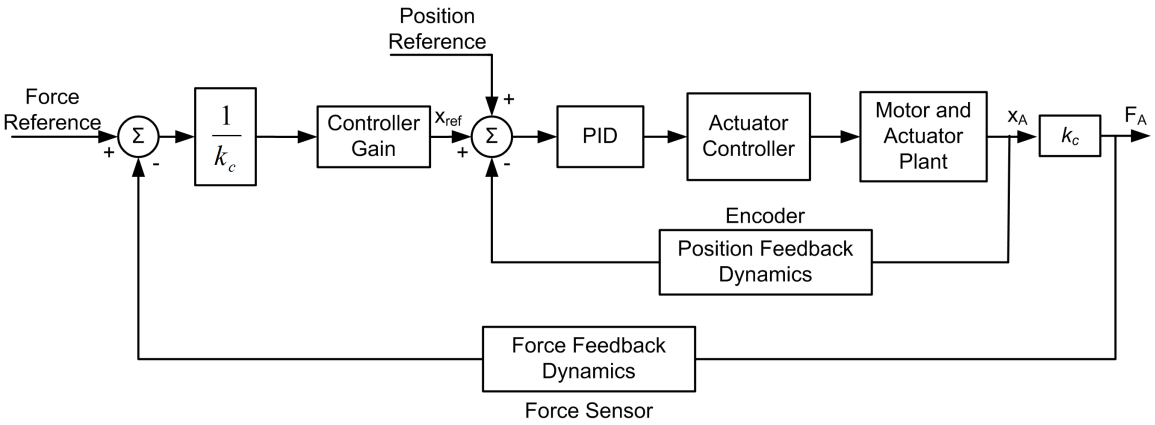

Figure 5.2: Block diagram of the cascaded force/torque control architecture. Based on information obtained from [83].

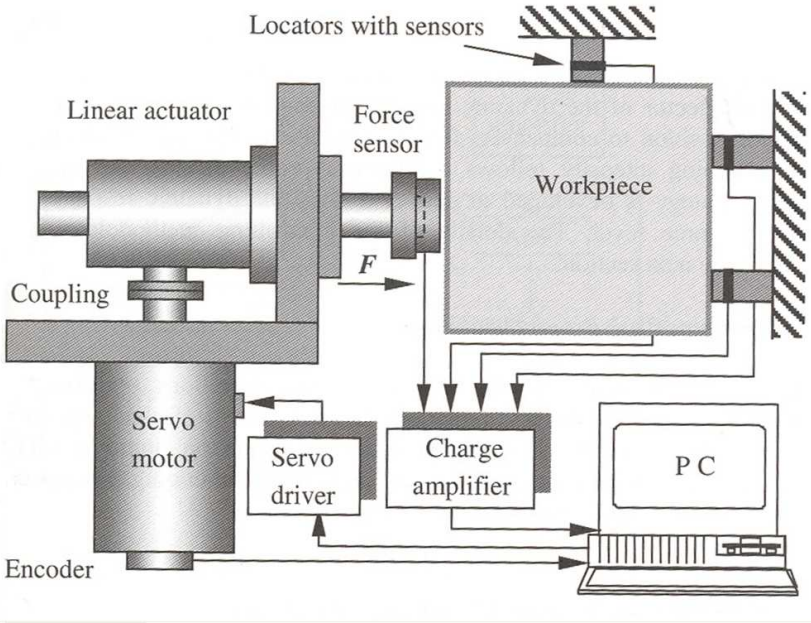

Figure 5.3: Schematic representation of the active clamp system operating under the cascaded force/position control scheme [98].

essary for controlling either the position or force applied from the actuators, deploy one controller per motion axis. This means that, for controlling the function of a linear actuator or a motor, only one feedback source can be used for each controller. As a result, only one feedback loop can be implemented through the available hardware. Some motion controllers can accommodate for a secondary position feedback source, used to measure displacement or position at the tip of the actuating element [95]. This architecture is used to improve positioning accuracy by removing backlash effects. However, a second controller for the second feedback source is not available. This means that the controller on one of the feedback loops in the cascaded architecture must be applied through software. This practice creates slower response of the overall system. Furthermore, when implemented through non-real-time operating systems, operating conditions, namely the control loop cycle time is variable. For the cascaded control architecture mentioned above, the force-feedback loop is the one implemented through software means.

This approach has been modelled and applied experimentally by [83] and [98]. In both cases the architecture remains the same to a great percentage. Both systems implement a Direct Current (DC) motor combined with a lead-screw to convert angular movement into linear. Another similarity is identified in the clamped workpiece. In both cases the active fixturing elements are in contact with a rigid workpiece, i.e. a solid block of metal. The cascaded position/force control scheme is used with the force-feedback loop constituting

the outer loop. The difference is located at the programmatically applied controller in the outer (force) closed loop. In [83] the applied controller has a simple proportional part with a stable gain. In [98] a Generalised Minimum Variance (GMV) controller is used. Results from both works are summarised in Figures 5.4 and 5.5.

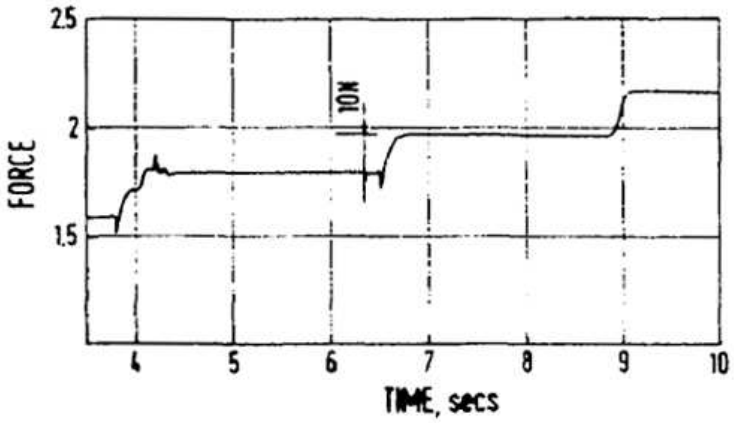

Figure 5.4: Response of a DC motor-based active clamping system to 10 N step inputs [83].

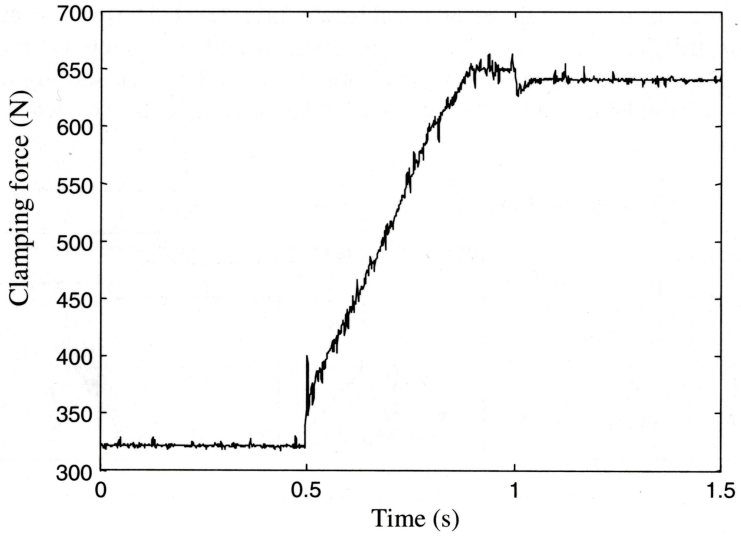

Figure 5.5: Response of a DC motor active clamping system to a ramp input [98].

In the case of [83], after both controllers of the system were tuned, results showed a response time of 200 ms for a force step of 10 N. The response presents no overshoot or steady state error. As the authors of this work comment, larger force steps are expected to require longer response times. Furthermore, it is also mentioned that increased workpiece stiffness leads to faster response, which is the expected behaviour.

In the case of [98], the best reported result involves the response of the aforementioned system to a 320 N force ramp from an initial condition of 320 N of clamping force. The system behaves reasonable well when faced with the request to perform the ramp increment

within 0.5 s. A small overshoot of 4.26% is noticed in the response. The system seems to stabilise at the overshoot value for approximately 206 ms. Afterwards, the force is lowered to the steady-state value.

The cascaded position/force-feedback algorithm is ideal when it is necessary to perform accurate tracking of both the position of the tip of the actuator and the force applied by it simultaneously. However, as one of the controllers is a software-based one, the approach suffers from the disadvantage of increased cycle-time. This time is dependent on the processing power of the available computer hardware, the speed of the communication ports used and the operating system of the controlling computer. Furthermore, the system needs to operate under non-variable cycle times. This dictates the need for utilising a real-time operating system. Non-deterministic cycle times could lead to inconsistent response and unwanted behaviour. Moreover, the cascaded position/force-feedback approach described earlier is based on positional feedback from an encoder mounted on the axis of the motor of the actuator. Tolerances in the actuator assembly and backlash significantly diminish the accuracy of actuator positioning. A linear relationship between angular position of the motor axis and linear displacement of the tip of the actuator can no longer be assumed. Backlash can be reduced or even eliminated by using specially designed hardware, such as backlash-free pre-stressed lead-screw nuts. Also, backlash effects can be drastically reduced by using a secondary position sensor (encoder or linear displacement sensor) positioned at the tip of the actuator [95].

The above disadvantages result in a system that requires higher capital investment for hardware, augmented implementation effort and presents increased response time when force control is necessary.

5.3.2.2 Direct Force/Torque Control Algorithm

The alternative to the previously described cascaded control algorithm is the direct force-feedback approach. This algorithm, despite its obvious advantages, has not been applied before on active fixturing. According to this strategy, the force value recorded by the force-sensing element of the active fixture element is passed through an amplifier and fed into the motion controller. There, it is directly compared to the reference input, i.e. the desired applied force value. The resulting error constitutes the input to the controller, which in turn adjusts the voltage input to the actuator controller and, hence, the applied current to

the armature of the motor of the actuator. This control scheme is depicted in Figure 5.6.

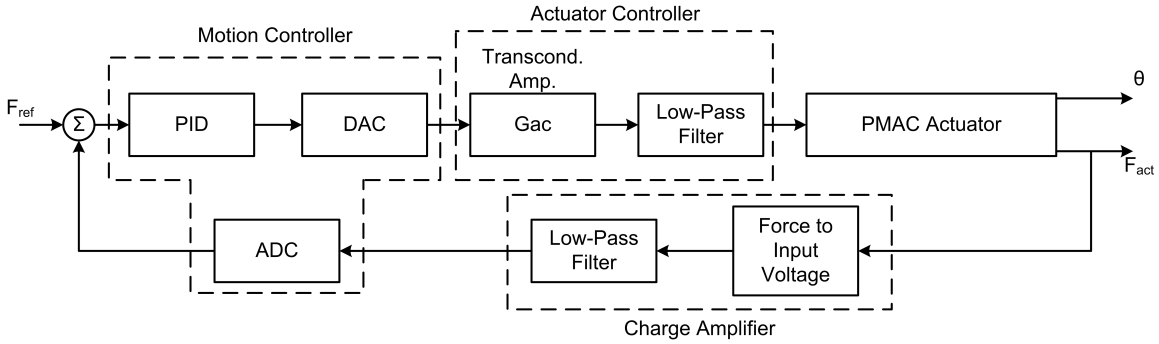

Figure 5.6: Block diagram of the direct force/torque control architecture.

In this approach the control loop can be implemented without the need for software-based controllers. The force signal from the sensor is amplified and conditioned from the charge amplifier and is fed directly into the motion controller. There it is converted into a digital signal and compared to the reference input. The resulting error value serves as the input to the PID controller. The output of the controller is transformed into an analogue voltage value using a Digital-to-Analogue Converter (DAC) with zero-order hold. This voltage is the input to the controller of the actuator.

The direct force-feedback architecture presents significant advantages. This architecture eliminates the need for software implementation of the close-loop operation. It is deployed through hardware alone. To achieve this, the force sensor is mapped as the primary feedback device and the force signal constitutes the direct input to the controller. The absence of software for the implementation of the control loop significantly reduces cycle time and eliminates the need for a special real-time operating system. A simple Windows-based PC can be used as the user interface between the motion controller and the operator, allowing the setting up of the controlling parameters. This reduces the cost of the overall system.

Furthermore, as the force sensor is placed as close to the point of application as possible, the force measurement is not affected by backlash. Please note however, that although backlash does not affect the measurement of the feedback variable, it can still affect adversely the behaviour of the system. Therefore, a reduced backlash actuator assembly is beneficial for this approach too, though not as critical as in the cascaded force/position control strategy, where backlash can lead to a wrong position steady-state value, despite the fact that the measurement arrangement indicates that the system has successfully reached the position reference input.

It should be noted that the direct force/torque control strategy does not completely eliminate the need for encoders or other sources of positional feedback in a fully-active fixturing system. This is attributed to the fact that the application of a user-selectable force value or profile is only one of the operations that the active elements need to be able to fulfil. As mentioned at the beginning of this chapter, the fixturing elements need to be able to move to a stand-by position. This involves moving the tips of the active elements to certain positions. For example, loading and unloading of components requires the elements to retract to avoid collision with the workpiece. The direct force control scheme cannot cater for such operations as it need to be in contact with the workpiece in order to operate correctly. Requesting the application of force from an element that is not in contact with the workpiece will result in the actuator accelerating rapidly and crashing. Modern controllers, however, do offer as standard the ability to change between two control schemes during operation. Therefore, a pure position control scheme can be used for positioning tasks and a pure force control scheme can be used for clamping tasks, without incurring extra costs.

5.3.3 Selection of Suitable Force/Torque Control Strategy

In machining-fixture applications, maintaining a specified clamping force profile is of paramount importance. Applying clamping forces that are higher than necessary, a situation also known as over-clamping, leads to elastic or even plastic workpiece deformation. This results in unwanted deviation from the nominal dimensions or irreversible damage to the part. On the other hand, applying too low clamping forces, also known as under-clamping, could result in the loss of contact between the fixture and the workpiece. The outcomes of such a scenario could be dimensional inaccuracy, reduced surface finish quality, damage on the workpiece, machine-tool breakdown or even serious injury to the operator.

As a result, active fixtures, not only need to exert the correct amount of forces on the workpiece, but also to react fast to sudden external stimuli like machining forces, in order to avoid excessive over- or under-clamping. The description and analysis of the different controlling strategies suggests that the implementation of the direct force control strategy can prove to be advantageous in terms of speed, accuracy and cost. In order to investigate this claim, the direct force control strategy is implemented on an experimental fully-active fixturing system. The system is described in detail in Chapter 3, Section 3.3.4 of this thesis.

Before any meaningful results can be extracted from the comparison between the various

control strategies, it is important to ensure that the controllers of the clamping elements of the fully-active fixturing system are properly tuned.

5.3.3.1 Tuning the Controller of the Experimental Fully-Active Fixture

The motion control hardware (motion controller) that was selected for the control of the experimental fully-active fixture deploys a PID controller for each axis of motion, i.e for each controlled actuator or motor. Therefore, the tuning process involves the identification of suitable proportional, derivative and integrative gains. The selected hardware limits the values of these gain variables to integer numbers only. Additionally, the motion controller offers the capability of tuning the controllers either automatically or manually. Automated tuning was found to be severely harsh, causing significant and violent oscillation of the active fixture elements that lead to plastic deformation of the test workpieces. Therefore, automated tuning was not feasible and manual tuning was preferred.

According to the manufacturers of the control equipment [95], the advised manual tuning method is the following. Firstly, the gain of the proportional part of the controller is increased to the point where the system presents oscillations. The derivative gain is then adjusted until the oscillation in the response of the system is removed. Finally, the integrative gain is increased until the steady-state error is completely removed and the system presents an acceptable overall behaviour. However, it was found that when applying even the smallest possible derivative gain ($K_D = 1$), oscillations in the response of the system were increased. As shown later in Section 5.5 of this chapter, this behaviour is expected. For this reason, the procedure that was followed is slightly changed. The proportional gain was increased until the output steady-state value for a step input presented no significant change between two consecutive proportional gain values. The integrative gain was then increased until the steady-state error was zero and the settling time was the shortest possible, without presenting significant overshoot. The derivative part of the controller was assigned a zero value, leading to a PI controller.

Following the above process, a PI controller with $K_p = 11$, $K_I = 86$ was established. This controller is implemented digitally, with a cycle time of 2 ms. Digital-value step commands where issued to the system. The magnitude of the step commands is measured in counts. Counts refer to the digital representation of an analogue, in this case force, value. The analogue-to-digital value correlation depends on a series of factors, such as the settings

of the force sensor amplifier, the voltage range of the controller's input channels, and the resolution of the digital-to-analogue converter (DAC) of the controller. More information on the matter is given in Section 5.4.1.2 of this chapter.

The response of the system with the previously-mentioned controller is shown in Figures 5.7 and 5.8. The first diagram reflects the step response of the system to a single 600 count (73.26 N) step input. The second diagram shows the response of the system to a train of step inputs. Each step has a magnitude of 600 counts and is either of increasing or decreasing amplitude. The three first steps are gradually increasing the magnitude of the applied clamping force, whilst the last three steps are gradually decreasing the magnitude of the clamping force. This diagram reflects the consistency and repeatability in the behaviour of the tuned system.

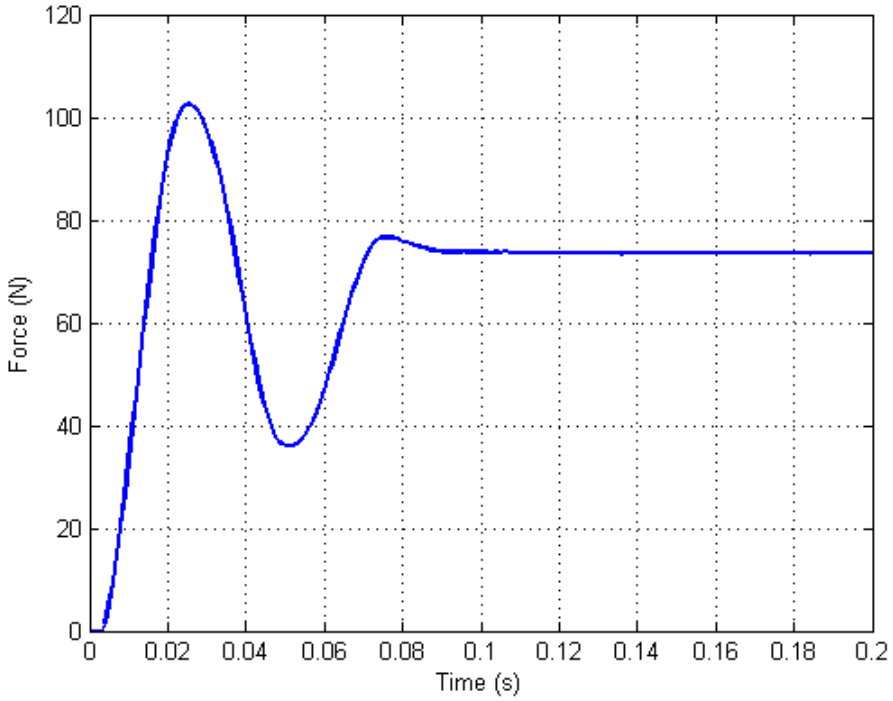

Figure 5.7: Transient response of a PMAC actuator-based active clamp with direct force control, in contact with a $150 \times 50 \times 3$ mm 7075-T6 aluminium plate, to a 600 count (73.26 N) step input.

5.3.3.2 Comparison of Control Strategies

The response obtained using the direct force/torque control strategy can be compared to the response of similar systems, which use the cascaded force/position control strategy found in literature (Figures 5.4 and 5.5). It should be noted here that the cascaded force/position

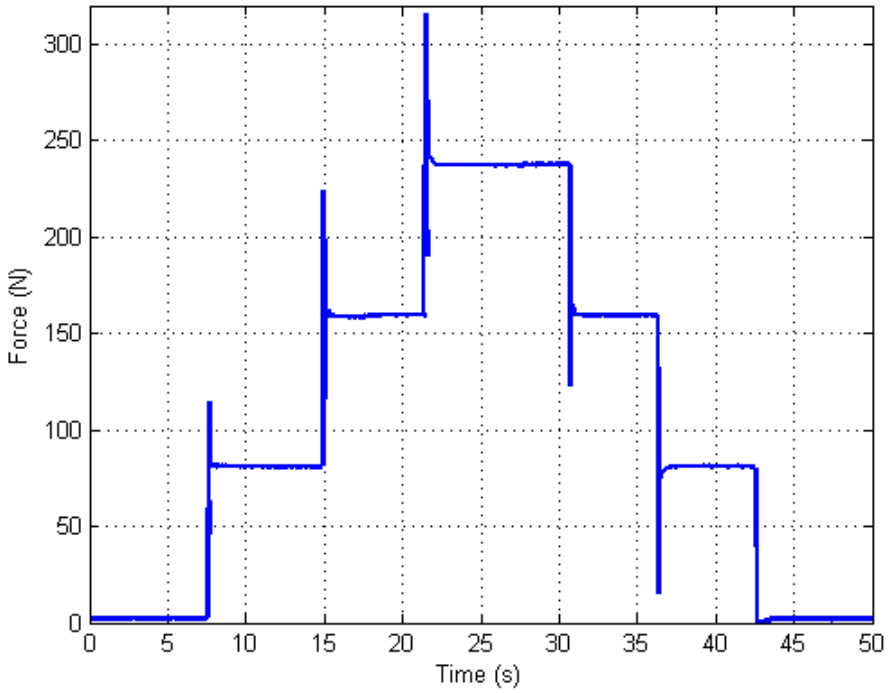

Figure 5.8: Transient response of a PMAC actuator-based active clamp with direct force control, in contact with a 150 × 50 × 3 mm 7075-T6 aluminium plate, to a train of ascending and descending 600 count (73.26 N) steps.

control algorithm was also applied on the active elements of the developed fixturing system. Nevertheless, the response characteristics obtained were inferior to the ones observed in literature. Therefore, it was preferred to perform the comparison of the two control strategies based on results from literature, as these set the performance benchmark. The comparison results are summarised in Table 5.1 and analysed in the following paragraphs.

Table 5.1: Comparison of the response characteristics of the system using the control strategy proposed by Mannan and Sollie [83] and the control strategy proposed by thus study.

Control Strategy	Response Characteristics		
	Rise Time (ms)	Settling Time (ms)	Overshoot (%)
Cascaded Force Control [83]	192.3	200	40.3
Direct Force Control	15.9	88.5	39.34
Difference (%)	91.73	55.75	2.38

Rise time. The DC motor-based active clamp system, in contact with a rigid workpiece [83, 98], operating under the cascaded force/position control algorithm, is characterised by a rise time of approximately 192.3 ms (Figure 5.4). The active element operating under

the control strategy that is proposed in this work presented a rise-time of 15.9 ms. Several comments should be made on the reported figures. Firstly, the rise time of the system from Mannan and Sollie [83] was observed for steps of 10 N. The authors of that work mention that, for larger force steps, the rise time is expected to be larger. Secondly, in the same work, it is mentioned that the stiffness at the contact between the active clamp and the workpiece also affects the response speed of the system. Higher stiffness results in faster response, ergo reduced rise time.

The PMAC-motor active clamp system proposed in the current work presents two characteristics that affect the rise time of the system in a negative manner. The clamp was tested for step force command inputs of approximately 72 N. Furthermore, the response of the clamp was obtained when the fixture element is in contact with a low-rigidity thin aluminium plate. Even so, the proposed system responded significantly faster, showing an improvement in rise time by 91.73%.

Settling time. The cascaded force/position control algorithm-based system presents a settling time of 200 ms. In comparison, the PMAC motor-based active clamp operating the direct force control algorithm proposed, manages to maintain a force value that is within ±2% of the steady-state value, after 88.5 ms. This translates in an improvement by 55.75%.

Overshoot. In most cases, the system proposed by Mannan and Sollie [83] presents no overshoot in its force response. A relatively large overshoot is observed during the first force step. This is approximately 40.3% of the amplitude of the step. However, no overshoot is observed in the next steps. Additionally, the same system during a ramp command input [98] (Figure 5.5) presents an overshoot of 3.1%. The direct force-controlled PMAC actuator system, that serves as the active element of the proposed fully-active fixture, exhibits significant overshoot (39.34%) in every step response (Figure 5.8).

Other response characteristics. As seen in Figure 5.4, in some cases, the response of the active fixture element, operating under the cascaded position/force control algorithm, presents an undershoot when the active clamp receives the step command. This means that the fixture element tends to move away from the workpiece, which causes the sudden reduction of clamping force. This initial undershoot, in the worst case, is approximately 34.4% of the step amplitude. Additionally , the active clamp, for every step command input,

appears to respond differently. In more detail, when executing the first step command, the output force increases to a certain value, at which it momentarily stabilises. Then the force continues to rise towards the steady-state value. Then, and before before settling to the final force value, it overshoots and oscillates. When executing the second and third step commands, no such behaviour is observed. Finally, at the third step command, no undershoot, overshoot or oscillation is observed in the response.

Figure 5.5 also reflects some interesting characteristics about the response of the DC motor-based active clamp, under the cascaded force/position control strategy. The clamping force in this case rises steadily and overshoots slightly (3.1%). It maintains this increased clamping force for about 63.6 ms and then the clamping force is reduced. A small undershoot is observed before the output force stabilises to the desired steady-state force value.

In comparison, the response of the direct-force-controlled PMAC actuator, proposed in this work, is more consistent. In all step commands, the system responds by presenting a relatively large overshoot and slight oscillation before stabilizing to the steady-state value. In some cases, the system stabilises momentarily at a force value, which is approximately 4.64% higher than the required steady-state value. Then, it ramps down until it reaches the steady-state value. This fluctuation in behaviour is attributed to the non-linearities and the stochastic characteristics in the system.

The above analysis outlines and highlights the advantages of the direct force/torque control scheme, when used to control the clamping forces exerted from the active clamping elements of a fully-active fixture, on the workpiece. Table 5.1 reveals that the proposed system responds significantly faster compared to a similar system that uses the cascaded position/force control approach. This means that the proposed system is better suited for active fixturing systems designed for machining processes, as it can adapt the clamping forces on the workpiece faster, minimising the transition effects from one clamping force to another, and more frequently. Additionally, the proposed system was proven to operate effectively in a wider range of forces, compared to that found in the literature [83]. This attribute is critical as the amplitude of machining forces can fluctuate heavily.

The response of the direct-force-controlled system, however, presents large overshoot in the force output. Large overshoot is also presented in the response of the system operating under the cascaded control strategy, however it constitutes the exception, since it was only

observed in the response to the first step input from a chain of steps. The overshoot can have an important impact in the surface profile of the processed workpiece. As the clamping force increases momentarily, so does the instantaneous depth of cut. This results in the formation of an unwanted groove on the surface of the workpiece. However, and as it will be discussed at a later point within this chapter (Section 5.5.3), this negative characteristic in the response of the proposed system could potentially be removed by a different set-up of the parameters of the controller. This shall be discussed in Section 5.5.3.

On the basis of the above analysis, the direct force/torque control scheme is deemed more appropriate for controlling the clamping forces applied by a fully-active fixturing system. Therefore, this control scheme will be incorporated in the comprehensive model of the fixture workpiece system. The rest of this chapter concentrates on creating the comprehensive fixture-workpiece system, when it operates in closed-loop under the direct force/torque control strategy.

5.4 Modelling the Closed-Loop Operation of the Clamps

In Chapter 4, the open-loop operation of the actuator in contact with a clamped-free-clamped-free (CFCF) plate workpiece was presented. The model also included the controller of the actuator, which was approximated as a transconductance amplifier with gain G_{ac} in series with an RC-circuit, playing the role of a low-pass filter. The PMAC actuator was approached as a DC motor actuator using the following relationships:

$$J_{tot}\ddot{\theta} + f_r\dot{\theta} = K_T I_m - T_e \tag{5.1}$$

$$L_m\dot{I}_m + R_m I_m = V_m - K_{emf}\dot{\theta} \tag{5.2}$$

where:

- J_{tot}: Moment of inertia of rotating components within the actuator in kg m^2
- θ: Angular displacement of motor in rad
- K_T: Motor torque constant in Nm/A
- f_r: Viscous damping co-efficient of motor in Nms/rad
- T_e: Externally applied torque in Nm
- I_m: Motor input current in A

V_m: Motor input voltage in V

L_m: Motor winding inductance in H

R_m: Motor winding resistance in Ω

K_{emf}: Electromotive force coefficient in Vs/rad

The actuator controller was modelled through equation:

$$V_m + RC\dot{V}_m = RG_{ac}V_{cc} \tag{5.3}$$

where R is the resistance of the RC-circuit, C is the capacitance of the RC-circuit, and V_{cc} is the command voltage applied on the actuator controller. The comprehensive fixture-workpiece model was generated by first coupling the model of the mechanical response of the actuator (Equation (5.1)) with the discretised workpiece model through implementing the following formula:

$$[S_C] = [S_w] \oplus [S_{ac}] \tag{5.4}$$

with $[S_w]$ being the system of second order equations of motion representing the discretised workpiece, $[S_{ac}]$ representing the 2^{nd} order equation of motion of the actuator, $[S_C]$ being the resulting coupled model, and $\oplus$ symbolising the impedance coupling process, presented in detail in Section 4.5. The coupled system of equations was then expressed as a system of 1^{st} order ordinary differential equations (ODEs), allowing the coupling of Equations (5.2) and (5.3) to system $[S_C]$, and the generation of the state-space model of the open-loop workpice-actuator system.

To expand the previously mentioned model to include the closed-loop behaviour of the actuator, the various components that comprise the entire system and their characteristics need to be first introduced. As shown in Figure 5.6, the closed-loop direct-force-feedback operation requires a motion controller and a charge amplifier. The former is constituted of a PID controller, an Analogue-to-Digital converter (ADC) and a Digital-to-Analogue converter (DAC). The charge amplifier, apart from converting the charge from the sensor to a voltage and amplifying it, it also contains a low-pass filter. All these components should be included in the overall fixture-workpiece model. Each component is discussed and analysed hereafter.

5.4.1 Modelling the Motion Controller

The motion controller is a digital controller. This means that the signals it treats need to be digital and therefore discrete. Nevertheless, it is a common approach to treat the system through a continuous-time model [51]. It is considered that the motion controller is constituted of the following parts:

5.4.1.1 PID Controller

The PID controller is perhaps the most commonly met controller in industrial applications. It comprises three parts; a proportional, an integral, and a derivative part. Each of them affects the output of the controller [50] and therefore the overall behaviour of the active fixturing elements. The continuous-time transfer function of the PID controller can be expressed as follows:

$$C_{PID}(s) = K_p\left(1 + \frac{K_I}{s} + K_D s\right) \tag{5.5}$$

In Equation (5.5) K_p is the gain of the proportional controller, K_I is called the integrative gain, K_D is called the derivative gain, and s is the Laplace variable. Defining the parameters of the PID controller is achieved through tuning. This is discussed later within this chapter.

5.4.1.2 Analogue-to-Digital Converter

The continuous-voltage signal from the force-sensor amplifier is transformed into a digital value through the ADC. The voltage signals are passed to the motion controller and the ADC through the input channels of the controller. The range of the voltage values, which the input signals are expected to have, is a parameter that needs to be defined in the settings of the controller. This ensures that the motion controller interprets the input signals correctly. In this work, the input signals range in value between 0 and 10 V, corresponding to 0 and 500 N, respectively. Therefore, the voltage range of the input channels of the motion controller is set to $0 \div 10$ V.

Furthermore, in order to define the transfer function of the ADC, it is necessary to define its resolution. The motion controller used here offers analogue inputs with a 12-bit resolution. The ADC can therefore be approached as a continuous transfer function with a constant gain of $H_{ADC}(s) = \frac{2^{12}}{10}$, measured in counts/V. The numerator reflects

the resolution of the ADC, whilst the denominator reflects the input voltage range. This transfer function defines the relationship between the digital unit of counts (bits) and the analogue value of the applied force.

5.4.1.3 Digital-to-Analogue Converter

The output of the PID controller inside the motion controller is a digital value measured in counts. This value needs to be transformed into a continuous voltage signal. The latter serves as the command signal to the controller of the actuator. The voltage value of this signal depends both on the resolution of the DAC and the output voltage range. Both of these depend, in turn, on the selected hardware. For the motion controller used in this work, the DAC resolution is 16 bits and the output voltage range is ±10 V. For modelling purposes, this can be expressed as a continuous transfer function with a static gain $H_{DAC}(s) = \frac{20}{2^{16}}$. This is measured in V/counts. The numerator represents the voltage range, whilst the denominator represents the resolution of the DAC.

5.4.2 Modelling the Charge Amplifier

The main role of the charge amplifier is to accept the charge generated at the piezoelectric force sensor as its input and transform it into a voltage signal with a $0 \div 10$ V range. Additionally, the produced voltage could be conditioned using a low-pass filter with user-selectable cut-off frequency. These features need to be reflected through appropriate transfer functions.

5.4.2.1 Force-to-Voltage Transformation

Piezoelectric force sensors produce a charge depending on the force that is applied on them. The charge produced per unit force is a characteristic of each sensor and is called charge sensitivity. It is measured in Coulomb per Newton (C/N) and it is denoted by Q_s. The produced charge from the sensor is therefore proportional to the applied force, i.e. $Q = Q_s F_A$, where Q is the charge change in Coulomb (C).

The charge amplifier transforms the produced charge into a voltage signal using a range capacitor. This voltage, in the majority of cases [69], can be calculated as shown below:

$$\frac{V_{in}}{F_A} = \frac{Q_s}{C_g} \tag{5.6}$$

where C_g is the capacitance of a range capacitor, measured in Farad (F). The force sensors used in this work were calibrated and found to present a charge sensitivity of $Q_s = 4.30$ pC/N. The value of the range capacitor depends on the output range of the amplifier, which is defined by the user. For this work, a range of 50 N/V is selected. This constitutes the amplification gain and translates into a measurement range of $0 \div 500$ N. By multiplying the range with the charge sensitivity, the capacitance of the range capacitor can be calculated. In this example, $C_g = 4.30 \times 50 = 215$ pF. These figures result in the amplifier outputting 0.02 V for every Newton of force observed by the load washer.

Equation (5.6) constitutes the transfer function of the force-to-voltage transformation process of the amplifier, when a low-pass filter is not used.

5.4.2.2 Low-Pass Filter of the Amplifier

In many applications where sudden changes in the force measurement are likely to occur, it is important to protect the hardware for electric voltage impulses. For this reason, the use of a low-pass filter is advisable. The amplifier used here (Kistler Type 5017A [69]) deploys a low-pass filter with user-selectable cut-off frequency. There is also the capability to turn the filter completely off. This low-pass filter should be present and is included in the developed model.

Just as in the case of the controller of the actuator, due to lack of information for the exact nature of the filter, a simple RC circuit is assumed. Therefore, the input voltage is related to the output voltage through the following equation:

$$V_{out} + R_f C_f \dot{V}_{out} = V_{in} \tag{5.7}$$

where R_f and C_f are, respectively, the resistance and the capacitance in the RC circuit. Transferring Equation (5.7) to the Laplace domain and solving for V_{out}/V_{in}, the transfer function of the low-pass filter in the amplifier can be established.

$$H_{af}(s) = \frac{1}{1 + R_f C_f s} \tag{5.8}$$

Due to the absence of arithmetic data on the values of the resistance and the capacitance of the elements in the RC filter, a $C_f = 500$ pF is assumed. The value of R_f can then be calculated through $F_c = 1/2\pi R_f C_f$, a relationship that interrelates the cut-off frequency,

the resistance and the capacitance of the low-pass filter. The random selection of the capacitance value does not subtract from the validity of the model. Both the frequency and step responses of the filter do not depend on the value of the capacitance. The behaviour of the filter is only affected by the inverse of the product of the resistance and the capacitance (cut-off frequency).

The combined transfer function of the the force sensor and the amplifier can be found through multiplication of the two separate transfer functions. This yields:

$$H_{amp}(s) = \frac{Q_s}{C_g(1 + R_f C_f s)} \tag{5.9}$$

As an example, the step response to a 1 N input and the Bode diagram of the full amplifier system, with a cut-off frequency of 10000 Hz is shown in Figure 5.9.

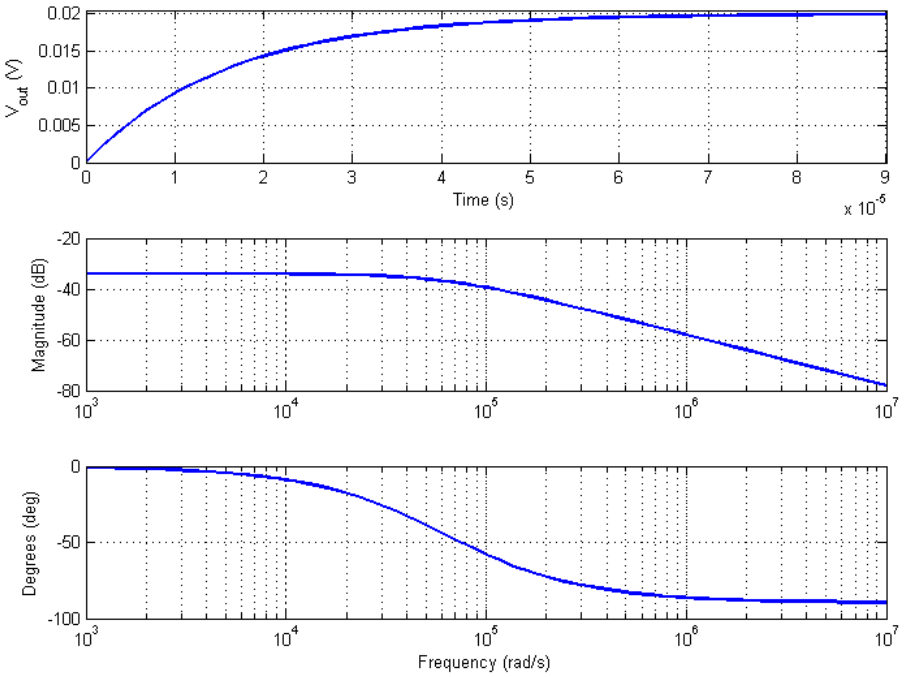

Figure 5.9: Step response and Bode diagram of the force sensor amplifier with the low-pass filter turned on ($F_c = 10000$ Hz).

5.4.3 Generating the Full System Model

Having established the dynamic models of all the elements that constitute the closed-loop system, it is possible to compile the comprehensive dynamic model of the fully-active fixture-workpiece system, operating under a direct-force-feedback force control algorithm.

To achieve this, the transfer function of the PID controller is multiplied with the transfer function of the DAC, i.e. $C(s) = C_{PID}(s) H_{DAC}(s)$.

The same process can be followed for the feedback branch. The overall transfer function of the feedback, denoted as $H_{fb}(s)$, can be estimated by multiplying the transfer functions of the different components that lie on the feedback branch. Based on Figure 5.6, this operation results in $H_{fb}(s) = H_{amp}(s) H_{ADC}(s)$.

Finally, the open-loop actuator-workpiece model that was generated in Chapter 4 (Equations (4.57)-(4.62)) needs to be introduced into the overall model. As this model is in state-space format, it first needs to be transformed in a transfer function. This is achieved by using the following formula [85], assuming zero initial conditions:

$$\mathbf{D}(s) = [H](s[I] - [F])^{-1}[G] + [J] \tag{5.10}$$

where $\mathbf{D}(s)$ is the transfer function of the open-loop actuator-workpiece system, $[I]$ is the unit matrix, and $[F]$, $[G]$, $[H]$, and $[J]$ are, respectively, the system, input, output, and direct transmission term matrices of the state-space model [50]. The block diagram of the system (Figure 5.6) is thus simplified to the one shown in Figure 5.10.

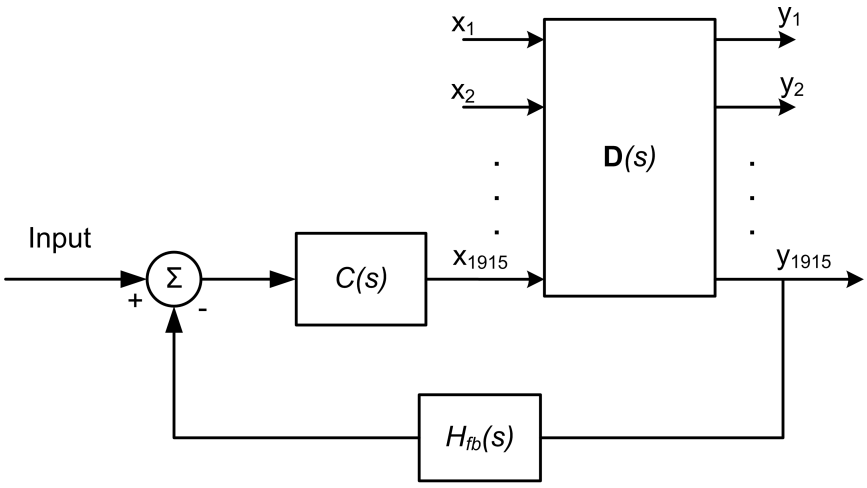

Figure 5.10: Simplified block diagram of the fixture-workpiece system. $C(s)$ is the resultant transfer function of the PID controller and the DAC, $\mathbf{D}(s)$ is the transfer function of the coupled actuator-workpiece system, and $H_{fb}(s)$ is the resultant transfer function of the amplifier and the ADC.

The open-loop actuator-workpiece model is a Multi-Input-Multi-Output (MIMO) model. This means that the transfer function $\mathbf{D}(s)$ encapsulates a number of SISO transfer functions $D_{(i,j)}$, which describe how each input u_i of the model affects each output y_j. The model that was formulated in Section 4.5 of Chapter 4 exhibits 1915 inputs and 1915 out-

puts.

The other transfer functions in Figure 5.10 express Single-Input-Single-Output (SISO) systems. Therefore, extra care needs to be taken in the formulation of the final model, in order to ensure that the output of the SISO models is applied to the correct input of the MIMO actuator-workpiece model. The same applies for the feedback loop. The feedback SISO model needs to be connected to the correct output of the MIMO model.

As explained in Section 4.5 of Chapter 4, the input voltage from the PID controller and the DAC corresponds to input u_{1915} of the actuator-workpiece model. This means that the transfer function $C(s)$ needs to be multiplied with all transfer functions of the MIMO model $\mathbf{D}(s)$ that describe the relationship between this input and the outputs of the model. In other words, the following operations need to be executed:

$$H_{(1915,j)}(s) = C(s)\, D_{(1915,j)}(s), \quad for\ j = 1, \ldots, 1915 \tag{5.11}$$

Moreover, the output of the MIMO fixture-workpiece model that related to the force that the active element exerts on the workpiece is the 1915^{th} output. Therefore, the complete closed-loop model is produced as shown below:

$$H_{sys_{(1915,1915)}}(s) = \frac{H_{(1915,1915)}(s)}{1 + H_{fb}(s)\, H_{(1915,1915)}(s)} \tag{5.12}$$

Equations (5.11) and (5.12) lead to the complete model of the fixture-workpiece system, operating in open loop. This is denoted hereafter as $\mathbf{H}_{sys}(s)$. With the generation of the entire closed-loop model, it is possible to compare the time-domain responses of the modelled and the experimental system. Nevertheless, before a direct comparison with the experimental implementation of the modelled system can be fulfilled, it is necessary to tune the controller of the modelled system.

5.5 Tuning the Controller of the Modelled System

There are various methods that can be employed to tune the controller of the modelled system [50]. Perhaps the most commonly used one is the Ziegler-Nichols method (ZN). This tuning method, along with manual tuning, are presented in the next section.

5.5.1 Ultimate Sensitivity Ziegler-Nichols Design Method

Ziegler and Nichols have developed two tuning methods for controller [50]. One is based on analysing the step response of the systems with an open-loop architecture. The other, which is the one applied here, is designed for systems that operate in a closed-loop fashion. The first step of this method involves the use of a controller with only a proportional part. The gain of this controller is increased to the point, where the system is brought to its stability limit. At this point the system exhibits continuous oscillation. The period of this oscillation is called the ultimate period, symbolised as P_u, and the gain at which this behaviour is observed is called the ultimate gain, symbolised by K_u. These two measures are used to tune the controller (P, PI or PID), through the formulas shown in Table 5.3.

Table 5.3: Controller parameter settings according to the Ziegler-Nichols ultimate sensitivity method, based on data from [50].

Type of Controller	Parameter Setting
P	$K_p = 0.5K_u$
PI	$K_p = 0.45K_u$ $K_I = \frac{1.2Kp}{P_u}$
PID	$K_p = 0.6K_u$ $K_I = \frac{2K_p}{P_u}$ $K_D = \frac{K_p}{8}P_u$

The ultimate gain of the comprehensive fixture-workpiece model was found to be $K_u = 20.88$. At the marginally stable condition, the period of oscillation was $P_u = 0.0375$ s. Using these values, the parameters of a P, a PI and a PID controller were estimated as shown in Table 5.4.

Table 5.4: Controller parameters after applying the Ziegler-Nichols ultimate sensitivity method.

Type of Controller	Parameter Setting
P	$K_p = 10.44$
PI	$K_p = 9.396$ $K_I = 300.672$
PID	$K_p = 12.528$ $K_I = 668.16$ $K_D = 0.0587$

5.5.2 Manual Tuning

Tuning the controller manually is based on trial and error. The procedure followed to tune the controller is similar to the one used to tune the controller for the active elements of the experimental fully-active fixture (see Section 5.3.3.1). The proportional gain is increased until the output steady-state value for a step input presented no significant change between two consecutive gain values. The integrative gain is then increased until the steady-state error is eliminated and the settling time is the shortest possible, without presenting significant overshoot. In this way, a PI controller is formulated. For establishing the parameters of a manually-tuned PID controller, the same process is repeated, but a derivative gain is also added. The gain is increased until the behaviour of the system is still acceptable, according to the design requirements. Finally, the proportional and integrative gains are increased to identify whether the behaviour of the system is improved.

Following the above process, a PI controller with $K_p = 9$, $K_I = 196$ and a PID controller with $K_p = 9$, $K_I = 236$ and $K_D = 0.08$ are identified as acceptable tuning parameters.

5.5.3 Discussion on the Tuning Results for the Modelled System

After establishing suitable controller parameters through various tuning methods, the behaviour of the model of the fixture-workpiece system can be extracted. Both the time-domain and frequency-domain response of the system with all the previously mentioned controllers are extracted. Figure 5.11 shows the response of the system to a 600 counts (73.26 N) step input. Figure 5.12 depicts the frequency response of the system. Table 5.5 summarises the results form the comparison of the time-domain responses of the system (modelled and experimental), operating under the different controller settings.

A series of observations, on the theoretically obtained time-domain responses can be made from Figure 5.11. From the force output response of the system the following can be concluded:

- A purely proportional controller does not constitute an acceptable solution due to the presence of a steady-state error.
- The addition of an integrative part in the controller (PI or PID) eliminates the steady-state error, as expected.

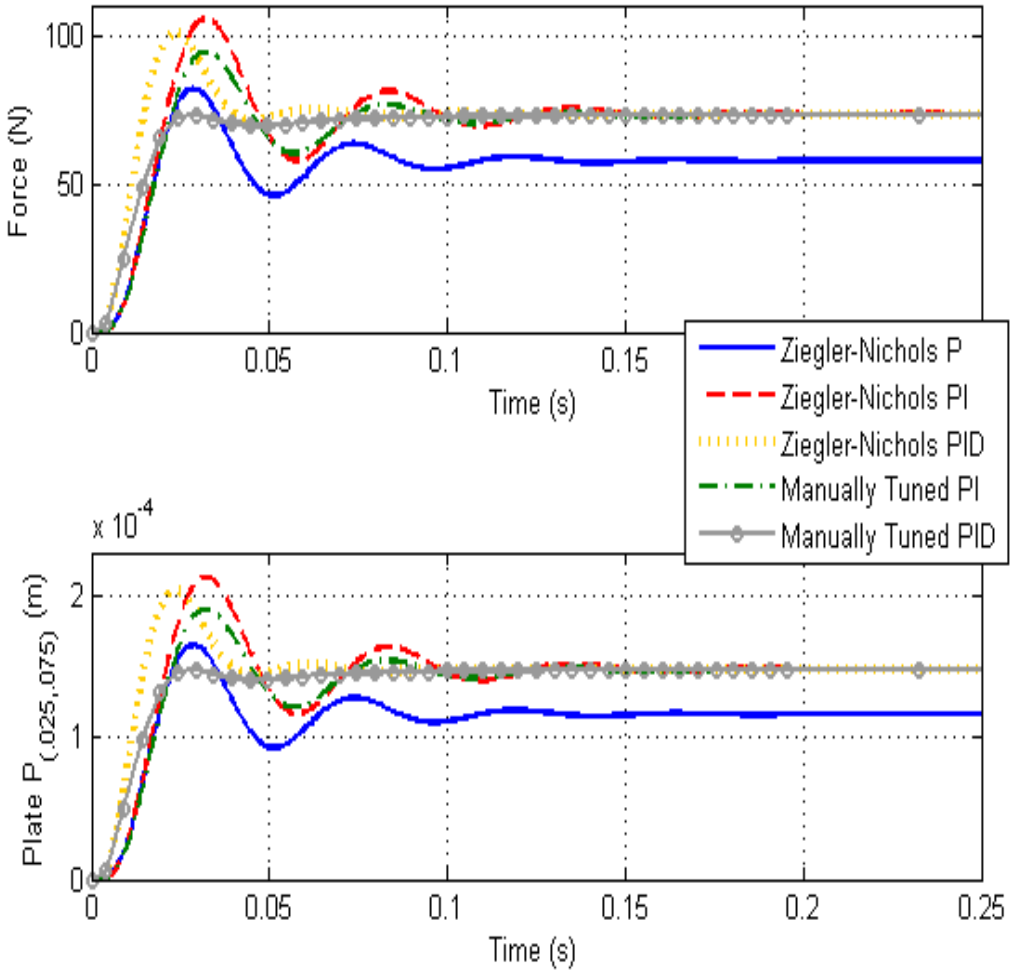

Figure 5.11: Response of the fixture-workpiece system with different controller parameters, to a 600 count force command input. From top: Actuator force output, angular velocity of the actuator motor axis, angular position of actuator motor axis, displacement of the midpoint (connecting point) of plate.

- All controllers that were the result of the Ziegler-Nichols ultimate sensitivity tuning method present significant overshoot and oscillation. The Ziegler-Nichols PI controller presents the largest overshoot (43.95%) compared to all other cases. The Ziegler-Nichols P and PID controllers present 41.78% and 37.31% overshoots, respectively. Furthermore, the PID controller presents the least oscillation. On the contrary, the PI controller presents the most intense oscillatory behaviour.

- The transient response of the system that utilises a PID controller, which was tuned using the Ziegler-Nichols ultimate sensitivity method, exhibits the briefest rise time (14.5 ms). The Ziegler-Nichols PI controller has a rise time of 20.8 ms, whilst the P

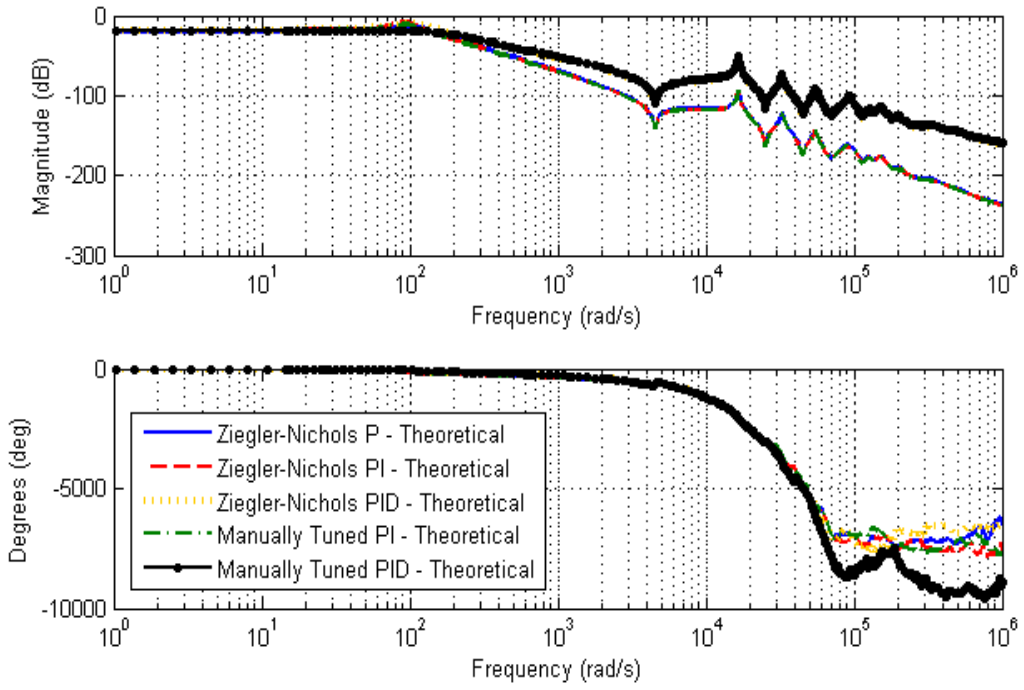

(a)

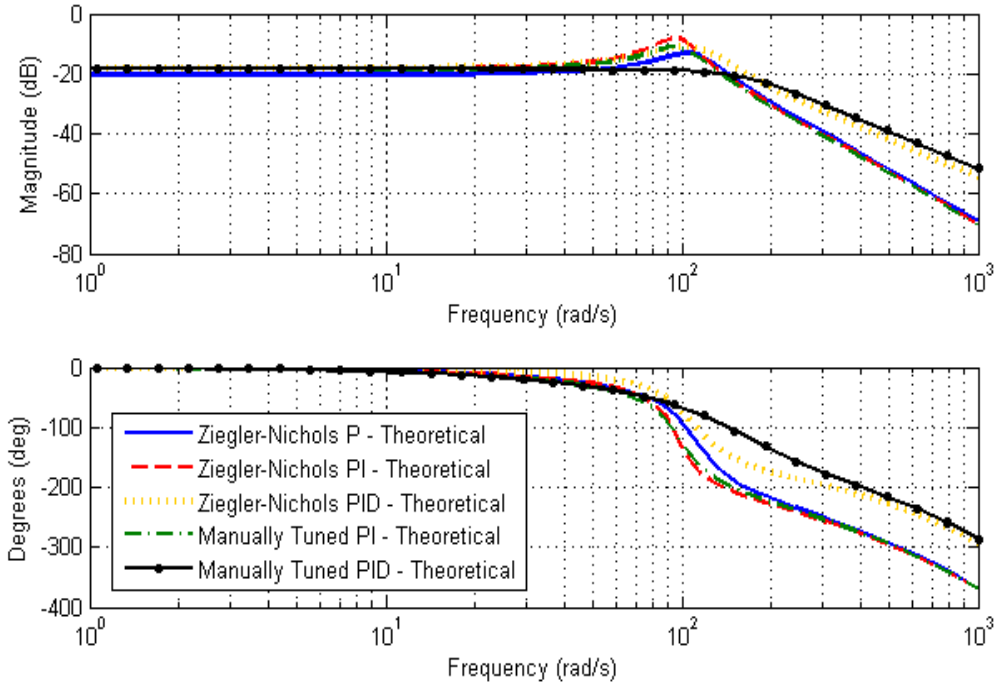

(b)

Figure 5.12: Frequency response of the force output of fixture-workpiece system with different controller parameters, to a force command input. (a) Response magnitude and phase in the 1 to 10^6 rad/s range, (b) A more detailed view of the response magnitude and phase in the 1 to 1000 rad/s range.

Table 5.5: Comparison between the time-response characteristics of the comprehensive fixture-workpiece system model under different controller parameters, and the manually tuned PI controller of the experimental fixture-workpiece system.

Tuning Method	Controller Type	Controller s Setting	Rise Time (ms)	Settling Time (ms)	Overshoot (%)
ZN	P	$K_p = 10.44$	22.6	123.3	41.78
ZN	PI	$K_p = 9.396$ $K_I = 300.672$	20.8	137.9	43.95
ZN	PID	$K_p = 12.528$ $K_I = 668.16$ $K_D = 0.0587$	14.5	49.7	37.31
Manual	PI	$K_p = 9$ $K_I = 196$	22	117.9	28.54
Manual	PID	$K_p = 9$ $K_I = 236$ $K_D = 0.08$	28.8	31.9	2.65
Experimental Manual	PI	$K_p = 11$ $K_I = 86$	15.9	88.5	39.34

controller exhibits a rise time of 22.6 ms.

- The manually tuned PID controller is superior to all other controllers in terms of settling time. The response of the system with this controller settles to the steady-state value after 31.9 ms. The Ziegler-Nichols P, PI and PID controllers settle after 123.3 ms, 137.9 ms, and 49.7 ms respectively.

- The system with the manually-tuned controllers presents smaller overshoot than the system that was tuned using the Ziegler-Nichols ultimate sensitivity method. Specifically, the manually-tuned PI controller-based system presents an overshoot of 28.54%, whilst the manually-tuned PID controller-based system has an overshoot of 2.65%.

- In general, the manually-tuned systems present slower transient response characteristics compared to their Ziegler-Nichols tuned counterparts. The manually-tuned PI controller-based system rises within 22 ms and settles after 117.9 ms. The manually-tuned PID controller-based system rises within 28.8 ms. However, the system with a manually tuned PID controller settles after 31.9 ms, i.e. faster than the system with a Ziegler-Nichols-tuned PID controller.

Based on this analysis, it is easily concluded that the implementation of a PID controller results in the fastest response characteristics and the smallest overshoot compared to the other controller architectures, i.e. P or PI. The ZN-tuned PI controller exhibits to the largest overshoot. The manually-tuned PI controller (theoretical) also leads to overshoot that is significantly larger compared to the manually-tuned PID controller. This leads to the conclusion that a PI controller leads to a system with increased overshoot, which can be dealt with by the addition of a derivative action in the architecture of the controller. This observations is of great importance. The experimentally applied PI controller (Figure 5.7) presents a large overshoot in its step response. This is a characteristic that is not desirable in fixturing applications, especially when low-rigidity workpieces are the focal point.

Furthermore, from Table 5.5, it is evident that the controller parameters of the tuned theoretical system are in a fair agreement with those of the experimental system. They present the same pattern, with small proportional and large integrative gains. A good agreement in the values of proportional gains is revealed, with a maximum difference between experimental and theoretical values being 18.18%, observed for the manually tuned controllers of the model. The integrative gains, however, are not close. The maximum observed difference occurs for the ZN-tuned PID controller, where the integrative gain of this controller is approximately 8 times larger than that of the experimental system. The smallest difference is observed for the modelled manually-tuned PI controller, the integrative gain of which is approximately 2.3 times larger than that of the experimentally deployed controller. This behaviour was expected as the experimental system is applied digitally, whilst the modelled system is treated in the continuous time-domain. Nevertheless, a full agreement between the parameters of the experimentally- and the theoretically-deployed controller was never sought after. The importance in the developed model lies primarily in the prediction of the time-response characteristics and the determination of an appropriate controller architecture, along with the interrelationship between the parameters of the controller.

As mentioned in Section 5.3.3.2, under machining conditions, the presence of overshoot would translate in a momentarily increased depth of cut, which would result in reduced surface quality and an uneven surface profile. According to the above results, the overshoot could be reduced, almost without compromise in the rise-time and the settling-time, by applying a small derivative gain value ($K_D = 0.08$). In practice, this was not feasible

as, due to the limitations in the selected equipment, the smallest derivative gain value that could be assigned was $K_D = 1$, which is significantly larger that the ones applied in the theoretically-tuned model. This value lead to unstable behaviour of the experimental system. However, the previous analysis constitutes a solid indication that a controller with more flexible tuning capabilities could further improve the behaviour of the system operating under the direct force/torque control strategy.

Continuing the discussion on the comparison between the theoretically-obtained results, the Ziegler-Nichols-tuned PID controller leads to the fastest rising system, and the shortest settling-time amongst the theoretically- and ZN-based tuned controllers. The results from the manually-tuned PID controller show that the settling-time and the overshoot could be reduced, to the expense of the rise-time, by decreasing the integrative action and increasing marginally the derivative action.

From the frequency response characteristics of the system, the following conclusions can be drawn:

- In all cases the system is stable, presenting positive gain margins and infinite phase margins. In detail, the Zeigler-Nichols tuned P, PI and PID controllers present gain margins of 19.3 dB, 14.2 dB and 26.4 dB, respectively. The manually-tuned PI and PID controllers lead to a system with gain margins of 17.8 dB and 31.2 dB, respectively. The system with the manually-tuned PID controller presents the highest stability margin as it has the largest gain margin.

- The system tracks the input reasonably well up to a frequency of 1.91 Hz for the manually-tuned cases, 2.07 Hz for the Ziegler-Nichols P and PI cases and 2.39 Hz for the Ziegler-Nichols PID case.

- In the manually-tuned PI and PID, and the Ziegler-Nichols tuned P and PI controller cases, the response of the system is trailing the input at a phase of 45^o, when the excitation frequency of the input is about 2.47 Hz. The system with the Ziegler-Nichols PID-tuned controller is trailing the input at the same phase, when the excitation frequency of the input is 2.71 Hz.

The previous analysis shows that the implementation of a PID controller leads to a stable system with higher stability margin. Additionally, a PID controller-based system

could grant the system with better input tracking capabilities. It should be noted that the manually-tuned PID controller is the solution is the solution with the highest stability margins but also the worst in terms of input tracking. The tracking capability is improved at the expense of overshoot. This can be seen by studying the frequency characteristics of the Ziegler-Nichols PID controller-based system. The latter presents the second highest gain margin and the and the most accurate tracking of the input. However, this system exhibits a relatively large overshoot. So long as the active clamps are required to change the forces they apply less frequently than 1.91 times a second, the manually-tuned PID controller is still the preferred controller solution.

Another important point that should be mentioned here is the following. The frequency response diagram for the system reveals that the electromechanical actuator that is being used in this work as an active clamping element is not suitable for applications where fast response to rapidly changing stimuli is necessary. However, the designed system is not intended for operation under such conditions. In other words, the active clamps are not intended to be used with vibration damping in mind. The active clamps are required to adapt the forces they apply almost one time per second (1 Hz). This, in combination with the constantly changing point of application of the clamping force is more than adequate to drastically improve the outcome of the machining process of thin-walled structures. This will be discussed further in Chapter 7 of this thesis.

In the next section, the time domain results from the model of the fully-active fixture-workpiece system that were presented earlier are compared to the experimentally obtained response of system. This is performed in order to examine the validity of the developed model.

5.6 Validation of the Fixture-Workpiece System Model

The previous section described the generation of a model that represents the active fixturing elements in contact with a thin-walled workpiece. The active elements operate in closed-loop manner under the direct force/torque control scheme. A series of P, PI and PID controllers were tuned and examined for their effect on the response of the system. In order to validate the developed model it is necessary to compare the response of the modelled system in terms of force output to the experimental results presented in Figure 5.7. This

comparison is executed graphically, through Figure 5.13. This figure shows the time domain response of the modelled system with both the manually-tuned PI and PID controllers, along with the response of an active clamping element from the fully-active fixture. The clamping element is in contact with a thin-walled workpiece that has the form of a thin plate, made of aluminium alloy (7075-T6).

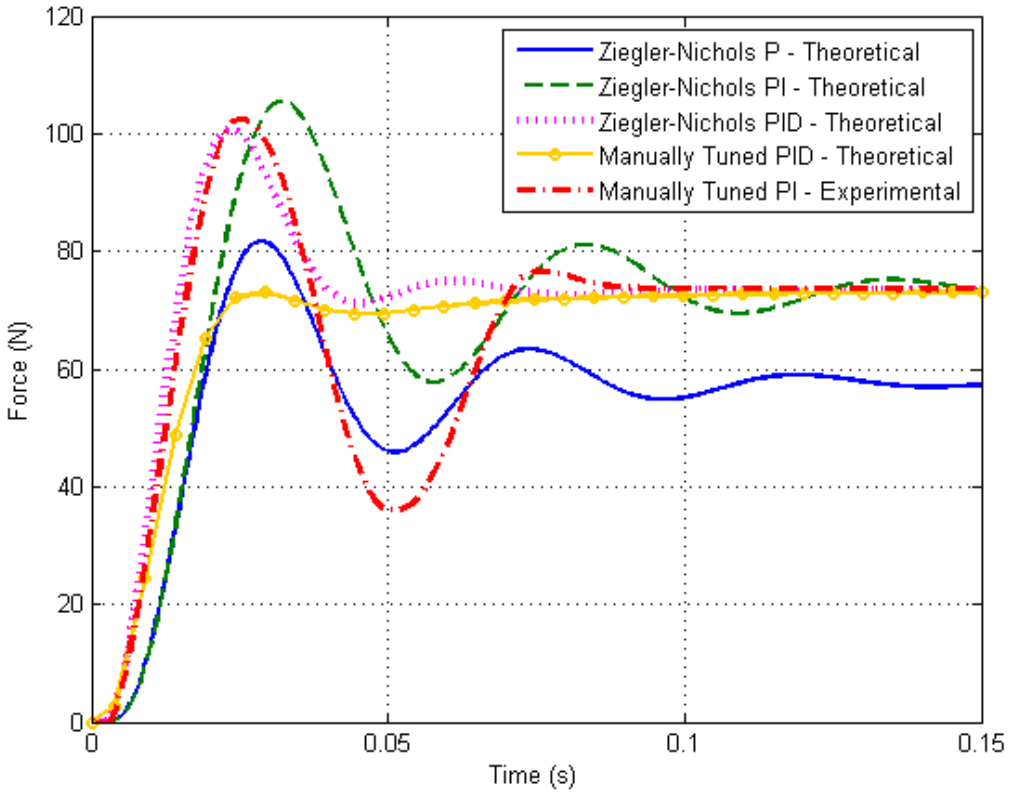

Figure 5.13: Step responses of the experimental and the modelled system, with various controller designs.

According to Figure 5.13, the experimentally-obtained response and the response of the modelled system are in very good agreement. This is reflected in Table 5.5. For convenience, the key characteristics of the response of the experimental and the theoretical system are re-iterated in Table 5.6. The overall behaviour of the modelled and the experimental systems is very similar. In all cases a slight delay can be observed at the first few milliseconds of the response. Then, the output force increases slowly, before it starts rising fast. An overshoot is observed in all cases apart from that of the manually-tuned PID controller. Additionally, the experimental system presents a large undershoot, something that is also present in the manually-tuned PI controlled system. In general, the developed comprehensive fixture-workpiece model represents the experimental system very well.

The controller parameters proposed by the tuning process applied on both the modelled and the experimental system, are not in good agreement. As discussed earlier the proportional gain values present a maximum difference of 18.18%. However, the integrative values of the theoretically-deployed controllers are 2.3 times higher than the integrative gain value of the experimentally-deployed controller. This behaviour was expected, as also stated earlier. This is attributed to the difference in which the experimental controller is applied (digital-discrete controller) and the way with which the modelled system was approached (continuous-time system). This difference in the controller paramaters was also observed by [83]. Nevertheless, the importance in the developed model lies primarily in the prediction of the time-response characteristics and the determination of an appropriate controller architecture, along with the interrelationship between the parameters of the controller. This has been achieved.

Table 5.6: Comparison of the time response performance between the experimental and the modelled system.

System	Rise Time (ms)	Settling Time (ms)	Overshoot %
Experimental Manual PI	15.9	83.3	39.53
Theoretical Manual PI	22.0	117.9	28.54
Theoretical Ziegler-Nichols PID	14.5	49.7	37.31
Theoretical Manual PID	28.8	31.9	2.65

Generally, the model that best reflects the behaviour of the actual system is the one with the Ziegler-Nichols-tuned PID controller. It presents the best agreement in terms of rise time (8.8%), settling time (40.33%) and overshoot (5.62%), as shown in Table 5.7. The reported agreement in terms of settling time is the second best. The model that presents the best agreement in terms of settling time is the one utilising the manually-tuned PI controller, exhibiting a difference of -33.22%) compared to the experimentally-recorded settling time.

To conclude, the presented results indicate that the developed model can be used with confidence as the basis of a design methodology for fully-active fixturing systems. The model that should be used in this design methodology is the one that deploys a PID controller with the parameters that were suggested by the Ziegler-Nichols ultimate sensitivity method ($K_p = 12.528$, $K_I = 668.16$, $K_D = 0.0587$), since this model approaches better the actual response of the fixture-workpiece system. The development of such a fixture design

methodology is the subject of the following chapter of the thesis.

Table 5.7: Comparison of the time response performance between the experimentally-deployed PI and the theoretical Ziegler-Nichols-tuned PID controllers.

System	Rise Time (ms)	Settling Time (ms)	Overshoot %
Experimental PI	15.9	83.3	39.53
Theoretical Ziegler-Nichols PID	14.5	49.7	37.31
Diff. (%)	8.8	40.33	5.62

5.7 Conclusions

This chapter focused on the control strategies that could be implemented for the control of the different operations that a fully-active fixture is called to execute. These operations were briefly presented and the attention was placed on one of the most critical aspects in fixturing applications, namely the application of clamping forces. A control strategy that leads to the best response of the active fixture elements to command inputs was selected. Furthermore, a comprehensive fixture-workpiece model, operating in a closed-loop manner, and best representing the experimentally-deployed PI controller-based system, was established. This model was validated experimentally. In more detail, the key conclusions from this chapter are:

- Two different control algorithms were presented. The first one is known as the cascaded position/force-feedback control strategy, and the second one is called direct force/torque control strategy.
- The direct force/torque control strategy was applied experimentally on a fully-active fixture test-bed and a thin-plate workpiece.
- The results from the application of the direct force/torque control strategy were compared to results from a similar system which operates under the cascaded position/force-feedback control strategy. These results were obtained from the open literature.
- A PI controller with $K_p = 11$ and $K_I = 86$ was utilised on the experimental system that deployed the direct force/torque control strategy. These values was obtained after manual tuning of the system.

- The comparison of the two systems (experimental and literature-obtained) revealed that the system under the direct force/torque control strategy exhibited faster rise time by 91.73%, and settling time by 55.75%. The response of the aforementioned system, however, presented large overshoot, something that was not present, at least in the majority of cases, in the system operating under the cascaded control strategy.

- The transfer function of a MIMO model of the fixture-workpiece system, operating in closed-loop using the direct force control strategy was established.

- The model was used to investigate theoretically the performance of different controller architectures with different controller-parameter values. These were obtained after tuning the controller of the model either manually or by implementing the ultimate sensitivity Ziegler-Nichols design method.

- A good agreement between the theoretically-obtained and the experimentally-obtained controller parameters was not achieved. Although the proportional gains presented a maximum difference of 18.18%, the integrative gain of the controllers of the theoretical system was at best 2.3 times higher, and at the worst case 8 times higher than the one that was obtained experimentally. This behaviour was expected, due to the difference in the implementation (digital-discrete) and simulation (continuous) of the system.

- It was shown that a purely proportional controller is not suitable as it does not eliminate the steady-state error.

- The Ziegler-Nichols-tuned systems presented large overshoots (max. 43.5%) compared to the manually tuned theoretical system (max. 28.8%).

- The PID-controller-based system presented the fastest settling time. The fastest settling time with a PID controller is 31.9 ms compared to 117.9 ms, which is the settling time of the manually-tuned theoretical PI-controller-based system.

- The manually-tuned theoretical system revealed that a careful selection of the controller parameters could reduce the overshoot to 2.65%.

- Based on the previous conclusion, the overshoot of the hardware system could be significantly reduced or even eliminated, by applying a small derivative action. This

was not feasible due to the parameter-adjustment limitations of the selected hardware.

- All trialled controller architectures lead to a stable system. The manually-tuned PID controller presents the highest gain margin (31.2 dB). All controllers lead to systems with infinite phase margins.

- The Ziegler-Nichols-tuned theoretical system with a PID controller presents the best input tracking characteristics. For this system, a phase angle of 45^o is observed when the system is excited at 2.71 Hz. All other theoretical systems present a response that trails by a 45^o phase angle the input, at an excitation frequency of 2.47 Hz.

- The selected system architecture, utilising the PMAC motor-based electromechanical actuators are not suitable for vibration cancellation operation, as expected. The selected system performs well so long as it is called to adapt the forces it applies on the workpiece at a rate of 1 to 1.5 times per second.

- The comparison between the experimental and the theoretically-derived responses are in very good agreement, thus verifying the developed model. Overall, the experimental system is best approximated by the fixture-workpiece model that utilises a Ziegler-Nichols-tuned PID controller. These two systems presented a good agreement in rise time (8.8%) and overshoot (5.62%). The agreement in terms of settling time (40.33%) was the second best.

- The modelled system with the Ziegler-Nichols-tuned PID controller ($K_p = 12.528$, $K_I = 668.16$, $K_D = 0.0587$) will be used as the basis of the fully-active fixture design methodology, presented in the next chapter.

Chapter 6

Fully-Active Fixture Design Methodology

6.1 Introduction

Modern manufacturing environments impose a continuous technological pull towards more flexible and efficient equipment. Customisation, low-cost quality products, rapid changes in volume and variant demand, all dictate the need for manufacturing systems and processes that are both highly reconfigurable and automated with no compromise in product quality. As it was revealed in the literature survey conducted and presented throughout Chapter 2 of this thesis, in the field of fixturing, research activities have focused so far on either flexibility/reconfigurability or enhanced performance, but not on both aspects simultaneously. The combination of these two aspects could lead to significant advantages as it will be shown in this chapter.

Active fixtures have been studied for their ability to reduce deflections of the processed workpiece through either maintaining optimal clamping forces [83, 98], or enhance surface finish by suppressing vibration [110, 131], or ensuring repeatable positioning of the workpiece relative to the machine-tool's reference frame [21, 22, 116]. Research work on reconfigurable fixtures on the other hand, has so far focused solely on the ability to cater for various workpieces [24, 66]. By combining these two aspects of fixturing great new potentials could be unleashed. As suggested by Nee *et al.* [98], a fully-active fixture, one that could change its clamping forces and fixturing element positions during the manufacturing process, could reduce workpiece deflection, hence significantly improve the end result of

the process. Especially, this holds true in the case of low-rigidity workpieces, where the structure flexes and vibrates more vigorously under the forces exerted by the manufacturing process. By changing the position of the fixturing elements, also known as fixels, the local stiffness of the workpiece can be increased. This reduces the static deflection of the workpiece as well as its dynamic response, ultimately leading to reduced amplitudes of vibration. The torque created between the pair of cutting tool force and clamping/reaction force at the moving fixel can also be reduced. Consequently, lower clamping forces are necessary to hold the workpiece in place, assisting in the reduction of static deflection and ameliorating form accuracy of the end product. Furthermore, clamping forces could also be actively adapted, further reducing workpiece deformation and vibration [131]. At the same time, such a fixture has the inherent capability to automatically change its layout. This attribute also allows the fixture to reconfigure for different part geometries. In general, a fully-active fixturing system could help to:

1. Reduce deformation and vibration of the processed structure by applying time varying clamping loads.

2. Reduce deformation and vibration amplitude by providing localised support and stiffness, allowing for a clamping or locating element of the fixture to be constantly in close vicinity to or exactly opposite the load from the manufacturing process.

3. Reduce deformation of the processed workpiece through the ability of the fixture to constantly change setup ensuring stable fixing with minimum clamping forces.

4. Minimise capital investment and increase flexibility through utilising the inherent reconfigurability of such a fixturing system to accommodate for different workpiece geometries and sizes.

In order to explore the capabilities and benefits of fully-active fixturing systems, it is important to look into the new fixturing strategies that such systems could render possible. These strategies are based on the fact that the fixture layout is no longer static, but dynamic. All fixturing elements can change their positions and the forces they exert on the workpiece throughout the manufacturing process. Therefore, the vibration amplitude of the workpiece is reduced and the surface finish quality increased.

Fully-active fixturing systems can ensure the presence of a fixturing element to the vicinity of the tool at all times. There are two ways to achieve this. One is by discretely moving the fixels to a predefined number of different points, whilst the tool is moving along a surface. The other is having a fixturing element always opposite the cutting tool. This means that the fixturing element constantly changes its position and practically imitates the movement of the tool. From the previous discussion it becomes apparent that there is a series of questions that seek answers in order to be able to apply these new strategies efficiently and effectively:

- Is it necessary to implement a fully-active fixturing strategy?
- Which strategy should be followed? Discrete or continuous moving fixels?
- How many contact points should the fixturing element pass through during the fully-active fixturing strategy?
- What are the coordinates of these points that the fixturing element should pass by (trajectory)?
- What are the minimum forces the clamps of the fixture need to apply in order to secure the part and achieve the required end results?

In order to provide the right answers to the previous questions in a concise and well-structured manner, it is necessary to formulate a suitable methodology. For this reason, this chapter shall focus on the development and description of a fixture design/planning methodology, which takes into account the capabilities of fully-active fixturing systems and outputs the parameters of the fixturing strategy that should be implemented to obtain the desired results. Firstly, the methodology shall be thoroughly described. Afterwards, a simple test case of a beam workpiece will be introduced. This intends to facilitate understanding and highlight the potential benefits of fully-active fixturing strategies.

6.2 Fixture Design Methodology

The fixture design methodology intends to capture the dynamic behaviour of a fixture-workpiece system under moving and time-variant (dynamic) loads exerted by the manufacturing process. Its outputs are the fixturing strategy that should be followed and its

parameters, in order to reduce the displacement of the workpiece below a user defined limit. The methodology can be split into three distinct phases:

1. Discretisation of the structure through the finite element (FE) method.
2. Formulation of the problem in Matlab [84].
3. Optimisation process.

A detailed walk-through of each phase is presented in the following paragraphs.

6.2.1 Discretisation of the Structure

The geometry of the workpieces that are processed in manufacturing process is most often complicated. For this reason it is rarely possible to use analytical expressions to describe the response of these workpieces under dynamic loading. Finite Element Analysis (FEA) [148] is a very powerful tool and can be used to simulate system response, regardless of the geometry of the structure. Using finite elements, it is possible to transform the continuous structure into a system of discrete masses, dampers and springs. The latter can be expressed through mathematical arrays, which are referred to as mass, damping and stiffness matrix, respectively. By exporting these matrices from the FEA software, the dynamic behaviour of the structure can be represented easily using the second-order equation of motion:

$$[M]\{\ddot{u}_w\} + [C]\{\dot{u}_w\} + [K]\{u_w\} = \{f_w\} \tag{6.1}$$

where $\{u_w\}$ represents the vector of spatial displacements or rotations, along or about any of the three axis in a Cartesian coordinate system, $[M]$ is the mass matrix, $[C]$ is the damping matrix, $[K]$ is the stiffness matrix, and $\{f_w\}$ is the vector of the external forces that are applied to the system. This system can be introduced in software like Matlab, and a solution can easily be obtained. Deriving a solution through Matlab presents significant advantages:

- Implementation of optimisation processes to obtain an optimal solution.
- Straightforward manipulation of matrices to accommodate for local structural modification [82], i.e. addition of discrete masses, springs, or dampers. The benefits of this

shall become apparent further on as more detail about the developed methodology is revealed.

- Coupling of FEA with non-FEA (e.g. analytical) models. An example of this was shown in Chapter 4.

The first phase of the methodology, schematically depicted in Figure 6.1, starts by inputting necessary information to the finite elements software. The output of this phase is the mass, damping and stiffness matrices of the discretised workpiece. In more detail, the required inputs are:

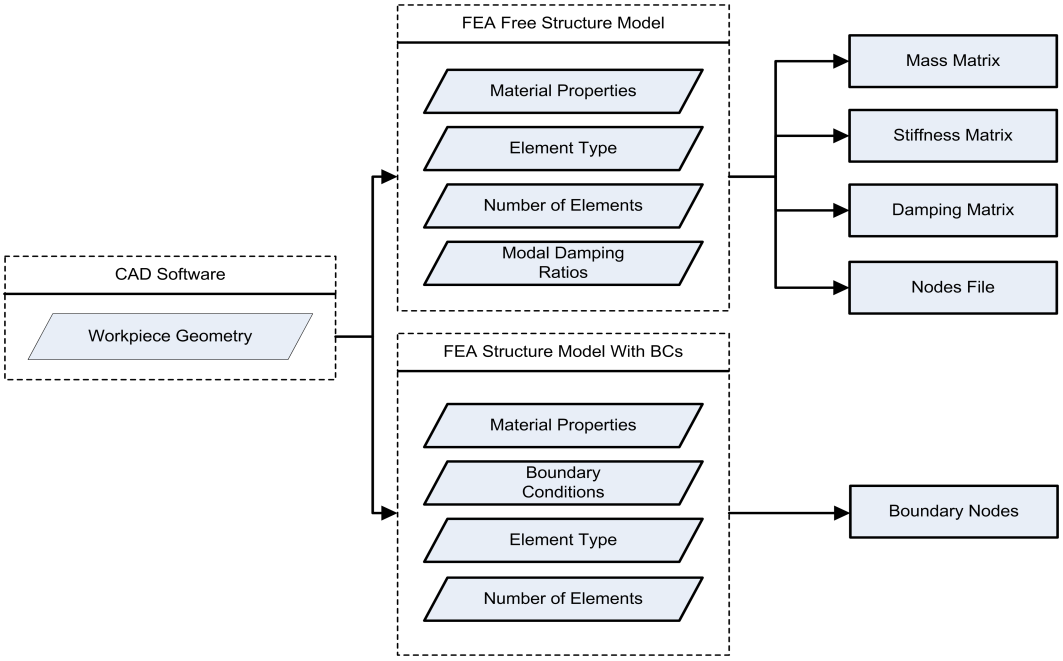

Figure 6.1: Schematic representation of the 1st phase of the Fixture Planning Methodology. Rhomboids signify user inputs, whilst rectangles signify processes.

6.2.1.1 Workpiece Geometry

Most commercial FEA packages, like Abaqus [127], used in this work, offer an environment within which the workpiece geometry can be electronically recreated. This entails the creation of a Computer Aided Design (CAD) drawing of the part. This environment, however, is fairly limited in terms of its capabilities. Therefore, and mainly for complicated geometries, the preferred method of developing an electronic representation of the workpiece is by formulating a CAD model in a dedicated CAD package (e.g. Catia, SolidWorks, Pro-Engineer etc.). This can then be imported in the FEA software. As soon as the model of the workpiece has been successfully introduced to the FEA software, the position of the

workpiece relative to a reference frame needs to be defined. All the resulting displacement values from the analysis will be displayed according to the relative position of the reference frame and the part.

6.2.1.2 Material Properties of the Workpiece

The material properties are necessary for the FEA package to be able to perform the requested analysis. The properties that need to be defined depend on the nature of the analysis itself. For structural problems within the elastic region of homogeneous materials, like the ones dealt with in this thesis, the necessary properties are the Young's modulus of elasticity, Poisson's ratio and material density.

6.2.1.3 Type and Number of Finite Elements

This step involves the definition of a grid of finite elements [48, 148]. This grid is used by the FEA software to perform the discretisation of the imported model and eventually output a solution. The selection of the type and number of finite elements is of paramount importance. It affects directly the outcome of the overall FE analysis. Selecting an inappropriate type of elements could lead to erroneous results and conclusions. FEA packages offer a wide range of different elements in order to cover the various problems they are called to solve. Each element type is also associated with a specific number of nodes. Therefore, the type of elements affects the total number of nodes in the FE problem. Moreover, the type of finite elements determines the number of degrees of freedom that each node has. This ultimately affects the number of elements in the matrices of the system. This number is the squared product of the number of nodes times the number of degrees of freedom per node, i.e. $\text{size}([S]) = (n \times d)^2$. In this formula $[S]$ is one of the system matrices, n is the total number of nodes in the FE problem and d is the number of degrees of freedom per node. The number of nodes must be carefully selected. Insufficient number of nodes could result in failing to converge to the correct solution, leading to significant over- or under-estimation of the solutions. On the other hand, too many nodes could lead to massive system matrices, rendering the problem computationally heavy. At the same time, if convergence is achievable with a smaller-sized model, then the redundant nodes lead to an unnecessary commitment of resources. Striking the right balance between element type and the number of elements and nodes is critical. The user of the methodology should perform

a comprehensive study in order to make a valid decision on the above matter. Such a study has been carried out within the context of this work and the results are presented in detail in Chapter 4 (Section 4.2) and Appendix A.

6.2.1.4 Damping Definition

In FEA software like Abaqus, damping is introduced into the system in many different ways [125, 126]. In the described methodology, two are the preferred ones, namely Rayleigh damping and critical damping factors, also known as damping ratios. The former is defined as a linear combination of the mass and stiffness matrices of the system. In mathematical terms, Rayleigh damping (proportional damping) is expressed as:

$$[C] = \alpha\,[M] + \beta\,[K] \tag{6.2}$$

where α and β are user selected constants. This way of introducing damping is straightforward and ensures that the equations of the system can be uncoupled and solved. When the damping exhibited by a structure is small, which is most often the case with real life structures, this approximation is acceptable. This way of defining damping is preferable when expressing the system in physical coordinates [82] or when no experimental modal analysis has been performed to extract the modal damping ratios.

Defining damping by critical damping factors is achieved through a series of damping ratios per mode. These ratios represent percentage of damping relative to the critical damping. For a single-degree-of-freedom system, the free response is given by:

$$m_s\ddot{u} + c_s\dot{u} + k_s u = 0 \tag{6.3}$$

where m_s, c_s, and k_s are the mass, damping, and stiffness coefficients of the system. Assuming a solution of the form

$$u = Ae^{\lambda t} \tag{6.4}$$

where A is a constant and

$$\lambda = -\frac{c_s}{2m_s} \pm \sqrt{\frac{c_s^2}{4m_s^2} - \frac{k_s}{m_s}} \tag{6.5}$$

The value of damping that makes the quantity below the square root equal to zero in Equation (6.5) is defined as critical damping:

$$c_{cr} = 2\sqrt{m_s k_s} \tag{6.6}$$

The damping ratios that need to be defined are expressed as:

$$\zeta = \frac{c_s}{c_{cr}} \tag{6.7}$$

This method of introducing damping is preferable, when the system is expressed in modal coordinates or when the damping ratios per mode have been acquired by experimental modal analysis.

6.2.1.5 Boundary Conditions

The final input to this first stage of the methodology is the incorporation of Boundary Conditions (BC's). The boundary conditions describe how the simulated workpiece interacts with its surroundings. In an FEA environment, boundary conditions are applied at the nodes of the discretised model. The nature and definition of BC's directly affect the solution of the problem and, therefore, these should be carefully selected and applied.

It should be noted that, when the intention is to extract the system's matrices through the FEA software, applying boundary conditions to the simulated part could lead to certain problems. In more detail, it is often the case that the necessary boundary conditions are expressed as constrained movement of specific degrees of freedom of some nodes. In other cases, boundary conditions are engineering elements, like springs and dampers, that are significantly stiffer than the workpiece itself. Many FEA software express the presence of zero-movement boundary conditions by adding very large stiffness values at the elements of the stiffness matrix that relate to the degree of freedom of the node, whose movement has been constrained. Engineering elements boundary conditions are introduced to the matrices of the system following the same process. This, however, can lead to numerical problems at a later phase of the methodology, when these matrices are introduced and manipulated in Matlab. Subsequently, it is necessary to perform the system matrix extraction on the completely free model of the part (no boundary conditions applied). Boundary conditions will need to be incorporated to the model later on in the methodology and outside of the FEA environment.

The outputs of this phase of the methodology are the following:

6.2.1.6 System Matrices

After having input all the necessary information, the generation of the three system matrices, namely mass, damping and stiffness matrices, can take place. To do that, an appropriate analysis step needs to be defined. In Abaqus, the generation and output of the global system matrices can be achieved via linear perturbation analysis steps [127]. Natural frequency extraction is such a step. It is also easy to implement, it requires reduced computational resources and allows for straight forward comparison with experimental data from modal analysis, thus facilitating validation. Therefore, the described methodology employs such a step. As mentioned earlier, the system matrices extraction step is performed on the free part. The outcomes of the step are three ASCII-format files with .mtx extension, one for each of the system matrices.

6.2.1.7 Map of Nodes

When the FEA software generates the grid of nodes, it also assigns a unique identifying number for each node. This numbering scheme is to a certain extend random. For example, node 1 does not always coincide with the origin of the Cartesian system of the model. Even if this happens, then there is no specific rule according to which the neighbouring nodes will be assigned specific numbers. However, the numbering of nodes affects directly the assembly of the global matrices of the system. To facilitate understanding of how node numbering affects the matrices of the system a brief example will be given. Assume a two-node element with three degrees of freedom per node (beam element [127]). If the node number is 4, the stiffness values for this node will be positioned between the $(3 \times 4 - 2) \times (3 \times 4 - 2)^{th}$ and the $(3 \times 4) \times (3 \times 4)^{th}$ elements of the overall (global) stiffness matrix of the system. The same applies for the mass and damping matrices. In a simple problem when a few nodes are used, identifying which elements in the global matrices correspond to which node is straightforward. However, as the number of nodes and degrees of freedom per node in the model increases, the above process becomes significantly complicated. Whenever it is necessary to manipulate the matrices outside of the FEA environment, it is of paramount importance to know where any changes should be applied, in order to be able to perform correctly even the simplest analysis. Consider for example the static analysis problem where a static load is applied to the middle of a beam. In matrix format, this problem can

be expressed as:

$$[K]\{u_w\} = \{f_w\} \tag{6.8}$$

The application of the load at a specific point on the beam within the FEA environment is easy. This is because the operator has a physical representation of the model in front of them. So when they want to place the load in the middle of the plate, they select the node that is physically in the middle of the plate. Then they assign a value to the force component that lies along the desired coordinate axis. When using the system matrices to solve the same problem, for example in Matlab, the physical representation of the system is missing. Assuming the model of the beam has three equidistant nodes and that each node has three degrees of freedom, then according to what was discussed earlier, the stiffness matrix $[K]$ of the beam should have $9 \times 9 = 81$ elements. The load vector $\{f_w\}$ should have 9 elements. If the load needed to be applied along the second degree of freedom of the middle node, and if the middle node were node 1, then the load vector should contain the load amplitude in its 2^{nd} element. All other elements would be zero. However, if the middle node were node 2, then the same load should be in the 5^{th} element of the load vector.

The previous example clearly illustrates the necessity of a map of nodes, one that will assist in applying the right changes to the right coordinates of the physical system. These changes include addition of point masses, springs and dampers, incorporation of boundary conditions, application of loads, etc. In Abaqus, this map can be obtained through the input file (.inp) of the model. This file contains a list of the numbers of all the nodes and their Cartesian coordinates. By knowing this information the map of nodes can be generated in Matlab as a matrix variable.

6.2.1.8 Boundary Condition Nodes

As mentioned earlier, the extraction of the matrices of the system from the FEA software should be executed only on the boundary condition free model. Consequently, boundary conditions should be applied in Matlab, after the matrices of the system have been introduced. In order to achieve this, it is necessary to know the identifying numbers of the nodes, where boundary conditions should be applied, and the degrees of freedom per node. This information can be extracted by generating the input file of the workpiece with the boundary conditions imposed. In this input file the numbers of the boundary nodes are

grouped as a set of nodes. This set can be easily transferred into Matlab as, for example, a vector variable, containing the number of the nodes within the set, in increasing order.

The previously describe files need to be in text (ASCII) format. To summarise, at the end of this phase the following files should have been generated:

1. Mass matrix file (.mtx file).
2. Damping matrix file (.mtx file).
3. Stiffness matrix file (.mtx file).
4. Nodes file (.txt file).
5. Boundary nodes file (.txt file).

With the generation of the above files, this phase of the methodology completes.

6.2.2 Formulation of Problem in Matlab

Having extracted all necessary information from the FEA software, the next phase of the methodology can commence. This phase, schematically summarised in the flow chart of Figure 6.2, uses as inputs the output files of the previous phase. The mass, stiffness and damping matrices are introduced first, followed by the information on the layout of the nodes (identifying number and coordinates) and the numbers of the nodes where boundary conditions should be applied. The output of the phase is the representation of the full fixture-workpiece system in Matlab. The desired output is achieved in two steps, namely the definition of boundary conditions and the definition of load vectors. Fixture elements are also introduced as boundary conditions.

6.2.2.1 Applying Boundary Conditions

As mentioned earlier, it is important to obtain the matrices of the system through solving the unconstrained case of the FEA problem. However, before the system of equations of the system can be solved, boundary conditions must be applied. If boundary conditions are not applied, then the stiffness matrix will be singular and, therefore, no solution can be reached [48, 148]. Two types of boundary conditions can be identified: prescribed displacement and engineering element boundary conditions. These are analysed hereafter.

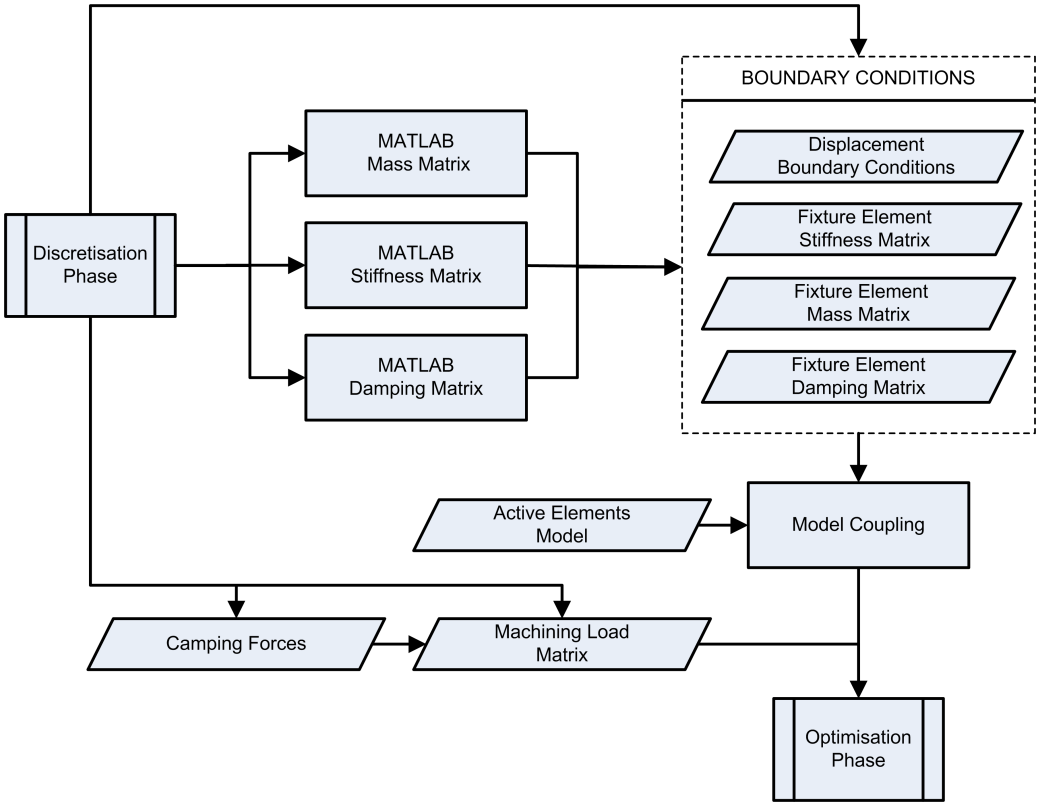

Figure 6.2: Schematic representation of the 2nd phase of the fully-active fixture design methodology. Rhomboids signify user inputs, rectangles signify processes and double rectangles refer to the predefined processes of phase 1 and phase 3.

Prescribed displacement boundary conditions. In a structural problem, like the ones dealt with in this research work, the most common type of boundary conditions is the one where prescribed displacements or rotations are assigned to specific support points on the structure. There are different ways with which the boundary conditions can be incorporated. One way, presented by [48], is described here using a simplified example. For this example the problem described by Equation (6.8) shall be deployed. To begin with, Equation (6.8) is written in more detail as:

$$\begin{bmatrix} k_{11} & k_{12} & \cdots & k_{1n} \\ k_{21} & k_{22} & \cdots & k_{2n} \\ \vdots & \vdots & \ddots & \vdots \\ k_{n1} & k_{n2} & \cdots & k_{nn} \end{bmatrix} \begin{Bmatrix} u_{w1} \\ u_{w2} \\ \vdots \\ u_{wn} \end{Bmatrix} = \begin{Bmatrix} f_{w1} \\ f_{w2} \\ \vdots \\ f_{wn} \end{Bmatrix} \tag{6.9}$$

where k_{ij} are elements of the stiffness matrix, n is the total number of degrees of freedom of the system, u_{wj} is the displacement along the j^{th} degree of freedom ($j = 1 \cdots n$), and f_{wi} is the force applied along the i^{th} degree of freedom. Assuming a boundary condition of

$u_{w2} = d$, where d is a constant, then, the equations in (6.9) can be rearranged as:

$$k_{i1}u_{w1} + 0 + \cdots + k_{in}x_{wn} = f_{wi} - k_{i2}d = f^*_{wi} \tag{6.10}$$

The leftmost part of the above equation is used to rewrite the stiffness matrix and the force vector, apart from the rows corresponding to the degree of freedom where the boundary conditions are applied, in this case u_{w2}. For these rows, the direct product of the stiffness matrix element corresponding to the boundary degree of freedom, with the prescribed displacement value of the degree of freedom equation is used. In this case, $k_{22}u_{w2} = f_{bc} = k_{22}d$. So (6.9) can be rewritten as:

$$\begin{bmatrix} k_{11} & 0 & \cdots & k_{1n} \\ 0 & k_{22} & \cdots & 0 \\ \vdots & \vdots & \ddots & \vdots \\ k_{n1} & 0 & \cdots & k_{nn} \end{bmatrix} \begin{Bmatrix} u_{w1} \\ u_{w2} \\ \vdots \\ u_{wn} \end{Bmatrix} = \begin{Bmatrix} f^*_{w1} \\ f_{bc} \\ \vdots \\ f^*_{wn} \end{Bmatrix} \tag{6.11}$$

Special mention should be given to the case where zero displacement boundary values are assigned. In essence, the same process, as the one described through Equations (6.9) to (6.11), is followed in this case too. However, as the displacement values are now zero, the entire columns and rows that are multiplied to that boundary degree of freedom do not contribute to the overall matrices of the system. For this reason, they can be removed completely from the system matrices and the force vector. This process reduces the overall size of the system, hence compressing the necessary computational power to solve the problem.

The above is one of the ways with which one can incorporate boundary conditions to a discretised system. The incorporation of displacement boundary conditions is a well-studied matter and not a part of the contributions of this work. Therefore, for more detailed information the interested reader is referred to well-established resources, such as [48, 148].

Engineering elements boundary conditions. Another type of boundary conditions is Engineering Elements. This includes springs, dampers and inertias (masses). A typical example of such conditions is a rectangular plate that is supported by four springs, one

on each of its corners. Fixture elements are in fact boundary conditions too and can be successfully represented by springs and dampers as shown in [87]. In fact, in the 3-2-1 principle based fixtures, the elements of the fixture are most often the only boundary conditions that are applied to the workpiece. Therefore, special attention shall be given to this type of boundary conditions. Fixturing elements in the form of engineering elements can be integrated in the matrices of the system using the principles of local structural modification. Structural modification is defined by Maia *et al.* [82] as "an area of study that deals with the effects if physical parameter changes on the dynamic properties of a structural system". The term physical parameters refers to the mass, damping and stiffness properties of the structure. The direct structural modification problem refers to the determination of changes in the dynamic characteristics of a system given a structural change in the system. The inverse problem deals with determining the structural changes a structure should undergo so as to obtain desired dynamic characteristics. Direct and inverse structural modification can be performed using either the spatial, modal or response models of the structure. Due to the nature of the objective of this methodology, i.e. the identification of fixture contact points for which the vibration amplitude of the structure is minimised, the knowledge of system matrices through FE analysis, and the fact that fixturing elements can be expressed as springs, dampers and masses, the spatial model is preferred. Provided that the fixturing elements engage with the workpiece through point contacts, or that the fixturing elements can themselves be discretised, Equation (6.1) is modified:

$$([M] + [\Delta M])\{\ddot{u}_w\} + ([C] + [\Delta C])\{\dot{u}_w\} + ([K] + [\Delta K])\{u_w\} = \{f_w\} \tag{6.12}$$

where $[\Delta M]$, $[\Delta C]$, and $[\Delta K]$ refer to the mass, damping, and stiffness matrix, respectively, of the fixturing elements. Equation (6.12) can also be expressed as:

$$[M^*]\{\ddot{u}_w\} + [C^*]\{\dot{u}_w\} + [K^*]\{u_w\} = \{f_w\} \tag{6.13}$$

The focus of this research work is point contacts, as they are the most generic fixturing interface with a vast variety of different geometry workpieces. It is reminded at this stage that reconfigurability is a sought after property of fully-active fixtures. If the fixturing elements are considered to be connected to the workpiece on one end and grounded on the

other, then the size of these incremental matrices is the same of that of the original system matrices. The elements that correspond to the nodes where the fixture elements are in contact with the workpiece contain the mass, damping or stiffness values of the fixturing elements. All other elements are zero.

The previous process is targeted towards incorporating passive fixturing elements to the workpiece model. Active fixturing elements require a slightly different approach. The actuating and sensing side of active elements need to be captured and modelled. This model can then be coupled to the structural model of the workpiece [82]. The model of an electromechanical actuator and the method to couple it with the structural model of a plate workpiece has already been described in detail in Chapter 4 of this thesis.

Generally, the outcome of the previously described process is a model of the fixture-workpiece system. In this model, the fixture elements are randomly positioned around the workpiece. Selecting the starting position of the fixels using fundamental rules of thumb for fixtures [96] can significantly reduce the time required by the optimisation process to reach a solution. A small clamping force value for each clamp could also also be assigned as a nodal force acting on the nodes where the clamping elements and the workpiece are physically coupled.

6.2.2.2 Definition of Load Vectors

With the introduction of the boundary conditions, the next necessary step in this phase of the methodology is the definition of the external forces applied both by the machining forces and the clamping elements of the fixture. In Equation (6.1) it can be seen that the loads applied to the workpiece should be included in the vector on the right hand side of the equation. Additionally, in Chapter 4 of this thesis (Section 4.2.2.2) it was shown that it is possible to capture the effects of dynamic moving loads by defining a set of loads along preselected nodes of the structure. These nodes are the ones above or in the vicinity of which the load passes as it moves along the structure. The amplitudes of the loads are varying over time. When the moving loads are within the boundaries of a finite element, then the simulated force loads on the nodes of the elements get a non-zero time-varying amplitude. On the contrary, all other loads on the nodes of the structure are zero. The same philosophy can be followed when simulating the system in Matlab. Each of the elements in the force vector of Equation (6.1) represents a specific degree of freedom of

a specific node. So by assigning the right load to the right element of the force vector it is possible to simulate the external loads on the workpiece-fixture system. The same philosophy is followed for the clamping loads from the fixture. The difference is that these loads are treated as concentrated ones and their point of application is always the same as the contact point between clamp and workpiece. Identifying the correct degrees of freedom where a load should be applied, can be achieved using the map of nodes extracted in the previous phase of the methodology.

Capturing the fact that only some nodes are loaded at any given time instant is critical. Perhaps the most straightforward way to simulate the moving machining loads and the clamping forces in Matlab is to create a force matrix. Each of the columns of the force matrix represents a force vector $\{f_w\}$, i.e. the loading conditions on the system at any given time instant. To construct this matrix it is necessary to first calculate the amplitude of each of the nodal loads at all the given time instants. Then careful placement of the nodal loads to the appropriate elements of the matrix is required. With this method, the equations of the system can be solved for all defined time instants. Obtaining a meaningful solution depends on how frequent these time instants are. It is of paramount importance to select the number of time instants with caution. A small number could result in misleading solution. On the other hand, too many time instants would increase the size of the force matrix. This, in combination with the number of nodes and degrees of freedom per node in the system could result in shortage of memory resources necessary to solve the problem. The appropriate number of columns (time instants) in the force matrix depends on the problem itself. High frequency harmonic forces, for example, need denser time instants to avoid aliasing effects [47]. In all cases, the number of nodes and the number of time instants that are used to simulate the moving and dynamic nature of the loads, need to be carefully checked for convergence.

6.2.3 Optimisation Process

The final phase of the fully-active fixture design methodology is the optimisation cycle. This cycle, shown schematically in Figure 6.3, receives as input the fixture-workpiece model, which was the outcome of the second phase of the methodology. The outputs of the optimisation phase, collectively referred to as fixturing process parameters, are:

- Number of position changes per tool pass for each fixture element - fixturing strategy.

- Position coordinates of each contact point between fixture elements and workpiece.
- Time scheduling of position changes.
- Clamping forces for every position of every clamping element.

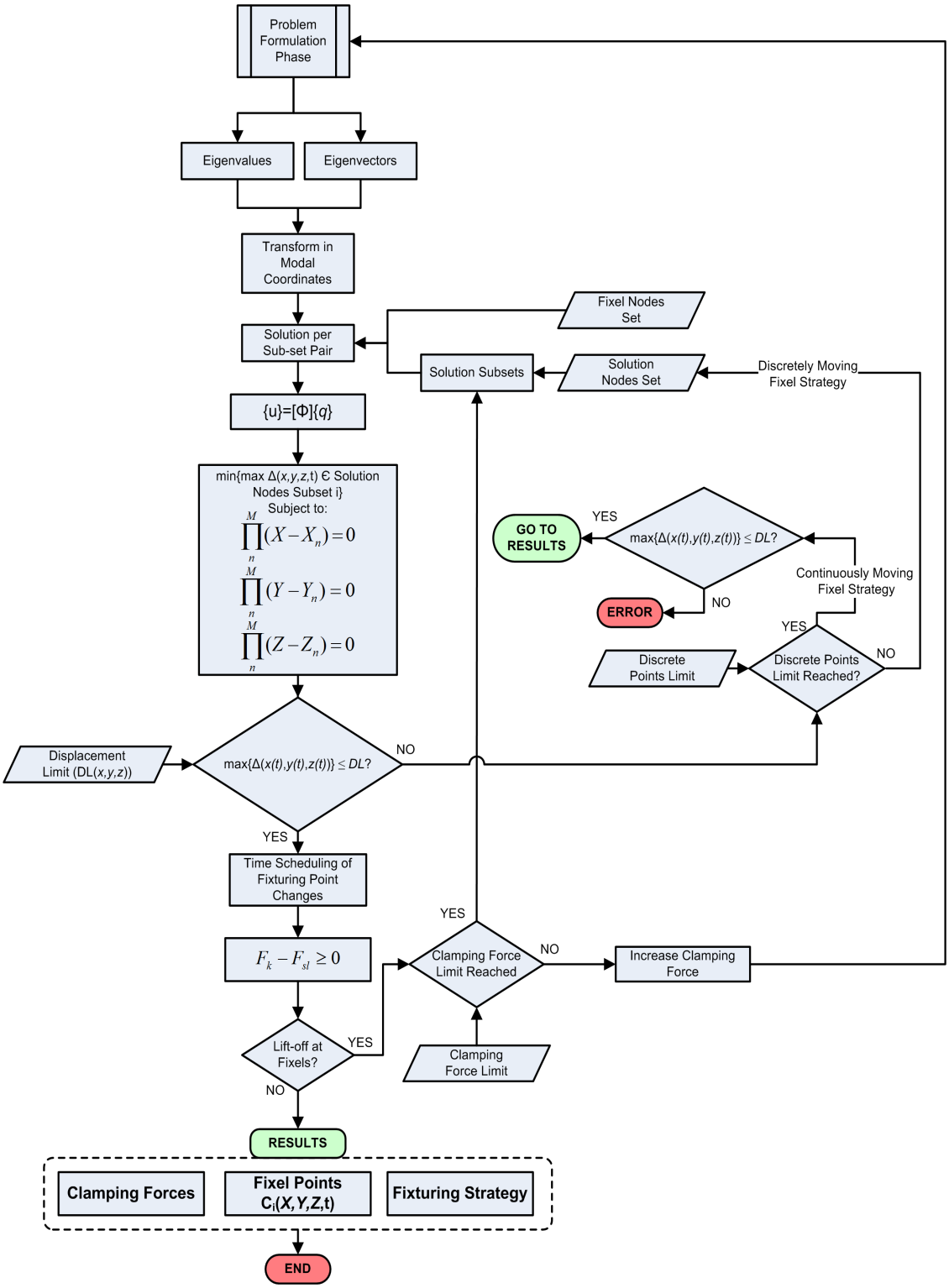

Figure 6.3: Schematic representation of the 3rd phase of the Fixture Planning Methodology.

Before the description of the methodology is adduced, it is important to highlight the assumptions and limitations, under which the methodology operates.

6.2.3.1 Assumptions and Limitations of the Methodology

Working area. In most real life applications, it is highly unlikely that each fixturing elements can achieve contact with the entire surface of the workpiece. Physical limitations, like the volume and the travel range of the movable fixels of a fully-active fixturing system, reduce the working area of each fixel to a fraction of the full workpiece surface. For this reason, each fixel is associated with a working area, i.e. a surface area on the workpiece within which the fixel can make contact. It is assumed that the working areas of fixels do not intersect, i.e. each fixel has their own unique working area.

Within the methodology, and because the workpiece is discretised by finite elements and their nodes, the nodes that belong to the surface of the workpiece that constitutes the working area of a fixel, are collectively referred to as Fixel Nodes Set (FNS).

Sequential operation. A key limitation of the methodology is that it does not produce the optimal fixturing process parameters for all fixture elements simultaneously. Each fixture element is treated independently. As a result, the fixture design methodology is applied to each element sequentially. When the methodology is applied on a fixel, all other fixture elements are treated as passive and non-moving. The order with which the elements are treated by the methodology depends on the machining process itself. This is explained further below.

Displacement solution area. The overarching target of the fixture design methodology is to improve the form accuracy and the surface quality of the machined area on the workpiece. To achieve this, it is necessary to minimise the displacement of the workpiece at the area that lies directly underneath the cutting tool.

Moreover, due to the discrete nature of the problem, it is only possible to obtain displacement solutions at the nodes of the workpiece model see Section 6.2.1). By combining the above two observations, it becomes apparent that it is sensible to define the machined area as a set of nodes.

Furthermore, it is assumed that the fixel, within whose working area the cutting tool moves and removes material, has the potential to impact the result of the process. This is

because the fixel, that lies within the vicinity of the cutting tool, can offer the maximum necessary local support leading to reduced elastic deformation and vibration. Therefore, only the nodes that belong to that area on the machined surface of the workpiece that is the closest to the working area (FNS) of a fixel need to be treated each time. The nodes that are contained within the machined area are grouped into one set of nodes, called the Solution Nodes Set (SNS).

From the above, it can also be deduced that the optimisation process targets only one pair of SNS and FNS, at a time. This means that the cutting tool cannot exit the working area of one fixture element and enter the working area of another, within one optimisation cycle. For example, in Figure 6.4, should the machining process take place on the surface that lies over the locators L2 and L3, then the optimisation process needs to be repeated twice. The machining area is split in two solution nodes sets, namely $\mathrm{SNS_{L2}}$ and $\mathrm{SNS_{L3}}$. The first time, assuming that the tool moves from right to left, the optimisation process targets the pair $\mathrm{FNS_{L3}}$ and $\mathrm{SNS_{L3}}$, and the second time the pair $\mathrm{FNS_{L2}}$ and $\mathrm{SNS_{L2}}$.

Please note that the FNS and the SNS are not necessarily different. For example, and for the plate workpiece that was modelled in Chapter 4 (Section 4.2), the workpiece is treated as a a two-dimensional (2D) body. Therefore, the nodes on the surface that experiences the machining and on the surface that is used to fixate the workpiece are the same, as there is no Z-dimension to separate the two surfaces. On the contrary, for the workpiece shown in Figure 6.4, the solution nodes sets (light grey areas) and the fixel nodes sets (dark grey areas) contain different nodes.

Sequencing of the application of the methodology. The sequence with which the pairs of SNS's and FNS's are treated depends on the motion path of the cutting tool. In the example of Figure 6.4, assuming that the cutting process starts in the position shown in the top figure, and that the cutter moves anticlockwise, the optimisation process is first applied to identify the optimal fixturing parameters for clamp C2. As soon as this is complete, the optimisation process is then applied on clamp C1, and so forth.

Displacements and rotations. It is assumed that the rotations that the workpiece experiences during the machining process are small and can be ignored [77]. Therefore, only displacements are considered.

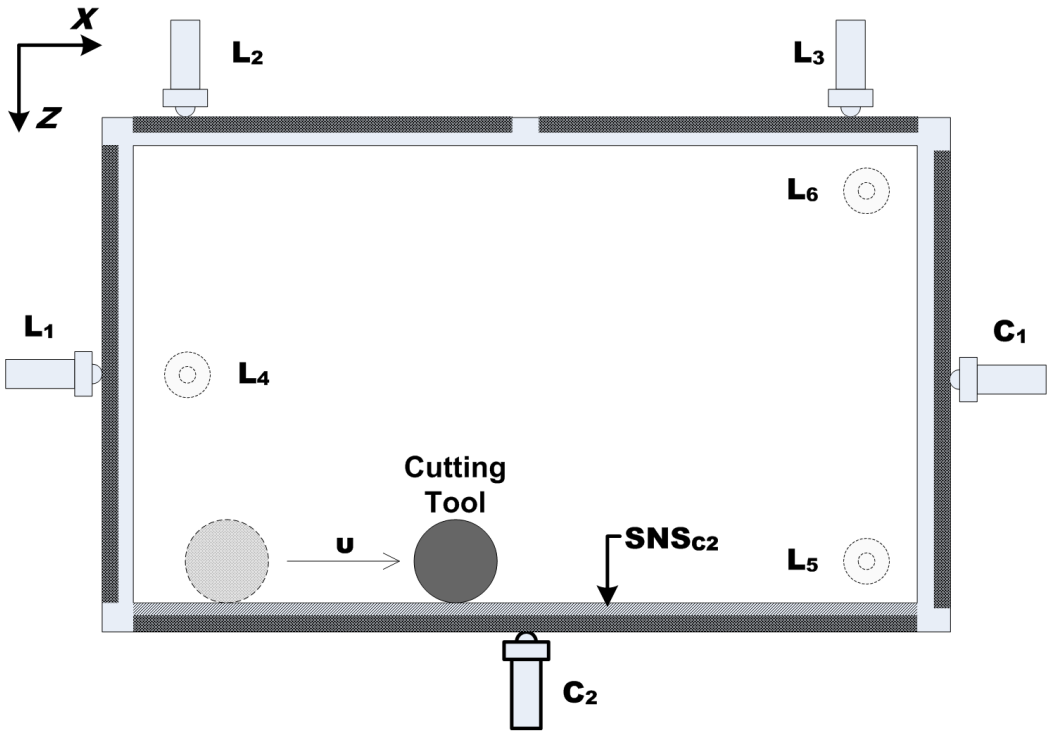

(a)

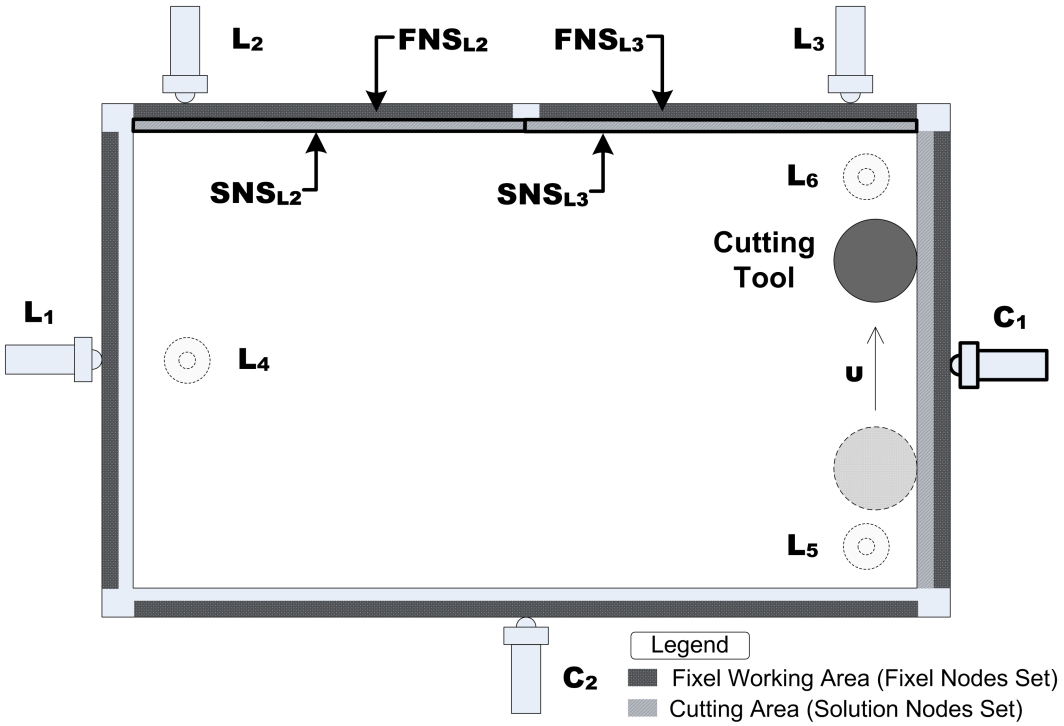

(b)

Figure 6.4: Illustrative representation of a five-sided-box-shaped workpiece held by a 3-2-1 fixture with point contacts. The machined area in each case is designated as light grey. The working area of each fixture is designated as dark grey. Locators are marked as L and clamps as C. (a) Optimisation process to be applied on clamp C2. (b) Optimisation process to be applied on clamp C1.

Damping. The damping in the systems on which the optimisation process is intended to be applied is considered proportional. The assumption that the damping in the system is proportional, i.e. the damping matrix can be expressed as a linear combination of the mass and the stiffness matrices (Equation (6.2)), is valid for a large percentage of structural analysis problems. This is because the damping of many physical structures is relatively small.

With the assumptions and limitations defined, and before the description of optimisation process can start, it is appropriate to define the objective function of and the constraints of the optimisation phase.

6.2.3.2 Objective Function

The overarching purpose of the methodology and the optimisation phase, as already expressed, is the minimisation of the elastic deformation of the workpiece. In other words, the optimisation process seeks to find the contact point between the fixture and the workpiece that lead to the minimisation of the maximum displacement of the machined workpiece surface. This, and because rotations are ignored, can be expressed mathematically as:

$$min\{max\{\Delta x_i(t),\Delta y_i(t),\Delta z_i(t)\}\} \tag{6.14}$$

where $\Delta x(t)$, $\Delta y(t)$, and $\Delta z(t)$ signify the elastic deformation of a point on the workpiece in the three Cartesian coordinates, at time t when the tool is directly over that point. The indicator i denotes the identification number of a node. Equation 6.14 constitutes the objective function of the methodology.

6.2.3.3 Nodal Solution Constraint

As stated previously, the optimisation process is applied each time to a pair of an SNS and an FNS. The process seeks to identify points (nodes) within an FNS that satisfy the optimisation function for the points within the corresponding SNS. Most available optimisation algorithms [71, 77] search for the optimal contact points in physical coordinates. Additionally, by using Cartesian coordinates, the solution becomes independent of the random nodes' numbering scheme, which was discussed in Section 6.2.1. Therefore, it is necessary to ensure that the algorithm accepts as feasible solutions only those points on the workpiece

that coincide with a node that belongs to a certain FNS. Assuming that an FNS contains a total of M nodes, and that each node is marked by a number n, the previously described constraint is expressed mathematically as:

$$\begin{aligned}
&\prod_{n=1}^{M}(X - X_n) = 0, \quad X \in [X_{b1}, X_{b2}] \\
&\prod_{n=1}^{M}(Y - Y_n) = 0, \quad Y \in [Y_{b1}, Y_{b2}] \\
&\prod_{n=1}^{M}(Z - Z_n) = 0, \quad Z \in [Z_{b1}, Z_{b2}]
\end{aligned} \tag{6.15}$$

In the above equations X_n, Y_n and Z_n signify the Cartesian coordinates of node n, and the indices $b1$ and $b2$ refer to the physical coordinates of the boundaries of the fixel nodes set. All constraints in (6.15) need to be satisfied simultaneously. It should be noted that the optimisation process is not necessary materialised through an optimisation algorithm. It could be performed manually, in which case it is also possible to search for the optimal positions of a fixel in terms of node numbers. In this case, the aforementioned constraints need to be updated as:

$$\prod_{j=1}^{M}(\mathrm{FNS}_j - n) = 0, \quad n \in \mathrm{FNS} \tag{6.16}$$

where FNS_j corresponds to the number of the j^{th} node within the fixel nodes set and n is the identifying number of the investigated-for-suitability node.

6.2.3.4 Separation Constraint

The final constraint that needs to be introduced is that there can be no separation between the workpiece and the fixture elements throughout the machining process. This constraint is of paramount importance. Should lift-off between fixture and workpiece occurs, then the workpiece would no longer be secured and changes in the workpiece's location relative to the machine tool's reference frame could take place. This could result in an unacceptable end-result, or even violent displacement of the workpiece that may cause damage to the machine tool and fixture or even serious injuries to the operator. When lift-off is about to occur then the forces experienced by the fixturing element become zero. In essence, in order to ensure that no separation between the fixels and the workpiece occurs, the sum of the forces that act in the direction of the fixels should never be zero. For increased safety,

it is possible to define a limit value, below which the sum of forces in the acting direction of the fixture elements cannot drop. This can be expressed as:

$$F_k(t) - F_{sl} \geq 0 \tag{6.17}$$

where $F_k(t)$ is the resultant force in the direction of fixture element k at time t, and F_{sl} is the user defined safety limit. It should be noted that this constraint needs to be satisfied for all fixels, regardless of the FNS-SNS pair that is being processed at any given time.

With the objective function and constraints defined, the optimisation problem has been fully formulated and the solution of the problem can commence.

6.2.3.5 Walk-Through of the Optimisation Phase

The optimisation phase, the flow-chart of which is presented in Figure 6.4, starts by accepting the model that was the output of the second phase of the design methodology. It is reminded that in this model the fixture elements have been positioned around the workpiece randomly, based on fixturing rules of thumb [96] or user intuition.

User inputs. For the optimisation phase to commence it is necessary for the user to define the pair of the fixture nodes set and solution nodes set on which the methodology will be applied. The user must also input a series of limits, which play an active role in the results of the optimisation process. More specifically, the user should input the maximum allowable displacement limit, denoted as DL, the clamping force limit, and the discrete points limit. The role of these limits will be explained later in this section.

Calculating the elastic deformation. With all necessary inputs introduced, the calculation of the elastic deformation of the nodes within the selected SNS can begin. Two cases are identified. The first one considers the fixture elements as being passive, i.e. not having the ability to adapt the forces they apply to the workpiece, or respond to the reaction forces exerted on them by the clamping or manufacturing process.

Passive fixture elements. In the case of passive elements, the elastic deformation of the nodes within the SNS is calculated by solving Equation (6.13). The latter can be solved for either the steady-state or the general response (transient and steady-state).

Steady-state solution. In the case where the steady-state solution is required, Equation (6.13), which describes the response of the coupled passive elements-workpiece system, can be solved either in spatial or modal coordinates. Solving the problem in modal coordinates is computationally less demanding and therefore preferred [47]. To obtain the modal solution, the eigenvalues ω_r^2 and the corresponding eigenvectors $\{\psi_r\}$ of the coupled system need to be calculated. For this, the following equations need to be solved:

$$\det|\left[K^*\right] - \omega^2\left[M^*\right]| = 0 \tag{6.18}$$

$$\left(\left[K^*\right] - \omega^2\left[M^*\right]\right)\{\psi\} = 0 \tag{6.19}$$

Solving Equation (6.18) for ω^2 yields the eigenvalues ω_1^2, ω_2^2, ..., ω_r^2 of the system. After the eigenvalues have been successfully extracted, they are used in (6.19) to solve for the eigenvectors $\{\psi_r\}$.

The eigenvalues are unique for every system, however the eigenvectors, are subject to an arbitrary scaling. If all eigenvectors are assembled together in one matrix, the result is the Mode Shape Matrix $[\Psi]$, also referred to as eigenvector matrix, or simply modal matrix. Provided that the damping of the system is proportional (see Equation (6.2)), by multiplying the matrices of the system from left with the transpose eigenvector matrix and from the right with the eigenvector matrix, the modal system matrices are obtained:

$$\begin{aligned} \left[\Psi\right]^T\left[M^*\right]\left[\Psi\right] &= \left[m_r\right] \\ \left[\Psi\right]^T\left[C^*\right]\left[\Psi\right] &= \left[c_r\right] \\ \left[\Psi\right]^T\left[K^*\right]\left[\Psi\right] &= \left[k_r\right] \end{aligned} \tag{6.20}$$

where $[m_r]$ is called the modal mass matrix, $[c_r]$ the modal damping matrix and $[k_r]$ the modal stiffness matrix. Matrices $[m_r]$, $[c_r]$, and $[k_r]$ are diagonal.

As mentioned earlier, the mode shape matrix is arbitrarily scaled. There are many ways of scaling this matrix, but perhaps one of the most convenient ways to do so, is by normalising it for unit mass matrix. When normalised for unit modal mass, the mode shape matrix presents interesting properties.

Mass-normalisation is achieved by dividing each eigenvector by the square root of the corresponding modal mass. This can be mathematically expressed as:

$$\{\phi\}_r = \frac{1}{\sqrt{m_r}}\{\psi\}_r \tag{6.21}$$

The mass-normalised modal matrix, marked as $[\Phi]$, is formulated by assembling all mass-normalised eigenvectors into a matrix. By post-multiplying the mass, damping and stiffness matrices by $[\Phi]$ and pre-multiplying by the transpose modal matrix $[\Phi]^T$ the following are obtained:

$$[\Phi]^T [M^*] [\Phi] = [I] \tag{6.22}$$

$$[\Phi]^T [C^*] [\Phi] = \begin{bmatrix} \ddots & & \\ & 2\zeta_r\omega_r & \\ & & \ddots \end{bmatrix} \tag{6.23}$$

$$[\Phi]^T [K^*] [\Phi] = \begin{bmatrix} \ddots & & \\ & \omega_r^2 & \\ & & \ddots \end{bmatrix} \tag{6.24}$$

with ζ_r being the modal damping ratio of mode shape r. Based on (6.22)-(6.24), Equation (6.13) can be re-written as follows:

$$[I]\,\ddot{q} + \begin{bmatrix} \ddots & & \\ & 2\zeta_r\omega_r & \\ & & \ddots \end{bmatrix} \dot{q} + \begin{bmatrix} \ddots & & \\ & \omega_r^2 & \\ & & \ddots \end{bmatrix} q = [\Phi]^T \{F\} \tag{6.25}$$

where q are called modal coordinates and their relationship with spatial coordinates is $\{u\} = [\Phi]\, q$. The use of mass-normalised eigenvector matrix presents significant advantages. As seen through (6.25), when expressed in modal coordinates by deploying the mass-normalised modal matrix, the system matrices of the coupled system are diagonal. As a result, the equations are uncoupled and can be solved easily. Furthermore, when solving the problem in spatial coordinates, then Equation (6.13) needs to be rearranged for $\ddot{x}$ and integrated twice. For this, it is necessary to multiply all terms of the equation with the inverse

mass matrix. This is not necessary when solving Equation (6.25) as the mass matrix has been transformed into a unity matrix. This reduces computational effort.

The steady-state solution for Equation (6.25), assuming purely harmonic forces with excitation frequency ω is given by:

$$X_j = \alpha_{jk} F_k \tag{6.26}$$

where α_{jk} is the individual frequency response function (FRF) that interrelates the response X_j of degree of freedom j, due to a force F_k, applied at degree of freedom k [47]. Individual FRF parameters can be calculated through the following formula:

$$\alpha_{jk}(\omega) = \sum_{r=1}^{N} \frac{(\phi_{jr})(\phi_{kr})}{\omega_r^2 - \omega^2 + i\eta_r\omega_r^2} \tag{6.27}$$

where $\eta_r = \beta + \alpha/\omega_r^2$ (see Equation (6.2)) is the structural damping loss factor at mode r, and i is the imaginary number $i = \sqrt{-1}$. The above procedure is not limited to simple harmonic excitations. As shown in Chapter 3 (Figure 3.1), machining forces can most often be described as a weighted sum of various simple harmonic forces. According to the principle of superposition, valid for linear systems, the response of a structure to an excitation force consisting of many harmonic forces can be calculated by superimposing the responses of the same structure to each of the individual harmonic forces.

Full/General solution. In some cases, where the transient behaviour of the system is quite prominent, the steady-state solution, produced above, is not adequate to accurately describe the behaviour of the system. In such a case, the use of the steady-state solution can lead to erroneous results from the optimisation process.

For the passive fixture elements case that is discussed in this section, calculating the general response of the workpiece-fixture system requires solving the second order ordinary differential equation (ODE) of the coupled system (see Equation (6.13)). The equations of motion of a structural problem, like the one dealt with here, constitute a system of non-homogeneous linear equations, provided

that damping is present. Theoretically, such a problem can be solved through well-established mathematical methods. In practice however, the solution to Equation (6.13) is obtained through the utilisation of the built-in integrators from available mathematical software, one of which is Matlab. For this, Equation (6.13) needs to be transformed into a system of first order ODE's, which is achieved by adopting the state-space representation of the coupled system. In its general form, the state-space model of the system is:

$$\{\dot{\mathrm{x}}_i\} = [F]\{\mathrm{x}_i\} + [G]\{\mathrm{u}_i\} \tag{6.28}$$

$$\{\mathrm{y}_i\} = [H]\{\mathrm{x}_i\} + [J]\{\mathrm{u}_i\} \tag{6.29}$$

where $\{\mathrm{x}_i\}$ are the state variables, $\{\mathrm{u}_i\}$ are the inputs of the model, $\{\mathrm{y}_i\}$ are the outputs of the model, $[F]$ is the system matrix, $[G]$ is the input matrix, $[H]$ is the output matrix and $[J]$ is the direct transmission term matrix [50]. The process of transferring a time-domain system in state space is a well-established process and has already been described in detail in Chapter 4 (Section 4.5). Therefore, for the sake of brevity, it will not be repeated in this section.

The selection of which solution should be followed in order to calculate the elastic deformation of the nodes of the coupled system, in the case of passive fixture elements, is left to the user. It is advised that both the steady-state and the general response of the coupled system are obtained and compared. A simpler, but still representative, version of the fixture-workpiece system could be used to reduce the necessary effort for the comparison to be performed. For example, a simpler loading condition could be used, like a concentrated harmonic load with similar amplitude and excitation frequency to that of the actual loads. If the difference between the general and the steady-state solutions is small (e.g. 5%), then the steady-state solution should suffice.

Active fixture elements. In the case where the workpiece is in contact with active fixturing elements, then only the general solution can be obtained. This is achieved by formulating the state-space representation of the system. The methodology to achieve this was exhibited in in Chapter 4 (Section 4.5) on an active fixturing system, comprising a single active element, which is based on electromechanical actuation,

and for a thin-walled plate-like workpiece. For an in-depth presentation of the methodology and the state-space-transformation method, please refer to Table 4.9 and Equations 4.42-4.62.

The presented methodology can be used to couple a single workpiece with more than one active elements. It is highlighted though, that the methodology does not account for the effects that the response of one active element has on the response of the other active elements. It can be expanded to reflect these effects, however this falls outside the scope of this study and shall not be further analysed here.

Repositioning the fixture element. After the elastic deformation of the nodes of the SNS, has been calculated for the fixture layout of the starting solution, the node of the SNS with the maximum displacement is identified and the displacement value is stored. It is reminded here that only the displacement at the points that lie directly underneath the cutting tool are of interest. Therefore, only the displacement values of the nodes, when the cutting tool is directly over them, are necessary to be stored.

With the required information saved, the fixturing element is placed at another point on the structure. This point is checked for its compliance with constraint (6.15) or (6.16). If that point coincides with a node from the fixel nodes set, the process to evaluate the elastic deformation at the SNS nodes is repeated.

This process continues until all nodes in the FNS have been used as fixture-workpiece contact points. The maximum displacements from each solution are compared and the one presenting the minimum value is selected as a candidate solution.

Comparison against displacement limit DL. This minimum maximum displacement value is compared against the user defined maximum allowable displacement limit mentioned earlier. Two cases are identified:

max$\{\Delta x(t), \Delta y(t), \Delta z(t)\} \leq DL$ **- Static fixel.** If the displacement value is smaller than the limit, then the position (or node) of the fixel that resulted in that displacement value is outputted as a provisional optimal fixture point. This result means that the objective function, the nodal solution constraint, and the displacement limit can be satisfied by positioning the fixel at a single point of the structure for the entire duration of the manufacturing process, or more precisely for the duration of the

manufacturing process that the cutting tool processes the area to which the nodes of the SNS belong. This constitutes the fixturing strategy for the specific fixel under investigation. In the aforementioned case, the strategy involves a traditional fixturing approach, i.e. one with static fixture elements, at least as far as the investigated fixture element is concerned. With the fixturing strategy and the position of the fixel identified, the optimisation process can proceed to the next step, which is the investigation of whether the separation constraint is satisfied or not.

max$\{\Delta x(t)$**,**$\Delta y(t)$**,** $\Delta z(t)\} > DL$**. Discretely-moving fixel.** Before investigating the satisfaction of the separation constraint, it is important to examine the case according to which the maximum observed elastic deformation is larger than the limit DL. In this case, and first of all, the optimisation process checks whether the discrete points limit has been reached or not. In order to understand the purpose of this limit, it is better to override it for the present and come back to it later.

If a fixturing position, within the FNS, that leads to displacement values that satisfy the maximum displacement limit could not be found, then the original SNS is split in half and the process is repeated for each of the two new solution nodes subsets. Note that the fixture nodes set is not affected. Now, a fixture-workpiece contact point that leads to a maximum elastic deformation below the DL value is sought for each solution nodes subset. Starting with the subset that corresponds to the workpiece area that is being machined first, the optimisation process checks the elastic deformation values of the nodes that belong to that subset. The displacement values of only the nodes that belong to the subset are compared, the minimum maximum displacement value is identified and compared to the displacement limit. The same process is repeated for the second subset.

Assuming that the minimum maximum elastic deformation of the nodes of each subset satisfy the displacement limit, then the methodology outputs the two fixture points that lead to the satisfaction of the objective function and the nodes solution constraint. In this case, the fixturing strategy involves one fixel repositioning during the manufacturing process. In detail, according to this strategy, when the processing of the workpiece area, which contains nodes of the first subset, starts the fixture is positioned at the fixturing point that was indicated by the methodology for this so-

lution nodes subset. As the cutting tool advances, it reaches a point after which the observed elastic deformation of the workpiece underneath the tool would be smaller if the fixel was placed on the second contact point suggested by the optimisation process. The time instant that the cutting tool reaches that point determined the timing of the position change. At that time instant, the cutting process pauses momentarily, allowing for the fixture element to be re-positioned to the second contact point that was the output of the optimisation process. The tool then re-engages the workpiece at the same point and finishes the cutting process. This fixturing strategy is named discretely-moving-fixel fixturing strategy, due to the discrete way with which the fixture element moves.

The scenario, where the displacement limit is not satisfied of one or both of the solution node subsets, needs to be discussed too. If the limit is not satisfied for one of the subsets, then this subset is split in two new subsets and the aforementioned process is repeated. If the limit is not satisfied for both of the subsets then the original SNS is split in three parts and the process is repeated. This approach has been adopted to minimise the fixturing positions that the fixel must occupy during the process. As it necessary for the tool to disengage the workpiece every time the fixel needs to change position, the total machining time increases. This is the reason that the earlier-mentioned discrete points limit has been incorporated in the methodology.

Discrete points limit - Continuously-moving fixel. The discrete points limit exists to ensure that a viable solution can be found, not only in terms of elastic deformation, but also in terms of time. The discrete-points-limit sets a boundary on the number of discrete fixel-position changes that take place during the manufacturing process. If that limit is reached, the optimisation process takes the original SNS and splits it down to as many subsets as possible. Of course, the maximum number of subsets is equal to the number of nodes. However, such a separation does not make sense. This is because only the elastic deformations of the nodes, at the time instant that the tool lies directly above the nodes, are of interest. Assuming that the contact area between the tool and the workpiece is small enough to be approximated by a straight line, as is the case in peripheral milling, the nodes belonging to this line constitute a solution subset.

For each of these subsets the maximum elastic deformation at the time when the cutting tool traverses them is retrieved and compared to the displacement limit. If the limit is satisfied for all subsets then the fixturing points that lead to the accepted maximum elastic deformations are outputted, along with the time instants at which these deformations occur. The time-instants information is used to create the sequence with which the fixture element occupies the fixturing points. This constitutes the motion path of the fixture element. It is accepted that the fixel moves in a continuous manner from one point of the path to the other, according to the previously-determined sequence. This strategy is called the continuously-moving-fixel strategy. In this strategy neither the cutting tool, nor the fixel need to disengage the workpiece. Therefore this strategy does not lengthen the processing time.

If the maximum displacement limit is not satisfied yet again, then the optimisation phase cannot produce a feasible solution. In such a case the displacement limit could be relaxed and/or the layout of the fixture elements that were not treated by the design methodology changed. Then the entire methodology could be restarted to check whether a solution can be produced after the aforementioned changes.

Satisfying the separation constraint - Specifying clamping forces. From the above procedure a candidate solution is produced. This solution contains the coordinates (node numbers) of the fixturing points, the number of fixturing points during the manufacturing process, the fixturing strategy and the time instants when the fixel changes position during the process. All the previous have been selected based on the satisfaction of the objective function and the adherence to the nodal solutions constraint (Equations (6.15) and (6.16)). In order for the above solution to be accepted, it needs to satisfy the separation constraint too.

This constraint, expressed mathematically through Equation (6.17), ensures that, during the process, the workpiece and the fixture elements stay always in contact. In order to check the solution's adherence to this constraint, the forces acting on all fixturing elements during the manufacturing process are calculated. These forces can be calculated in two ways. If the model used to calculate the elastic deformation of the workpiece is in state-space form, then the forces on the elements can be requested as an output of the model, as shown in Section 4.5 of Chapter 4. If the modal coordinates model is used, then the forces

on the elements can be calculated by multiplying the workpiece displacement and velocity of the contact nodes with the contact stiffness co-efficient and the damping co-efficient of the spring and damper element, through which the contact behaviour is simulated.

The resultant force in the direction of each fixture element, and for every position they occupy during the manufacturing process, is calculated, including the clamping force for the case of clamps. The difference of the resultant force and the user specified safety limit F_{sl} must be greater than zero. If this is the case, then the optimisation phase accepts the solution that was produced from the previous steps as the final solution. The clamping forces that were assigned to the clamping elements at the generation of a provisional fixturing solution, are accepted as the clamping forces of the final solution.

If the separation criterion is violated at a clamping element, then the clamping force from this element is increased. If the separation criterion is violated at a locating element, then the clamping force from the clamping element that lie opposite, or nearly opposite, that element is increased.

Every time the forces are increased, the elastic deformation of the workpiece for the provisional fixturing solution needs to be recalculated and the results checked against the displacement limit again. The process is repeated until clamping force that ensure that the separation constraint is satisfied for all fixels are found, or until the user defined clamping force limit has been reached. In the former case, the optimisation process concludes, outputting all the requested fixturing process parameters.

However, if the limit is violated then the optimisation process either returns to the elastic deformation calculation phase or flags that a solution cannot be reached. The materialisation of either of the previous choices depends on the fixturing strategy that was accepted as a candidate solution before the step of checking the satisfaction of the separation constraint started. In detail, if the discrete points limit has not been reached, then the original nodes subset is further divided into subsets and the whole process is repeated.

If, the fixturing strategy within the provisional solution involves as many discrete fixturing point changes as the discrete points limit, then the continuously-moving-fixel strategy is adopted and the process repeated. If, however, the provisional solution involved the continuously-moving-fixel strategy, then, as no further division of the solution nodes set is possible, the optimisation phase concludes without being able to produce a solution.

All the phases of the methodology that were presented through this chapter, can be summarised schematically through the flow-chart shown in Figure 6.5. This flow-chart merges together the flow-charts that were presented for each phase of the methodology separately.

6.3 Beam Workpiece Test Case

In order to facilitate understanding of the fully-active fixture design methodology that was presented in this chapter, a simple test case has been devised. This involves a simple planar beam with the same properties as those shown in Table 3.1. Both ends of the beam are fully constrained, i.e. no translational or rotational movement is allowed. Also, the beam is in contact with a fixture that comprises only one fixturing element. This element is passive and applies no force onto the beam, i.e. it is a locating element.

The methodology described in the previous section will be applied step-by-step to the beam test case. The optimisation process shall be completed in Matlab by means of simple programming language statements, such as 'for' loops. With this approach, the displacements of the beam are calculated for every different fixturing scenario. This can then be used to find the optimal solution. Alternatively, an optimisation algorithm could have been used. However, the complexity of the problem is low and the problem can be solved in a simpler manner. Additionally, complex optimisation algorithms fall outside the scope of this thesis. Nevertheless, the methodology has been formulated to be independent of the implementation method.

The process starts by representing electronically the geometry of the workpiece within the FEA environment. The geometry of a beam is very simple, so no specialised CAD software is necessary. The beam is simulated in Abaqus as a one-dimensional part with dimensions as shown in Table 3.1. The cross-section of the beam is defined separately as rectangular. For the discretisation of the part 6 beam elements are used. Each element has a length of 25 mm and possesses two nodes. Each node has three degrees of freedom, namely displacement along the X- and the Y-axis and rotation about the Z-axis. This means a total of 7 nodes and 21 degrees of freedom are used to describe the beam. The discretised beam along with the assigned numbering of the nodes is presented in Figure 6.6. Please note that the aforementioned mesh does not lead to a convergent solution. However,

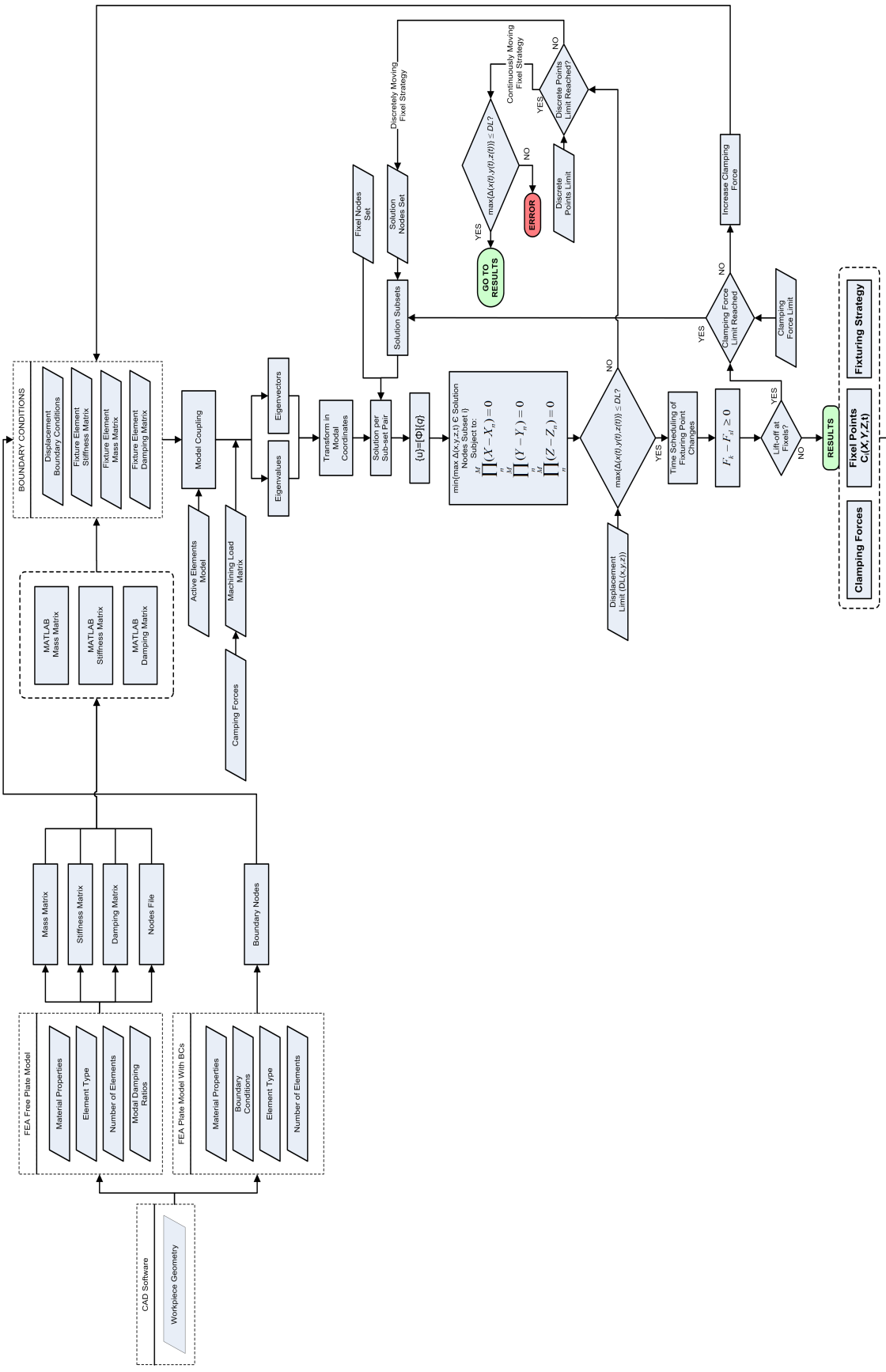

Figure 6.5: Schematic representation of the overall fully-active fixture planning methodology.

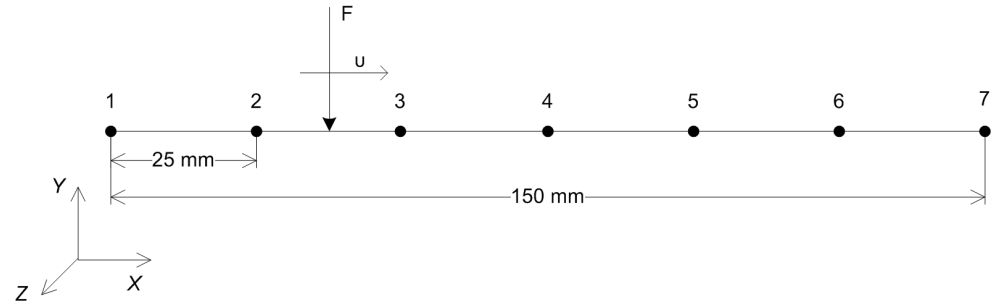

Figure 6.6: Beam workpiece FEA model. Numbering of the nodes was automatically generated by the FEA software.

this is not a problem as this test case is not used in order to improve the end-result of an actual process, but merely for theoretical demonstration purposes. Damping in the beam and at the contact interface between the workpiece and the fixel is assumed negligible. A reference frame is assigned to the above model, with the origin of the Cartesian axes at node 1. The positive directions of the axes are shown in Figure 6.6. A natural frequency analysis step is then defined to extract the natural frequencies of the system. Afterwords, the code of the input file for this problem is updated to output the stiffness and mass matrices of the beam. The problem is solved and the .mtx files containing the elements of the system matrices are generated. Also, the nodes and their numbers and coordinates are copied from the input file into a text file, thus generating the nodes file. Finally, boundary conditions are imposed on the beam workpiece, so that nodes 1 and 7 are not allowed to move in any direction. The input file of the updated problem is generated. A set of nodes containing nodes 1 and 7 appears. This information is used in the second phase of the methodology. With this, the discretisation phase concludes.

The problem formulation phase starts by importing the system matrices into Matlab and transforming them into Matlab variables. Each matrix has a size of 21×21, as expected. The next step is to apply boundary conditions. To do this the map of nodes is necessary. The formulation of this map for the beam test case is simple. The coordinates of the nodes differ only in their X-coordinate. The node at the left-most side of the beam, coinciding with the origin of the Cartesian coordinate system, is node 1. The rest of the nodes are numbered sequentially from left to right. The last node in the right-most end of the beam is node 7. Therefore the map of nodes is a vector containing the numbers of the nodes in increasing order.

According to the process described in Section 6.2.2, zero displacement conditions are

reflected by removing the relevant rows and columns from the system matrices. Node 1 corresponds to the first three rows and columns, whilst node 7 to the last three rows and columns of the system matrices. These are completely removed, reducing the size of the matrices to 15×15. Furthermore, in this test case there is only one fixturing element in contact with the beam workpiece. Therefore, no other boundary conditions should be applied at the structure at this stage.

The next step is the formulation of the moving load matrix. The load in this test case is a concentrated moving force, applied along the Y-axis. It has a constant amplitude of $F = 100$ N and it moves from node 1 to node 7 at a rate of 25 mm/s. As the load moves from one side of the beam to the other, it passes through different elements. When the load moves within the span of an element, it is simulated by the reaction forces it induces on the nodes of that element. No forces are applied to the other nodes. This approach is depicted in Figure 6.7. The time taken for the load to travel the entire length of the beam is split in 601 time instants. Therefore, a load matrix with dimensions 21×601 is created. The boundary conditions need to be reflected in the force matrix as well. For this reason, the first and the last three rows of this matrix are removed, reducing its size to 15×601. As mentioned earlier, the test case focuses on a locating element. As a result, no clamping loads need to be introduced into the load matrix.

Additionally, the locating element is passive so the model coupling process presented in Equation (6.12) is adopted. More specifically, the fixel is first placed on node 2. The element itself is treated as rigid, while the contact behaviour is simulated via a spring with stiffness 100 MN/m. One of the ends of the spring is in contact with the workpiece, whilst the other is grounded. Also, the fixturing element contacts the beam along the Y-direction. As the locator is placed on node 2, the contact stiffness value should be added to element (2,2) of the stiffness matrix that resulted from the addition of boundary conditions. This completes the problem formulation phase.

The final phase of the methodology is the optimisation phase. The process starts by requesting the user to input all necessary information for the optimisation step to produce a solution. This information includes the FNS and SNS pair, the maximum allowable displacement limit, the clamping force limit, and the discrete points limit. The FNS contains all nodes on the workpiece apart from the boundary nodes, i.e. node $2 \div 6$. The SNS in this test case is the same as the FNS. The displacement limit is set to $DL = 0.7$ μm and

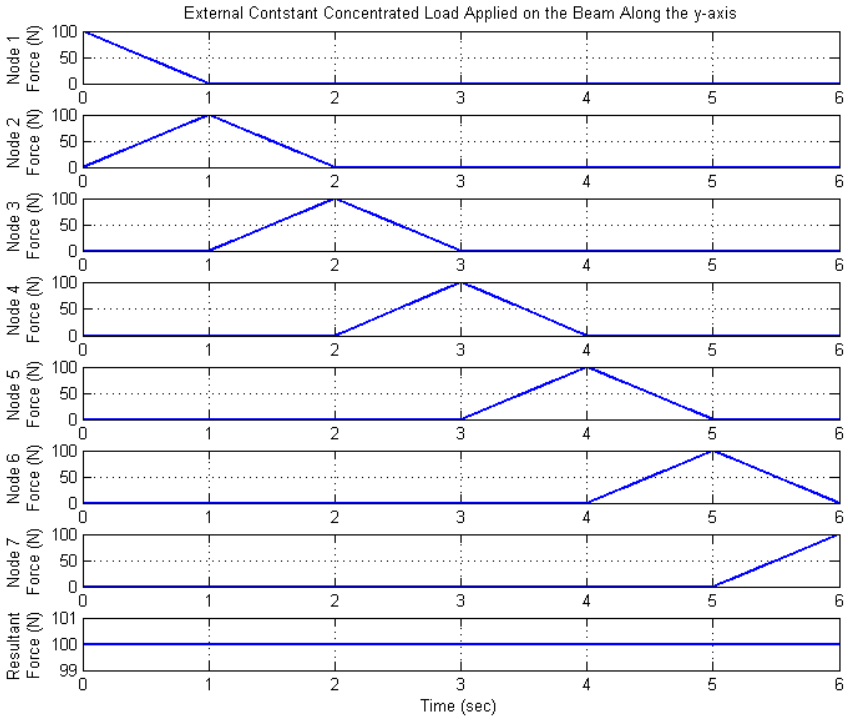

Figure 6.7: Concentrated constant moving load and the reactions it induces to the nodes of the beam workpiece.

applies only for the transverse direction (Y-axis). The clamping force limit is set to zero, since there are no clamping elements present. The discrete points limit is set to 3.

The calculation of the elastic deformation at the nodes of the SNS can then commence. At first, the displacement of the nodes under the initial fixturing set-up is investigated. For this, the eigenvalues and mass-normalised mode-shape matrix of the system are calculated and the system is transformed into modal coordinates (see Equation (6.25)).

At this stage a decision needs to be made as per which solution method should be followed. For this, the general and the steady-state solutions of the clamped beam without any fixturing elements are obtained. The load used to solve the forced response of the system is the one described above and shown in Figure 6.7. The above system constitutes a simplified version of the actual fixture-workpiece system. Figure 6.8 presents the transverse displacement of the midpoint of the beam over time. From this figure it becomes apparent that there is virtually no difference between the two solution methods. Therefore, for this example, the steady-state solution will be used, as it is computationally less expensive. To obtain the steady-state solution, Equations (6.26) and (6.27) are used.

As the set maximum allowable transverse displacement limit is 0.7 μm, it becomes apparent that it is not possible to produce an acceptable fixturing strategy through a single

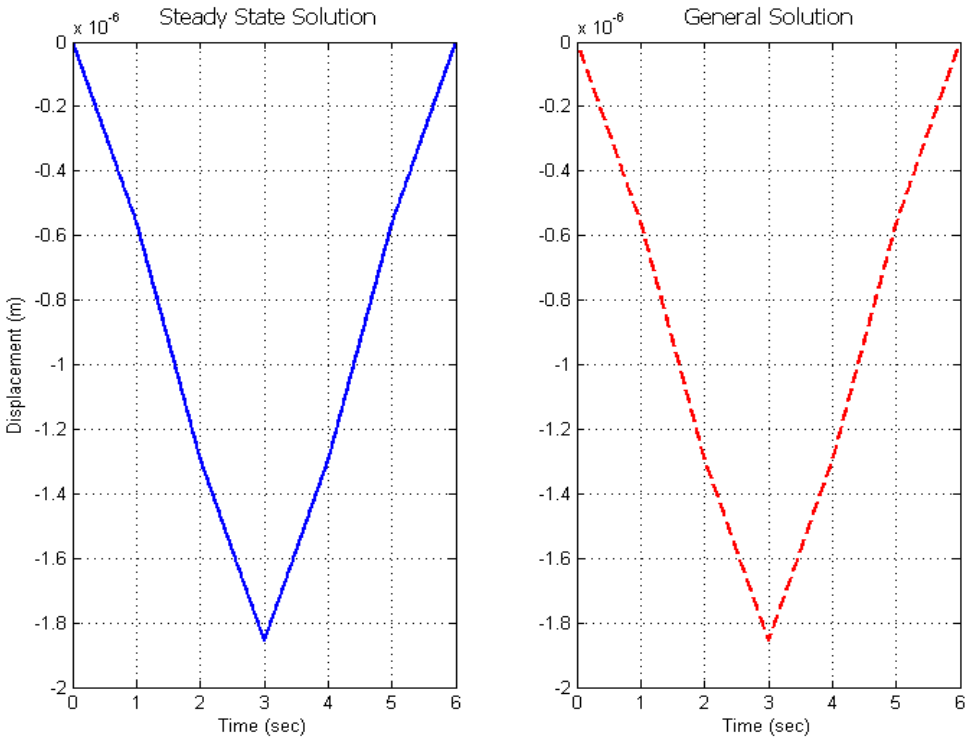

Figure 6.8: Dynamic response of the midpoint of the beam to a moving constant and concentrated load of 100 N magnitude. Left: Steady-state response. Right: Full dynamic response.

locating element. This means that a moving fixturing element is necessary. Therefore, it should be investigated which fully-active fixturing strategy is preferable. To do that, the solution nodes set is divided in two subsets. The first contains nodes 2,3 and 4 and the second one nodes 5 and 6. For the first solution subset, and according to Table 6.1, the minimum maximum displacement is observed when the locating element is placed at node 4. The maximum displacement value is 0.93 μm and it is presented by node 3. For the second solution subset the minimum maximum displacement is observed when the locator is at node 5. In this case, the value of the minimum maximum displacement is 0.60 μm and is presented at node 5.

Table 6.1: Maximum transverse displacement of planar beam workpiece under various static fixture scenarios.

	Max. Displacement at Nodes (μm)				
Locator Node	Node 2	Node 3	Node 4	Node 5	Node 6
2	0.43	1.22	1.68	1.46	0.75
3	0.55	0.60	1.19	1.24	0.71
4	0.65	0.93	0.65	0.93	0.65
5	0.71	1.24	1.19	0.60	0.55
6	0.75	1.46	1.68	1.22	0.43

After the responses of the nodes of the SNS for the initial system layout have been obtained, the results are stored and the fixture element is positioned on another node. The elastic deformation of the beam is calculated for the new fixturing scenario. The process is repeated until the fixturing element has been positioned on all five nodes that belong to the FNS. The results for the different fixture element placement scenarios are summarised in Table 6.1. It should be noted, that as the load applied to the workpiece is exciting the workpiece only the Y-direction, the displacement in the X-direction is significantly smaller and has, therefore, been ignored. The rotational degree of freedom has also been ignored on the basis of the assumption and limitations governing the optimisation phase (see Section 6.2.3).

The minimum maximum elastic deformation observed amongst the nodes of the second solution nodes subset is below the displacement limit. Therefore, positioning the locating element at node 5 is a candidate solution. On the contrary, the minimum maximum elastic deformation observed amongst the nodes of the first solution nodes subset is above the displacement limit. As a result, the first subset is split in two new subsets. The first of these contains nodes 2 and 3. The second contains node 4. The minimum maximum displacement for the first solution subset is observed at node 3, when the locator is at node 3. That displacement value is 0.60 μm. For the second subset, the minimum maximum displacement value of 0.65 μm is observed at node 4 when the locator is at node 4.

Having verified that the displacement criterion is satisfied the next step is the identification of the time instants when the fixture element changes position. Since the tool moves from the left to the right of the beam, the first position ($t = 0$ s) where the fixel is positioned is node 3. The displacement of the beam at the position of the tool, and as the tool moves along the beam, is shown in Figures 6.9 (a). More specifically, this figure shows the displacement of the workpiece at the position of the tool, assuming that the fixel remains put at node 3 (blue continuous line) or at node 4 (red dashed-dotted line). What this figure shows, is that if the fixel remained at node 3, then at $t = 2.38$ s, the displacement at the position of the tool would be bigger, than if the fixel was positioned at node 4. Therefore, and in order to keep the elastic deformation to a minimum, the fixel must be removed from node 3 and be repositioned at node 4 when $t = 2.38$ s. Similarly, and through Figure 6.9 (b), which shows the same information as Figure 6.9 (a), but for the fixel positioned at nodes 4 and 5, the fixel must be removed from node 4 and be repositioned at

node 5 at $t = 3.62$. The fixel then remains at node 5 until the end of the manufacturing process.

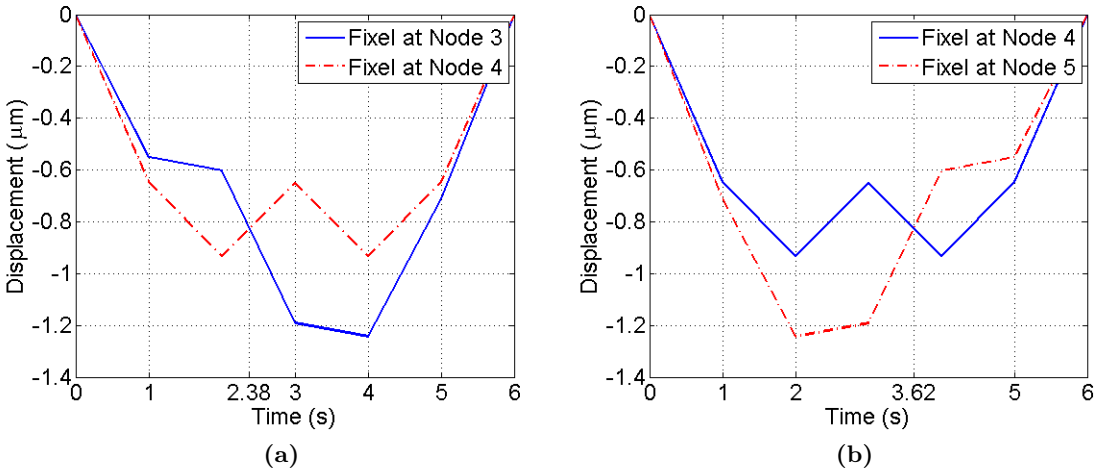

Figure 6.9: Displacement of the workpiece at the point of the cutting tool, when the fixture element is positioned at (a) nodes 3 and 4 and (b) nodes 4 and 5.

Base on the thus far information, the optimisation process has identified a candidate solution. This involves:

1. A discretely-moving-fixel fixturing strategy is necessary.
2. Three discrete position changes are required to satisfy the displacement limit.
3. The coordinates of these points (in mm) are:
   (a) (50,0,0) from $t = 0$ s to $t = 2.38$ s.
   (b) (75,0,0) from $t = 2.38$ s to $t = 3.62$ s.
   (c) (100,0,0) from $t = 3.62$ s to $t = 6$ s.

The final step involves making sure that no seperation between the fixel and the workpiece occurs. For this, it is necessary to check the resultant force on the fixel for the duration of the manufacturing process. This is presented in Figure 6.10. The figure highlights that the resultant force on the fixture element is always greater than zero. Therefore, no separation occurs and the provisional solution is outputted as the final solution.

By applying the fully-active fixture design methodology on a simple planar beam workpiece and a fixture with a single passive locating element, a significant reduction in terms of elastic deformation is noticed. Compared to a traditional fixturing approach, where a

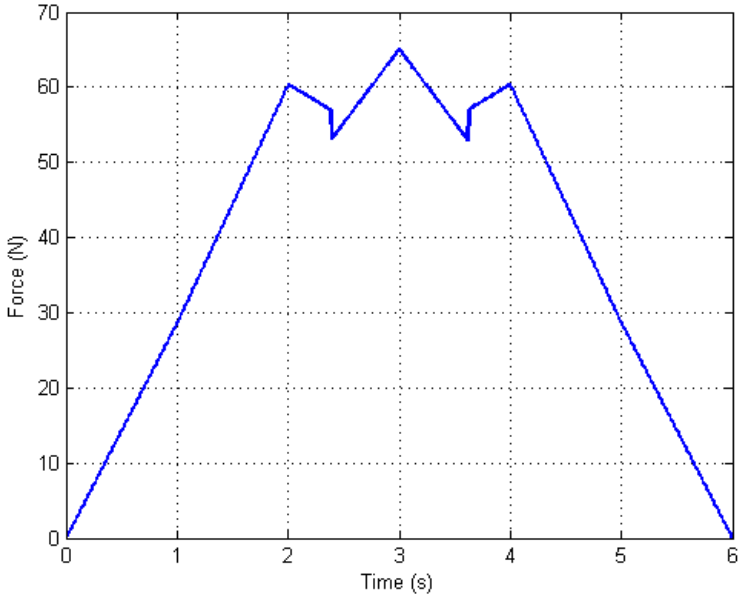

Figure 6.10: Resultant force at the fixturing element during the manufacturing process. The figure reflects all positions that the fixel occupies during the discretely-moving-fixel strategy.

single passive element would be used, the discretely-moving-fixel fixturing strategy results to a maximum reduction in elastic deformation of 35.48%, as shown in Table 6.2.

Table 6.2: Comparison of static and fully-active fixturing strategies.

	Max. Displacement at Nodes (μm)				
Fixturing Scenario	Node 2	Node 3	Node 4	Node 5	Node 6
Static fixture @ Node 4	0.65	0.93	0.65	0.93	0.65
Fully-active fixture	0.55	0.60	0.65	0.60	0.55
% Difference	19.62	35.48	0.00	35.48	19.62

6.4 Conclusions

In this chapter a methodology for the planning and design of fully-active fixturing systems has been presented. The main conclusions can be summarised through the following points:

- A fixture design methodology to assist in the establishment of the fixturing parameters that minimise the maximum elastic deformation of a workpiece has been formulated.
- The methodology takes into account the capabilities of fully-active fixtures. Both active and passive elements are considered.
- The proposed fully-active fixture design methodology comprises three core steps:

1. The discretisation phase, which is executed with the aid of FEA software.
2. The formulation in Matlab phase, where the data produced by the FEA software are input in Matlab and used to establish the coupled fixture-workpiece system model.
3. The optimisation phase, were the model from the previous step is used to identify the optimal fixturing parameters.

- The fixturing parameters that the methodology outputs are:
  1. The fixturing strategy, namely whether static, discretely-moving or continuously-moving fixture elements should be used.
  2. The number of discrete fixturing points per fixel, if a discretely-moving-fixel strategy is suggested.
  3. The time instants when the fixel needs to change position (discretely-moving-fixel case), or the motion path of the fixel (continuously-moving-fixel case).
  4. The minimum clamping forces that the clamps of the fixture need to apply to avoid fixture-workpiece separation.
- The methodology was applied on a theoretical test case involving a beam and a fixture composed of a single passive fixel.
- The results of the test case revealed that by deploying the fully-active fixture design methodology and a fixture with the ability of changing the position of its elements during the manufacturing process, the elastic deformation of the beam workpiece can be reduced by up to 35.48%.

Chapter 7

Verification of the Fixture Design Methodology

7.1 Introduction

As discussed in the previous chapters of this thesis, one of the most determinant factors for the outcome of a manufacturing process in terms of final product quality is fixtures. The layout and contact characteristics of these workholding devices affect the static and dynamic behaviour of the workpiece. Static deformation due to constant clamping loads, displacement from the clamping process, lift-off and slippage due to the selection of non-optimal clamping forces, dynamic deformation due to forced excitation from machining loads, are all factors that can reduce the quality of the end product of a manufacturing process. Fully-active fixtures constitute a promising approach with the ability to adapt fixturing parameters, like clamping forces and fixture layout, in order to reduce or eliminate the aforementioned problems. Fully-active fixtures allow for continuous and on-line adaptation of fixturing parameters according to the instantaneous conditions and needs, thus moving away from the-worst-case-scenario approach of traditional fixtures.

Modelling and predicting the behaviour of such fixturing systems was presented in Chapters 4 and 5 of the thesis. Chapter 6 concentrated on establishing a design methodology that reflects the capabilities of fully-active fixtures. Such a methodology does not treat the fixture layout as a static entity, but as one with the ability to reposition its fixturing elements during the manufacturing process. The core outputs of the methodology are the layout of the fixture and the optimal clamping forces for any given instant in time.

The desired result from the design methodology is a fixturing case that minimises the static deflection and the amplitude of vibration that the workpiece experiences due to the applied clamping forces and the externally applied machining forces.

This chapter focuses on the experimental verification of the advantages of the fully-active fixture design methodology. In order to achieve this, the chapter is split in three distinct parts. In the first part, the fully-active fixture design methodology is applied on a test case involving a thin-walled plate workpiece undergoing a material removal operation via peripheral (down) milling. Different theoretical maximum allowable elastic deformation are set to highlight the decision-making process within the methodology. The results from the test case are presented in Section 7.2. The second part deals with the experimental set-up, including the implementation of a fully-active fixture prototype, its key design features, and how the latter were selected (Section 7.3). The experimental procedure that is followed in order to verify the design methodology is described in Section 7.4. The third part covers the results, which were obtain from the execution of experiments (Section 7.5). These results are then analysed and discussed in Section 7.6. The chapter closes with a summary of the main conclusions.

7.2 The Thin Plate Test Case

The application of the fully-active fixture methodology, which was described in depth in Chapter 6, on a test case involving a workpiece that has the geometry of a thin-plate, is presented in this section. The theoretical application of the fully-active fixture design methodology on the previously-mentioned test case intents to supply the fixturing parameters for a fixture-workpiece system that can also be deployed experimentally. This way, a direct comparison between theoretical and experimental results can be achieved. In this way, the applicability and the usefulness of the methodology, as well as the potential positive impact of fully-active fixtures can be verified.

The geometrical features and the material of the thin-plate test workpiece were selected based on multiple reasons. To begin with, as expressed in Section 3.2.1.1 of Chapter 3 of the thesis, the developed models and methodologies are expected to have a greater impact on low-rigidity structures. Such structures are often met in industrial sectors like the automotive and aerospace. Their geometrical features, in many cases, resemble basic

structural elements, like plates [86].

Furthermore, the production of large amounts of plate-like workpieces for experimental processes is significantly more cost-efficient and less time-consuming compared to more complex-geometry workpieces. Plate workpieces can be produced in bulk from a larger-sized aluminium sheet.

Finally, the selected material for the thin-plate workpieces, is a high-grade aluminium alloy, namely the aluminium 7075-T6 alloy, which is often met in the aerospace and the automotive industries.

For all the above reasons, it is regarded that, a thin-plate workpiece is an ideal test case for the fixture design methodology to be applied on.

In the described test case the thin plate workpiece is held in place by a clamping arrangement, the geometry and characteristics of which are presented in Section 7.3.4 of this chapter. The fully-active fixture that holds the thin plate is constituted of a single passive clamping element. This arrangement was chosen in order to facilitate the experimental application of the results of the methodology and to isolate the effects of the methodology-derived fixturing strategies from factors like the geometrical inaccuracies which complex fixtures may exhibit.

In this section, the step-by-step theoretical application of the methodology is presented, along with the results it produced. It is reminded here that the methodology comprises three phases. These are described hereafter.

7.2.1 Phase 1: Discretisation of the Structure

For the first phase to commence the following inputs are defined:

Workpiece geometry. The application of the methodology starts by creating a model of the workpiece. For this, the thin-plate workpiece, shown in Figure 7.1, is drawn in the Finite Element Analysis (FEA) software Abaqus [127]. The plate is represented as a 3-dimensional deformable, planar, and solid object. The thickness of the plate is 3.17 mm, the width is 50 mm, and the length is 150 mm.

Material properties. Next, the material properties are introduced. In this case, the thin plates are made of aluminium 7075-T6. The properties of this material are summarised in Table 7.1.

Type and number of finite elements. Next, the workpiece is discretised using finite elements (FE). A total of 300 S4 elements [127] are used to discretise the plate in this test case. The FE model is therefore created using 341 equidistant nodes, each exhibiting 6 degrees of freedom (DOF). The selection of these elements was explained in detail in Section 4.2 of Chapter 4.

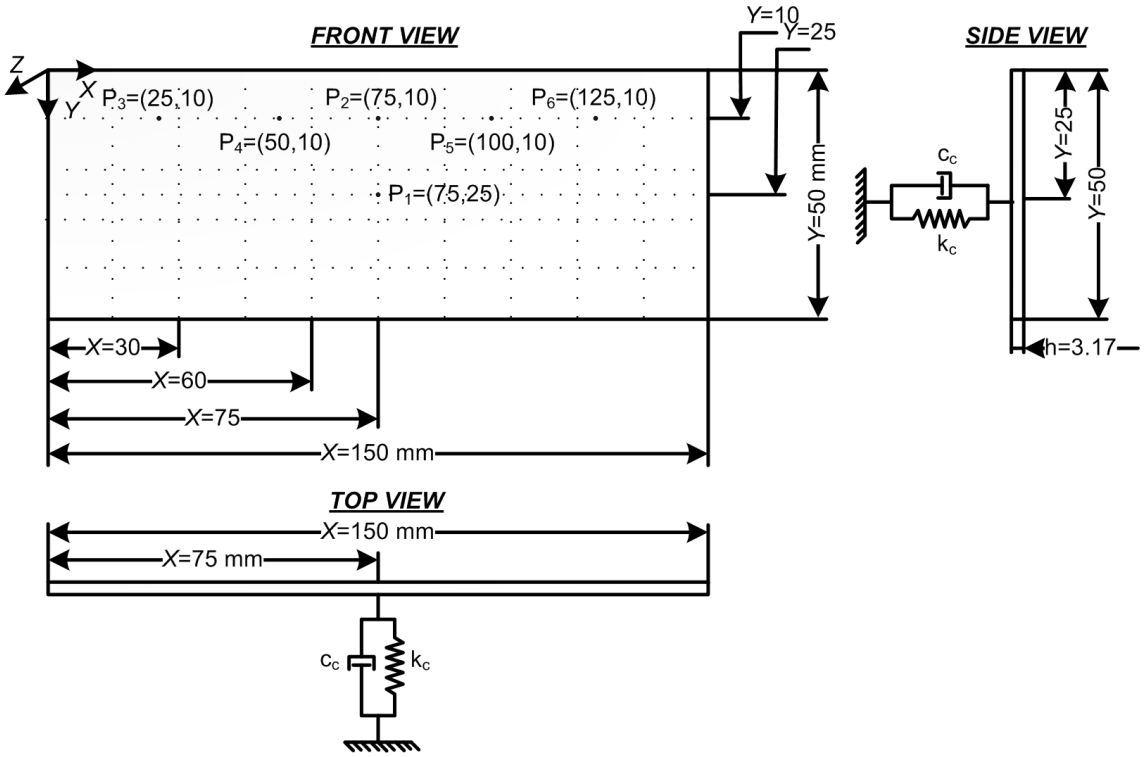

Figure 7.1: Schematic representation of the geometric model of thin-plate workpiece. The spring and damper, shown in the side and top views, represent a passive fixture element. The position of the passive element constitutes the initial solution for the optimisation step of the fixture design methodology, applied on the thin-plate test case (Section 7.2.3). Key points on the surface of the plate are highlighted. All coordinates are expressed in millimetres.

Table 7.1: Mechanical properties of aluminium 7075-T6.

Properties	
Density	2810 kg/m^3
Young's Modulus	71.7 GPa
Shear Modulus	26.9 GPa
Poisson's Ratio	0.33

Damping definition. The damping matrix was decided to be manually created in the next step of the methodology,. For this the proportional damping formula, described in Equation (7.1), is used. This was decided to avoid repetition, since the method to

introduce damping into the FEA model would be the same. Further information on the definition of the damping matrix in this test case are presented in Section 7.2.2, where the second phase of the design methodology is analysed.

Definition of boundary conditions. In this test case, the two shorter edges of the plate are fully constrained. In detail, all degrees-of-freedom are removed along the boundary nodes at the short edges the plate. No degrees-of-freedom are removed from the nodes along the longer edges of the plate. These conditions simulate those that exist at the edges of the plate when it is part of a monolithic workpiece. It is reminded here that, although translational and rotational spring boundary conditions might be more appropriate, as suggested by Meshreki *et al.* [86], the boundary conditions used (Clamped-Free-Clamped-Free or CFCF) can be implemented experimentally in a more straightforward way.

Having defined all necessary inputs, the first phase of the methodology leads to the subsequent outputs:

System matrices. The first output of the discretisation phase of the methodology is the system matrices. For the thin plate test case, the mass and stiffness matrices are generated in this step. The damping matrix will be defined directly in the next phase of the methodology, as discussed earlier. In order to extract the required system matrices, a natural frequency extraction step is defined as the desired FE analysis step. The problem is first solved with all the ends of the plate being free to move in all directions, i.e. without applying any type of boundary conditions. This is to avoid any numerical issues in the next steps of the methodology. The process generates two separate files, each one containing the elements of one of the two system matrices.

Map of nodes. With the system matrices outputted, the map of nodes file needs to be generated. This is automatically done by Abaqus, as the coordinates and the identifying numbers of all nodes can be found within the file of the FEA model, i.e. the input file.

Boundary conditions nodes. For this file to be generated, the model needs solving once more, this time with the boundary conditions applied. For this, fully-constrained boundary conditions are applied on the two shorter edges of the workpiece model.

The input file of the updated model is then created, within which the boundary nodes can then be found.

7.2.2 Phase 2: Formulation of the Problem in Matlab

Just as in the first phase, the second phase starts by introducing the necessary inputs, i.e. the results from the previous phase.

Introduction of FEA-generated files. The second step of the methodology starts by introducing the files from Abaqus, which contain the elements of the system matrices, into Matlab. As mentioned in the previous section, the mass and stiffness matrices are defined directly from the input files. The damping matrix, however, is defined manually, using the proportional damping formula:

$$[C] = \alpha\,[M] + \beta\,[K] \tag{7.1}$$

where $[C]$ is the damping matrix, $[M]$ is the mass matrix, $[K]$ is the stiffness matrix, and α and β are the Rayleigh damping constants. The latter were defined by means of trial and error and were selected based on the modal damping ratios that were extracted during the experimental modal analysis of the plate workpiece. In detail, if $[\Phi]$ is the mass-normalised mode-shape matrix, then the following equation applies:

$$[\Phi]^T\,[C]\,[\Phi] = \mathrm{diag}[2\zeta_r\omega_r] \tag{7.2}$$

In Equation (7.5), ζ_r and ω_r are the damping ratio and the frequency of mode r. The constants α and β were selected so that the above equation is valid. The values $\alpha = 90\ \mathrm{s}^{-1}$ and $\beta = 7 \cdot 10^{-7}$ s were chosen.

The map-of-nodes file is then introduced in Matlab, followed by the boundary-nodes file.

Applying boundary conditions. The process to apply the boundary conditions can be found in Section 6.2.2 of the previous chapter and will not be repeated here, for the sake of brevity. It is only mentioned that, since there are 22 six-degree-of-freedom boundary nodes and because these nodes are fully constrained, a total of $22 \times 6 = 132$

rows and 132 columns are removed from the system matrices. This reduces the size of the matrices to 1914×1914.

Part of the boundary-condition-implementation step is also the coupling of the discretised workpiece model to that of the fixturing elements. For this test case it is assumed that the fixture consists of a single clamping element. The element is treated as a passive linear spring element with a constant stiffness of $k_c = 10^8$ N/m, while $c_c = 0$ (see Figure 7.1). The process behind the coupling of passive fixture elements can be found in Section 6.2.2 of Chapter 6.

Definition of load vectors. The load vectors is the final part of the model that needs to be defined. The details behind the method to fulfil this requirement can be found in Section 6.2.2. However, the specifics behind the machining loads, as simulated in this test case, need to be discussed in this paragraph. The machining loads are approximated as a simple harmonic force with an excitation frequency of $\omega = 200$ Hz, acting along the direction normal to the surface of the plate. The excitation frequency stems from the fact that a down-milling operation is assumed to be the process that the thin plate undergoes, and that the parameters of this process involve a spindle speed of 3000 rpm and a 4-flute cutting tool. An evenly distributed profile, from $Y = 0$ mm to $Y = 25$ mm of the plate (Figure 7.1), is assigned to the load, simulating the axial depth of cut. The amplitude of the load is given by $P(t) = 3+2.8\cos(\omega t)$ N/mm. This amplitude is an approximation of the traverse-direction component of the actual cutting load, which was measured experimentally. The load traverses the plate with a speed of $c = 300$ mm/min, or $c = 5$ mm/s. The load is first applied at $X = 15$ mm and travels to $X = 135$ mm.

Based on the speed with which the load traverses the plate surface, the machining process lasts 24 s. This time span is divided into time instants that are spaced at $dt = 757.5$ ns. This time increment value was selected to ensure that the Nyquist criterion is met. According to this criterion the sampling frequency needs to be at least twice that of the measured frequency. By selecting the previously-mentioned time increment value, a 'sampling frequency' of approximately 1320 Hz is assumed, which is six times higher than the frequency of excitation of the machining force. This 6-to-1 ratio was selected for increased confidence in the reproduction of the machining

force profile in the developed model.

From this analysis, it is derived that the load matrix will be of size 1914×31684 after the application of non-displacement boundary conditions. The number of row stems from the number of nodes that the discretised workpiece model exhibits. The number of columns reflects the time instants, which the 24 s time span has been divided into. Each column represents the load vector, which excites the fixture-workpiece system at the corresponding time instant.

Moreover, a clamping load of 20 N is applied at the point where the fixel is in contact with the plate workpiece. This small starting clamping force is selected for practical reasons, since in real-life applications it is always advisable for clamps to apply at least a small clamping force to avoid slippage between the fixture and the workpiece. This practice is also followed during the experimental procedure and is therefore incorporated into the fixture-workpiece model.

The second phase of the methodology uses all the previously defined input to generate its sole output, namely a comprehensive model of the fixture workpiece system that is accepted by the next step of the methodology as an initial solution. The generation of this is described below:

Initial solution generation. For this test case, the fixture comprises a single passive clamping element. By following basic fixturing rules-of-thumb, it is reasonable to accept as a feasible initial solution that, where the passive fixture element is in contact with the workpiece at the midpoint of the plate, namely point P1 (Figure 7.1) with coordinates $(X, Y) = (75, 25)$ in millimetres. The fixture element is positioned in the traverse direction of the workpiece. Point P1 corresponds to node 171. Due to the application of the boundary conditions, the six DOFs from 11 nodes with identifying number smaller that that of the fixture contact node have been removed from the matrices of the system. This means that in order to generate the stiffness matrix of the coupled system, the fixel stiffness value $k_c = 10^8$ N/m needs to be added to the element of the workpiece stiffness matrix with indices $(957, 957)$, since $(171 - 11) \times 6 - 3 = 957$. The -3 in the previous formula is used to ensure that the fixture element is placed along the Z-direction of the plate, which is the third DOF from the six that each node exhibits. The mass and damping matrices do not need

to be updated as it is assumed that the fixture elements do not present damping or inertia.

7.2.3 Phase 3: Optimisation Process.

The optimisation phase commences by defining the fixel nodes set (FNS), which contains all possible fixturing points, the solution nodes set (SNS), which contains the nodes of which the elastic deformation must satisfy the objective function for a solution to be reached, the objective function, the solution constraints, and the various user-selected limits need to be defined.

Solution nodes set. As described above, the machining loads travel from $X = 15$ mm to $X = 135$ mm and the axial depth of cut is 25 mm, from $Y = 0$ mm to $Y = 25$ mm. This means that the SNS should contain all nodes with coordinates in the intervals of $X \in [15, 135]$ and $Y \in [0, 25]$.

Fixel nodes set. The fixture elements can be positioned on any point on the large surface of the plate that is not being traversed by the cutting tool. However, the geometric model of the workpiece is a two-dimensional one, which means that the workpiece is simulated as a rectangular surface. This surface contains all the nodes of the FEA model. Hence, the FNS contains all the nodes of the workpiece model apart from the boundary nodes. The latter are exempt from the FNS as the system matrix elements that correspond to the boundary nodes have been removed. Therefore, a coupling of the fixture element-workpiece model on those nodes is impossible.

Objective function. The optimisation process commences by accepting the fixture-workpiece model created above, along with the load vectors as an initial solution. As the loads in this test case are applied only along the Z-direction of the plate (see Figure 7.1), the objective of the optimisation phase is to identify the fixturing strategy and the fixture-workpiece contact points that lead to the minimisation the maximum elastic deformation of the plate in the Z-direction, and at the points of application of the machining forces as the cutting tool traverses the surface of the plate. The elastic deformation in the other directions is considered significantly smaller that the one in the Z-direction and is, therefore, ignored. Subsequently, the objective function of the

optimisation phase can be expressed mathematically as:

$$min\{max\{\Delta z_i(t)\}\} \tag{7.3}$$

where $\Delta z(t)$ signify the elastic deformation of point i on the workpiece in the Z-direction, at time t when the tool is directly over that point.

Additionally, all solutions that the optimisation process produces must obey the following constraints:

Nodal solution constraint. As explained in Chapter 6 (Section 6.2.3), the optimisation process can only accept as possible fixture-workpiece contact points, those that coincide with a node of the workpiece model. For this test case, the optimisation phase is applied in Matlab by means of simple programming language statements, such as 'for' loops. Therefore, it is preferable to look for the fixture-workpiece contact points that satisfy the objective function in terms of nodes and not physical coordinates. As a result, the nodal solution constraint is expressed as:

$$\prod_{j=1}^{M} (\mathrm{FNS}_j - n) = 0, \quad n \in \mathrm{FNS} \tag{7.4}$$

where FNS_j corresponds to the number of the j^{th} node within the fixel nodes set and n is the identifying number of the investigated-for-suitability node. In this test case, and since the FNS contains all nodes in the workpiece model, this constraint is always satisfied.

Separation constraint. As discussed in the previous chapter, no separation between the workpiece and the fixture element is allowed. This means that the resultant force in the direction of the fixel cannot be zero, which is expressed mathematically as:

$$F_k(t) - F_{sl} \geq 0 \tag{7.5}$$

where $F_k(t)$ is the resultant force in the direction of fixture element k at time t, and F_{sl} is the user defined safety limit. In this test case, no force safety limit is defined, i.e. $F_{sl} = 0$.

User-defined limits. There are three limits that the need to be defined in order for the optimisation process to output a solution. These are the maximum allowable displacement limit, denoted as DL, the clamping force limit, and the discrete points limit. The clamping force limit is set to 50 N to avoid excess deformation of the plate. The discrete points limit is set to 5. For the purposes of the test case and in order to highlight the potential benefits of fully-active fixtures, the displacement limit is not strictly defined. It takes several values so that the design methodology and the optimisation phase lead each time to different fixturing parameters results. More information on this matter are presented in the following sections.

With all the previous aspects of the optimisation phase defined, the next step is the calculation of the elastic deformation of the workpiece. The coupled fixture model produced in the second phase of the methodology is accepted as the starting point of the optimisation phase. The model is transferred into modal coordinates, as explained in Section 6.2.3.5, and the elastic deformation of the nodes within the SNS is calculated using the steady-state-solution approach. For the initial solution, where the fixture element is in contact with P1 of the plate (Figure 7.1), the predicted displacement at the nodes of the plate, and when the tool passes directly above these nodes, is depicted graphically in Figure 7.2.

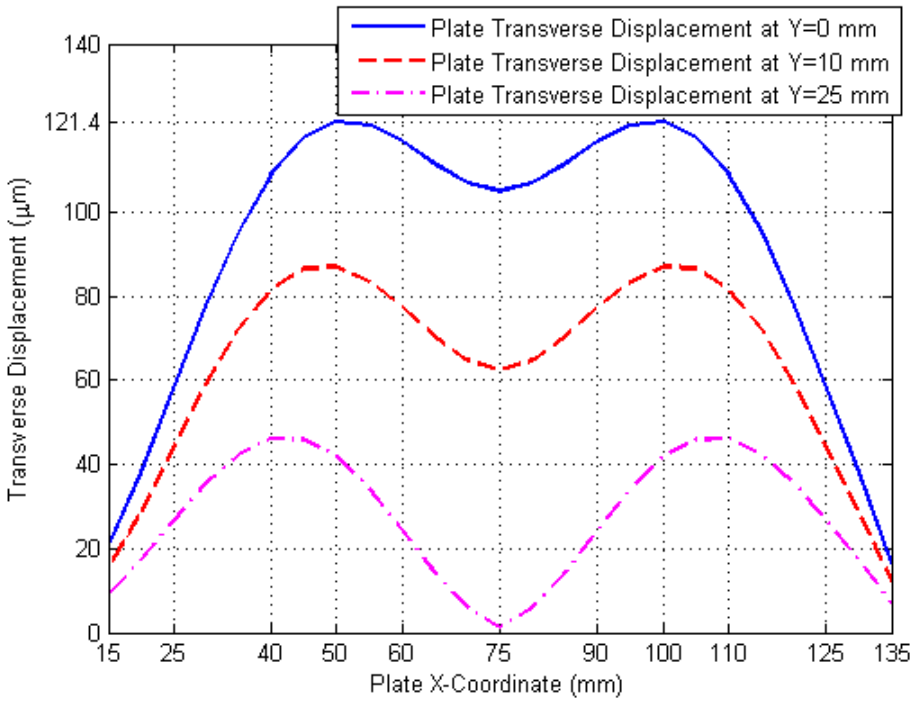

Figure 7.2: Transverse elastic deformation of the workpiece, as the cutting tool traverses the plate, as predicted by the fixture-workpiece model. A single clamping element positioned at P1 (Figure 7.1) is used. The applied clamping force is 20 N

Based on the selection of the displacement limit, the following cases are identified.

7.2.3.1 Passive and Static Clamping Element

If the maximum allowable displacement limit is set to $DL = 80$ μm, it becomes apparent from Figure 7.2 that the initial solution is not acceptable. For this reason, and as described in Section 6.2.3.5, the fixture element and the workpiece are coupled at another node and the elastic deformations of the new system are calculated. The process is repeated until the fixture element has been positioned on all nodes in the FNS. Then, the position of the fixture element that leads to the minimum maximum deformation is identified.

In this case the optimum position of the passive clamping element is node 78, which coincides with point P2 $(X, Y) = (75, 10)$ (see Figure 7.1). The predicted elastic deformation results from this fixturing scenario are presented in Figure 7.3. From this figure it can be seen that the maximum elastic deformation is 79.26 μm and it is observed at $(X, Y) = (40, 0)$ and $(X, Y) = (110, 0)$. The fact that there are two points on the plate that present the maximum elastic deformation makes sense, due to the symmetric nature of the problem.

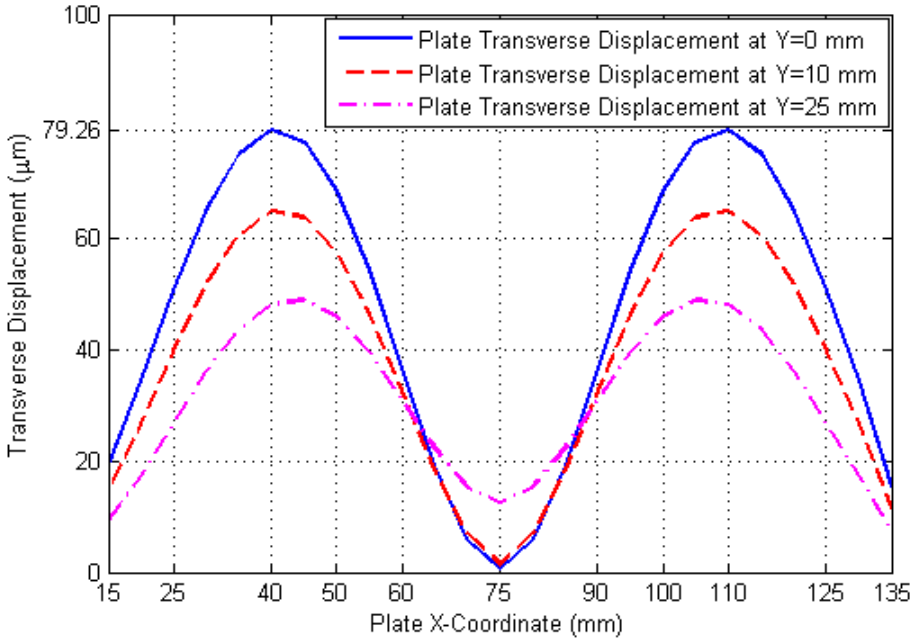

Figure 7.3: Transverse elastic deformation of the workpiece, as the cutting tool traverses the plate, after the optimisation phase of the design methodology has been applied. A single clamping element is positioned at point P2, as shown in Figure 7.1.

With the optimal position for the clamp defined, the next step is to check whether there is a violation of the separation constraint. Figure 7.4 shows the resultant force that the

fixture element receives over the history of the machining process. It can be seen clearly in this figure that the resultant force in the direction of the fixel remains greater than zero, which means that Equation (7.5) is satisfied. Therefore, a statically applied passive clamping element at point P2 of the plate is accepted as a viable solution that satisfies all constraints.

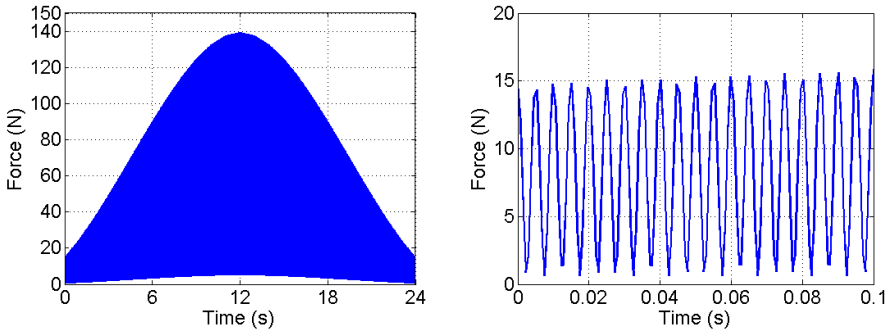

(a) **(b)**

Figure 7.4: Elastic deformation of the point of contact between locator and workpiece (P2), as the load traverses the plate. (a) Full time history and (b) a closer look at $t = 0 \div 0.1$ s, where the resultant force is closer to violating the minimum force criterion.

7.2.3.2 Passive and Moving Clamping Elements - Discrete Motion

If a tighter displacement limit is set, for example $DL = 30$ μm, then it becomes apparent from the previous analysis that this cannot be achieved by using a statically positioned element. In this case, and as explained in detail in Section 6.2.3.5 of Chapter 6, the fixturing methodology splits the original solution nodes set into two equal or almost equal sub-sets. Then, the methodology tries to find a position for the fixture element that minimises the displacement of nodes belonging to each solution nodes sub-set. If a solution cannot be found for either of the sub-sets, then the original SNS is split into three equal parts and so forth.

When applied in this test case, the methodology could not find an acceptable solution when the original SNS was split in two, three or four equal sub-sets. On the contrary, a solution was identified when five sub-sets were used. These sub-sets were the following:

Solution nodes sub-set 1. This includes nodes with coordinates that satisfy the following coordinate-related criteria: $X \in [15, 35]$ and $Y \in [0, 25]$.

Solution nodes sub-set 2. This includes nodes with coordinates that satisfy the following coordinate-related criteria: $X \in [35, 60]$ and $Y \in [0, 25]$.

Solution nodes sub-set 3. This includes nodes with coordinates that satisfy the following coordinate-related criteria: $X \in [60, 90]$ and $Y \in [0, 25]$.

Solution nodes sub-set 4. This includes nodes with coordinates that satisfy the following coordinate-related criteria: $X \in [90, 115]$ and $Y \in [0, 25]$.

Solution nodes sub-set 5. This includes nodes with coordinates that satisfy the following coordinate-related criteria: $X \in [115, 135]$ and $Y \in [0, 25]$.

The position of the fixture element that minimises the maximum traverse elastic deformation at the nodes of each sub-set is then identified. By applying the design methodology, it is found that the aforementioned value is minimised when the following fixture points are used:

From sub-set 1. The suggested fixture contact point has coordinates $(X, Y) = (25, 10)$ and is marked as point P3 in Figure 7.1.

From sub-set 2. The suggested fixture contact point has coordinates $(X, Y) = (50, 10)$ and is marked as point P4 in Figure 7.1.

From sub-set 3. The suggested fixture contact point has coordinates $(X, Y) = (75, 10)$ and is marked as point P2 in Figure 7.1.

From sub-set 4. The suggested fixture contact point has coordinates $(X, Y) = (100, 10)$ and is marked as point P5 in Figure 7.1.

From sub-set 5. The suggested fixture contact point has coordinates $(X, Y) = (125, 10)$ and is marked as point P6 in Figure 7.1.

All these points correspond to nodes of the discretised workpiece model, and, therefore, they constitute acceptable solutions. The resulting elastic deformation of the plate, as the tool traverses the length of the plate workpiece is shown in Figure 7.5.

However, the above solution is not complete before the time instants, at which to position of the fixel changes, are calculated. For this, and following the corresponding procedure as described in Section 6.2.3.5, the elastic deformation of the plate for two consecutive fixturing points are checked each time. At first, the elastic deformation of the plate, for the case where the fixture element is at position P3, is compared to the elastic

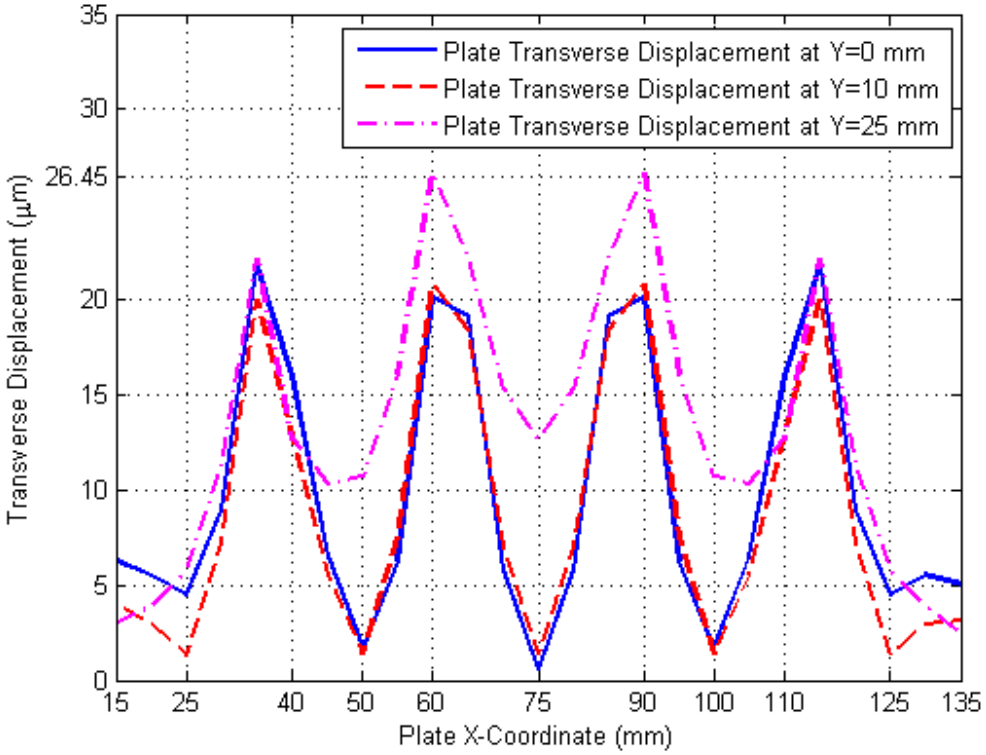

Figure 7.5: Transverse elastic deformation of the workpiece, as the cutting tool traverses the plate, after the optimisation phase of the design methodology has been applied. The clamping element moves, in discrete steps, from point P3 to point P6, as presented in Figure 7.1.

deformation of the plate at $Y = 25$ mm, when the fixture element is at position P4. As always, the deformation of the plate at the direct vicinity of the cutting tool is of interest. The deformation of the plate under the previously-mentioned fixturing cases is presented and compared graphically in Figure 7.6. From this figure, it can be observed that, should the fixture element be maintained at position P3, then the plate will start experiencing greater elastic deformation than the one it would if the fixel was at P4, when the tool has surpassed the point with X-coordinate $X = 32.05$ mm. This means that, with the velocity with which the tool traverses the plate, the time instant when the fixel needs to be moved from P3 to P4 is $t_1 = 3.41$ s. Following the same process for the other fixture-element-position changes, it is established that the latter need to take place at $t_2 = 9.18$ s (tool at $X = 60.93$ mm) for the change from P4 to P2, $t_3 = 14.81$ s (tool at $X = 89.07$ mm) for the change from P2 to P5, and $t_4 = 20.59$ (tool at $X = 117.96$ mm) for the change from P5 to P6.

The final step of the methodology is to check whether the separation criterion is met at every point of contact between the fixture and the workpiece. Indicatively, two graphs,

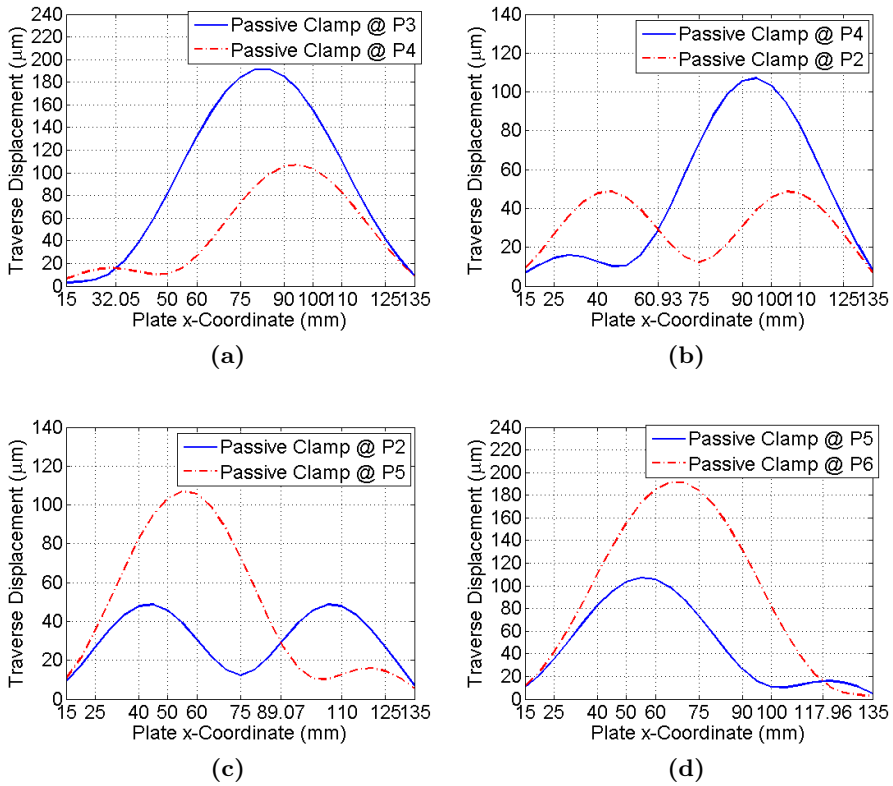

Figure 7.6: Comparison of the elastic deformation of the thin-plate workpiece at $Y = 25$ mm, for different positions of the fixture element. (a) The cases where the fixture element is at P3 and at P4. (b) The cases where the fixture element is at P4 and at P2. (c) The cases where the fixture element is at P2 and at P5. (d) The cases where the fixture element is at P5 and at P6. These graphs are used for determining the time instants, when the fixture element needs to change positions, during the discrete-moving-fixel case.

depicting the force experienced by the clamping element at two of the positions it occupies during the milling process, specifically positions P3 and P4, are shown in Figure 7.7. From this figure, it is evident that the resultant force on the fixture element, in the direction normal to the surface of the thin plate, never violates the set constraint. In other words, the resultant force on the fixel is always greater than zero. In general, the minimum force criterion is satisfied for all contact points so, according to the methodology, the previously mentioned fixturing scenario is accepted as the final solution.

7.2.3.3 Passive and Moving Clamping Elements - Continuous Motion

Assuming a further tightening of the maximum dynamic displacement limit requirements ($DL = 13$ μm), and because a maximum number of 5 discrete changes in the position of the fixture element are allowed, according to the design methodology, a continuously-moving fixturing element would be the preferred fixturing strategy. The path of the fixturing element in relation to the workpiece and the cutting tool needs to be, therefore, decided.

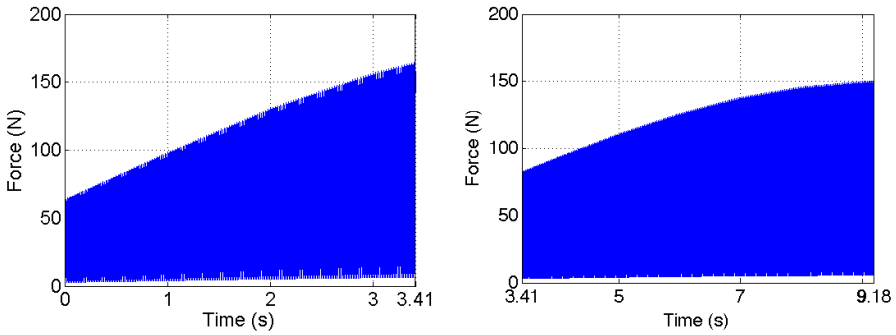

Figure 7.7: The resultant force on the fixture element at two positions during the discrete-moving-fixture-element case. (a) Resultant force on the fixel while it is positioned at P3. (b) Resultant force on the fixel while it is positioned at P4.

For this, the methodology divides the original solution nodes set to sub-sets, each of which contain nodes with the same X-coordinate and with with Y-coordinates $Y \in [0, 25]$. This way each solution nodes sub-set forms a straight line parallel to the Y-coordinate axis of the workpiece (Figure 7.1). The node, from each sub-set, that minimises the maximum dynamic displacement of the thin-plate workpiece, is regarded as a point on the plate, over which the fixture element needs to pass. Moreover, it is important to estimate the time instants at which the fixture element needs to be over each solution node from each solution sub-set. The ensemble of all the optimal nodes from all sub-sets, along with the timing information, form the path that the fixel needs to follow during the process.

Based on the results that were presented in the previous paragraphs, and more specifically Figures 7.2, 7.3, and 7.5, it is anticipated that the maximum reduction in the dynamic displacement of the thin plate should be observed when the tool is exactly over the fixture element. This is also confirmed by calculating the elastic deformation of the plate, and for every possible position of the fixture element. For each solution nodes sub-set, it is found that the node that minimises the elastic deformation is that with Y-coordinate $Y = 10$ mm. Also, the minimum elastic deformation, as expected, is observed when the fixturing element is at the same level with the cutting tool. This translates into a fixturing strategy, where the fixture element traverses the plate in a straight line, parallel to the X-axis and at $Y = 10$ mm. In other words, the fixture element is first positioned at point $(X, Y) = (15, 10)$, it starts traversing the plate at the moment when the tool engages the workpiece, and follows the movement of the tool until it reaches the point $(X, Y) = (135, 10)$. The resulting anticipated deformation of the plate, at various points

on its surface, is shown in Figure 7.8. This diagram shows the deformation of the plate for the points that lie directly underneath the cutting tool, as it travels along the workiece.

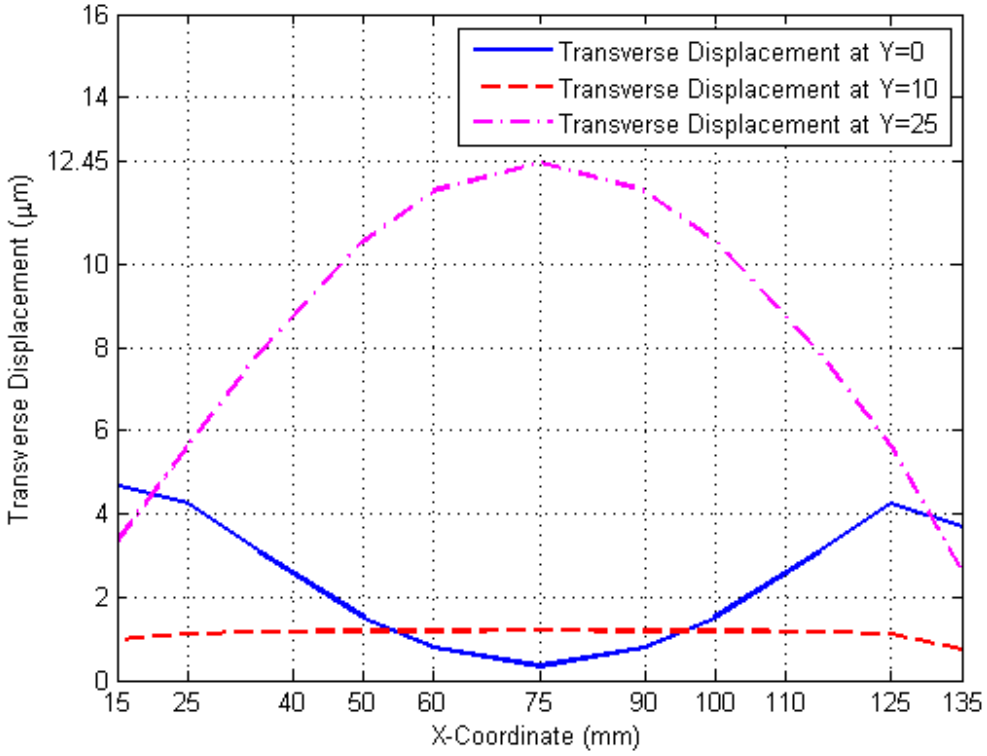

Figure 7.8: Transverse elastic deformation of the thin-plate workpiece, at various points on its surface, with $Y = 0$, $Y = 10$, and $Y = 25$, as the cutting tool traverses the plate, after the optimisation phase of the design methodology has been applied. The clamping element moves continuously, following exactly the movement, of the tool.

Finally, the resultant force on the fixture element, as it moves along the plate, is shown in Figure 7.9. From this figure it is deduced that this fixturing scenario satisfies by the largest margin the separation constraint, rendering it the most stable solution.

7.2.3.4 Short Discussion on the Results of the Methodology

From the theoretical results so far it can be concluded that the fully-active fixturing approach, even when passive fixture elements are used, can have a big impact in reducing the amplitude of vibration of a thin-walled low-rigidity workpiece. Unsurprisingly, the presence of the fixture element in the vicinity of the cutting tool, increases the local stiffness of the workpiece. This results in less deformation, which in turn means that the cutter is removing the desired amount of material, as the depth of cut is better maintained throughout the process. Also, the increased stiffness translates in reduced amplitudes of vibration. This leads to reduced deviations of the instantaneous depth-of-cut, which should improve the

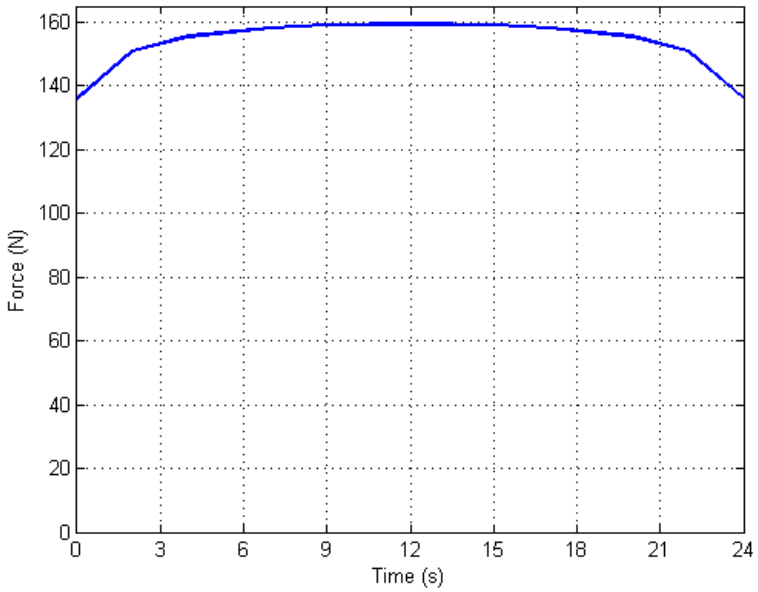

Figure 7.9: The resultant force on the fixture element as it traverses the plate, continuously following the motion of the tool.

finish of the surface of the workpiece.

The reduction in the maximum elastic deformation of the thin-plate workpiece, under the various fixturing scenarios that resulted from the application of the fully-active fixture design methodology (Chapter 6), are summarised in Table 7.2. This table clearly highlights the level of potential reduction of the displacement of the workpiece during a manufacturing process, which must translate into relevant improvement of the dimensional accuracy and surface finish of the end-result. This will be demonstrated by experimental results.

Table 7.2: Summary of maximum elastic deformation reduction, as the direct result of the application of the fully-active fixture design methodology on a thin-plate workpiece test case. A passive fixture element is assumed.

	Static Fixel at P1	Statc Fixel at P2	Moving Fixel Discrete	Moving Fixel Continuous
Max. Deformation (μm)	121.4	79.26	26.45	12.45
Reduction Compared to Static @ P1 case (%)	n/a	34.71	78.21	89.74
Reduction Compared to Static @ P2 case (%)	n/a	n/a	66.63	84.29

7.3 Experimental Set-Up

In order to verify the benefits from using the fully-active fixture methodology and further investigate the potential of fully-active fixtures, the results of the methodology are also applied experimentally. In order to achieve this, a fully-active fixture prototype was designed and built, as part of the activities for this research work. The concept of the fixture has already been presented in Chapter 3, Section 3.3.3. In this section, the hardware implementation of that concept for the purposes of experimental verification of the fully-active fixture design methodology, is described.

7.3.1 Fixture Hardware

The fully-active fixture that is used during experimentation (Figure 7.10) consists of a single transport component, with a pair of linear guides bearing a pair of runners. One runner moves along each linear guide. The linear guides are the SHW-21CR1-ZZ-C1+400LP model, supplied by THK [133]. They are made of martensite stainless steel for increased strength and rigidity. Each runner incorporates end seals, side seals, inner seals and metal scrapers. These protect the bearing mechanism inside from contaminants like swarf, and allow for trouble-free operation even when cutting fluids are used. The linear guides mounted on an in-house designed and manufactured Transport Component Base, which is machined out of high grade steel.

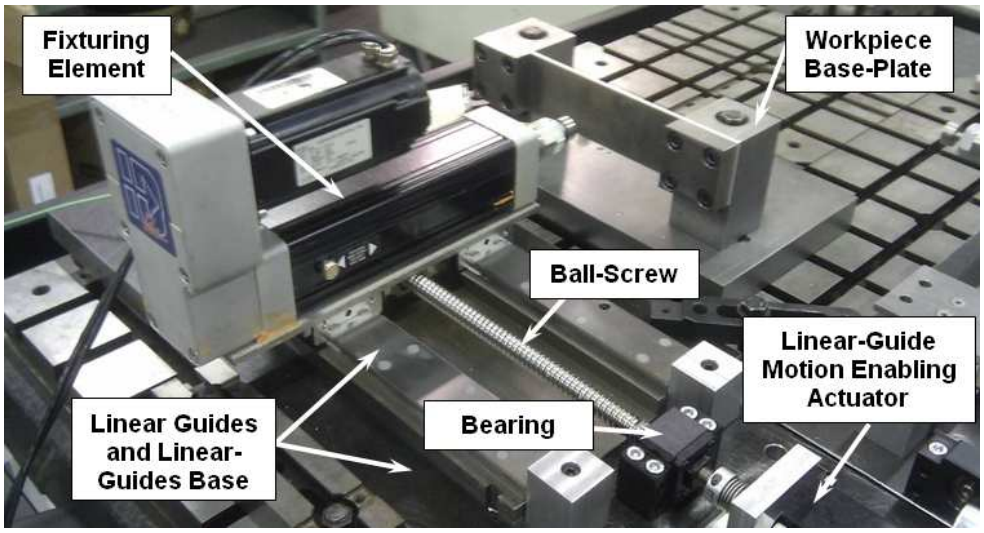

Figure 7.10: Picture of the fully-active fixture used for the experimental verification of the design methodology. The fixture comprises a single clamping element that can operate in both passive and active modes. The position of the element on the linear guides is controlled by the LGME actuator.

The two runners are bolted together through a custom-built runner base, also made of high grade steel. Below the runner base, and between the two linear guides, the nut of the ball screw is bolted. This formation positions the main axis of the ball screw main in the centreline between and parallel to the two linear guides, avoiding the generation of torque while driving the runner base. This torque would tend to twist the runner base around the direction normal to its surface and would reduce the performance of the fixture. The ball screw axis and nut is the BNT1404-3.6-WW-G0+530LC-J1K also sourced from THK [133]. The pitch of the ball screw is 4 mm.

Two ball bearings, one on each end of the ball screw, are used to secure the balls-screw axis in place. A THK-sourced BK10 bearing [133] is used on one side, providing fixed support. A THK BF10 bearing [133] is used on the other side, simply supporting the ball screw shaft. The bearings are bolted directly on the transport component base.

At one end of the ball screw, a Linear-Guide-Motion-Enabling (LGME) actuator is used. This is a Kollmorgen AKM23C Permanent Magnet Alternating Current (PMAC) motor, supplied by Danaher Motion [31]. This motor incorporates a rotary quadratic encoder, which is used to monitor the position of the runners on the linear guides. The ball screw shaft and the LGME actuator are connected by a flexible coupling. This caters for any minor misalignment between the motor axis and the ball screw axis. The LGME actuator is mounted on the transport component base via a custom-designed steel mounting plate.

On the runners, the fixture element is bolted. This is a linear electromechanical actuator EC2-BK23S-100-16B from Kollmorgen [32]. This actuator consists of four parts: a Permanent Magnet Alternating Current (PMAC) servomotor with integrated rotary encoder, a gearbox, a ball screw, and an extension shaft. The servomotor is positioned parallel to the ball screw shaft axis, and it is used to drive the gearbox, which in turn drives the ball screw axis. The nut of the ball screw transforms the rotational motion into linear motion of the extension shaft. At the free end of the extension shaft the fixturing tips, i.e. the parts of the fixture that are in direct contact with the surfaces of the workpiece, are mounted. Two types of tips can be used. One has the formation of a half-sphere with 5 mm diameter (Figure 7.11 (a)). The other is a roller, made of a cylindrical part with 10 mm diameter, that can rotate freely around its axis (Figure 7.11 (b)). Both of them are made of high strength steel. The first tip is used when a static or a discretely-moving fixture element strategy is deployed. The second one is used when a continuously-moving fixture element

strategy is applied.

(a) **(b)**

Figure 7.11: The two active element tips used for the fully active fixture. (a) A normal point-contact fixture tip that is used when the active elements maintain their position or change it in a discrete fashion. (b) A rolling point-contact tip enabling constant movement of the active elements with the need to disengage the workpiece surface.

The actuation direction of the element is perpendicular to the motion direction of the linear guides. This design grants the fully-active fixture with two degrees-of-freedom. Moreover, and because the integrated encoder is incremental, an inductive switch that acts as a reference point, is used to initialise the actuator at the start-up phase, or after a potential power failure.

Between the fixture tip and the free end of the extension shaft of the fixture element, a Kistler Type 9101A [70] piezoelectric (PZT) single component load washer is placed. This is used to monitor the reaction forces on the fixture element and ensure that the desired clamping force value is applied, when the element is used in passive mode. In active mode, the force sensor constitutes the force-feedback source that closes the control loop of the clamping element.

Finally, two Cherry DH3C-B1LA [147] micro-mechanical switches are used at either end of the linear guides. These mark the end-of-travel of the runners. They also serve as home switches, in order to initialise the axis-of-motion of the LGME actuator, as an incremental encoder is integrated in this actuator too.

All the above are assembled, directly or indirectly, on the transport component base. This rendered the entire experimental hardware a single module that could be easily added to or removed from the machine tool bed. The fully-active fixture module that was used during experimentation is shown in Figure 7.10.

7.3.2 Controlling Hardware

In order to operate the actuators of the experimental fully-active fixture, control the force it applies, the positions of the fixture-element body and tip, and utilise the information from the position (encoders) and force sensor, appropriate control hardware needs to be deployed. This includes a personal computer (PC), the controller of the fixture element (actuator), the controller of the LGME actuator, a motion control card, an amplifier and a controlling-hardware interface board.

Personal computer. A PC was utilised as the human-machine-interface point. The PC is equipped with a Pentium 4 processor, and is running on Microsoft Windows XP. The operation of the actuators was controlled through this PC. The controlling commands were issued through the National Instruments Measurement & Automation Explorer, a software which is supplied together with the motion control card [92]. Also, the PC hosts the motion controller card, which bears the PID controller that regulates the force of the active fixture element and the position of the of the runners on the linear guides. The motion controller is the hardware that issues the commands to the rest of the controlling hardware. More detail on the motion controller are given below.

Actuator controllers. Also known as drive units, the controllers of the actuators regulate and provide the power to the motor of the actuator, condition the voltage and current signals that control the speed and torque (force) of the actuator, supply the position feedback from the rotary encoders to other controlling hardware, and stop the operation of the actuator in case a safety issue occurs. The selected model for the controllers is the Kollmorgen S200VTS drive unit [35]. One controller per actuator was used.

Motion control PCI card. This is a peripheral component interconnect (PCI) local-bus card that is mounted inside the personal computer that acts as the overarching control unit of the fixture and the human-machine interface (HMI) point. It incorporates a trajectory generator and a digital controller per motion axis. The selected card was the National Instrument PCI-7344 motion control card [92]. This can control the motion or torque of up to 4 axis of motion (degrees-of-freedom). Two control axis of the motion control card are used during the experiments, one for controlling the motor of the fixture element, and one for controlling the LGME actuator.

Furthermore, the card incorporates analogue-to-digital (ADC) and digital-to-analogue (DAC) converters. The ADC is used to transform the analogue signal from the amplifier of the force sensor to a digital value that can be processed by the motion control card. The digital signal from the card is transformed to the analogue voltage that controls the actuator controllers, via the DAC. The card also caters for emergency stopping of motion. Finally, the parameters of the card can be adapted to the user needs, rendering it a very flexible piece of equipment, which is ideal for the experimental fixture.

Controlling hardware interface board. As the various controlling hardware was supplied from different manufacturers, one issue is the integration of all the equipment into one fully functional system. For this, the National Instruments UMI-7774 [94] was selected. This external board serves as a pass-through device for any signal that goes to and from the motion control card. Moreover, it provides visual signals to the user for the status of the system.

Amplifier. The amplifier is necessary in order to condition and amplify the signal from the piezoelectric load washer. It recognises the change in the charge of the sensor, due to compression and transforms it into a voltage. The latter is then amplified to a $0 \div 10$ V value. A Kistler Type 5017A charge amplifier [69] was used for this task. This amplifier can accommodate up to eight different sensors and can accept user adjustable settings.These include the Charge-to-Force ratio (Charge Sensitivity - C_s), the Force-to-Voltage ratio (Operating Range), the utilisation or not of a low-pass filter, and the cut-off frequency of the low-pass filter. The first two settings define the Charge-to-Voltage ratio, which is selected after proper calibration of the force sensor.

The control architecture of the experimental fixture is shown in Figure 7.12. Apart from the fixture and its controlling hardware, the experimental set-up also consists of two other main components: the workpiece and the workpiece baseplate. These were carefully designed to ensure that the boundary conditions assumed during the theoretical modelling of the fixture-workpiece system are also applied during experimentation.

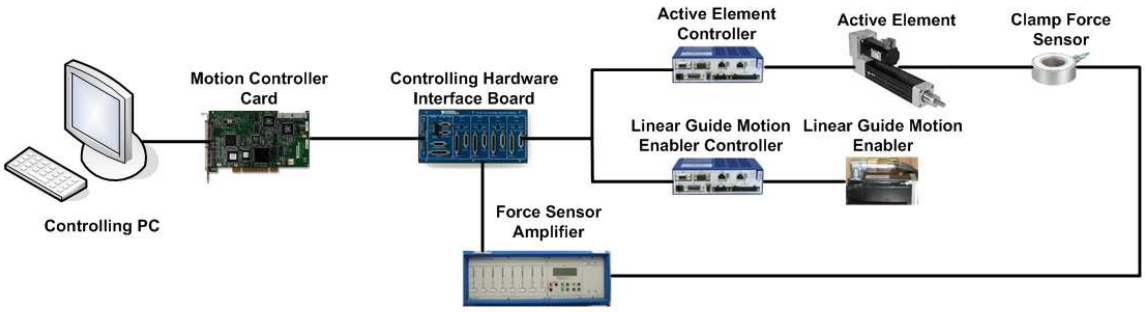

Figure 7.12: Schematic representation of the control architecture of the fully-active fixture used during the experiments.

7.3.3 Workpiece

In order to ensure that the workpiece, which is used for experimental purposes, is the same as the one that was modelled for the application of the fully-active fixture design methodology, its geometrical features had to be carefully selected. The workpiece must exhibit a free span of 150 mm, and be perfectly clamped, preventing any motion at the two shorter edges. For this, the workpiece that is shown in Figure 7.13 was adopted. This workpiece has a total span of 250 mm, allowing for a length of 50 mm on both ends to be used for clamping. The nominal thickness of the plate is $h = 0.125$ inches or $h = 3.17$ mm, and was determined by the availability of aluminium 7075-T6 alloy in sheet form. The properties of this material are shown in Table 7.1.

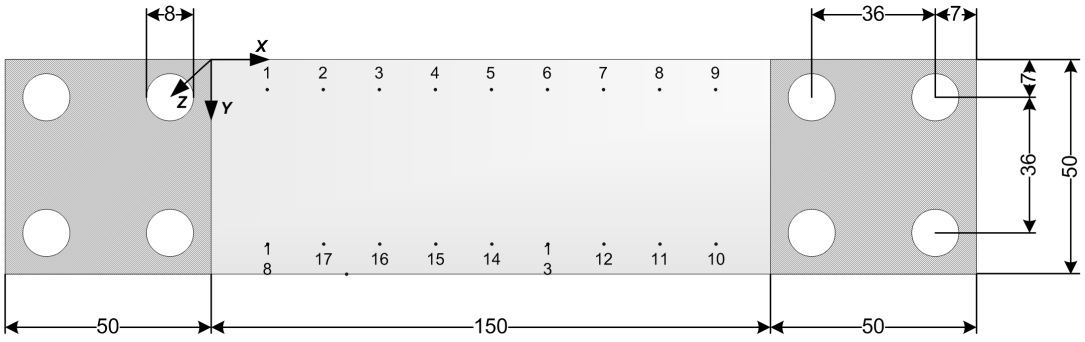

Figure 7.13: Drawing of the rectangular thin-plate workpiece. All dimensions are in mm. The thickness of the plate is $h = 3.17$ mm. The shaded areas with four through-holes designate the parts of the workpiece that are used for clamping.

The two clamping areas of the plate workpiece bear four through-holes each, arranged at the corners of an imaginary square. They are used as locating holes, but also to secure the plate in place. The pattern of these locating holes and the additional length for clamping were selected using experimental modal analysis, performed on a test workpiece. The modal analysis was performed in two stages. In the first one a 3 mm thick test workpiece made

of aluminium 6068 alloy was used. All other dimensions were the same as the ones shown in Figure 7.12. The reason for using this workpiece instead of the one used in the actual experiments, was that plates made of aluminium 7075-T6 alloy were not readily available when the experimental modal analysis was performed. The second stage was executed when the aluminium 7075-T6 plates became available. The experimental process that was followed during the two steps is explained below.

For the modal analysis on the aluminium 6068 plates, the test workpiece was clamped using the workpiece baseplate, which is described in detail in paragraph 7.3.4. This baseplate was first checked for its impact in the dynamic response of the workpiece. This was also achieved through experimental modal analysis (Section 7.3.4). The plate is positioned with a vertical orientation, so that the direction normal to its primary surface is parallel to the ground.

The modal testing was performed after mounting the workpiece baseplate securely on the T-slot baseplate of the prototype fixture, which was described in Chapter 3, Section 3.3.3. A PCB Piezotronics 086C03 instrumented impact hammer [105] with a PZT force sensor was used to excite the workpiece. A total of 18 points where marked on the structure, on the free span area of the plate. From these, 9 points were 10 mm below the top free edge and the other 9 were 10 mm above the lower free edge of the workpiece. In each of these sets, each point is 15 mm apart from its neighbouring points. All points are numbered in increasing order starting from the top leftmost corner with number 1 and, in a clockwise direction, finishing in the leftmost bottom corner with number 18 (Figure 7.13). A PCB Piezotronics 353B18 accelerometer [104] was mounted exactly behind the first point, at the leftmost top corner, using wax. The measurement axis of the accelerometer is normal to the primary surface of the plate and coincides with the direction of excitation from the impact hammer. This is also the same direction as that of the machining loads, as simulated in the thin-plate test case (Section 7.2). A 'Quattro' data-acquisition board from Data Physics Corporation [36] was used to sample the data from the accelerometer. The 'SignalCalc/ACE' software [36], also from Data Physics Corporation, was used to display and monitor the recorded data.

Using the instrumented hammer, a sharp impulsive impact was applied on each of the marked points on the surface of the plate. The impact direction was the same as the direction of measurement of the accelerometer. The response of the structure at the point

where the accelerometer was mounted was recorded. Three response measurements were taken for each point of excitation. The average of each set of the three measurements was used to obtain the frequency response of that point. The modal test was performed for a bandwidth of $0 \div 5000$ Hz.

The experimentally-obtained first five natural frequencies of the plate are compared to those from finite element- (FE-) based modal analysis and Kirchhoff plate theory. The FE modal analysis was performed on the workpiece shown in Figure 7.1 using Abaqus/CAE [127]. For this analysis 300 S4 finite elements [127], made of 341 nodes, were utilised. The nodes are separated by a distance of 5 mm. The selection of this finite element type is justified in detail in Chapter 4 and in Appendix B. The natural frequencies of the plate, as predicted by Kirchhoff plate theory, were obtained directly from literature [57]. The results from this comparison are presented in Table 7.3. The results indicate that the boundary conditions that are applied on the workpiece during the experimental process are the same as the simulated ones, since the measured and the FE-estimated natural frequencies present a maximum deviation of 2.69%. Figure 7.14 shows the frequency response of the test workpiece, when excited at the point, behind which the accelerometer was mounted, i.e. point 1 (Figure 7.13). This point is often referred to as drive point.

Table 7.3: The first five natural frequencies of the thin-plate aluminium 6068 workpiece extracted using different methods. Experimental and FE-based results are compared.

Mode	Nat. Freq. FEA (Hz)	Nat. Freq. Plate Theory (Hz)	Nat. Freq. Experimental (Hz)	Diff. FEA vs Exp. (%)
1	718.32	715.32	728.51	1.42
2	1508.2	1527.0	1519.7	0.76
3	1973.3	1970.7	1920.1	-2.69
4	3264.2	3309.0	3312.8	1.49
5	3865.0	3876.6	3961.8	2.48

The mode shapes, that correspond to each of the measured frequencies, were also compared to those that were estimated through FEA. This was to ensure that the compared frequencies belong to the same mode shapes. For the sake of brevity graphic comparison of the mode-shapes is not presented here. It shall suffice to mention that there is a full match between the mode shapes of the compared frequencies.

Based on the in-depth modal analysis on the aluminium 6068 workpiece, the analysis performed on the aluminium 7075-T6 plates with 3.17 mm thickness was brief, with the

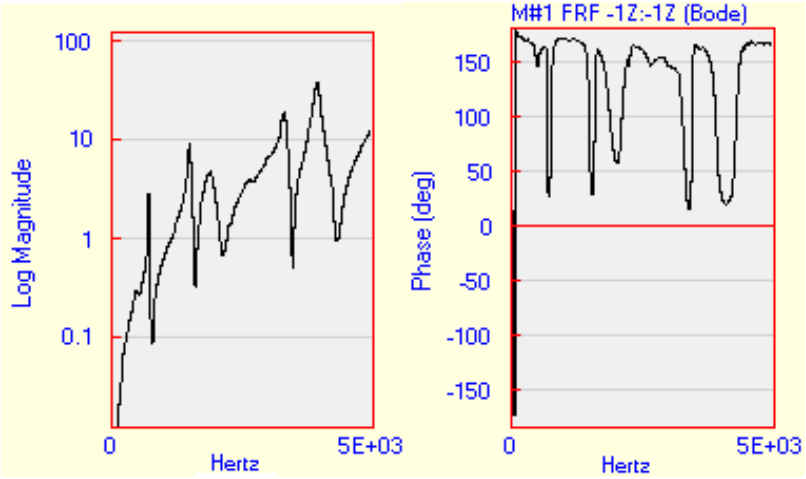

(a) **(b)**

Figure 7.14: The frequency response plot of the aluminium 6068 test workpiece. (a) Response magnitude in dB. (b) Response phase in degrees.

purpose of extracting the natural frequencies of the plate. The procedure included the same set-up as the one described previously. However, this time, the workpiece was excited only at one random point. Three measurements were obtained, the average of which was used to calculate the first three natural frequencies of the plate. These were then compared to the ones predicted through FEA. The results are shown in Table 7.4. The similarity between the predicted and measured natural frequencies for this workpiece too, prove beyond any doubt that the simulated boundary conditions are applied accurately in the experimental set-up.

Table 7.4: The first three natural frequencies of the thin-plate aluminium 7075-T6 workpiece extracted using FE-based calculations and experimental modal analysis.

Mode	Nat. Freq. FEA (Hz)	Nat. Freq. Experimental (Hz)	Diff. (%)
1	748.19	745.31	-0.39
2	1570.0	1531.25	-2.53
3	2065.3	2021.88	-2.15

7.3.4 Workpiece Baseplate

The workpiece baseplate, shown in Figure 7.15 with the workpiece clamped, is another critical component for the experimental procedure. This is the part that provides the desired boundary conditions to the thin-plate workpiece. It is also used to locate the workpiece in relation to the transport component of the fully-active fixture. The workpiece

baseplate is mounted so that the larger edges of the plate are parallel to the axis of motion of the linear guides.

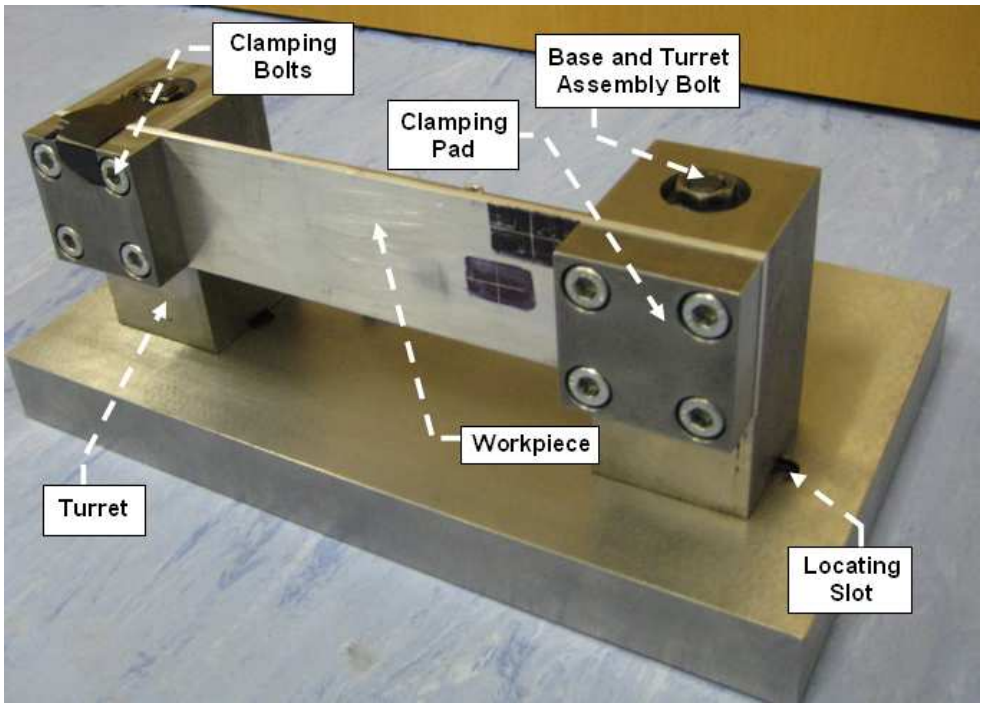

Figure 7.15: The workpiece baseplate with the thin-plate workpiece. Some of the most important features are highlighted in this photograph.

The workpiece baseplate comprises five pieces: a base, two turrets and two clamping pads. The base is a rectangular block with 4 through-holes. Two of them are used to locate and bolt it to the fixture baseplate. The other two are used to bolt the turrets on the base.

Each turret has eight threaded holes on one of its surfaces normal to the fixture baseplate. These are divided into two sets of four holes. One set is used to locate the plate at a height, where the fixture element can come in contact with the points on the plate surface with Y-coordinate $Y = 25$ mm (see Figure 7.1). The other set is used to locate the plate in a height, where the fixture element can come in contact with the points on the plate surface with Y-coordinate $Y = 10$ mm. This is to accommodate for the lack of motion of the experimental fixture along the Y-direction. Each set of four holes mimics the pattern of the locating/clamping holes on the thin-plate workpiece (Figure 7.13) and the clamping pads. This allows for proper clamping of the plate. The direction of all holes is towards the transport component and the fixture element.

The turrets also bear a through-hole that permits assembly with the base of the workpiece baseplate. At the point of interface between the base and the turrets, each part bears a 2 mm deep slot, which, in combination with a rectangular wedge, assists in accurately

locating the turrets. This design ensures that the surfaces of the turrets, which are in contact with the workpiece, are perfectly parallel. Moreover, the turrets are carefully placed so that their inner surfaces are exactly 150 mm apart. This affects the free span of the plate workpiece. Finally, the width of each turret is 50 mm to ensure that the entire 50 mm wide clamping area on the workpiece is properly utilised.

The clamping pads are a square block of stainless steel. The clamping surface has an area of 50×50 mm^2. They also have 4 through-holes with the same formation as the ones on the workpiece and the threaded holes on the turrets (see Figure 7.15). The clamping pads are bolted on top of the plate and the turrets to clamp the workpiece securely in its place.

According to Ewins [47], performing modal testing on a workpiece is straightforward only in the case when no boundary conditions are applied to it. In all other cases, like the one dealt with here, it is imperative to ensure that the apparatus that imposes the boundary conditions on the workpiece does not affect its dynamic response. For this reason, modal analysis was performed on the workpiece baseplate too. The measurement direction is the same as the principal direction of the machining loads, i.e. the traverse direction of the plate. The workpiece baseplate is then excited at one point on each turret and in the same direction as the measured one, using the instrumented impact hammer. The frequency response functions for the two excitation points are obtained. These are presented in Figure 7.16. These frequency response diagrams, when compared to Figure 7.14, reveal that the amplitude of the response of the workpiece baseplate is more than an order of magnitude less than that of the thin-plate workpiece at frequencies in the range of $0 \div 5000$ Hz. This satisfies the criterion set by Ewins [47] and ensures that the workpiece baseplate does not affect the dynamic response of the workpiece. Please note that the modal analysis of the workpiece baseplate must be and was performed prior to that of the workpiece itself.

7.4 Experimental Procedure

The previously described workpiece, mounted on the workpiece baseplate, and the fully-active fixture, comprising a single transport component, were securely mounted on the stable bed of a Hurco VM1 machining centre [65]. The workpiece baseplate and the transport component were positioned in such a way, that the normal to the surface of the plate is

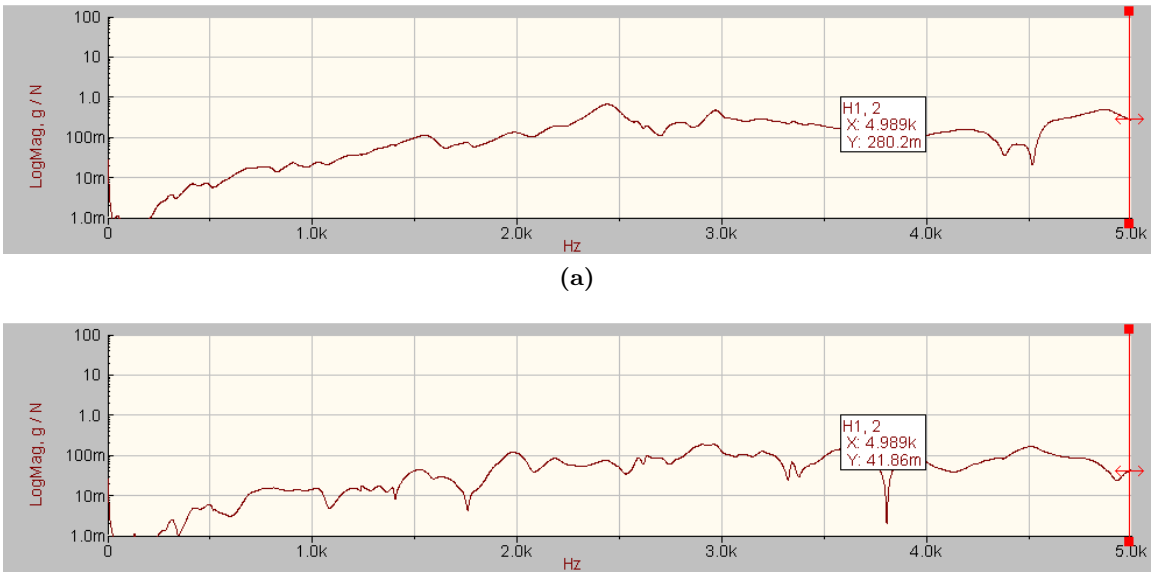

Figure 7.16: The frequency response of the workpiece baseplate. (a) Response of the baseplate when excited at the turret with the accelerometer. (b) Response of the baseplate when excited at the turret without the accelerometer.

parallel to the axis of motion of the fixture element. Furthermore, the plate was positioned vertically. A 4-flute EMH-4WL end-mill cutter from Swiss-Tech [29] was selected as the cutting tool. This cutter has a diameter of 20 mm, a flute length of 75 mm, and it is made of high speed steel with 8% cobalt. Also, the cutter is free from any type of coatings. The set-up with which the experiments were executed is presented in Figure 7.17. The figure shows the bench with the controlling hardware and the machine tool. The fixture and the workpiece baseplate, when mounted inside the machine tool are shown in Figure 7.18.

A total of thirty thin-plates was used during the experiments. A cut of 120 mm was performed on each plate. The cutting tool engaged the workpiece at $X = 15$ mm and disengaged the workpiece at $X = 135$ mm. In all cases, the same cutting parameters were used. These are summarised in Table 7.5.

Table 7.5: Cutting process parameters.

Parameters	
Spindle Speed:	3000 rpm
Direction of Rotation:	Forward - Climb Milling
Radial Depth of Cut:	0.5 mm
Axial Depth of Cut:	25 mm
Feed Rate:	300 mm/min
Cutting Length:	120 mm
Cutting Fluid:	Oil

Figure 7.17: A view of the experimental set-up and equipment. The controlling hardware arrangement is shown positioned next to the machine tool.

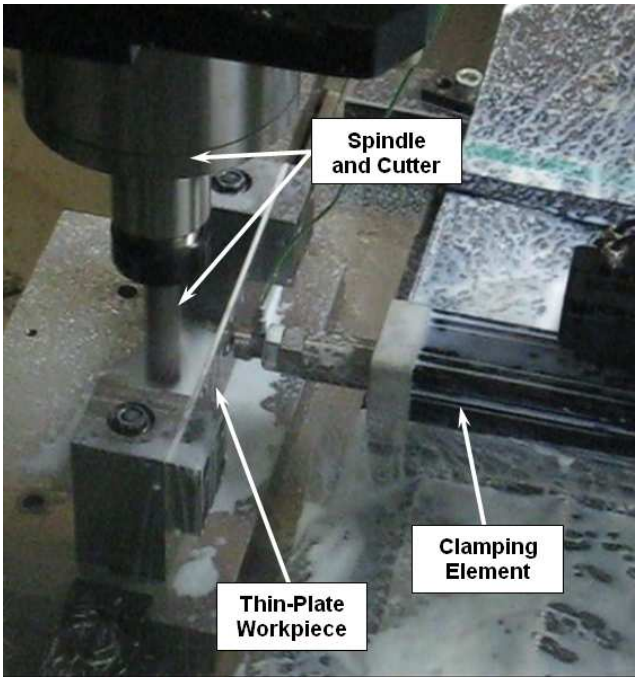

Figure 7.18: The fully-active fixture with one transport component and one active clamp, positioned on the bed of the Hurco VM1 machining centre.

The plates were made of Aluminium 7075-T6 alloy with the dimensions shown in Figure 7.13. Six different fixturing scenarios were used during the experiments. For every scenario five plate were used. The fixturing parameters of each scenario are shown in Table 7.6. The parameters of the first four fixturing scenarios were selected based on results from the application of the fully-active fixture design methodology on the thin-plate test case, which was presented in Section 7.2. These involve a passive element that applies a constant

clamping force of 20 N. The four scenarios correspond to the four fixturing scenarios that were presented during the application of the fixture design methodology on the thin plate test case. These include the initial solution, the static and passive clamping element, the discretely-moving passive clamping element, and the continuously-moving passive clamping element.

Table 7.6: The parameters of the fixturing scenarios used during the experiments.

Case No.	Fixture Strategy	Coordinates of Clamp Positions (mm)	Clamping Force	Active Clamping
1	Static Clamp	$(X, Y) = (75, 25)$	20 N	No
2	Static Clamp	$(X, Y) = (75, 10)$	20 N	No
3	Moving Clamp - Discrete	$(X, Y) = (25, 10)$ $(X, Y) = (50, 10)$ $(X, Y) = (75, 10)$ $(X, Y)) = (100, 10)$ $(X, Y) = (125, 10)$	20 N	No
4	Moving Clamp - Continuous	$X \in [15, 135]$	20 N	No
5	Static Clamp	$(X, Y) = (75, 10)$	20 N	Yes
6	Moving Clamp - Continuous	$X \in [15, 135]$	20 N	Yes

The last two scenarios, involve an active fixture element that is called to maintain a camping force of 20 N. At first, the active element is statically-positioned on point P2 (see Figure 7.1). in the last scenario the active element is moving continuously following the path of the continuously-moving passive element, as resulted from the theoretical application of the methodology. All scenarios and the results they produce will be discussed in Section 7.5 of this chapter.

A total of eight randomly selected thin-plate workpiece samples had their surface roughness measured prior to the execution of the experiments. This was to confirm the uniformity of the surface quality on all samples and to ensure that the original surface quality would not affect the final result. If the thin-plate workpieces present a rough surface with profile characterised by intense peaks and valleys, then, as the tool passes over this surface, the instantaneous depth-of-cut changes. As a result, the resulting reaction force on the workpiece has a time-varying amplitude, which leads to unwanted vibration. This is known as regenerative vibration or chatter [26, 128], and could affect the experimental result if not minimised.

The surface roughness measurement was performed on a Talysurf CLA 1000 by Taylor Hobson [132], which was housed in a temperature-controlled room. The measurement equipment utilises an inductive sensor and a stylus with a tip of 2 μm radius and 90^{o} helix angle. The resolution of the sensor is 40 nm.

The measurement process is as follows. As the stylus is 'dragged' along the length of the plate in a straight-line path, the peaks and valleys on the measured surface force the stylus to move upwards and downwards. An inductive sensor records the variations in the position of the stylus, thus regenerating the surface profile. The focus was placed on three surface roughness variables, namely the average surface roughness R_a, the maximum profile height R_t, and the Japanese Industrial Standard (JIS) Ten Point Average Roughness ($R_{z\text{JIS}}$). The average roughness is an arithmetic average of the absolute measured values. The maximum profile height is the height difference between the lowest measured valley and the highest measured peak. Finally, the JIS ten point average roughness is calculated by averaging the five highest peaks and the five lowest valleys from the measured profile. There are a lot more measures of the roughness of a surface, however, the proposed three are more than enough to provide a solid indication of the condition of the thin-plate surface after machining.

The surface measurement equipment was calibrated at the beginning of every measurement day using a sample with a known average surface roughness value of $R_a = 6$ μm. After calibration, and for measuring the surface quality of the thin-plate samples before machining, lengths of 80 mm ($X = 35$ to $X = 115$ mm) at $Y = 5$, $Y = 10$, $Y = 15$ and $Y = 20$ mm (see Figure 7.1) of the thin plates were sampled using the stylus to obtain the surface quality values of interest. A typical measurement profile is shown in Figure 7.19.

When measuring the resultant surface of the workpieces after the machining process has taken place, lengths of 97 mm ($X = 26.5$ to $X = 123.5$ mm) at $Y = 5$, $Y = 10$, $Y = 15$ and $Y = 20$ mm were measured. The results from these measurements are presented below.

The average surface roughness of the sample shown in Figure 7.19 is $R_a = 0.052$ μm, the profile height is $R_t = 2.54$ μm, and the JIS ten point average is $R_{z\text{JIS}} = 0.40$ μm. These values, in conjunction with the minimal deviation from flatness, as depicted in Figure 7.19, indicate that the original state of the workpiece will not affect the outcome of the experimental process, as the surface characteristics are smooth, hence drastically reducing the appearance of regenerative vibration.

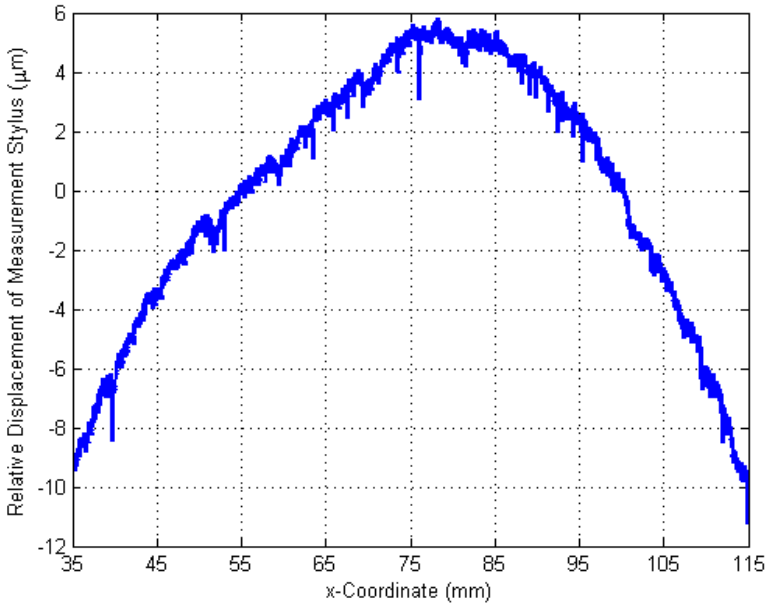

Figure 7.19: A typical surface profile of the aluminium 7075-T6 thin-plate workpieces. Obtained at $Y = 5$ mm and from $X = 35$ mm to $X = 115$ mm on the surface of a thin-plate workpiece that is to be machined.

7.5 Results

Following the procedure described above, the results shown in Table 7.7 were obtained from the experiments. The results in this table are analysed in more detail hereafter.

7.5.1 Passive and Static Clamp at P1 (X, Y)=(75,25)

For this fixturing strategy, the point contact fixturing tip was used. The fixture element was accurately positioned at point P1 through careful measurement using calibrated measurement blocks. The shaft of the actuator, which plays the role of the clamp, was extended until a clamping force of 20 N was recorded. After one pass of the cutting tool, the resulting surface was measured for roughness, as described above. A typical profile from the results of the measurements are shown in Figures 7.20 and 7.21. Results from all the measurements are summarised in Table 7.7. For the workpiece presented here, the surface roughness characteristics are $R_a = 2.459$ μm, $R_t = 39.669$ μm, and $R_{z\text{JIS}} = 9.090$ μm. These are highlighted in bold in Table 7.7 and correspond to plate 5.

Table 7.7: Detailed results from the surface characteristics analysis. Bold letters and numbers indicate measurement results that were obtained from machined plates, the profile of which is also presented graphically.

Plate No.	Fixture Strategy	R_a (μm)	R_t (μm)	$R_{z\text{JIS}}$ (μm)
1		3.235	33.951	11.902
2	Static Passive Clamp	4.221	49.608	15.217
3	at P1	3.499	35.815	23.693
4	$(X, Y) = (75, 25)$	3.696	37.448	13.203
5		**2.459**	**39.669**	**9.090**
6		2.483	46.532	9.466
7	Static Passive Clamp	2.606	30.455	9.690
8	at P2	**2.472**	**34.693**	**9.277**
9	$(X, Y) = (75, 10)$	2.346	21.328	8.9359
10		2.494	31.968	9.448
11		0.645	11.969	2.424
12	Moving Passive Clamp	0.894	12.833	3.309
13	Discrete	**0.957**	**11.673**	**3.482**
14	Motion	0.822	10.513	3.122
15		0.819	10.2124	3.035
16		0.531	5.990	2.076
17	Moving Passive Clamp	0.421	5.879	1.663
18	Motion	0.352	4.453	1.382
19	Continuous	**0.156**	**2.260**	**0.704**
20		0.117	1.347	0.561
21	Static Active Clamp	0.159	8.166	0.723
22	at P2	0.156	4.395	0.723
23	$(X, Y) = (75, 10)$	0.179	6.640	0.754
24		**0.202**	**7.806**	**0.839**
25	Moving Active Clamp	0.131	5.843	0.625
26	Continuous	0.150	5.980	0.677
27	Motion	**0.150**	**5.980**	**0.630**
28		0.166	7.794	0.732

7.5.2 Passive and Static Clamp at P2 (X, Y)=(75,10)

The same process, as the one described for the static clamp at point P1, was used for this set of experiments too. The plate was repositioned to the second set of locating holes on the turrets of the workpiece baseplate. In this way, the clamp could be deployed at the desired Y-coordinate on the plate. The position of the clamping element along the X-axis was confirmed by calibrated measurement blocks. A representative surface profile, after one pass of the cutting tool is shown through Figures 7.22 and 7.23. For this profile the average surface roughness, surface profile and JIS ten point average roughness are, respectively, $R_a = 2.472$ μm, $R_t = 34.693$ μm, and $R_{z\text{JIS}} = 9.277$ μm. These are highlighted in bold in

Table 7.7 and correspond to the results shown for plate 8. The results from the measurement of the surface profile of the all the plates from this set of experiments is shown in the same table.

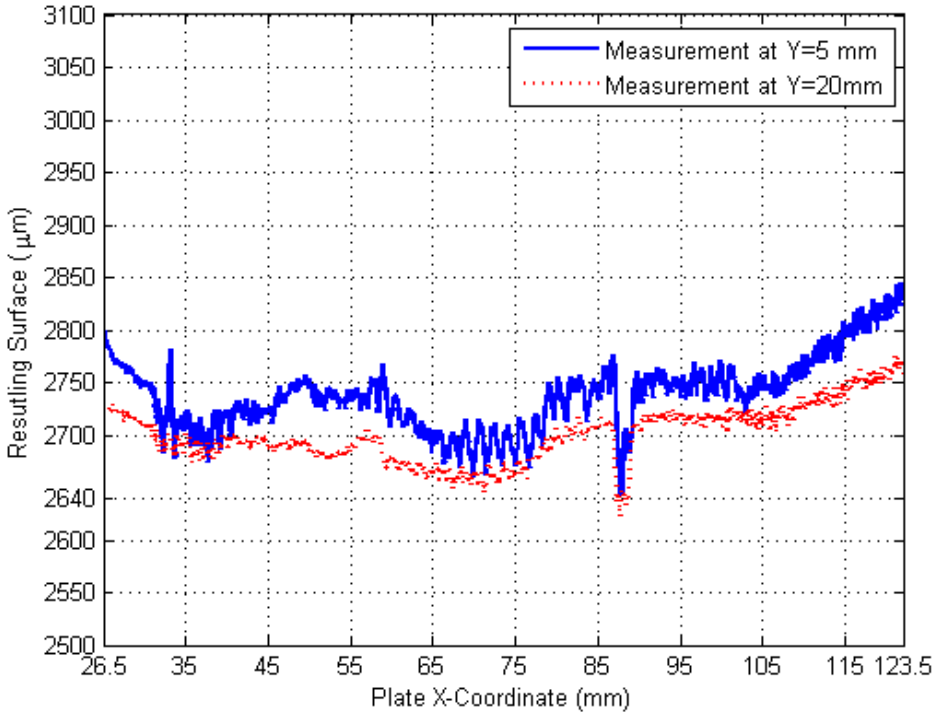

Figure 7.20: Surface measurement results for the fixturing scenario, where a passive clamp (F_c = 20 N) is constantly positioned at P1 with coordinates $(X, Y) = (75, 25)$, as shown in Figure 7.1.

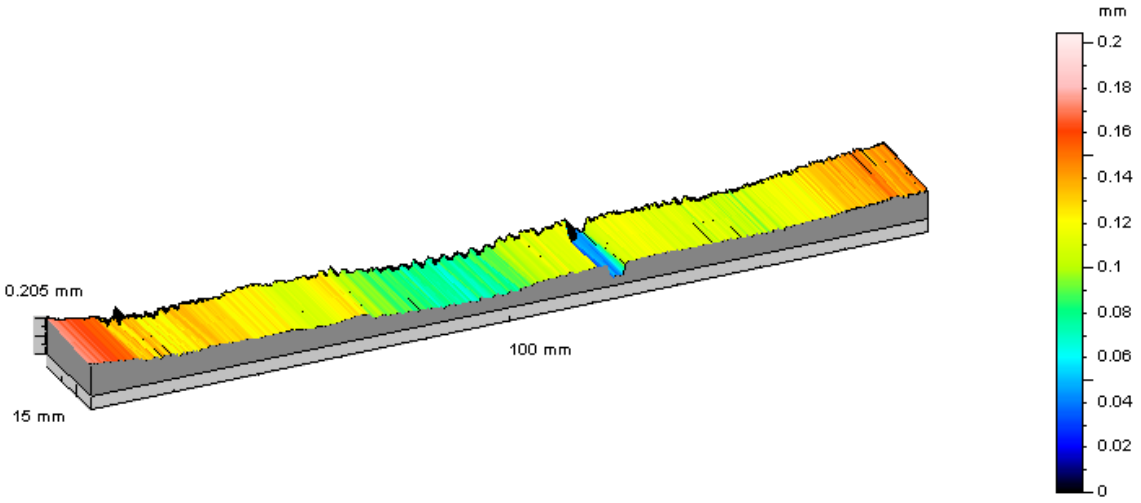

Figure 7.21: Three-dimensional representation of the measured surface profile of a thin-walled workpiece machined under the fixturing scenario where a passive clamp (F_c = 20) N is positioned at P1 with coordinates $(X, Y) = (75, 25)$.

The motion of the cutting tool is also discrete. After the clamp is positioned at point P3, the tool engages the plate at X = 15 mm and moves until X = 32.05 mm. This is

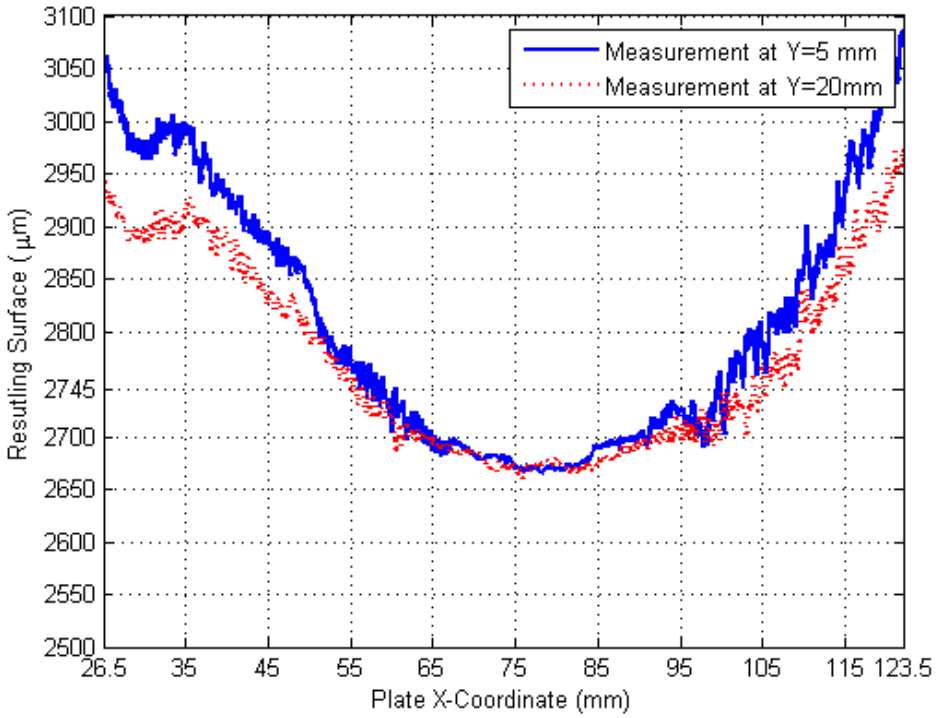

Figure 7.22: Surface measurement results for the fixturing scenario, where a passive clamp (F_c = 20 N) is constantly positioned at P2 with coordinates $(X, Y) = (75, 10)$. This is the point that was indicated after the application of the methodology on the thin-plate test case, and when a static fixture layout was assumed.

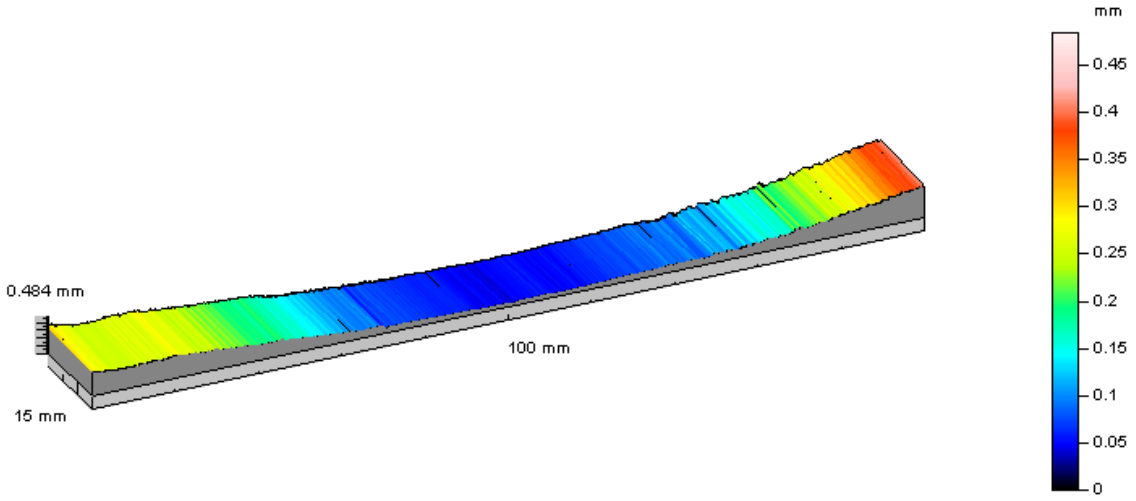

Figure 7.23: Three-dimensional representation of the measured surface profile of a thin-plate workpiece machined under the fixturing scenario, where the passive clamp (F_c = 20) N is positioned at P2 $(X, Y) = (75, 10)$.

the travel length that was suggested by the fixture methodology. At this point, the tool disengages the plate. Then the clamping element is retracted from point P3, moves above point P4, and then contacts the plate at P4. The tool then re-engages with the plate exactly where it stopped cutting, i.e. at $X = 32.05$ mm, and continues cutting until it reaches the point where $X = 60.93$ mm. The tool then disengages from the workpiece and the fixture

element is re-positioned to the next clamping point. The same process is repeated until the tool scans the entire surface area, from which material is to be removed, and the fixture element has pass through all previously-mentioned points. The cutting steps that the tool performs are summarised in Table 7.8.

A representative surface profile, this set of experiments is presented through Figures 7.24 and 7.25. The average surface roughness, surface profile and JIS ten point average roughness of the depicted profile are, respectively, $R_a = 0.957$ μm, $R_t = 11.673$ μm, and $R_{z\text{JIS}} = 3.482$ μm. These are highlighted in bold in Table 7.7 and correspond to the results shown for plate 13. The results from all the surface profiles from this set of experiments is shown in the same table.

Table 7.8: Cutting process parameters.

Fixture-Workpiece Contact Points vs. Cutting Steps		
Sequence	Contact Point (mm)	Cutting Length (mm)
1	P3 $(X, Y) = (25, 10)$	$X = 15$ to $X = 32.05$
2	P4 $(X, Y) = (50, 10)$	$X = 32.05$ to $X = 60.93$
3	P2 $(X, Y) = (75, 10)$	$X = 60.93$ to $X = 89.07$
4	P5 $(X, Y) = (100, 10)$	$X = 89.07$ to $X = 117.96$
5	P6 $(X, Y) = (125, 10)$	$X = 117.96$ to $X = 135$

7.5.3 Passive and Moving Clamp - Continuous Motion

For this set of experiments the rolling point-fixturing tip was used (Figure 7.11 (b)). At the beginning of the process the tip was positioned accurately at the point with coordinates $(X, Y) = (15, 10)$, and the actuator was extended to the point where a 20 N of clamping force was applied. Then, as soon as the tool engaged with the workpiece, the fixture element was commanded to move at exactly the same speed as that of the tool (feed rate). A representative surface profile, created from the machining of thin-plate workpieces, using the previously described fixturing method, is presented through Figures 7.26 and 7.27. The average surface roughness, surface profile and JIS ten point average roughness of the depicted profile are $R_a = 0.156$ μm, $R_t = 2.260$ μm, and $R_{z\text{JIS}} = 0.704$ μm. Table 7.7 summarises the results from the other surface profile measurements from this set of experiments. The results from the surface profile shown here (plate 19), through Figures 7.26 and 7.27, are highlighted in bold.

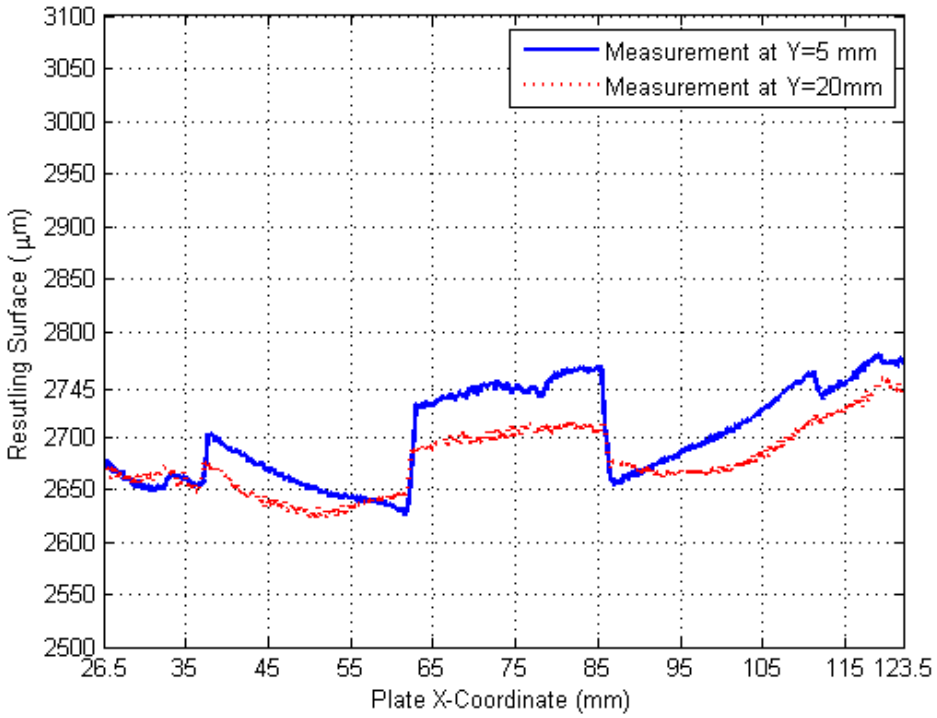

Figure 7.24: Surface measurement results for the fixturing scenario, where a passive clamp (F_c = 20 N) is moving along the surface of the plate in a discrete manner occupying five points, as shown in Table 7.8.

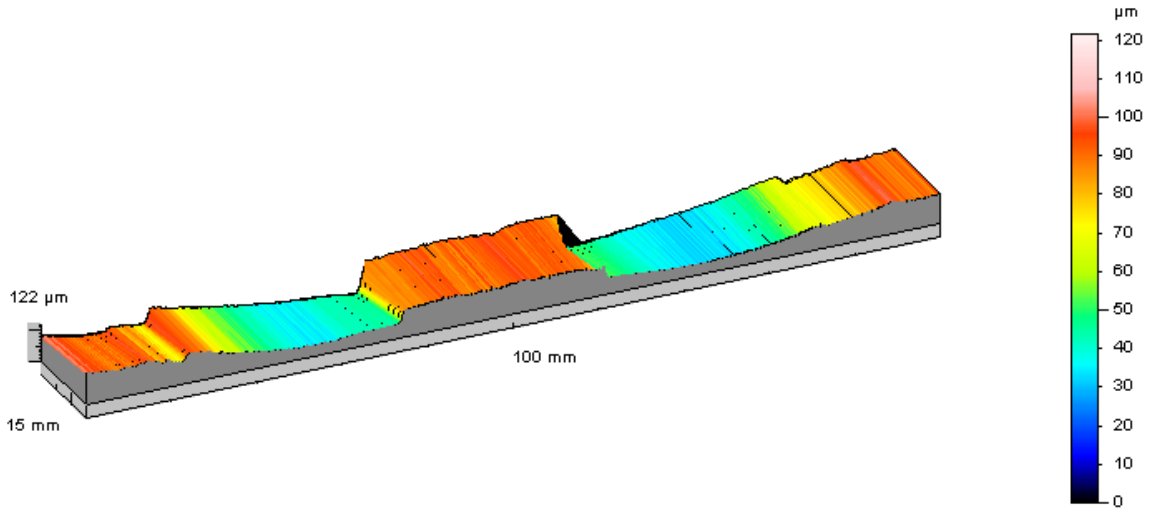

Figure 7.25: Three-dimensional representation of the measured surface profile of a thin-plate workpiece machined under the fixturing scenario, where the passive clamp ($F_c = 20$) N moves in a discrete manner, occupying the five points that were suggested by the fully-active fixture design methodology (see Table 7.8).

7.5.4 Active and Static Clamp at P2 (X, Y)=(75,10)

For these experiments, the normal static fixture tip was used (Figure 7.11 (a)). At the beginning of the process, the tip was positioned accurately at point P1 $(X, Y) = (75, 10)$. After coming in contact with the plate, the system was adjusted to operate using the direct

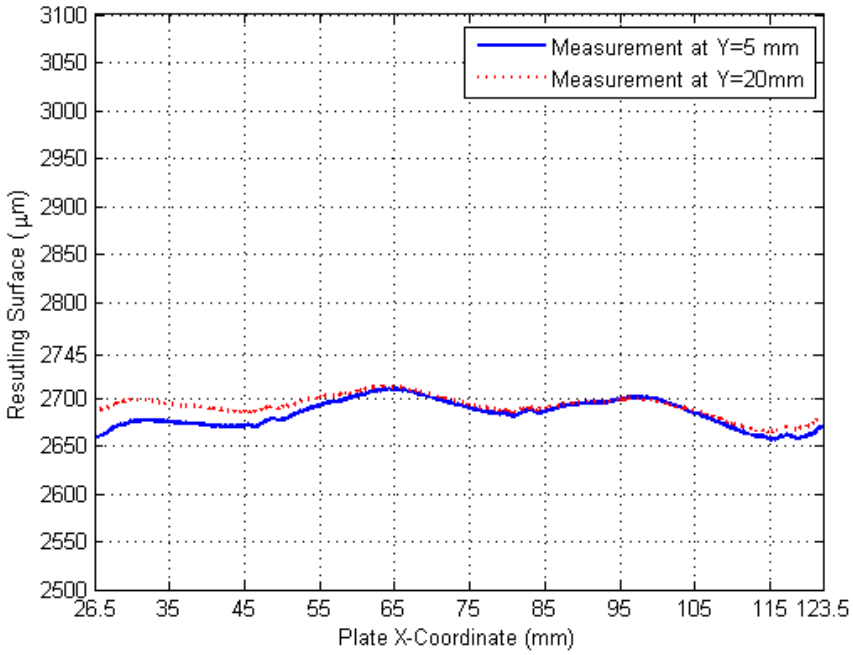

Figure 7.26: Surface measurement results for the fixturing scenario, where a passive clamp (F_c = 20 N) is moving along with the cutting tool. The path of the fixture element is a straight line with Y-coordinate $Y = 10$ mm.

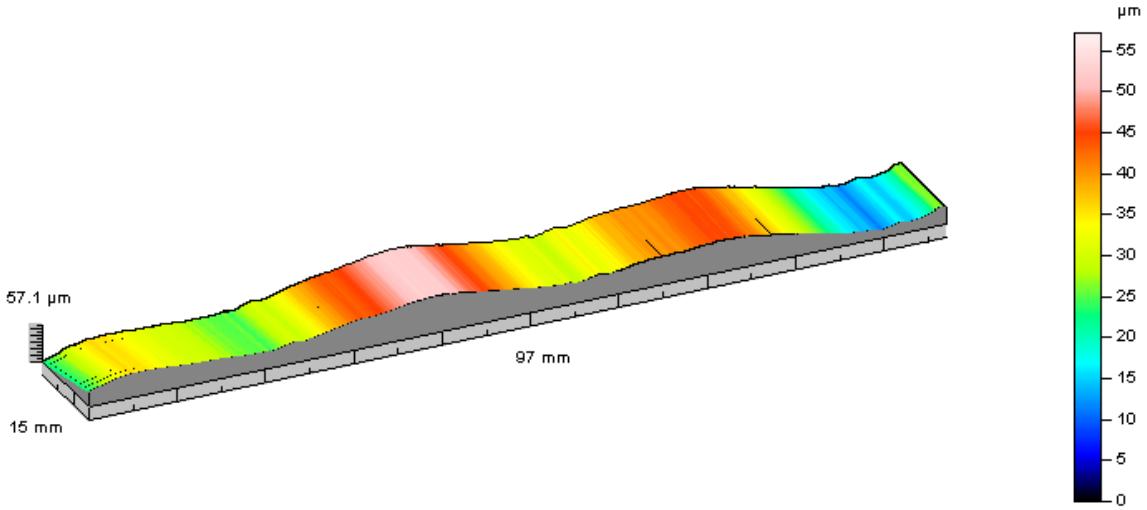

Figure 7.27: Three dimensional representation of the measured surface profile of a thin-plate workpiece machined under the fixturing scenario, where the passive clamp (F_c = 20) N is continuously moving, following the motion of tool.

force/torque control algorithm, described in Section 5.3.2.2 of Chapter 5. The PI controller, with the parameters described in Section 5.3.3.1, was used. In detail, the controller has a proportional gain of $K_p = 11$ and an integrative gain of $K_I = 86$. The fixture element then applied a clamping force of 20 N. Enough time was given afterwards to allow any transient effects from the actuation of the clamping element to wear out. The tool then was brought in contact with the workpiece to machine the desired length of 120 mm.

The characteristics of a representative surface profile, resulting from this set of experiments, is presented through Figures 7.28 and 7.29. The results from the measurements are summarised in Table 7.7. It should be noted that for this fixturing scenario, only four out of the five machined plates were measured. The results from the profile depicted in the aforementioned figures are $R_a = 0.202$ μm, $R_t = 7.806$ μm, and $R_{z\text{JIS}} = 0.839$ μm, and they correspond to plate 24.

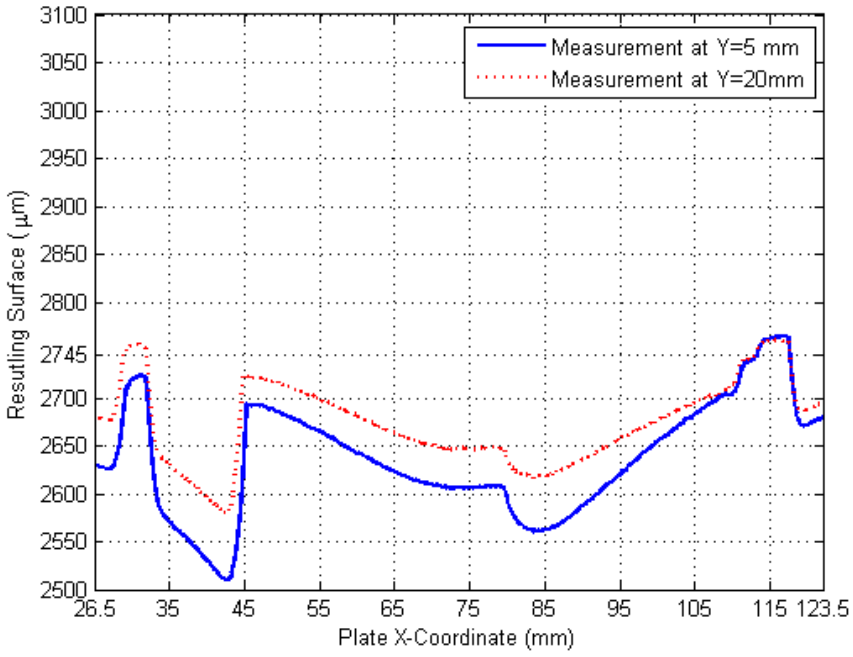

Figure 7.28: Surface measurement results for the fixturing scenario, where an active clamp (F_c = 20 N) is constantly positioned at P2 with coordinates $(X, Y) = (75, 10)$.

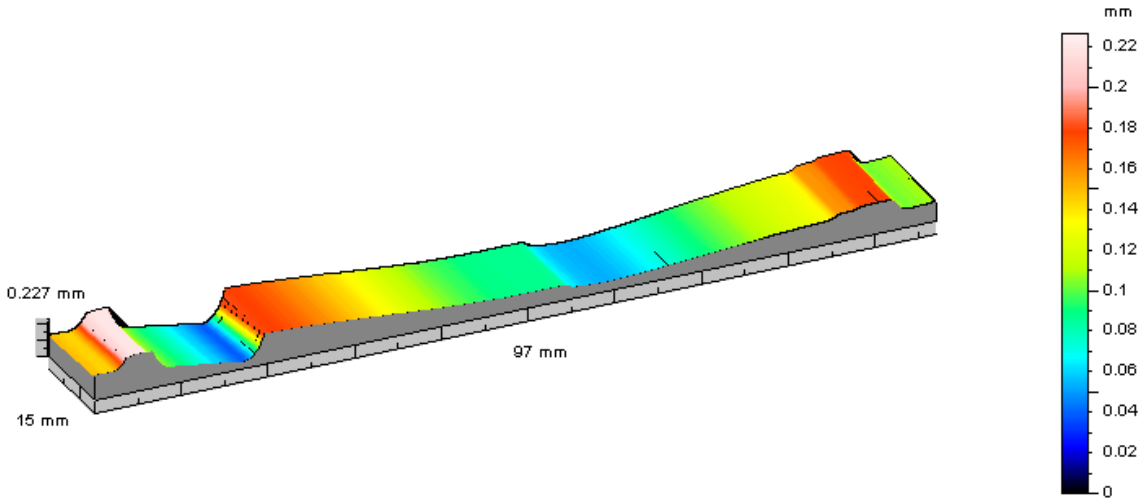

Figure 7.29: Three-dimensional representation of the measured surface profile of a thin-plate workpiece machined under the fixturing scenario, where an active clamp (F_c = 20) N is positioned at P2 $(X, Y) = (75, 10)$.

7.5.5 Active and Moving Clamp - Continuous Motion

This fixturing scenario was also executed purely experimentally. The exact process as that in the passive and continuously moving clamping element fixturing scenario (Section 7.5.3) was followed in these experiments. The only difference is that the fixture element was brought in contact with the plate at the point with coordinates $(X, Y) = (15, 10)$ and then the system was switched to force control mode, utilising the direct force/torque control algorithm, and a force of 20 N was then applied. The movement of the clamp along the workpiece was initiated manually in this case too. The characteristics of a representative resulting surface from this set of experiments is shown in Figures 7.30 and 7.31. The results from the measurements are summarised in Table 7.7. It is noted that for this fixturing scenario, only four out of the five machined plates were measured. This is for the sake of brevity, as small deviations in the surface characteristics were observed. The results from the profile depicted in the aforementioned figures are $R_a = 0.150$ μm, $R_t = 5.980$ μm, and $R_{z\text{JIS}} = 0.630$ μm, and they correspond to plate 27 on Table 7.7.

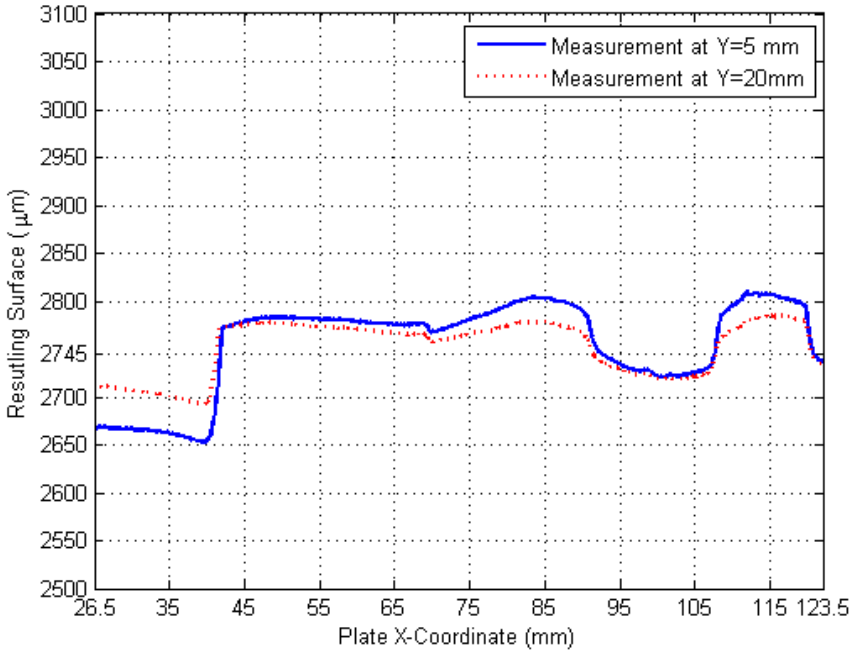

Figure 7.30: Surface measurement results for the fixturing scenario, where an active clamp (F_c = 20 N) is moving along with the cutting tool. The path of the fixture element is a straight line with coordinate $Y = 10$ mm.

Table 7.9 shows the reduction in the surface roughness values, which were achieved experimentally, following the results from the application of the fully-active fixture design methodology on the thin-plate test case. To produce the presented statistical results, the

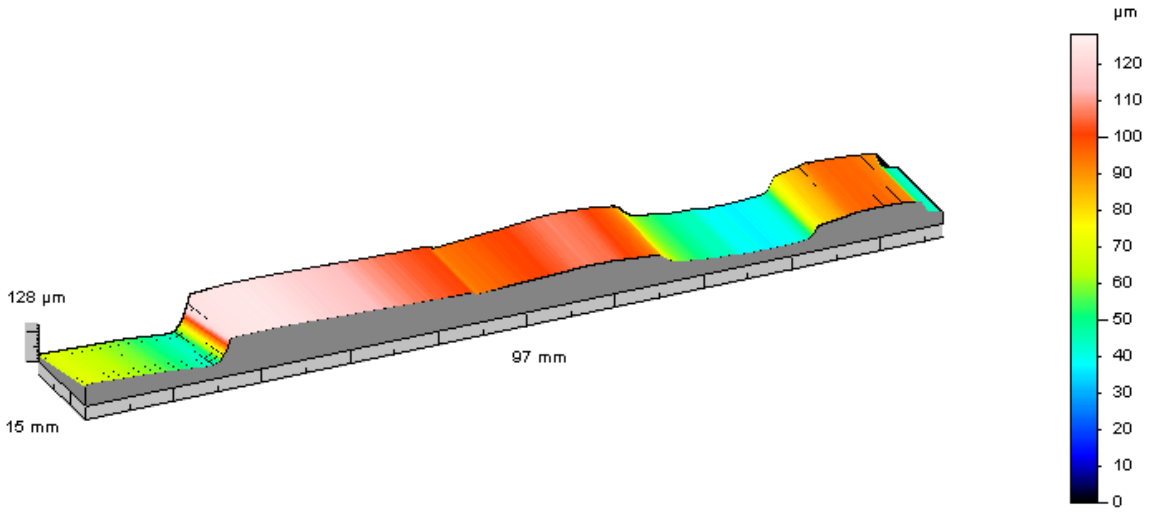

Figure 7.31: Three-dimensional representation of the measured surface profile of a thin-plate workpiece machined under the fixturing scenario, where an active clamp (F_c = 20) N is continuously moving, following the motion of tool.

values of each surface roughness measure from all the measurements belonging to a single fixturing strategy were averaged. They were then compared to the average of the surface roughness measures from the fixturing strategy, where a single passive clamping element was positioned at P2 (see Figure 7.1). This fixturing strategy constitutes the performance benchmark, as it is considered that it corresponds to a traditional, but well-designed fixturing solution. Mathematically, the percentage reduction in the surface roughness values is estimated as follows:

$$\text{Av. Reduction} = \frac{\text{Average } R_x \text{ of Passive Clamp at P2} - \text{Average } R_x \text{ of Strategy x}}{\text{Average } R_x \text{ of Passive Clamp at P2}} \times 100\% \tag{7.6}$$

with R_x being one of R_a, R_z or $R_{z\text{JIS}}$. Table 7.10 compares the resulting surfaces from the passive and continuously-moving clamp (PCMC) strategy and the active and fully-active fixturing strategies. Mathematically, this is achieved as follows:

$$\text{Av. Reduction} = \frac{\text{Average } R_x \text{ of PCMC} - \text{Average } R_x \text{ of (Fully-)Active Strategy}}{\text{Average } R_x \text{ of PCMC}} \times 100\% \tag{7.7}$$

Positive percentages signify a decrease, whilst negative values signify an increase in the values of the selected surface quality indicators, compared to the ones achieved for the passive and continuously-moving clamp strategy.

Table 7.9: Statistical comparison of surface measurement results. Results shown are in comparison to the static, passive clamp at P2 fixturing strategy (Eq. (7.6)).

Fixturing Strategy	Av. Reduction of R_a (%)	Av. Reduction of R_t (%)	Av. Reduction of $R_{z\text{JIS}}$ (%)
Moving Passive Clamp Discrete Motion	66.65	65.33	67.17
Moving Passive Clamp Continuous Motion	87.28	87.98	86.36
Static Active Clamp at P2 $(X, Y) = (75, 10)$	92.98	79.54	91.89
Moving Active Clamp Continuous Motion	93.99	81.52	92.89

Table 7.10: Statistical comparison of surface measurement results. Results shown are in comparison to the passive and continuously moving clamp strategy (Eq. (7.7)). Positive values indicate a reduction, whilst negative values indicate an increase, compared to the passive continuously-moving clamp strategy.

Fixturing Strategy	Av. Reduction of R_a (%)	Av. Reduction of R_t (%)	Av. Reduction of $R_{z\text{JIS}}$ (%)
Static Active Clamp at P2 $(X, Y) = (75, 10)$	44.81	-70.18	40.51
Moving Active Clamp Continuous Motion	52.75	-53.66	47.85

7.6 Discussion

The results that were presented in the previous section depict the improvements, in both the form accuracy and the surface finish, which can be achieved through the fully-active fixture paradigm. They also verify the fully-active fixture design.

With regards to the results from the set of experiments, where a passive clamp was positioned at point P1 $(X, Y) = (75, 25)$ of the plate (see Figure 7.1), it is immediately evident that the surface, resulting from the milling process, is very rough. The software that was charged with the analysis of the measurements from the Talysurf 1000 CLA indicates a maximum average surface roughness of $R_a = 4.221$ μm. This value however is a lot lower than the one expected, based on visual observation. In more detail, the average surface roughness was also measured using standardised pre-calibrated samples. These samples are used to derive through visual observation an estimate of the average surface roughness of a machined surface. On the basis of this measurement, the average surface roughness

of the surface of the plate that were machined under the previously mentioned fixturing scenario was found to be $R_a = 50$ μm. The difference is attributed to the integrated cut-off filter in the software. This filter is used to differentiate large profile variations, which are in some cases desirable, from the smaller deviations of the height of the surface, from which the surface texture is created. This filter could not be de-activated. Nevertheless, the values of the surface characteristic indicators that were suggested by the software were used for comparison purposes. This is because the values of the surface roughness indicators that were measured using the Talysurf 1000 CLA constitute a best-case measurement. This means that the observed reduction in the values of the indicators when applying the various fixturing scenarios are the minimum-observed.

Another interesting observation on the experimental results of the aforementioned set of experiments relates to the thickness of the removed material. The original thickness of the plate was measured as $h = 3.245$ μm, and the desired thickness of the removed material is 0.5 mm. It can be noted in Figure 7.20, that more material has been removed from the central area of the workpiece, and less from the region towards the edges. This is attributed to the fact that the workpiece was not well supported by the fixture, as there was no support within the axial depth-of-cut, the tool was losing contact with the workpiece. This explains the fact that less material was removed from these areas, where the amplitude of vibration is expected to be larger, as predicted by the design methodology. As for the central area, due to the increased local stiffness, the workpiece presented a smaller amplitude of vibration, as predicted by the methodology. This, in combination with the applied clamping force that deflects the workpiece towards the tool, explains why more material has been removed from the central region.

Similar observations can be made of the fixturing case, where a passive clamping element is positioned at point P2 of the plate (Figure 7.1). Less material than intended is removed from the side areas of the plate and more material is removed from the centre areas. In detail, the edges of the plate present a maximum deviation from the desirable dimension of $+340$ μm. Similarly, the central, area of the plate shows a difference from the nominal dimension of -80 μm. The justification is the same as before. The difference is that a larger deviation from the desired profile is observed in this case. This is due to the vibration amplitude being considerably smaller, so the tool remains in contact with the workpiece. The smaller amplitude of vibration, which is predicted by the fully-active fixture

design methodology, is reflected in the considerable improvement of the surface roughness parameters.

A significant improvement in both form accuracy and surface quality is observed in the set of experiments, where the discretely-moving passive clamp fixturing strategy is implemented. A reduction in the range of 66% in all surface roughness parameters is observed, compared to the single passive clamp at point P2 fixturing strategy (see Table 7.9). The flatness of the surface appears significantly improved. The maximum positive and negative deviation from the nominal dimension of 2745 μm is $+21.8$ μm and -124.4 μm, respectively. The surface roughness characteristics are also significantly improved, recording a reduction of approximately 87% in the average surface roughness, the profile height, and the JIS ten point average roughness (Table 7.7). The surface profile at the areas towards the ends of the plate workpiece present a small degree of inclination. This is a direct result from the profile of the plate as it statically deforms under the applied loads. It is not observed at the centre due to the symmetric deformation profile, resulting from a load being applied in the middle of the length of the plate. Furthermore, the profile of the resulting surface presents a number of steps, equal to the number of the positions that the clamp takes over the manufacturing process. This characteristic was also predicted by the design methodology.

A further improvement is observed when the continuously-moving passive element fixturing strategy is applied. The flatness of the surface (Figures 7.26, 7.27) and its roughness appear considerably improved (Table 7.7). A small deviation from the desirable thickness of the removed material is also observed. The maximum observed value is -80 μm. This improvement in the surface characteristics were also indicated by the fully-active fixture design methodology.

Moreover, the surface of the thin plate presents fluctuations that resemble a wave. This formation presents a certain amount of periodicity, with a "wave-length" of approximately 32.3 mm. This is attributed to the out-of-roundness tolerances of the rolling-contact tip (Figure 7.11 (b)). The diameter of the rolling tip is 10 mm, which translates into a perimeter of 62.8 mm. If the actual shape of the tip approached that of an ellipse, then this would justify the observed frequency of the wave on the surface of the plate, since $62.8/2 = 31.4$ mm. Such an ellipsoid shape could have been created by the manufacturing process. Furthermore, assuming that the transverse and the conjugate diameters of the ellipse differ in length by 40 μm, then this would justify the amplitude of the "waves",

which is approximately 20 μm. Such a deviation on the roundness of the rolling tip was confirmed by a measurement with a hand-held digital vernier caliper.

In the active-fixture cases, which were investigated purely experimentally, a series of interesting observations can be made. To begin with, in both active fixturing cases, there are relatively large deviations in the machined depth. This is because of the occasional large over- or under-shoot in the response of the active element, which was also observed and commented on in Chapter 5, Section 5.3.3.1. Unfortunately, the experimentally applied control parameters were the best that could be achieved. As it was observed in Chapter 5 (Section 5.5.3), however, the possibility to apply a PID controller, should drastically improve the response of the active clamps. This is based on the theoretical results presented in the previously mentioned sections of Chapter 5.

The resulting surface quality in both active fixturing cases appears noticeably improved compared to the passive fixturing cases, even the case where the passive clamp is moving continuously by following the motion of the tool. In more detail, and as presented in Table 7.10, the static and active fixture element strategy resulted in a reduction of 44.81% of the average surface roughness and 40.51% of the JIS ten point average roughness. The adoption of the active and continuously-moving clamp fixturing strategy (fully-active) led to a reduction by 52.57% in average roughness, and 47.85% in the ten point average roughness value. However, the large overshoot in the response of the active element, led to a significant increase in the surface profile values, namely by 70.18% in the active and static clamp, and by 53.66% in the fully-active fixturing case.

The aforementioned observations lead to the conclusion that a fast responding actuator, even when statically positioned could lead to significant improvement in the roughness characteristics of a machined surface. This, as expected, is in agreement with previous related work on the field [98, 110]. However, the moving-fixture-element strategies appear to improve the form accuracy of the resulting surface, whilst reducing the roughness of the surface. The gains from this approach are expected to be greater as the free span of thin-walled low-rigidity structures increases.

Finally, apart from the qualitative correlation that is observed in the predictions of the fully-active fixture design methodology and the experimental results, there appears to be a good agreement between the percentage reduction in the maximum elastic deformation of the plate and the measured surface roughness parameters. This is shown in Table 7.11.

It is reminded here that a direct quantitative agreement between the fully-active fixture design methodology and the surface measurement results is not the intention of this work, nor was it expected. This is due to various reasons. To begin with, the simulated loads in the methodology are only applied in the traverse direction of the plate. In reality, the machining loads are applied in all Cartesian directions. However, the transverse component of the force is in fact the most dominant one, followed by that with direction parallel to the surface of the plate, namely the X-direction as depicted in Figure 7.1. Moreover, the simulated loads are simple harmonic ones. In reality, machining loads are a superposition of various harmonic forces and noise. In practice, this should affect the response amplitude and phase of the workpiece. Moreover, the contact stiffness profile used in this work, i.e. a linear spring constant, constitutes a linearised and simplified representation of the fixture-workpiece contact behaviour. Additionally, the spring constant that was used in the thin-plate test case was randomly selected. The contact stiffness affects the natural frequencies of the systems and, therefore, its dynamic response. An experimentally measured stiffness profile would enhance the prediction accuracy of the methodology.

Nevertheless, bearing in mind that the primary goals of this chapter are the investigation of the performance of the fully-active fixtures paradigm and the qualitative verification of the design methodology, it is considered that these goals have been successfully achieved.

Table 7.11: Statistical comparison of experimental results and the percentile reduction in the maximum elastic deformation of the plate, as predicted by the fully-active fixture design methodology, when applied on the thin-plate test case. Results shown are in comparison to the fixturing strategy where a static and passive clamp is positioned at point P2 $(X, Y) = (75, 10)$ of the plate.

Fixturing Strategy	Av. Reduction of R_a (%)	Av. Reduction of $R_{z\text{JIS}}$ (%)	Methodology Reduction (%)
Moving Passive Clamp Discrete Motion	66.65	67.17	66.63
Moving Passive Clamp Continuous Motion	87.28	86.36	84.29

7.7 Conclusions

This chapter focused on the verification of the fully-active fixture design methodology, presented in Chapter 6. The chapter began with the application of the methodology on a

test case involving a thin-plate workpiece undergoing a climb-milling operation. The results from the methodology were applied experimentally. The experimental set-up, along with the justification behind key design decisions, were also presented.

Both the experimental results and those from the application of the design methodology revealed the potential of fully-active fixturing systems. In detail the following key conclusions can be drawn:

- A careful placement of the clamping element, based on the proposed fixture design methodology, can noticeably improve the surface quality characteristics.
- A fixturing strategy where a single passive element is used on a thin-walled low-rigidity plate workpiece results in significant deviation from flatness, by approximately 420 μm.
- A passive and discretely-moving clamping element, could lead to significant improvement in both form accuracy and surface quality. More specifically, deviations from the nominal dimensions appear reduced by a maximum of 123.4 μm. The surface quality characteristics are improved by 67%. These figures are based on the experimental observations.
- A fixturing strategy, according to which a fixture element changes position in a discrete manner, leads to a surface profile characterised by step formations.
- A fixturing strategy, where a passive clamping element traverses the length of a thin-plate workpiece, leads to the best combination of form accuracy and surface finish. Compared to the static-passive element strategy (optimum placement), a reduction of 87.28% and 87.98% was achieved in the average surface roughness and the profile height respectively.
- The passive and continuously-moving clamp fixturing strategy results in a surface with small deviation from flatness. The surface exhibits a wave-like finish, with the amplitude of the waves being 20 μm. The radial depth of cut appears increased by 80 μm compared to the nominal value. The wave formations on the surface are attributed to the dimensional tolerances and the out-of-roundness of the rolling fixture tip.

- The static and active element fixturing strategy improved the average surface roughness by 92.98% and the JIS ten point average roughness by 91.89%, compared to the static and passive element fixturing strategy. Also, a reduction of at least 40.51%, compared to the passive and continuously-moving element strategy, was observed in the surface roughness parameters.

- The active and continuously-moving element fixture strategy led to a further improvement of the surface roughness parameters by at least 47.85%, compared to the passive and continuously moving element fixturing strategy.

- Due to the limitation in the adjustment of the PID-controller parameters, the response of the active element in the active and fully-active fixturing strategies strategies was characterised by occasional overshooting and undershooting, which affected the form accuracy of the machined surface negatively. The maximum deviation from the nominal dimensions was 240 μm in the static and active element strategy, and 95 μm in the continuously-moving and active element strategy.

- All the previously mentioned observations were indicated successfully by the fully-active fixture design methodology, revealing a clear correlation between the experimental and the predicted results. This correlation, however, is qualitative and not quantitative, due mainly to the simplifications behind the load profile and the contact-stiffness constant value.

- A correlation between the percentile-reduction of the experimentally-obtained surface roughness parameters, and the methodology-predicted reduction in the maximum elastic deformation of the workpiece, was also observed.

Chapter 8

Conclusions and Future Work

8.1 Contributions

Fixtures are devices that are designed to repeatedly and accurately locate the processed workpiece in a desired position and orientation, and securely hold it in that location throughout the manufacturing process. Additionally, fixtures are charged with the task of adequately supporting the workpiece to minimise its deflection under the externally applied loads from the manufacturing process. From the above definition, it becomes evident that fixtures have a large impact on the outcome of a manufacturing process. In the case of machining, an improperly-designed fixture could result in large deformations and intense vibrations that can lead to large deviations from the nominal machined surface profile and surface finish quality. This is instantiated more profoundly in the case of low-rigidity thin-walled components.

In traditional manufacturing environments, where thin-walled components are produced, the adopted fixturing solutions are dedicated to a specific workpiece geometry. This ensures maximum support and localisation accuracy of the workpiece, relative to the machine tool coordinate frame, to achieve the target geometrical and surface-finish characteristics. However, in the recent decades a clear trend towards mass customisation has appeared. According to this manufacturing paradigm, each manufactured part is unique and adapted to the needs of the customer. This results in the need for manufacturing environments that can produce fast and efficiently large number of small-sized batches of products, without compromise in the quality of the produced parts, which often constitutes the competitive edge of western manufacturers. This has created a technological

pull towards manufacturing equipment, like Computer Numerically Controlled (CNC) machine tools that exhibit high production rates, increased flexibility/reconfigurability, and machining precision.

Fixtures are not exempt from this technology pull. On the contrary, fixtures have been the focal point of a plethora of research work. However, the vast majority of that work has focused on either reconfigurability, or intelligent fixturing solutions that help augment the quality of the produced parts. Reconfigurable fixtures are defined as fixtures that can, manually or automatically, have their layout re-arranged to accept a workpiece with a different geometry. Intelligent fixtures, also referred to as adaptive or active fixtures, incorporate an array of actuators and sensors, that allow the fixture to adapt the clamping forces it applies throughout the manufacturing process. The combination of the active fixturing and the reconfigurable fixturing paradigms could have a significant impact in fixturing technology. The impact is not limited to the immediately apparent benefits. The aforementioned combination leads to the birth of a new fixturing paradigm, where the fixture layout is not static but changes dynamically during the manufacturing, providing increased support to the workpiece, thus reducing vibration amplitude and elastic deformation. This, especially when the processed workpiece exhibits low rigidity, results in a tighter adherence to the nominal dimensions of the machined profile and an improved surface-finish quality. At the same time, the fixture retains the abilities to adapt the forces it exerts on the workpiece, which has been proven to improve the end result of a machining process, and to reconfigure before the start of a manufacturing process to accept a workpiece with a different geometry. A fixture with the previously mentioned capabilities is referred to as fully-active fixture.

In order to investigate the impact that such a fixturing solution could have on the quality of a machined thin-walled low-rigidity workpiece, a structured research methodology was first proposed. This comprises four steps:

8.1.1 Literature Survey

A detailed literature review was conducted to establish the state-of-the-art in the relevant fields of fixturing research. The key conclusions from and the knowledge gaps that were identified through the literature survey are summarised bellow:

- The field of modelling and predicting the response of the structure of a workpiece to dynamic loads has received considerable amount of attention.

- The majority of the models that intend to predict the dynamic deformation experienced by the workpiece, treat the problem as static or pseudo-static.
- The workpiece is treated as rigid in a large percentage of the aforementioned work. This renders the proposed modelling approaches invalid for low-rigidity workpieces.
- The moving point of application of external loads, such as machining forces, is often ignored even in research activities that deal with the dynamic response of fixture-workpiece systems.
- The effect of the closed-loop operation of active fixture elements within active fixtures is not reflected in the vast majority of the proposed models.
- There is a lack of work on studying the performance and capabilities of fully-active fixtures.
- There is a lack of a fixture design methodologies that can support fully-active fixtures.

8.1.2 Identification of Research Objectives, Assumptions and Limitations

Based on the identified knowledge gaps the following research objectives were set:

1. The generation of a model that adequately describes the active fixture-workpiece system's response to external moving and oscillating loads.
2. The definition of appropriate control algorithms and strategies for the seamless operation of a fully-active fixture.
3. The composition of a fixture design methodology, which accounts for the capabilities of fully-active fixtures, and assists in drastically improving the results of a machining process in terms of surface quality and form accuracy.

The assumptions and limitations that govern the activities towards achieving the set research objectives are summarised bellow:

- The developed models and methodologies are targeted towards low-rigidity workpieces.

- The proposed models, concepts and methodologies are based on point-contact fixturing and the 3-2-1 fixturing paradigm.
- External loads are assumed to comprise a single component applied in the transverse direction of the workpiece.
- The loads are simple harmonic in nature.
- Peripheral milling is assumed to be the source of external excitation. The rigidity and mass of the cutting tool are not taken into consideration.

8.1.3 Fulfilment of the Research Objectives

The main contributions towards achieving the research objectives are presented hereafter, along with key conclusions.

8.1.3.1 Open-Loop Model of Coupled Actuator and Workpiece System

A methodology to generate model of an actuator-workpiece system, reflecting the open-loop response of an active element, the moving harmonic loads applied in the traverse direction during machining operation, and the effects of these on the workpiece was proposed. The development of the model involves the discretisation of the structural model of the workpiece in finite elements, the establishment of a way to simulate moving machining loads, the development of a model that reflects the dynamics of the active elements and their drive units, and the coupling of the previous models. The main key developments and findings from these activities are:

- The tetrahedron four-node shell elements (S4) are the most appropriate for discretising the structural model of the workpiece, and for simulating the dynamic response of a thin-walled plate-like workpiece. This is based on the capability of these elements to accurately predict the natural frequencies and the elastic deformation of the workpiece, with the lowest possible density of nodes. The S4 elements outperformed all other investigated elements, underestimating the natural frequencies of a thin plate by 0.47% on average, and overestimating the elastic deformation of the plate by 3.78% on average. These percentages stem from the comparison of FEA results to results from Kirchhoff plate-theory and the analytical model of a thin plate subjected to

moving loads, respectively. The total number of nodes used to obtain these results is 341, which is the lowest compared to other types of finite elements.

- Traverse, distributed, moving, line loads can be simulated through their resultant nodal shearing loads at the nodes of the finite element they traverse at any time instant. This approach is valid even when the nodes are positioned 5 mm apart.

- A first-principle-based model for the Permanent Magnet Alternating Current (PMAC) motor-based actuator was established. The model includes the behaviour of the drive unit which is necessary for the actuator to work. The model treats the motor as a direct current one. This approximation is valid, provided that the PMAC motor exhibits high resistance. The validity of this approximation was verified experimentally.

- The contact interface between the actuator and the workpiece is approached via a combination of a spring and a damper with constant coefficients of stiffness and damping, respectively.

- The workpiece, moving loads, and active element (actuator) models were coupled using the impedance coupling technique in physical coordinates in order to provide the second-order differential equations (ODEs) of the workpiece-actuator model. The first-order equations were added after transferring the entire system in state space.

- The experimental verification process revealed that, due to non-linearities in the actual system, the experimentally-obtained responses present different force amplitudes for two different-form but same-amplitude signals. This non-linearity can be accounted for by calibrating the reverse efficiency factor in the coupled workpiece-fixture model. For the step response the efficiency factor was set to $\eta_2 = 65\%$, while for the sinusoidal response it was set to $\eta_2 = 37.5\%$.

8.1.3.2 Investigation of Clamping Force Control Strategies

Two force-control strategies were investigated, namely the direct force/torque control and the cascaded position/force-feedback control strategies. The former was applied experimentally, whilst results on the performance of the latter were derived from the open literature. The key developments and findings from this activity are:

- The direct force/torque control strategy exhibits faster rise time by 91.73% and settling time by 55.75%, compared to the cascaded control approach. This was observed after manual tuning, which resulted in a PI controller with $K_p = 11$ and $K_I = 86$.
- The direct force/torque control is the preferred control strategy for regulating the clamping forces applied from a PMAC motor-based electromechanical actuator.
- The response of the direct-force control-based system presents significant overshoot (39.53%). A better performing controller could be tuned, if a higher flexibility in the parameter adjustment was allowed by the hardware. A PID controller with a small derivative gain is advisable, based on the theoretical results.

8.1.3.3 Development of a Closed-Loop Comprehensive Model

On the basis of the control-strategy results, the fixture-workpiece model described earlier was further expanded to reflect the closed-loop behaviour of the active elements of a fully-active fixture. For this, the models for the various components of the system, including the motion controller and the force-sensor amplifiers, were developed and expressed in the Laplace domain as transfer functions. The open-loop model of the system was also expressed as a transfer function. The model was used to theoretically investigate the performance of different controller architecture. The model was verified experimentally. The following conclusions were drawn:

- A PID controller is the preferred controller architecture. Careful selection of the controller parameters could result in a fast response with minimal overshoot.
- All examined controller architectures lead to a stable system.
- The system that simulates more accurately the response of the experimental test bed is the one that includes a PID controller tuned via the Ziegler-Nichols ultimate sensitivity method.

8.1.3.4 Development of a Fully-Active Fixture Design Methodology

A methodology to establish the parameters of a fixturing process based on the fully-active fixturing paradigm was developed. The methodology accepts the previously developed

model and is used to identify whether a discretely-moving or a continuously-moving fixture element strategy is necessary, the number and the coordinates of the contact points that constitute the path of the fixture element, the time instants when the moving fixture element needs to change position, and the clamping forces that the fixture needs to apply at each contact point. The methodology was applied on two test cases. One involved a planar-beam workpiece, which was verified analytically. The other dealt with a thin-walled plate workpiece. In both cases, the fixture elements were treated as passive. The results of the methodology were applied experimentally on a thin-plate workpiece undergoing a peripheral milling operation. Additionally, the cases involving a static active element (active fixture) and a continuously-moving active element (fully-active fixture) were examined experimentally. The main conclusions from these are:

- The methodology, at its present state, produces results that can be used only in a qualitative manner. This was expected as the machining forces and the contact behaviour are largely simplified in this work.

- The methodology predicts correctly (qualitatively) the improvement of the form accuracy and the surface quality of the workpiece that can be achieved by adopting the proposed fixturing parameters.

- A careful placement of the clamping element, based on the proposed fixture design methodology, can noticeably improve the surface-quality characteristics.

- A fixturing strategy where a single passive element is used on a thin-walled low-rigidity plate workpiece results in significant deviation from flatness, by approximately 420 μm.

- A passive and discretely-moving clamping element, could lead to significant improvement in both form accuracy and surface quality. More specifically, and based on experimental observations, deviations from the nominal dimensions appear reduced by a maximum of 123.4 μm. The surface quality characteristics are improved by 67%.

- A fixturing strategy, where a passive clamping element traverses the length of a thin-plate workpiece, leads to the best combination of form accuracy and surface finish. Compared to the static-passive element strategy (optimum placement), a reduction

of 87.28% and 87.98% was achieved in the average surface roughness and the profile height, respectively.

- The passive and continuously-moving clamp fixturing strategy results in a surface with small deviation from flatness. The surface exhibits a wave-like finish, with the amplitude of the waves being 20 μm. The radial depth of cut appears increased by a maximum of 80 μm compared to the nominal value.

- The static and active element fixturing strategy improved the average surface roughness by 92.98% and the JIS ten-point average roughness by 91.89%, compared to the static and passive element fixturing strategy. Also, a reduction of at least 40.51%, compared to the passive and continuously-moving element strategy, was observed in the surface roughness parameters.

- The active and continuously-moving-fixel strategy led to a further improvement of the surface-roughness parameters by at least 47.85%, compared to the passive and continuously-moving-element fixturing strategy.

- Due to the limitation in the adjustment of the PID-controller parameters, the response of the active element in the last two strategies was characterised by occasional overshooting and undershooting, which negatively affected the form accuracy of the machined surface. The maximum deviation from the nominal dimensions was 240 μm in the static and active element (active fixturing) strategy, and 95 μm in the continuously-moving and active-element strategy (fully-active fixturing strategy).

The above clearly outline the potential impact of fully-active fixtures on the form accuracy and surface finish of a machined thin-walled component.

8.1.4 Validation of the Developed Model and Methodology

Both theoretical and experimental validation practices have been implemented in order to verify the proposed models and the design methodology. Theoretical validation was primarily based on the analytical model of a thin-plate workpiece subjected to moving loads, and finite element analysis results. Experimental validation and verification procedures were executed on a prototype fully-active fixture that was conceptualised and materialised for the needs of this work.

8.2 Future Work

The research study presented through this thesis has proposed tools, models, and methodologies that can help advance the technological state-of-the-art and has revealed new potential fixturing practices that can greatly benefit the industry. At the same time, the presented results inevitably lead to new questions that seek scientific investigation. The models and the design methodology that was proposed in this thesis can be further enriched and expanded in the following ways:

- The stiffness of the spring elements used to simulate the contact behaviour between the workpiece and the fixture elements could be enhanced to reflect a more accurate contact profile.
- The incorporation of friction in the contact model could further improve the fixture workpiece system to reflect the non-linear effects that are present in the fixtrure-workpiece interface.
- A more accurate model of the actuator system could capture the non-linear effects that were not accounted for in this work.
- The profile of the machining force could be obtained experimentally or simulated via a plethora of accurate machining-force prediction models that are in existence.
- Machining forces acting in all three physical dimensions could be applied to the already developed model.
- The introduction of the stiffness of the cutting tool in the fixture-workpiece model could improve the model's prediction capability in terms of workpiece elastic deformation.
- The application of the developed methodology to a more generic, real-life industrial component could help emphasise further the capabilities and benefits of fully-active fixtures.
- The incorporation of vibration damping capabilities in a fully-active fixture could lead to an additional improvement in performance.

Bibliography

[1] *EC Series Electric Cylinders User's Manual*, 2007. Revision 1.0.

[2] Abou-Hanna, J., and Okamura, K. Mechanical Properties of Steel Pellets in Particulate Fluidized Bed Fixtures. *Journal of Manufacturing Systems 10*, 4 (1991), 307–313.

[3] Abou-Hanna, J., and Okamura, K. Finite Element Approach to Modeling Particulate Bed Fixtures. *Journal of Manufacturing Systems 11*, 1 (1992), 1–12.

[4] Abou-Hanna, J., Okamura, K., and McGreevy, T. Dynamic Behavior and Creep Characteristics of Flexible Particulate Bed Fixtures. *Journal of Manufacturing Systems 12*, 6 (1993), 469–505.

[5] Abou-Hanna, J., Okamura, K., and McGreevy, T. Experimental Study of Static and Dynamic Rigidities of Flexible Particulate Bed Fixtures Under External Vertical and Torque Loads. *Journal of Manufacturing Systems 13*, 3 (1994), 177–189.

[6] Abou-Hanna, J., Okamura, K., and McGreevy, T. Sinkage Characteristics of Workpieces in Flexible Particulate Bed Fixtures: An Experimental and Numerical Investigation. *Journal of Manufacturing Systems 13*, 5 (1994), 359–369.

[7] Ahn, S. H., and Wright, P. K. Reference Free Part Encapsulation (RFPE): An Investigation of Material Properties and the Role of RFPE in a Taxonomy of Fixturing Systems. *Journal of Manufacturing Systems 21*, 2 (2002), 101–110.

[8] Al-Habaibeh, A., Gindy, N., and Parkin, R. M. Experimental Design and Investigation of Pin-Type Reconfigurable Clamping System for Manufacturing Aerospace Components. *Journal of Engineering and Manufacture 217* (2003), 1771–1777.

[9] Aoyama, T. Development of Gel Structured Electrorheological Fluids and Their Application for the Precision Clamping Mechanism of Aerostatic Sliders. *CIRP Annals - Manufacturing Technology 53*, 1 (2004), 325 – 328.

[10] Aoyama, T., and Kakinuma, Y. Development of Fixture Devices for Thin and Compliant Workpieces. *CIRP Annals - Manufacturing Technology 54*, 1 (2005), 325–328.

[11] Bakker, O. J. *Control Methodology and Modelling of Active Fixtures*. PhD thesis, University of Nottingham, 2010.

[12] Bakker, O. J., Popov, A., and Ratchev, S. Control of a Workpiece Holder with Piezo-Electric-Mechanical Actuation. *Journal of Machine Engineering 8*, 3 (2008), 17–28.

[13] Bakker, O. J., Popov, A. A., and Ratchev, S. M. Investigation into Feedback Control of Part-Fixture Systems Undergoing Dynamic Machining Forces. In *Proceedings of the International Conference on Noise and Vibration Engineering (ISMA2008)* (Leuven (Heverlee), September 2008), P. Sas and B. Bergen, Eds., ISMA2008 - International Conference on Noise and Vibration Engineering, Katholieke Universiteit Leuven - Departement Werktuigkunde, pp. 131–140.

[14] Bakker, O. J., Popov, A. A., and Ratchev, S. M. Fixture Control by Hydraulic Actuation Using a Reduced Workpiece Model. *Proceeding of the Institution of Mechanical Engineers, Part B: Journal of Engineering Manufacture 223* (2009), 1553–1566.

[15] Bakker, O. J., Popov, A. A., and Ratchev, S. M. Model-Based Control of an Advanced Actuated Part-Fixture System. In *Proceedings of 2009 ASME International Manufacturing Science and Engineering Conference* (October 2009), no. MSEC2009-84175, ASME.

[16] Behzadi, M. R., and Arezoo, B. Static and Dynamic Models for Predicting the Effects of Supports on Machining Flatness and Roughness. *Proceeding of the Institution of Mechanical Engineers, Part B: Journal of Engineering Manufacture 216* (2002), 735–743.

[17] Bi, Z. M., and Zhang, W. J. Flexible Fixture Design and Automation: Review, Issues and Future Directions. *International Journal of Production Research 39*, 13 (2001), 2867–2894.

[18] Blevins, R. D. *Formulas for Natural Frequencies and Mode Shapes*, reprint ed. Krieger Publishing Company, Malabar, Florida, 2001.

[19] Brost, R. C., and Peters, R. R. Automatic Design of 3-D Fixtures and Assembly Pallets. In *Proceedings of the 1996 IEEE Interntional Conference on Robotics and Automation* (Minneapolis, Minnesota, April 1996).

[20] Bukowski, A., Kwansy, W., and Jedrzejewski, J. Mechatronic Approach to the Development of an Intelligent Fixturing Device Test-Bed. *Journal of Machine Engineering 8*, 3 (2008), 66–76.

[21] Chakraborty, D., De Meter, E. C., and Szuba, P. S. Part Location Algorithm for an Intelligent Fixturing System Part 1: System Description and Algorithm Development. *Journal of Manufacturing System 20*, 2 (2001), 124–134.

[22] Chakraborty, D., De Meter, E. C., and Szuba, P. S. Part Location Algorithm for an Intelligent Fixturing System Part 2: Algorithm Testing and Evaluation. *Journal of Manufacturing System 20*, 2 (2001), 135–148.

[23] Chan, K. C., Benhabib, B., and Dai, M. Q. A Reconfigurable Fixturing System for Robotic Assembly. *Journal of Manufacturing Systems 9*, 3 (1990), 206–221.

[24] Chan, K. C., and Lin, C. S. Development of a Computer Numerical Control (CNC) Modular Fixture - Machine Design of a Standard Multifinger Module. *International Journal of Advanced Manufacturing Technology 26* (1996), 18–26.

[25] Chou, Y. C., Srinivas, R. A., and Saraf, S. Automatic Design of Machining Fixtures: Conceptual Design. *International Journal of Advanced Manufacturing Technology 9* (1994), 3–12.

[26] Chryssolouris, G. *Manufacturing Systems: Theory and Practice*, 2nd ed. Mechanical Engineering Series. Springer Science and Business Media, Inc., New York, 2006.

[27] Couey, J. A., Marsh, E. R., Knapp, B. R., and Vallance, R. R. Monitoring Force in Precision Cylindrical Grinding. *Precision Engineering 29* (2005), 307–314.

[28] Craig Jr., R. R., and Kurdila, A. J. *Fundamentals of Structural Dynamics*, 2nd ed. John Wiley & Sons, Hoboken, New Jersey, 2006.

[29] Cromwell Group (Holdings) Ltd. SwissTech® 4 Flute End Mills. `http://www.cromwell.co.uk/SWT1631006A`. Last accessed on 10/12/2010.

[30] Daimon, M., Yoshida, T., Kojima, N., Yamamoto, H., and Hoshi, T. Study for Designing Fixtures Considering Dynamics of Thin-Walled Plate- and Box-Like Woekpieces. *Annals of the CIRP 34/1* (1985), 319–322.

[31] Danaher Motion. Kollmorgen AKM-Series Brushless Servomotors. `http://www.kollmorgen.com/website/com/eng/products/motors/brushless_motors/conventional_rotary_servomotors/akm_series.php`. Last accessed on 10/12/2010.

[32] Danaher Motion. Kollmorgen EC-Series Linear Actuators. `http://www.kollmorgen.com/website/com/eng/products/electric_cylinders.php`. Last accessed on 10/12/2010.

[33] Danaher Motion. *Kollmorgen AKM Series Motor Catallogue*, 2006.

[34] Danaher Motion. *Kollmorgen AKM Servomotor Product Manual*, 2008.

[35] Danaher Motion. *S200 High Performance Compact Brushless Servo Drives- Reference Manual*, 2008. Revision C.

[36] Data Physics Corporation. SignalCalc ACE: Dynamic Signal Analyser. `http://www.dataphysics.com/products/analyzerfamily/ace/index.htm`. Last accessed on 10/12/2010.

[37] de Faria, A. R., and Oguamanam, D. C. D. Finite Element Analysis of the Dynamic Response of Plates Under Traversing Loads Using Adaptive Meshes. *Thin-Walled Structures 42* (2004), 1481–1493.

[38] De Meter, E. C., and Hockenberger, M. J. The Application of Tool Path Compensation for the Reduction of Clamping Induced Geometric Errors. *International Journal of Production Research 35*, 12 (1997), 3415–3432.

[39] Deiab, I. M. On the Effect of Fixture Layout on Part Stability and Flatness During Machining: A Finite Element Approach. *Proceeding of the Institution of Mechanical Engineers, Part B: Journal of Engineering Manufacture 220* (2006), 1613–1620.

[40] Deiab, I. M., and Elbestawi, M. A. Effect of Workpiece/Fixture Dynamics on the Machining Process Output. *Proceeding of the Institution of Mechanical Engineers, Part B: Journal of Engineering Manufacture 218* (2004), 1541–1553.

[41] Deng, H. *Analysis and Synthesis of Fixturing Dynamic Stability in Machining Accounting for Material Removal Effect.* PhD thesis, Georgia Institute of Technology, Atlanta, Georgia, USA, December 2006.

[42] Deng, H., and Melkote, S. N. Analysis of Fixturing Dynamic Stability in Machining. In *Proceedings of the 2005 IEEE/ASME International Conference on Advanced Intelligent Mechatronics* (Monterey, California, USA, July 2005), pp. 869–874.

[43] Deng, H., and Melkote, S. N. Determination of Minimum Clamping Forces for Dynamically Stable Fixture. *International Journal of Machine Tools and Manufacture 46* (2006), 847–857.

[44] Du, H., and Lin, G. C. I. Development of an Automated Flexible Fixture for Planar Objects. *Robotics & Computer-Integrated Manufacturing 14* (1998), 173–183.

[45] Du, H., Lin, G. C. I., Zhao, J., and Gol, O. An Approach to Enhancing the Intelligence of a Three-Fingered Automated Flexible Fixturing System by Using Adaptive Control Theory. *Robotics & Computer-Itegrated Manufacturing 15* (1999), 101–110.

[46] EU-AFFIX FP6 Project. Aligning, Holding and Fixing Flexible and Difficult to Handle Components . `http://www.affix-ip.eu/`. Last accessed on 13/12/2010.

[47] Ewins, D. J. *Modal Testing Theory, Practice and Application*, 2nd ed. Research Studies Press Ltd., Hertfordshire, England, 2000.

[48] Fagan, M. J. *Finite Element Analysis: Theory and Practice*. Prentice Hall, London, 1992.

[49] Fang, B., DeVor, R. E., and Kapoor, S. G. Influence of Friction Damping on Workpiece-Fixture System Dynamics and Machining Stability. *Journal of Manufacturing Science and Engineering 124* (2002), 226–233.

[50] Franklin, G. F., Powell, J. D., and Emami-Naeini, A. *Feedback Control of Dynamic Systems*, 5th ed. Addison-Wesley Publishing Company, Upper Saddle River, New Jersey, 1994.

[51] Franklin, G. F., Powell, J. D., and Workman, M. L. *Digital Control of Dynamic Systems*, 2nd ed. Addison-Wesley Publishing Company, Boston, Massachusetts, 1990.

[52] Frýba, L. *Vibration of Solids and Structures Under Moving Loads*, 3rd ed. Thomas Telford Ltd, Prague, Czech Republic, 1999.

[53] Gallagher, R. H. *Finite Element Analysis Fundamentals*. Prentice Hall Inc., Englewood Hills, New Jersey, 1975.

[54] Gandhi, M. V., and Thompson, B. Automated Design of Modular Fixtures for Flexible Manufacturing Systems. *Journal of Manufacturing Systems 5*, 4 (1986), 243 – 252.

[55] Gandhi, M. V., and Thompson, B. S. Phase Change Fixturing for Flexible Manufacturing Systems. *Journal of Manufacturing Systems 4*, 1 (1985), 29–40.

[56] Gandhi, M. V., Thompson, B. S., and Maas, D. J. Adaptable Fixture Design: An Analytical and Experimental Study of Fluidized-Bed Fixturing. *Journal of Mechanisms, Transmissions, and Automation in Design 108* (1986), 15–21.

[57] Gorman, D. J. *Free Vibration Analysis of Rectangular Plates*. Elsevier, Amsterdam, The Netherlands, 1982.

[58] Grippo, P. M., Gandhi, M. V., and Thompson, B. S. The Computer-Aided Design of Modular Fixturing Systems. *The International Journal of Advanced Manufacturing Technology 2*, 2 (1987), 75–88.

[59] Grochowski, M., Bukowski, A., and Jedrzejewski, J. Modelling of Mechatronic Workpiece-Fixture System Focusing on Active Compensation of Displacements. In *Proceedings of the 21st International Conference on Computer-Aided Production Engineering (CAPE 2010)* (Edinburgh, Scotland, UK, April 2010).

[60] Gupta, S., Bagchi, A., and Lewis, R. Sensor Based Fixturing System. In *Recent Developments in Production Research* (Amsterdam, 1988), A. Mital, Ed., Elsevier Science Publishers B.V., pp. 11–16.

[61] Hameed, R. A., Mannan, M. A., and Nee, A. Y. C. The Cutting Force Measurement in a Fixturing Setup with Instrumented Locators. *International Journal of Advanced Manufacturing Technology 23* (2004), 783–793.

[62] Hargrove, S. K., and Kusiak, A. Computer-Aided Fixture Design: A Review. *International Journal of Production Research 32*, 4 (1994), 733–753.

[63] Hoffman, E. G. *Modular Fixturing*. Manufacturing Technology Press, Lake Geneva, Wisconsin, 1987.

[64] Hunter, R., Rios, J., Perez, J. M., and Vizan, A. A Functional Approach for the Formalization of the Fixture Design Process. *International Journal of Machine Tools and Manufacture 46* (2006), 683–697.

[65] Hurco Europe Ltd. Hurco Europe General Website. `www.hurco.com`. Last accessed on 10/12/2010.

[66] Hurtado, J. F., and Melkote, S. N. A Model for Synthesis of Fixturing Configuration in Pin-Array Type Flexible Machining Fixtures. *International Journal of Machine Tools and Manufacture 42* (2002), 837–849.

[67] Hurtado, J. N., and Melkote, S. N. Workpiece-Fixture Static Friction Under Dynamic Loading. *Wear 231* (1999), 139–152.

[68] Kamarthi, S., Bohle, N., and Zeid, A. Investigating the Design and Development of Truly Agile Flexible Fixtures Based on Electrorheological Fluids. *International Journal of Rapid Manufacturing 1*, 1 (2009), 99–110.

[69] Kistler Instruments Ltd. Type 5017A Charge Amplifier. http://www.kistler.com/. Legacy product. Specifications sheet and operation manual available on request from the supplier.

[70] Kistler Instruments Ltd. Type 9101A Load Washer Specifications. http://www.kistler.com/gb_en-gb/13_Productfinder/App.9101A.5/Load-washer-0-...-20-kN.html. Last accessed on 10/12/2010.

[71] Kulankara, K., Satyanarayana, S., and Melkote, S. Iterative Fixture Layout and Clamping Force Optimization Using the Genetic Algorithm. *Journal of Manufacturing Science and Engineering 124* (2002), 119–125.

[72] Kurz, K., Craig, K., Wolf, B., and F.Stolfi. Design and Development of a Flexible, Automated, Fixture Device for Manufacturing. In *Proceedings of the ASME Dynamics Systems and Control Division* (New Orleans, Louisiana, USA, 1993), vol. 50, pp. 99–105.

[73] Kurz, K., Craig, K., Wolf, B., and Stolfi, F. Developing a Flexible Automated Fixture Device. *Mechanical Engineering 116*, 7 (1994), 59–63.

[74] Lam, S. L., and Lim, B. S. An Integrated Robotics Off-line Programming System for Modular Fixture Assembly. *Journal of Mechanical Workholding Technology 20* (1989), 261–271.

[75] Lee, E., and Sarma, S. E. Reference Free Part Encapsulation: Materials, Machines and Methods. *Journal of Manufacturing Systems 26* (2007), 22–36.

[76] Lee, E., Valdivia, P., Fan, W., and Sarma, S. E. The Process Window of Reference Free Part Encapsulation. *Transactions of the ASME 124* (2002), 358–368.

[77] Li, B., and Melkote, N. Optimal Fixture Design Accounting for the Effect of Workpiece Dynamics. *International Journal of Advanced Manufacturing Technology 18* (2001), 701–707.

[78] Liao, Y. G., and Hu, S. J. An Integrated Model of a Fixture-Workpiece System for Surface Quality Prediction. *The International Journal of Advanced Manufacturing Technology 17* (2001), 810–818.

[79] Lin, G. C. I., and Du, H. Design and Development of an Automated and Flexible Fixture. In *4th International Conference on Automation Technology* (Hsinchu, Taiwan, 1996), pp. 475–481.

[80] Liu, H., Lu, B., Ding, Y., Tang, Y., and Li, D. A Motor-Piezo Actuator for Nano-Scale Positioning Based on Dual Servo Loop and Nonlinearity Compensation. *Journal of Micromechanics and Microengineering 13* (2003), 295–299.

[81] Lu, S. S., Chu, J. L., and Jang, H. C. Development of a Novel Coordinate Transposing Fixture System. *International Journal of Advanced Manufacturing Technology 13* (1997), 350–358.

[82] Maia, N. M. M., Silva, J. M. M., He, J., Lieven, N. A. J., Lin, R. M., Skingle, G. W., To, W. M., and Urgueira, A. P. V. *Theoretical and Experimental Modal Analysis*. Research Studies Press Ltd., Hertfordshire, England, 1997.

[83] Mannan, M. A., and Sollie, J. P. A Force-Controlled Clamping Element for Intelligent Fixturing. *Annals of the CIRP 46/1* (1997), 265–268.

[84] The MathWorks, Inc. *Matlab Getting Started Guide*, 2010.

[85] The MathWorks, Inc. *Signal Processing Toolbox 6: User's Guide*, 2010.

[86] Meshreki, M., Kövecses, J., Attia, H., and Tounsi, N. Dynamics Modeling and Analysis of Thin-Walled Aerospace Structures for Fixture Design in Multiaxis Milling. *Journal of Manufacturing Science and Engineering 130* (2008), 031011–1 – 031011–12.

[87] Mittal, R. O., Cohen, P. H., and Gilmore, B. J. Dynamic Modeling of Fixture-Workpiece System. *Robotics & Computer-Itegrated Manufacturing 8*, 4 (1991), 201–217.

[88] Molfino, R., Zoppi, M., and Zlatanov, D. Reconfigurable Swarm Fixtures. In *ASME/IFToMM International Conference on Reconfigurable Mechanisms and Robots* (London, United Kingdom, June 2009), pp. 730–735.

[89] Motlagh, H. E., Hamedi, M., and Nikkhah-Bahramy, M. Application of the Armstrong Friction Model to Study Dynamic Transient Response in Workpiece-

Fixture Systems. *Proceeding of the Institution of Mechanical Engineers, Part B: Journal of Engineering Manufacture 218* (2004), 737–747.

[90] Munro, C., and Walczyk, D. Reconfigurable Pin-Type Tooling: A Survey of Prior Art and Reduction to Practice. *Journal of Manufacturing Science and Engineering 129* (2007), 551–565.

[91] National Instruments. PCI-6031E 100 kS/s, 16-Bit, 64-Analog-Input Multifunction DAQ. `http://sine.ni.com/nips/cds/view/p/lang/en/nid/1055`. Last accessed on 13/12/2010.

[92] National Instruments. PCI-7344: 4-Axis Stepper/Servo Controller for PCI. `http://sine.ni.com/nips/cds/view/p/lang/en/nid/13244`. Last accessed on 10/12/2010.

[93] National Instruments. SCB-100 Noise Rejecting, Shielded I/O Connector Block.

[94] National Instruments. UMI-7774: 4-Axis Universal Motion Interfaces for Industrial Applications. `http://sine.ni.com/nips/cds/view/p/lang/en/nid/12534`. Last accessed on 10/12/2010.

[95] National Instruments. *Motion Control, NI-Motion User's Manual*, 2006.

[96] Nee, A., Whybrew, K., and Senthil Kumar, A. *Advanced Fixture Design for FMS*. Springer-Verlag London Limited, Tyne & Wear, Engalnd, 1995.

[97] Nee, A. Y. C., Senthil Kumar, A., and Tao, Z. J. An Intelligent Fixture with Dynamic Clamping Scheme. *Proceeding of the Institution of Mechanical Engineers, Part B: Journal of Engineering Manufacture 214* (2000), 183–196.

[98] Nee, A. Y. C., Tao, Z. J., and Senthil Kumar, A. *An Advanced Treatise on Fixture Design and Planning*, vol. 1 of *Series on Manufacturing Systems and Technology*. World Scientific Publishing Co. Pte. Ltd, Singapore, 2004.

[99] Neelakantan, V. A., Washington, G. N., and Bucknor, N. K. Model Predictive Control of a Two Stage Actuation System Using Piezoelectric Actuators for Controllable Industrial and Automotive Brakes and Clutches. *Journal of Intelligent Material Systems and Structures 19* (2008), 845–857.

[100] Ngoi, B. K. A., Tay, M. L., and Wong, C. S. Development of an Automated Fixture Set-up System for Inspection. *The International Journal of Advanced Manufacturing Technology 13* (1997), 342–349.

[101] Padmanaban, K. P., and Prabhaharan, G. Dynamic Analysis on Optimal Placement of Fixturing Elements Using Evolutionary Techniques. *International Journal of Production Research 46*, 15 (2008), 4177 – 4214.

[102] Papastathis, T. N., Ryll, M., Bone, S., and Ratchev, S. Development of a Reconfigurable Fixture for the Automated Assembly and Disassembly of High Pressure Rotors for Rolls-Royce Aero Engines. In *Precision Assembly Technologies and Systems* (Chamonix, France, February 2010), pp. 283–289. Proceedings of the International Precision Assembly Seminar (IPAS2010).

[103] Papastathis, T. N., Ryll, M., and Ratchev, S. Rapid Reconfiguration and Part Repositioning with an Intelligent Fixturing System. In *Proceedings of the 2007 International Manufacturing Science and Engineering Conference (MSEC2007)* (Altanta, Georgia, USA, October 2007).

[104] PCB Piezotronics Inc. Acceleromenter Model 353B18: Specifications Sheet. `http://www.pcb.com/spec_sheet.asp?model=353B18`. Last accessed on 10/12/2010.

[105] PCB Piezotronics Inc. Impulse Hummer Specifications Sheet. `http://www.pcb.com/spec_sheet.asp?model=086C03`. Last accessed on 10/12/2010.

[106] Pham, D. T., Nategh, M. J., and de Sam Lazaro, A. A Knowledge-Based Jig-and-Fixture Designers' Assistant. *International Journal of Advanced Manufacturing Technology 4* (1989), 26–45.

[107] Phuah, H. L. *Part-Fixture Behaviour Prediction for Fixture Design Verification.* PhD thesis, University fo Nottingham, School of Mechanical, Materials and Manufacturing Engineering, 2005.

[108] Qu, Z. Q. *Model Order Reduction Techniques: with Applications in Finite Element Analysis.* Springer-Verlag, London, 2004.

[109] Raibert, M. H., and J.Craig, J. Hybrid Position/Force Control of Manipulators. *Journal of Dynamic Systems, Measurement, and Control 102* (1981), 126–133.

[110] Rashid, A., and Nicolescu, C. M. Active Vibration Control in Palletised Workhodling System for Milling. *International Journal of Machine Tools and Manufacture 46* (2006), 1626–1636.

[111] Ratchev, S., Phuah, K., Lämmel, G., and Huang, W. An Experimental Investigation of Fixture-Workpiece Contact Behaviour for the Dynamic Simulation of Complex Fixture-Workpiece Systems. *Journal of Materials Processing Technology 164-165* (2005), 1597–1606.

[112] Ratchev, S., Phuah, K., and Liu, S. FEA-based Methodology for the Prediction of Part-Fixture Behaviour and its Applictations. *Journal of Materials Processing Technology 191* (2007), 260–264.

[113] Rieker, J. R., and Trethewey, M. W. Finite Element Analysis of an Elastic Beam Structure Subject to a Moving Distributed Mass Train. *Mechanical Systems and Signal Processing 13*, 1 (1999), 31–51.

[114] Rong, Y., Tao, R., and Tang, X. Flexible Fixturing with Phase-Change Materialls. Part 1. Experimental Study of Magnetorheological Fluids. *International Journal of Advanced Manufacturing Technology 16* (2000), 822–829.

[115] Ryll, M. *Towards a Software Framework for Reconfigurable and Adaptive Fixturing Systems*. PhD thesis, University of Nottingham, 2010.

[116] Ryll, M., Papastathis, T. N., and Ratchev, S. Towards an Intelligent Fixturing System with Rapid Reconfiguration and Part Positioning. *Journal of Materials Processing Technology 201* (2008), 198–203.

[117] Sarma, S. E., and Wright, P. K. Reference Free Part Encapsulation: A New Universal Fixturing Concept. *Journal of Manufacturing Systems 16*, 1 (1997), 35–47.

[118] Sayeed, Q. A., and De Meter, E. C. Machining Fixture Design and Analysis Software. *International Journal of Production Research 32*, 7 (1994), 1655–1674.

[119] Sela, M. N., Gaundry, O., Dombre, E., and Benhabib, B. A Reconfigurable Modular Fixturing System for Thin-walled Flexible Objects. *The International Journal of Advanced Manufacturing Technology 13* (1997), 611–617.

[120] Senthil Kumar, A., Fuh, J. Y. H., and Kow, T. S. An Automated Design and Assembly of Interference-Free Modular Fixture Setup. *Computer-Aided Design 32* (2000), 583–596.

[121] Senthil Kumar, A., Subramaniam, V., and Teck, T. B. Conceptual Design of Fixtures Using Machine Learning Techniques. *International Journal of Advanced Manufacturing Technology 16* (2000), 176–181.

[122] Shen, C. H., Lin, T. T., Agapiou, J. S., Jones, G. L., Kramarczyk, M. A., and Bandyopadhyay, P. An Innovative Reconfigurable and Totally Automated Fixture System for Agile Manufacturing Applications. *Transactions of the NAMRI/SME 31* (2003), 325–402.

[123] Shirinzadeh, B. Issues in the Design of the Reconfigurable Fixture Modules for Robotic Assembly. *Journal of Manufacturing Systems 12*, 1 (1993), 1–14.

[124] Shirinzadeh, B. Flexible and Automated Workholding Systems. *Industrial Robot 22*, 2 (1995), 29–34.

[125] SIMULIA, Dassault Systèmes S.A. *Abaqus Analysis User's Manual, Edition 6.7-1.* Providence, Rhode Island, 2007.

[126] SIMULIA, Dassault Systèmes S.A. *Abaqus Theory Manual, Edition 6.7-1.* Providence, Rhode Island, 2007.

[127] SIMULIA, Dassault Systèmes S.A. *Abaqus/CAE User's Manual, Edition 6.7-1.* Providence, Rhode Island, 2007.

[128] Stephenson, D. A., and Agapiou, J. S. *Metal Cutting Theory and Practice.* Marcel Dekker Inc., New York, 1997.

[129] Subramaniam, V., Senthil Kumar, A., and Seow, K. C. A Multi-Agent Approach to Fixture Design. *Journal of Intelligent Manufacturing 12* (2001), 31–42.

[130] System3R. VDP: Vibration-Damped Palletisation. http://www.system3r.com/3r/en/products--services/products/precision-production/vdp.aspx. Last accessed on 13/12/2010.

[131] Tan, E. Y. T., Senthil Kumar, A., Fuh, J. Y. H., and Nee, A. Y. C. Modelling, Analysis and Verification of Optimal Fixturing Design. *IEEE Transactions on Automation Science and Engineering 1*, 2 (2004), 121–132.

[132] Taylor Hobson Ltd. Surface Profilers: Ultra Precision PGI Range. http://www.taylor-hobson.com/ultra-precision-pgi-range.html. Last accessed on 10/12/2010.

[133] THK. Linear Motion Systems. http://www.thk.com/uk/products/index.html. Last accessed on 10/12/2010.

[134] Thompson, B. S., Gandhi, M. V., and Desai, D. J. Workpiece-Fixture Interactions in a Compacted Fluidized-Bed Fixture under Various Loading Conditions. *International Journal of Production Research 27*, 2 (1989), 229–246.

[135] Timoshenko, S., and Goodier, J. *Theory of Elasticity*, 2nd ed. McGraw-Hill Book Company, Inc. and Kōgakusha Company, Ltd., Tokyo, Japan, 1951.

[136] Timoshenko, S., and Woinowski-Krieger, S. *Theory of Plates and Shells*, 2nd ed. McGraw-Hill Book Company, Inc., Singapore, 1959.

[137] Trappey, A. J. C., and Liu, C. R. Automated Fixture Configuration Using Projective Geometry Approach. *International Journal of Advanced Manufacturing Technology 8* (1991), 297–304.

[138] Tuffentsammer, K. Automatic Loading of Machining Systems and Automatic Clamping of Workpieces. *Annals of the CIRP 30*, 2 (1981), 553–558.

[139] Walczyk, D. F., and Longtin, R. S. Fixturing of Compliant Parts Using a Matrix of Reconfigurable Pins. *Transactions of the ASME 122* (2000), 766–772.

[140] Wang, Y. F., Fuh, J. Y. H., and Wong, Y. S. A Model-Based Online Control of Optimal Fixturing Process. In *Proceedings of the 1997 IEEE International Conference on Robotics and Automation* (Albuquerque, New Mexico, USA, April 1997).

[141] Wu, J. J. Dynamic Analysis of a Rectangular Plate under a Moving Line Load using Scale Beams and Scaling Laws. *Computers and Structures 83* (2005), 1646–1685.

[142] Wu, J. J., Whittaker, A. R., and Cartmell, M. P. The Use of Finite Element Techniques for Calculating the Dynamic Response of Structures to Moving Loads. *Computers and Structures 78* (2000), 789–799.

[143] Wu, N. H., and Chan, C. A Genetic Algorithm Based Approach to Optimal Fixture Configuration. *Computers and Industrial Engineering 31*, 3/4 (1996), 919–924.

[144] Xu, Y.-C., Liu, G., Tang, Y., Zhang, J., Dong, R., and Wu, M. *Flexible Manufacturing Systems*. IFS Publications, Bedford, 1985, ch. A Modular Fixturing System for Flexible Manufacturing, pp. 227–233.

[145] Yeh, J. H., and Liou, F. W. Contact Condition Modeling for Machining Fixture Setup. *International Journal of Machine Tools and Manufacture 39* (1999), 787–803.

[146] Youcef-Toumi, K., and Buitrago, J. H. Design and Implementation of Robot-Operated Adaptable and Modular Fixtures. *Robotics & Computer-Itegrated Manufacturing 5*, 4 (1989), 343–356.

[147] ZF Electronics UK, Ltd. Cherry DH-Series Ultra Miniature Snap Action Switches. `http://www.cherrycorp.com/english/switches/submini/dh.htm`. Last accessed on 10/12/2010.

[148] Zienkiewicz, O. C., Taylor, R. L., and Zhu, J. Z. *The Finite Element Method: Its Basis and Fundamentals* . Elsevier Butterworth-Heinemann, Oxford, Great Britain, 2005.

Appendix A

Validation of FEA and Analytical Workpiece Models

A.1 Validation of Natural Frequencies Obtained from the Literature

When transporting information and data from literature into a usable format, errors could be introduced. Typographical mistakes could also affect the results and lead to false conclusions. For these reasons the eigenvalues and natural frequencies that were obtained from literature should be validated.

This can be achieved by comparing the literature-derived natural frequencies of the plate workpiece with the ones calculated using beam theory. The main difference between a thin plate and a thin beam is their Length-to-Width ratios. In order for a structure to be considered a beam, it needs to have width-to-length and thickness-to-length ratios of 1/10 or less. If the width-to-length ratio is greater than the given figure, then the structure can be approached as a plate. However, when the width-to-length ratio of a plate is close to that of a beam, then the natural frequencies of the structure can be predicted fairly accurately by using the analytic expressions designed for beams. This can be used as basic theoretical validation of the results obtained through plate analysis. The natural frequencies of a simply supported beam are given by the following equation.

$$\omega_{(j)} = \left(\frac{j\pi}{l_y}\right)^2 \sqrt{\frac{EJ}{\mu}} \tag{A.1}$$

with

$$J = \frac{l_y h^3}{12} \tag{A.2}$$

where:

E: Young's Modulus

ω_j: The j$^{\text{th}}$ natural frequency of the structure

J: Moment of inertia of the beam's cross section

l_y: Width of the beam

μ: Mass per unit length

h: Beam thickness

To calculate the approximate natural frequencies of the plate, the same formula can be used, substituting EJ with $D = \frac{Eh^3}{12(1-\nu^2)}$. Hence the following equation can be used too.

$$\omega_{(j)} = \left(\frac{j\pi}{l_y}\right)^2 \sqrt{\frac{D}{\mu}} \tag{A.3}$$

Using the above, the first 8 natural frequencies of the plate were calculated and compared to the respective ones from Plate Theory [57]. The results are presented in Table A.1.

Table A.1: Comparison between natural frequencies of the aluminum plate with $\phi = 1/3$ calculated using beam theory and Kirchhoff plate theory [57]. Values in Hz.

i	1	2	3	4	5	6	7	8
Beam Theory	323.53	1294.1	2911.7	5176.4	8088.2	11647	15853	20706
Gorman (1982)	307.12	1242.9	2822.8	5050.8	7924.3	11444	15613	20424
% Diff.	5.34	4.12	3.15	2.49	2.07	1.77	1.54	1.38

A.2 Validation of Analytical Model of SFSF Plate Subjected to Moving Load

As already mentioned, beams and plates are two structural elements that, under certain conditions behave fairly similar. For this reason, the analytical model described in Section 4.2.2.2, can be validated through a beam model. As the beam is a one-dimensional body, only concentrated loads moving along the length of the beam can be simulated. Furthermore, the simplest beam model to implement is the one where the load is no longer

time-varying but constant. As a result, and in order to reduce the effort for validation of the full model, a simplified version of the plate model shall be used, one where the load is constant and concentrated along the middle of the plate, i.e. $\eta = l_y/2$. The analytical expression for the transverse displacement of a plate subjected to a moving load, which was presented in Chapter 4, can be rewritten for a constant, concentrated load, moving along $\eta = l_y/2$ as:

$$\begin{aligned} w(x,y,t) &= \sum_{i=1}^{\infty}\sum_{j=1}^{\infty} \frac{2P}{l_x W_j} \frac{1}{\omega_{(i,j)}^2 - \omega_x^2} \sin\left(\frac{i\pi x}{l_x}\right) w_{(j)}(y) w_{(j)}(\eta) \times \\ &\quad \left[\sin(\omega_x t) - \frac{\omega_x}{\omega_{(i,j)}} \sin\left(\omega_{(i,j)} t\right)\right] \end{aligned} \tag{A.4}$$

Furthermore, the equation of motion of a beam under a constant concentrated moving load is given by:

$$EJ\frac{\partial \upsilon^4(x,t)}{\partial x^4} + \mu\frac{\partial \upsilon^2(x,t)}{\partial t^2} + 2\mu\omega_b\frac{\partial \upsilon(x,t)}{\partial t} = \delta(x-ct)P \tag{A.5}$$

where:

- x: length coordinate. Origin is at the left hand side end of the beam
- t: Time
- $\upsilon(x,t)$: Beam deflection at point x at time t
- E: Young's Modulus
- J: Moment of inertia of the beam's cross section
- ω_b: Circular damped frequency of the beam
- μ: Mass per unit length
- P: Constant load magnitude
- δ: Dirac function
- c: Constant load speed

The natural frequencies of a simply supported beam can be calculated through:

$$\omega_{(j)}^2 = \frac{j^4\pi^4}{l^4}\frac{EJ}{\mu} \tag{A.6}$$

In the above equation l is the length of the beam. If $\alpha = {}^{\omega}/_{\omega(1)}$,where ω is the excitation

circular frequency ($\omega = {}^{\pi c}/_{l}$) and assuming zero damping then, for $\alpha \neq j$, the displacement $\upsilon(x,t)$ of the beam is given by:

$$\upsilon(x,t) = \upsilon_0 \sum_{j=1}^{\infty} \sin\left(\frac{j\pi x}{l}\right) \frac{1}{j^2(j^2-\alpha^2)} \left[\sin(j\omega t) - \frac{a}{j}\sin\left(\omega_{(j)}t\right)\right] \tag{A.7}$$

where:

$$\upsilon_0 = \frac{2Pl^3}{\pi^4 EJ} \tag{A.8}$$

For $\alpha = n$, where $n = 1, 2, 3, \cdots$, then:

$$\begin{aligned} \upsilon(x,t) &= \upsilon_0 \frac{1}{2n^4}\left[\sin(n\omega t) - n\omega t\cos(n\omega t)\right]\sin\left(\frac{n\pi x}{l}\right) + \\ &\quad \upsilon_0 \sum_{j=1, j\neq n}^{\infty} \sin\left(\frac{j\pi x}{l}\right) \frac{1}{j^2(j^2-\alpha^2)} \left[\sin(j\omega t) - \frac{a}{j}\sin\left(\omega_{(j)}t\right)\right] \end{aligned} \tag{A.9}$$

Substituting $P = 300$ N, $c = 0.033$ m/sec, $E = 71.7$ GPa in the above equations, the transverse displacement of the beam can be calculated and compared directly to the ones from the plate. Comparison results are summarised in Table A.3. This table shows a clear agreement between the behaviour of the beam and the plate, under the same conditions. This is a strong indication that the analytic model used to calculate the plate transverse displacement is correct. However, it is important to make sure that the beam model used, is itself correct. For this reason two other tests need to be performed. These are described in the following paragraphs.

A.2.1 Static Deflection of Beam Versus Deflection of Beam Under Slowly Moving Load

When the speed of the moving load approaches a zero value, then the problem is almost equivalent to the static loading of a beam. The deformation at any point of a simply supported beam under a static load (Figure A.1), is given by the following equations.

For span a:

$$y_{AB} = \frac{Fbx}{6EJl}(x^2 + b^2 - l^2) \tag{A.10}$$

For span b:

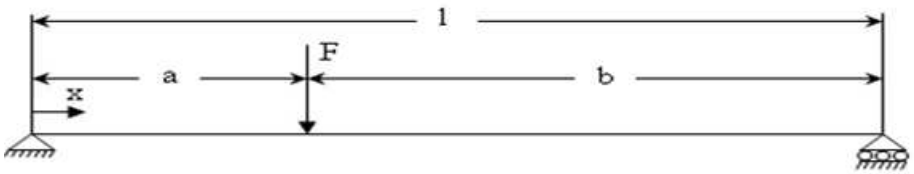

Figure A.1: Graphical Representation of a simply supported beam subjected to a static load.

$$y_{BC} = \frac{Fa(l-x)}{6EJl}(x^2 + a^2 - 2lx) \tag{A.11}$$

If the load is applied in the middle of the beam, then $y_{AB} = y_{BC} = \frac{Fax}{48EJ}(4x^2 - 3l^2)$. When calculating the analytic model presented in Equations (A.7) to (A.9) with a very slow speed for the moving load, e.g. $c = 0.1$ mm/sec and comparing it to static deflection results from Equations (A.10) and (A.11), good agreement is expected. The results form this comparison are summarised in Table A.4. It is evident from this table that the agreement between the static and the slowly moving load cases is very good.

A.2.2 Deflection of Beam Under Moving Load Versus Literature Results

Using the algorithm created for the transverse displacement of a beam excited by a moving load, different values to c can be assigned, permitting comparison of analytical results with the ones presented in [52]. The transverse deflection of the beam excited by a moving load at the following speeds was calculated:

- 0.1 mm/sec
- 33 mm/sec
- 45810 mm/sec, half the critical speed $\left(c_{cr} = \frac{\pi}{l}\sqrt{\frac{EJ}{\mu}}\right)$
- 91620 mm/sec, equal to the critical speed
- 100000 mm/sec

The response of the midpoint of the beam under these speeds is shown in Figure A.2a. This diagram can be compared directly to results presented in [52] (Figure A.2b). The results from all the above clearly indicate that the analytic model for a simply supported-free plate traversed by a moving distributed load is correct and can be used as means of validation for the FEA model of the workpiece.

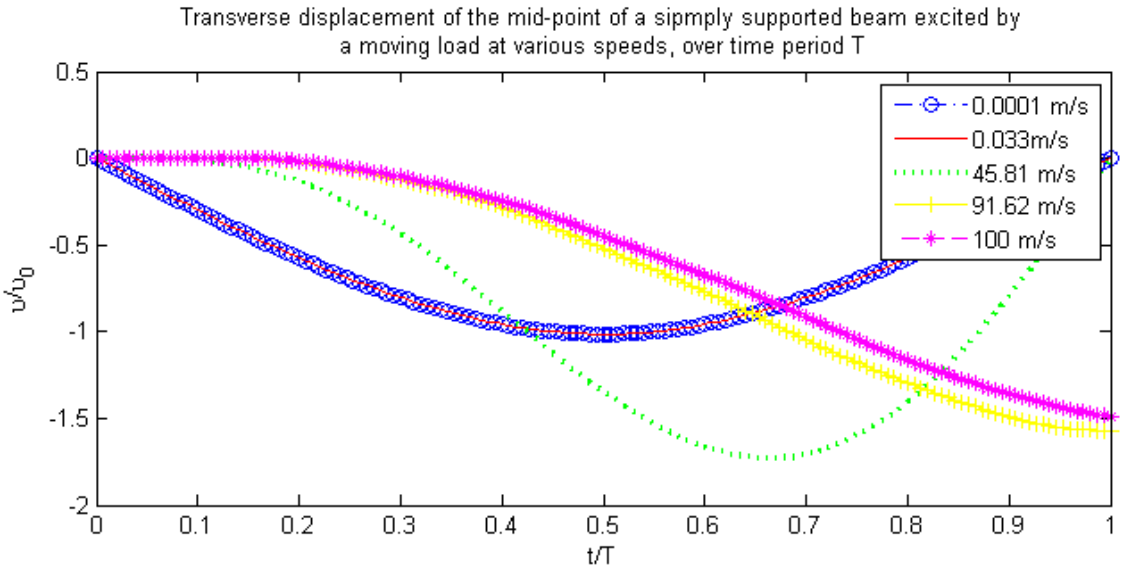

(a)

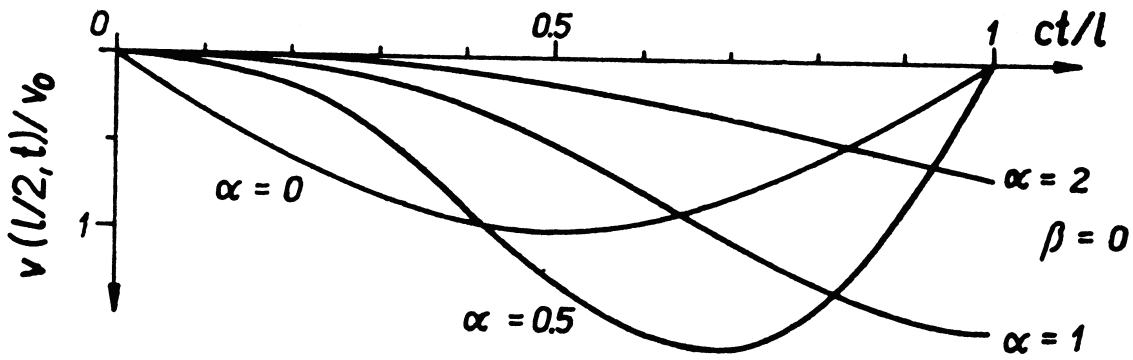

(b)

Figure A.2: Response of the midpoint of a simple supported beam excited by a moving constant load, under different speed cases (a) as calculated using Equations (A.7) and (A.9) and (b) as presented in [52]. In this figure α designates ratio of load speed to critical speed, β refers to damping, $T = ct/l$ is the time period necessary for the load to travel one full length of the beam.

Table A.3: Comparison of transverse deflection between a simply supported beam and a simply supported plate (values from $y = 25$ mm) under a 300 N moving load ($c = 33$ mm/s). All displacement values in μm.

Time=0.1515 s, Load @ x=5 mm				
	x=5	x=25	x=50	x=75
Beam	-43.44	-176.92	-257.76	-261.12
Plate (y=25mm)	-42.16	-170.66	-248.36	-252.33
% Diff.	**2.94**	**3.54**	**3.65**	**3.37**
Time=0.7575s, Load @ x=25mm				
Beam	-176.92	-807.12	-1226.82	-1259.10
Plate (y=25mm)	-170.67	-777.49	-1179.87	-1218.54
% Diff.	**3.53**	**3.67**	**3.83**	**3.22**
Time=1.515s, Load @ x=50mm				
Beam	-257.76	-1226.82	-2066.22	-2227.65
Plate (y=25mm)	-248.17	-1178.89	-1994.31	-2150.27
% Diff.	**3.72**	**3.91**	**3.48**	**3.47**
Time=2.272s, Load @ x=75mm				
Beam	-261.12	-1259.10	-2227.65	-2615.06
Plate (y=25mm)	-252.25	-1218.21	-2151.68	-2529.16
% Diff.	**3.40**	**3.25**	**3.41**	**3.28**

Table A.4: Comparison of transverse deflection of a simply supported beam under a 300 N static load, applied at different positions along the span of a beam and the same beam under a slow moving 300 N load ($c = 0.1$ mm/s). All displacement values in μm.

Load @ x=5 mm				
	x=5	x=25	x=50	x=75
Beam Static	-43.44	-176.92	-257.76	-261.12
Beam Moving Load	-44.04	-179.53	-261.55	-264.94
% Diff.	**-1.38**	**-1.48**	**-1.47**	**-1.46**
Load @ x=25 mm				
Beam Static	-176.92	-807.12	-1226.82	-1259.10
Beam Moving Load	-179.53	-818.91	-1244.81	-1277.59
% Diff.	**-1.48**	**-1.46**	**-1.47**	**-1.47**
Load @ x=50 mm				
Beam Static	-257.76	-1226.82	-2066.22	-2227.65
Beam Moving Load	-261.55	-1244.81	-2096.51	-2260.33
% Diff.	**-1.47**	**-1.47**	**-1.47**	**-1.47**
Load @ x=75 mm				
Beam Static	-261.12	-1259.10	-2227.65	-2615.06
Beam Moving Load	-264.94	-1277.59	-2260.34	-2653.39
% Diff.	**-1.46**	**-1.47**	**-1.47**	**-1.47**

Appendix B

Detailed Natural Frequency Prediction Results

In the following pages, detailed results on the natural frequency prediction capabilities of a variety of finite elements shall be presented. Results from the Simply supported-Free-Simply supported-Free (SFSF) boundary conditions case are adduced first, in Tables B.1-B.6. The Clamped-Free-Clamped-Free case is presented in Tables B.7 and B.8.

Table B.1: Natural frequencies of a thin plate with SFSF boundary conditions as predicted using (a) S4 finite elements (341 nodes) and (b) S4R finite elements (341 nodes). Values in Hz.

(a)

			j		
			1	2	3
i	1	PT	307.12	1276.3	7124.8
		FEA	307.43	1258.0	7096.4
		% Diff.	**0.10**	**-1.45**	**-0.40**
	2	PT	1242.9	2780.3	8573.3
		FEA	1245.8	2743.8	8462.0
		% Diff.	**0.23**	**-1.33**	**-1.31**
	3	PT	2822.8	4684.9	10745
		FEA	2837.6	4635.2	10530
		% Diff.	**0.52**	**-1.07**	**-2.04**
	4	PT	5050.8	7101.2	13509
		FEA	5098.6	7050.1	13193
		% Diff.	**0.94**	**-0.72**	**-2.40**

(b)

			j		
			1	2	3
i	1	PT	307.12	1276.3	7124.8
		FEA	307.41	1257.5	7092.6
		% Diff.	**-0.03**	**-1.79**	**-1.61**
	2	PT	1242.9	2780.3	8573.3
		FEA	1245.6	2740.3	8446.3
		% Diff.	**-0.27**	**-1.84**	**-2.60**
	3	PT	2822.8	4684.9	10745
		FEA	2836.8	4624.5	10492
		% Diff.	**-0.58**	**-1.98**	**-3.34**
	4	PT	5050.8	7101.2	13509
		FEA	5096.5	7027.3	13120
		% Diff.	**-0.98**	**-2.27**	**-4.00**

Table B.2: Natural frequencies of a thin plate with SFSF boundary conditions as predicted using (a) S8R finite elements (981 nodes) and (b) S3 finite elements (341 nodes). Values in Hz.

(a)

			j		
			1	2	3
i	1	PT	307.12	1276.3	7124.8
		FEA	306.96	1252.3	6994.4
		% Diff.	**-0.05**	**-1.88**	**-1.84**
	2	PT	1242.9	2780.3	8573.3
		FEA	1238.4	2726.2	8340.7
		% Diff.	**-0.36**	**-1.94**	**-2.72**
	3	PT	2822.8	4684.9	10745
		FEA	2800.7	4585.4	10364
		% Diff.	**-0.78**	**-2.12**	**-3.55**
	4	PT	5050.8	7101.2	13509
		FEA	4983.7	6922.9	12938
		% Diff.	**-1.33**	**-2.51**	**-4.23**

(b)

			j		
			1	2	3
i	1	PT	307.12	1276.3	7124.8
		FEA	307.40	1244.9	7081.0
		% Diff.	**0.09**	**-2.52**	**-0.62**
	2	PT	1242.9	2780.3	8573.3
		FEA	1265.0	2763.7	8533.1
		% Diff.	**1.75**	**-0.60**	**-0.47**
	3	PT	2822.8	4684.9	10745
		FEA	2834.8	4679.3	10732
		% Diff.	**0.42**	**-0.12**	**-0.12**
	4	PT	5050.8	7101.2	13509
		FEA	5087.8	7126.4	13575
		% Diff.	**0.73**	**0.35**	**-0.49**

Table B.3: Natural frequencies of a thin plate with SFSF boundary conditions as predicted using (a) STRI65 finite elements (7701 Nodes) and (b) C3D8 finite elements (7904 Nodes). Values in Hz.

(a)

			j		
			1	2	3
i	1	PT	307.12	1276.3	7124.8
		FEA	307.03	1257.1	7025.2
		% Diff.	**-0.03**	**-1.50**	**-1.40**
	2	PT	1242.9	2780.3	8573.3
		FEA	1239.4	2736.4	8384.7
		% Diff.	**-0.28**	**-1.58**	**-2.60**
	3	PT	2822.8	4684.9	10745
		FEA	2805.3	4616.3	10426
		% Diff.	**-0.62**	**-1.46**	**-2.97**
	4	PT	5050.8	7101.2	13509
		FEA	4997.2	6953.6	13032
		% Diff.	**-0.98**	**-2.08**	**-3.60**

(b)

			j		
			1	2	3
i	1	PT	307.12	1276.3	7124.8
		FEA	327.33	1225.4	7217.7
		% Diff.	**6.58**	**-3.99**	**1.30**
	2	PT	1242.9	2780.3	8573.3
		FEA	1310.0	2904.0	8525.9
		% Diff.	**5.40**	**4.45**	**-0.55**
	3	PT	2822.8	4684.9	10745
		FEA	2933.3	4760.5	10524
		% Diff.	**3.91**	**1.61**	**-2.06**
	4	PT	5050.8	7101.2	13509
		FEA	5123.4	7152.9	13102
		% Diff.	**1.44**	**0.73**	**-3.01**

Table B.4: Natural frequencies of a thin plate with SFSF boundary conditions as predicted using (a) C3D8R finite elements (7904 Nodes) and (b) C3D20 finite elements (4947 Nodes). Values in Hz.

(a)

			j		
			1	2	3
i	1	PT	307.12	1276.3	7124.8
		FEA	289.36	1149.5	6572.8
		% Diff.	**-5.78**	**-9.93**	**-7.75**
	2	PT	1242.9	2780.3	8573.3
		FEA	1164.0	2669.5	7846.6
		% Diff.	**-6.35**	**-3.98**	**-8.48**
	3	PT	2822.8	4684.9	10745
		FEA	2615.2	4398.2	9755.9
		% Diff.	**-7.35**	**-6.12**	**-9.20**
	4	PT	5050.8	7101.2	13509
		FEA	4554.7	6587.0	12180
		% Diff.	**-9.82**	**-7.24**	**-9.84**

(b)

			j		
			1	2	3
i	1	PT	307.12	1276.3	7124.8
		FEA	306.72	1221.4	7001.5
		% Diff.	**-0.13**	**-4.49**	**-1.76**
	2	PT	1242.9	2780.3	8573.3
		FEA	1234.2	2875.9	8386.3
		% Diff.	**-0.70**	**3.32**	**-2.18**
	3	PT	2822.8	4684.9	10745
		FEA	2775.9	4680.6	10443
		% Diff.	**-1.69**	**-0.09**	**-2.89**
	4	PT	5050.8	7101.2	13509
		FEA	4869.3	6990.1	13054
		% Diff.	**-3.73**	**-1.59**	**-3.49**

Table B.5: Natural frequencies of a thin plate with SFSF boundary conditions as predicted using (a) C3D20R finite elements (4947 Nodes) and (b) C3D15 finite elements (6812 Nodes). Values in Hz.

(a)

			j		
			1	2	3
i	1	PT	307.12	1276.3	7124.8
		FEA	306.65	1214.2	7001.6
		% Diff.	**-0.15**	**-5.11**	**-1.76**
	2	PT	1242.9	2780.3	8573.3
		FEA	1233.2	2862.3	8360.1
		% Diff.	**-0.79**	**-2.55**	**-2.55**
	3	PT	2822.8	4684.9	10745
		FEA	2771.1	4662.5	10399
		% Diff.	**-1.87**	**-0.48**	**-3.33**
	4	PT	5050.8	7101.2	13509
		FEA	4856.0	6962.8	12990
		% Diff.	**-4.01**	**-1.99**	**-4.00**

(b)

			j		
			1	2	3
i	1	PT	307.12	1276.3	7124.8
		FEA	306.68	1216.5	7000.7
		% Diff.	**-0.14**	**-4.92**	**-1.76**
	2	PT	1242.9	2780.3	8573.3
		FEA	1233.6	2866.2	8369.3
		% Diff.	**-0.75**	**3.00**	**-2.44**
	3	PT	2822.8	4684.9	10745
		FEA	2773.1	4669.1	10417
		% Diff.	**-1.79**	**-0.34**	**-3.15**
	4	PT	5050.8	7101.2	13509
		FEA	4860.3	6974.1	13020
		% Diff.	**-3.92**	**-1.82**	**-3.76**

Table B.6: Natural frequencies of a thin plate with SFSF boundary conditions as predicted using (a) SC8R finite elements (1500 Nodes) and (b) SC6R finite elements (1504 Nodes). Values in Hz.

(a)

			j		
			1	2	3
i	1	PT	307.12	1276.3	7124.8
		FEA	306.93	1214.4	6890.5
		% Diff.	**-0.06**	**-5.10**	**-3.40**
	2	PT	1242.9	2780.3	8573.3
		FEA	1237.8	2858.9	8211.1
		% Diff.	**-0.41**	**2.75**	**4.41**
	3	PT	2822.8	4684.9	10745
		FEA	2795.3	4653.3	10202
		% Diff.	**-0.98**	**-0.68**	**-5.32**
	4	PT	5050.8	7101.2	13509
		FEA	4929.2	6968.9	12757
		% Diff.	**-2.47**	**-1.90**	**-7.32**

(b)

			j		
			1	2	3
i	1	PT	307.12	1276.3	7124.8
		FEA	306.81	1215.1	6927.9
		% Diff.	**-0.10**	**-5.04**	**-2.84**
	2	PT	1242.9	2780.3	8573.3
		FEA	1235.7	2858.2	8342.7
		% Diff.	**-0.58**	**2.73**	**-2.76**
	3	PT	2822.8	4684.9	10745
		FEA	2788.2	4667.2	10453
		% Diff.	**-1.24**	**-0.38**	**-2.79**
	4	PT	5050.8	7101.2	13509
		FEA	4902.6	7013.7	13158
		% Diff.	**-3.02**	**-1.25**	**-2.67**

Table B.7: Natural frequencies of a thin plate with CFCF boundary conditions as predicted using (a) S4 finite elements (341 Nodes) and (b) S3 finite elements (341 Nodes). Values in Hz.

(a)

			j		
			1	2	3
i	1	PT	715.25	1527.0	7211.5
		FEA	715.11	1502.2	7172.4
		% Diff.	**-0.02**	**-1.65**	**-0.55**
	2	PT	1970.7	3309.0	8873.1
		FEA	1974.7	3260.6	8726.5
		% Diff.	**0.20**	**-1.48**	**0.01**
	3	PT	3876.6	5521.6	11312
		FEA	3895.2	5456.4	11037
		% Diff.	**0.48**	**-1.19**	**-2.49**
	4	PT	6427.9	8263.0	14373
		FEA	6486.6	8197.1	13972
		% Diff.	**0.90**	**-0.80**	**-2.87**

(b)

			j		
			1	2	3
i	1	PT	715.25	1527.0	7211.5
		FEA	715.40	1516.0	7170.0
		% Diff.	**0.02**	**-0.73**	**-0.58**
	2	PT	1970.7	3309.0	8873.1
		FEA	1973.9	3295.3	8836.1
		% Diff.	**0.16**	**-0.42**	**-0.42**
	3	PT	3876.6	5521.6	11312
		FEA	3890.7	5520.5	11311
		% Diff.	**0.36**	**-0.02**	**-0.01**
	4	PT	6427.9	8263.0	14373
		FEA	6473.6	8293.7	14460
		% Diff.	**0.71**	**0.37**	**-0.60**

Table B.8: Natural frequencies of a thin plate with CFCF boundary conditions as predicted using (a) SC8R finite elements (1500 Nodes) and (b) C3D20 finite elements (4947 Nodes). Values in Hz.

(a)

			j		
			1	2	3
i	1	PT	715.25	1527.0	7211.5
		FEA	708.46	1481.1	6954.8
		% Diff.	**-0.94**	**-3.01**	**-3.56**
	2	PT	1970.7	3309.0	8431.5
		FEA	1956.8	3208.6	8836.1
		% Diff.	**-0.71**	**-3.03**	**-0.42**
	3	PT	3876.6	5521.6	11312
		FEA	3858.1	5355.3	10623
		% Diff.	**-0.48**	**-3.01**	**-6.09**
	4	PT	6427.9	8263.0	14373
		FEA	6419.8	8018.7	13392
		% Diff.	**-0.13**	**-2.96**	**-6.83**

(b)

			j		
			1	2	3
i	1	PT	715.25	1527.0	7211.5
		FEA	705.72	1492.0	7080.0
		% Diff.	**-1.33**	**-2.29**	**-1.82**
	2	PT	1970.7	3309.0	8431.5
		FEA	1940.3	3227.5	8617.3
		% Diff.	**-1.54**	**-2.46**	**-2.88**
	3	PT	3876.6	5521.6	11312
		FEA	3801.9	5369.6	10881
		% Diff.	**-1.93**	**-2.75**	**-3.81**
	4	PT	6427.9	8263.0	14373
		FEA	6274.1	7999.2	13715
		% Diff.	**-2.39**	**-3.19**	**-4.58**

Appendix C

Detailed Elastic Deformation Prediction Results for Plate

In this Appendix, the elastic deformation of the plate workpiece traversed by a distributed harmonic load is presented in detail. In all cases the plate is simply supported along both its smaller edges and is free at the longer edges. The dynamic load changes its amplitude at a frequency of $\omega = 198.02$ Hz. It has a mean value of 150 N and an amplitude of 150 N. Its amplitude can be mathematically described by:

$$P(t) = 150\,(1 + \cos \omega t) \tag{C.1}$$

The load moves along the x-axis of the plate at a constant speed of $c = 0.033$ m/s. It is applied parallel to y-axis from $y = 0$ mm to $y = 25$ mm, i.e. the centreline of the plate. The results obtained using S4 finite elements are first presented, followed by the ones obtained using S3 elements. Both cases are also compared to results from the analytical model presented in Chapter 4 [52]. All coordinate values are in mm, whilst all displacement values are in μm.

C.1 Elastic Deformation of a SFSF Plate Calculated Using S4 Finite Elements

Table C.1: Elastic deformation of a SFSF plate at time $t = 0.1515$ s - S4 Elements.

$t = 0.1515$ s, Tool @ $x = 5$ mm					
		x=5	x=25	x=50	x=75
y=0	Plate	-63.16	-257.82	-372.75	-381.32
	FEA	-65.93	-273.75	-387.64	-399.86
	Diff (%)	4.20	5.82	3.84	4.63
y=10	Plate	-57.33	-238.99	-353.16	-365.31
	FEA	-58.88	-251.56	-366.76	-381.84
	Diff (%)	2.62	4.99	3.71	4.33
y=25	Plate	-50.35	-218.08	-332.60	-349.15
	FEA	-51.57	-227.48	-344.63	-363.22
	Diff (%)	2.37	4.13	3.49	3.87
y=40	Plate	-45.41	-205.30	-322.22	-342.16
	FEA	-46.72	-212.45	-333.18	-354.30
	Diff (%)	2.79	3.37	3.29	3.43
y=50	Plate	-44.37	-202.83	-321.47	-342.66
	FEA	-45.20	-208.52	-331.71	-353.95
	Diff (%)	1.83	2.73	3.09	3.19

Table C.2: Elastic deformation of a SFSF plate at time $t = 0.7575$ s - S4 Elements.

$t = 0.7575$ s, Tool @ $x = 25$ mm					
		x=5	x=25	x=50	x=75
y=0	Plate	-257.84	-1170.86	-1776.31	-1841.12
	FEA	-274.74	-1227.29	-1857.47	-1918.98
	Diff (%)	6.15	4.60	4.37	4.06
y=10	Plate	-239.01	-1091.76	-1682.05	-1761.48
	FEA	-253.32	-1138.66	-1754.46	-1833.29
	Diff (%)	5.65	4.12	4.13	3.92
y=25	Plate	-218.09	-1004.58	-1583.15	-1680.39
	FEA	-227.23	-1043.38	-1645.67	-1745.03
	Diff (%)	4.02	3.72	3.80	3.70
y=40	Plate	-205.30	-952.85	-1532.80	-1644.02
	FEA	-212.47	-986.63	-1588.30	-1712.79
	Diff (%)	3.37	3.42	3.49	4.02
y=50	Plate	-202.83	-944.05	-1528.63	-1645.68
	FEA	-208.61	-973.81	-1580.73	-1711.74
	Diff (%)	2.77	3.06	3.30	3.86

Table C.3: Elastic deformation of a SFSF plate at time $t = 1.515$ s - S4 Elements.

$t = 1.515$ s, Tool @ $x = 50$ mm					
		x=5	x=25	x=50	x=75
y=0	Plate	-372.20	-1773.59	-3007.21	-3252.20
	FEA	-386.18	-1855.59	-3118.95	-3371.05
	Diff (%)	3.62	4.42	3.58	3.53
y=10	Plate	-352.61	-1679.40	-2848.59	-3101.91
	FEA	-363.98	-1752.23	-2946.26	-3208.40
	Diff (%)	3.12	4.16	3.32	3.32
y=25	Plate	-332.04	-1580.53	-2680.39	-2947.11
	FEA	-341.63	-1643.19	-2764.17	-3038.88
	Diff (%)	2.81	3.81	3.03	3.02
y=40	Plate	-321.65	-1530.14	-2592.24	-2873.81
	FEA	-330.46	-1586.00	-2666.51	-2954.35
	Diff (%)	2.67	3.52	2.79	2.73
y=50	Plate	-320.88	-1525.90	-2584.98	-2873.18
	FEA	-329.21	-1578.56	-2652.90	-2947.85
	Diff (%)	2.53	3.34	2.56	2.53

Table C.4: Elastic deformation of a SFSF plate at time $t = 2.272$ s - S4 Elements.

$t = 2.272$ s, Tool @ $x = 75$ s					
		x=5	x=25	x=50	x=75
y=0	Plate	-381.08	-1840.00	-3255.77	-3828.90
	FEA	-402.40	-1926.31	-3412.85	-4015.90
	Diff (%)	5.30	4.48	4.60	4.66
y=10	Plate	-365.06	-1760.38	-3105.39	-3641.41
	FEA	-383.33	-1840.57	-3250.18	-3811.05
	Diff (%)	4.76	4.36	4.45	4.45
y=25	Plate	-348.90	-1679.31	-2950.53	-3444.89
	FEA	-364.78	-1752.88	-3081.73	-3597.16
	Diff (%)	4.35	4.20	4.26	4.23
y=40	Plate	-341.89	-1642.94	-2877.28	-3345.98
	FEA	-356.52	-1712.89	-2999.53	-3486.97
	Diff (%)	4.10	4.08	4.08	4.04
y=50	Plate	-342.38	-1644.57	-2876.74	-3341.45
	FEA	-356.76	-1713.38	-2995.30	-3475.98
	Diff (%)	4.03	4.02	3.96	3.87

C.2 Elastic Deformation of a SFSF Plate Calculated Using S3 Finite Elements

Table C.5: Elastic deformation of a SFSF plate at time $t = 0.1515$ s - S3 Elements.

$t = 0.1515$ s, Tool @ $x = 5$ mm					
		x=5	x=25	x=50	x=75
y=0	Plate	-63.16	-257.82	-372.75	-381.32
	FEA	-66.07	-272.57	-387.90	-398.62
	Diff (%)	4.41	5.41	3.90	4.34
y=10	Plate	-57.33	-238.99	-353.16	-365.31
	FEA	-59.22	-250.80	-367.10	-380.94
	Diff (%)	3.18	4.71	3.80	4.10
y=25	Plate	-50.35	-218.08	-332.60	-349.15
	FEA	-52.06	-227.16	-345.26	-362.62
	Diff (%)	3.29	4.00	3.67	3.71
y=40	Plate	-45.41	-205.30	-322.22	-342.16
	FEA	-47.31	-212.46	-334.14	-353.94
	Diff (%)	4.00	3.37	3.57	3.33
y=50	Plate	-44.37	-202.83	-321.47	-342.66
	FEA	-46.00	-208.63	-333.02	-353.95
	Diff (%)	3.54	2.78	3.47	3.19

Table C.6: Elastic deformation of a SFSF plate at time $t = 0.7575$ s - S3 Elements.

$t = 0.7575$ s, Tool @ $x = 25$ mm					
		x=5	x=25	x=50	x=75
y=0	Plate	-257.84	-1170.86	-1776.31	-1841.12
	FEA	-272.98	-1226.02	-1855.75	-1918.47
	Diff (%)	5.54	4.50	4.28	4.03
y=10	Plate	-239.01	-1091.76	-1682.05	-1761.48
	FEA	-250.68	-1145.85	-1753.34	-1833.08
	Diff (%)	4.65	4.72	4.07	3.91
y=25	Plate	-218.09	-1004.58	-1583.15	-1680.39
	FEA	-227.11	-1043.86	-1645.36	-1745.43
	Diff (%)	3.97	3.76	3.78	3.73
y=40	Plate	-205.30	-952.85	-1532.80	-1644.02
	FEA	-212.42	-987.90	-1588.80	-1704.74
	Diff (%)	3.35	3.55	3.52	3.56
y=50	Plate	-202.83	-944.05	-1528.63	-1645.68
	FEA	-208.58	-975.60	-1581.65	-1704.61
	Diff (%)	2.76	3.23	3.35	3.46

Table C.7: Elastic deformation of a SFSF plate at time $t = 1.515$ s - S3 Elements.

$t = 1.515$ s, Tool @ $x = 50$ mm					
		x=5	x=25	x=50	x=75
y=0	Plate	-372.20	-1773.59	-3007.21	-3252.20
	FEA	-388.02	-1853.63	-3137.98	-3391.43
	Diff (%)	4.08	4.32	4.17	4.11
y=10	Plate	-352.61	-1679.40	-2848.59	-3101.91
	FEA	-366.53	-1751.10	-2965.87	-3229.88
	Diff (%)	3.80	4.09	3.95	3.96
y=25	Plate	-332.04	-1580.53	-2680.39	-2947.11
	FEA	-344.63	-1643.01	-2785.32	-3062.40
	Diff (%)	3.65	3.80	3.77	3.76
y=40	Plate	-321.65	-1530.14	-2592.24	-2873.81
	FEA	-333.68	-1586.49	-2689.83	-2980.50
	Diff (%)	3.60	3.55	3.63	3.58
y=50	Plate	-320.88	-1525.90	-2584.98	-2873.18
	FEA	-332.69	-1579.41	-2678.09	-2975.93
	Diff (%)	3.55	3.39	3.48	3.45

Table C.8: Elastic deformation of a SFSF plate at time $t = 2.272$ s - S3 Elements.

$t = 2.272$ s, Tool @ $x = 75$ mm					
		x=5	x=25	x=50	x=75
y=0	Plate	-381.08	-1840.00	-3255.77	-3828.90
	FEA	-399.08	-1918.64	-3395.93	-3994.29
	Diff (%)	4.51	4.10	4.13	4.14
y=10	Plate	-365.06	-1760.38	-3105.39	-3641.41
	FEA	-380.86	-1833.00	-3234.25	-3791.52
	Diff (%)	4.15	3.96	3.98	3.96
y=25	Plate	-348.90	-1679.31	-2950.53	-3444.89
	FEA	-362.51	-1745.17	-3066.62	-3580.74
	Diff (%)	3.75	3.77	3.79	3.79
y=40	Plate	-341.89	-1642.94	-2877.28	-3345.98
	FEA	-353.94	-1704.61	-2984.77	-3473.40
	Diff (%)	3.40	3.62	3.60	3.67
y=50	Plate	-342.38	-1644.57	-2876.74	-3341.45
	FEA	-353.69	-1704.60	-2980.36	-3464.26
	Diff (%)	3.20	3.52	3.48	3.55